

**MARGIN AND SENSITIVITY METHODS
FOR
SECURITY ANALYSIS
OF
ELECTRIC POWER SYSTEMS**

by
Scott Greene

A dissertation submitted in partial fulfillment
of the requirements for the degree of

Doctor of Philosophy
(Electrical Engineering)

University of Wisconsin – Madison
1998

Supervised by Ian Dobson
Department of Electrical and Computer Engineering
University of Wisconsin – Madison
1415 Engineering Drive, Madison WI 53706 USA

© Copyright by Scott Greene 1998
All Rights Reserved

Abstract

Reliable operation of large scale electric power networks requires that system voltages and currents stay within design limits. Operation beyond those limits can lead to equipment failures and blackouts. Security margins measure the amount by which system loads or power transfers can change before a security violation, such as an overloaded transmission line, is encountered.

This thesis shows how to efficiently compute security margins defined by limiting events and instabilities, and the sensitivity of those margins with respect to assumptions, system parameters, operating policy, and transactions. Security margins to voltage collapse blackouts, oscillatory instability, generator limits, voltage constraints and line overloads are considered. The usefulness of computing the sensitivities of these margins with respect to interarea transfers, loading parameters, generator dispatch, transmission line parameters, and VAR support is established for networks as large as 1500 buses.

The sensitivity formulas presented apply to a range of power system models. Conventional sensitivity formulas such as line distribution factors, outage distribution factors, participation factors and penalty factors are shown to be special cases of the general sensitivity formulas derived in this thesis. The sensitivity formulas readily accommodate sparse matrix techniques.

Margin sensitivity methods are shown to work effectively for avoiding voltage collapse blackouts caused by either saddle node bifurcation of equilibria or immediate instability due to generator reactive power limits. Extremely fast contingency analysis for voltage collapse can be implemented with margin sensitivity based rankings.

Interarea transfer can be limited by voltage limits, line limits, or voltage stability. The sensitivity formulas presented in this thesis apply to security margins defined by any limit criteria. A method to compute transfer margins by directly locating intermediate events reduces the total number of loadflow iterations required by each margin computation and provides sensitivity information at minimal additional cost. Estimates of the effect of simultaneous transfers on the transfer margins agree well with the exact computations for a network model derived from a portion of the U.S grid. The accuracy of the estimates over a useful range of conditions and the ease of obtaining the estimates suggest that the sensitivity computations will be of practical value.

*This thesis is dedicated to the caring educators
of my youth.*

Acknowledgments

I cherish the friendships that accompanied my studies here at the University of Wisconsin. I thank my wife, my children, my parents, and my sister for their enduring love and support.

I appreciate the guidance, dedication, and exemplary academic standards of my advisor, Professor Ian Dobson. I am also indebted to Professor Fernando Alvarado for his counsel, insight, and encouragement. I thank Professor Chris DeMarco for numerous enlightening discussions and his willingness to entertain my aberrant questions. I have enjoyed the instruction and advisement of Professor Bill Long since before starting graduate school, and I am thankful for his participation on my thesis committee. I am grateful to Joel Robbin, Professor of Mathematics, for many hours of tutoring and for giving me an entirely different perspective on engineering.

Professor Claudio Cañizares of the University of Waterloo developed software that started this research and I thank him for his support and friendship.

I thank Dr. Arthur Ekwue and the National Grid Company plc of the United Kingdom for their interest in our work and for providing the test data and motivation for the research presented in Chapter 7.

I thank the Grainger Foundation for their generosity and support of the power engineering program at the University of Wisconsin.

Funding in part from National Science Foundation PYI grant ECS-9157192 and from the Electric Power Research Institute under contracts RP8010-30, RP8050-03, WO8050-03 is gratefully acknowledged. Funding in part from the Empire State Electric Energy Research Corporation and New York State Electric and Gas under ES-EERCO project EP 95-11 is gratefully acknowledged. The support of the Power System Engineering Research Center (PSerc) is gratefully acknowledged.

Contents

Abstract	i
Acknowledgments	iii
1 Introduction	1
1.1 Motivation	1
1.2 Margins and sensitivity	2
1.3 Literature review	3
1.4 Summary	4
2 Assumptions	7
2.1 Power system operation	7
2.2 Assumptions	10
3 Margin Computations	17
3.1 Previous work	17
3.2 Anatomy of margin computations	18
3.2.1 Description of margin computation program	25
3.3 Summary	27
4 Sensitivity Computations	29
4.1 Methods of sensitivity analysis	29
4.2 Sensitivity formulas	35
4.2.1 Derivation	35
4.2.2 Normal vector to the event boundary in parameter space	38
4.2.3 General derivation	39
4.2.4 Fold bifurcation	44
4.2.5 Hopf bifurcation and eigenvalue sensitivity	45
4.3 Traditional sensitivity	47
4.4 Penalty factors, β coefficients, and normal vectors	53
4.5 Example: line overload	55
5 Voltage Collapse	59
5.1 Introduction	59
5.2 Theoretical background and assumptions	62

5.3	Informal derivation	63
5.4	Application to test system	64
5.4.1	Emergency load shedding	65
5.4.2	Direction of load increase	67
5.4.3	Reactive power support	67
5.4.4	Area interchange	67
5.4.5	Load model	71
5.4.6	Line susceptance	71
5.4.7	Generator dispatch	71
5.5	Discussion	74
5.6	Conclusions	76
5.7	Appendices	77
5.7.A	Derivation of sensitivity formulas	77
5.7.B	Construction of Ψ	78
5.7.C	Locally closest fold bifurcation.	79
6	Contingency Analysis for Voltage Collapse	81
6.1	Introduction	81
6.2	Previous work	83
6.3	Results	85
6.3.1	1390 bus system	85
6.3.2	All single contingencies of the 118 bus system	86
6.3.3	Multiple contingencies of 118 bus system	88
6.4	Discussion	90
6.5	Computations	91
6.5.1	Linear estimate formula	92
6.5.2	Quadratic estimate formula	93
6.5.3	Computational efficiency	94
6.6	Conclusion	95
7	Margin Sensitivity Applications	97
7.1	Introduction	98
7.2	Nominal voltage collapse margin	98
7.3	Loading margin sensitivity	103
7.4	Contingency ranking for voltage collapse	108
7.5	Voltage collapse due to VAR limits	114
7.6	Ranking for voltage collapse due to VAR limits	117
7.7	Large deviation contingency analysis	123
7.8	Conclusions	125

8	Sensitivity of Transfer Capability Margins	129
8.1	Introduction	129
8.2	Overview of transfer capability determination	130
8.3	Sensitivity	134
8.3.1	Assumptions	134
8.3.2	Sensitivity formulas	135
8.4	Example	136
8.4.1	40 bus system	137
8.4.2	1500 bus system	142
8.4.3	Sensitivity of the transfer capability to transactions	144
8.4.4	Computational efficiency	147
8.5	Discussion	148
8.6	Conclusions and Future Work	148
9	Interarea Oscillations	149
9.1	Introduction	149
9.2	Assumptions and model	150
9.3	Motivation	154
9.4	Computations	155
9.5	Results	158
9.6	Discussion and conclusions	168
9.7	Appendix	170
10	Conclusions and Future Research	175
10.1	Conclusions	175
10.2	Future work	177
	Bibliography	181

List of Figures

1	Phase portraits and equilibrium trajectory as parameter changes and state remains within each basin of attraction	12
2	Phase portraits and equilibrium trajectory as parameter changes and state does not remain within each basin of attraction	13
3	Equilibria trajectories for different values of the parameter p	30
4	Nominal trajectory and boundary as function of the parameter p	32
5	Nominal trajectory and estimated boundary	34
6	Nose curves as parameter p varies	61
7	Loading margin as parameter p varies	61
8	Effect of load shedding on voltage collapse margin	66
9	Effect of assumed loading direction on voltage collapse margin	68
10	Effect of shunt capacitance on voltage collapse margin	69
11	Effect of import into critical area on voltage collapse margin	70
12	Effect of composition of load model on voltage collapse margin	72
13	Effect of susceptance on voltage collapse margin	73
14	Effect of generator dispatch on voltage collapse margin	75
15	Nominal and contingency nose curves	82
16	Effect of load increase at Indian Queens on the loading margin to voltage collapse	109
17	Effect of load decrease at Indian Queens on the loading margin to voltage collapse	110
18	Effect of load decrease at Indian Queens on the loading margin to voltage collapse and critical VAR limit	111
19	Effect of variation in VAR limits at Exeter on the loading margin to voltage collapse	112
20	Critical bus voltage versus transfer to Area 3	137
21	Effect of simultaneous transfer on transfer capability limited by low voltage	138
22	Effect of simultaneous transfer on transfer capability limited by voltage collapse	139
23	Effect of generator dispatch on transfer capability limited by low voltage	140

24	Effect of load variation at a critical bus on transfer capability limited by low voltage	141
25	Effect of reactive power support on transfer capability limited by low voltage	142
26	Effect of simultaneous transfer on margin to first flow limit	145
27	Effect of simultaneous transfer on margin to voltage limit	146
28	One line diagram of 3 bus test system	158
29	Effect of generation dispatch on Hopf margin	159
30	Effect of generation dispatch on Hopf margin, extended variation . . .	160
31	Trajectory of critical eigenvalues as generator dispatch is varied for generator terminal voltage of 1.00 p.u.	161
32	Trajectory of critical eigenvalues as generator dispatch is varied for generator terminal voltage of 1.05 p.u.	162
33	Trajectory of critical eigenvalues as generator dispatch is varied for generator terminal voltage of 1.10 p.u.	163
34	One line diagram of 9 bus test system	164
35	Least damped eigenvalues at base case of 9 bus system.	165
36	Movement of least damped eigenvalues as transfer to Area 3 increases.	166
37	Movement of critical eigenvalue as transfer to Area 3 increases.	166
38	Damping of critical mode versus linear estimate as function of transfer to Area 3 in 9 bus system.	167
39	Linear estimate and actual margin to oscillations as function of export to Area 2 in 9 bus system.	167
40	Effect of interarea exchange on damping of 37 bus system	169

List of Tables

1	Estimated loading margins for all 500kV line outages in a critical area of the 1390 bus system.	87
2	Estimated loading margins for the 25 worst outages of the 118 bus system.	89
3	Transformer data	99
4	Branch data	100
5	Nominal stable operating point	101
6	Reactive power limits	102
7	Direction of load increase	102
8	Nominal point of collapse	104
9	Left eigenvector corresponding to the zero eigenvalue of the system Jacobian at the nominal point of collapse	105
10	Estimated and actual changes in the loading margin to fold bifurcation resulting from severe non-radial line outages	114
11	Estimated and actual changes in the loading margin to fold bifurcation resulting from radial line outages	115
12	Estimated and actual changes in the loading margin to fold bifurcation resulting from less severe non-radial line outages	116
13	Estimated and actual changes in the loading margin to voltage collapse resulting from severe non-radial line outages	117
14	Estimated and actual changes in the loading margin to voltage collapse resulting from radial line outages	118
15	Estimated and actual changes in the loading margin to voltage collapse resulting from less severe non-radial line outages	119
16	The loading margins to fold bifurcation and voltage collapse for all line outages causing an immediate instability prior to fold bifurcation . .	120
17	Comparison of the normal vectors to the parameter set corresponding to fold bifurcation (W) and immediate instability (N)	122
18	Comparison of linear estimated changes in the loading margin to voltage collapse resulting from severe non-radial line outages	123
19	Comparison of linear estimated changes in the loading margin to voltage collapse resulting from less severe non-radial line outages	124

20	Comparison of linear, quadratic, and large deviation estimates for changes in the loading margin to voltage collapse resulting from severe non-radial line outages	126
21	Comparison of linear, quadratic, and large deviation estimates for changes in the loading margin to voltage collapse resulting from less severe non-radial line outages	127
22	Area exports at base case, nominal transfer limit, and contingency transfer limit	143
23	Sensitivities of the transfer margin with respect to area exports . . .	144

Chapter 1

Introduction

This thesis concerns the stability and security of large electric power systems with an emphasis on static or longer term stability. One contribution of this thesis is the establishment of a coherent, consistent, and general framework for margin and sensitivity analysis applicable to a variety of security criteria. This thesis shows how to efficiently compute the security margins defined by limiting events and instabilities, and the sensitivity of those margins with respect to any model parameter. This chapter introduces the important concepts and includes an explanation of the most relevant previous work and a brief summary of the thesis. Chapter 2 states assumptions defining admissible power system models. Chapters 3 and 4 detail computational methods for computing margins and their sensitivities. Chapters 5, 6, and 7 describe applications regarding voltage collapse. Chapter 8 describes applications regarding transfer capability. Chapter 9 describes applications regarding oscillatory instabilities. Chapter 10 contains a summary of the thesis and outlines possible avenues for future work.

1.1 Motivation

Power systems are affected by events that depend upon the state (voltages and currents) of the power system. The state of the power system is influenced by both controllable and uncontrollable factors.

For instance, as loads increase, the system generation must increase to keep power balance and maintain reserve and security margins. Often, at high load levels, generators reach real and reactive power limitations and the flows on lines exceed limits. Any of these events can initiate a change in the operation of the power system. The change in operation is reflected by a change in the equations that model the power system, or the nature of the solutions that the equations yield. Fundamental questions of system security, and the questions addressed by this thesis, are:

“How close is the system to the next event?”

“Will the system remain stable after the next event?”

“How can the margin to the next event be increased?”

1.2 Margins and sensitivity

Some parameters can be set or controlled and others, like loads, are mostly uncontrolled. The uncontrolled parameters can vary with time and affect the behavior of the power system. The difference between the parameter values corresponding to an event and the current or nominal parameters defines the margin to the event. For instance, when an increase in loading causes the flow on a line to exceed its rating, the distance to the line overload can be measured by a suitable norm of the vector difference in loads, a loading margin. Depending on the application, security margins can be measured in parameter space with respect to load levels, load model parameters, import levels, temperature, or time. When the security margin measures the distance to an event that causes the system to become unstable, it is called a stability margin.

In some instances, it may be practical to measure the security margin with a state variable or a function of state. For example, the amount of additional real power flow on a line that would cause overload is an easily understood measure of closeness to overload of that line. Examples of margins measured in state space are increments in line flows, generator VAR outputs, and voltage levels.

The system equilibrium, and thus margins to events, is affected by both controllable and uncontrollable parameters. The sensitivity of margins with respect to uncontrollable parameters quantifies the effects of different assumptions, forecasts, and measured data. System operation also requires knowledge of how the controllable parameters can be adjusted to keep the system secure as the uncontrollable parameters change. One way of quantifying the effectiveness of controls is by computing the sensitivity of the security margin with respect to the control parameter.

Consider the case of a line approaching overload. By computing the sensitivity of the line flow with respect to different loading patterns, one can estimate the worst case loading pattern — the one that increases the line flow most rapidly. The loading margin for this load pattern can then be computed by solving for a continuation of equilibria as the loading level is gradually increased.¹

Once the loading level at which the line reaches overload is located and hence the loading margin found, the sensitivity of the loading margin with respect to any parameters can be calculated. For example, computing the sensitivity of the margin with respect to the area export set points can be used to assess the possibility of avoiding the overload by changing the export schedules.

¹The continuation neglects the transients and dynamics of the power system. However, the locus of equilibria approximates the trajectory of the system state for sufficiently stable dynamics and slowly varying load level.

This thesis describes how to compute margins to several events, compute the sensitivity of the margins with respect to any parameters, and investigates applications for the margin and sensitivity computations.

1.3 Literature review

This section contains a brief review of literature helpful for understanding the material presented in this thesis. The references in this section are relevant to the thesis as a whole and to the material presented in Chapters 2,3, and 4 in particular.

Several textbooks outside the field of power engineering were particularly useful for this thesis. The derivations and computational methods presented in Chapters 3 and 4 require an understanding of multivariable calculus. The first two chapters of [Spivak] and the first chapter of [GP] are recommended. [GV] is an excellent reference for matrix computations and [HJ] for matrix theory. [BN] is an accessible and clear reference for differential equations. [GH] is a popular reference for bifurcations but is not as accessible to the engineer as [Seydel]. [Seydel] is a valuable reference concerning computations and bifurcations and is most frequently cited in power systems papers concerning voltage collapse computations. [GZ] presents an exceptional explanation of the path following, or continuation methods, that form the backbone of the methods in this report.

The fundamentals of modeling electric power systems are covered in [Bergen], [WW], [Kundur], and [SauPai]. [Bergen] is the most understandable. [Kundur] is the most comprehensive and contains a good analysis of generator reactive power limits. [WW] best describes utility interconnections and economics. [SauPai] has the clearest explanation of small signal stability, the effects of load models, and Hopf bifurcations. [Heydt] is the most complete text describing power system computations but is becoming outdated.

Supplemental to these texts, two survey papers provide good explanation of static [Sto74] and dynamic [Sto79] power system models and computations. [PPTT], [SM79], and [DT68] are landmark papers concerning sensitivity, optimization, and computation in power systems.

Van Cutsem [VC91, VC95, VC293, VC96] has forwarded an approach to steady state stability analysis influential to this thesis. Specifically, Van Cutsem embraces the use of loading margins that are path dependent and account for discrete events, utilizes sensitivities and promotes the use of path following methods as static simulation tools. Van Cutsem also provided the useful interpretation of margin sensitivities in terms of the Lagrange multipliers of an optimization problem. The new text [VCK] contains the aggregate of Van Cutsem's work and a complete description of voltage

stability theory and application.

[WF93] and the discussion by Wu, Fischl, and Nwankpa in [GDA97] has also influenced this thesis, suggesting the use of continuation and sensitivity methods to assess interarea transfer margins, proposing the use of first and second order Taylor series estimates for contingency analysis [GDA98], and presenting the transfer margin computation as an optimization problem.

Chapters 5, 6, and 7 concern voltage collapse in electric power systems. [DCL, Davos, IEEE1] cover the full breadth of case studies, research and opinions on voltage collapse. [GDA97] is a concise version of Chapter 5 and computes Taylor series estimates of the bifurcation set for a practical power system model accounting for generator reactive power limits. Chapter 9 concerns oscillatory instability in power systems. [IEEE1] contains a broad range of ideas and experiences concerning interarea oscillations in power systems.

The research contained in this thesis builds upon earlier work conducted at the University of Wisconsin. [AJ89] presents a direct method to locate a saddle node bifurcation point of a power system model and [CA93] compares a continuation method with a direct method. A more tutorial and detailed presentation is found in [CañPhD] and [CA91] incorporating models for HVDC systems. Several papers [Dob93, DL93, ADH94] concern locating the closest saddle node bifurcation to an operating point or optimizing the distance in parameter space to a bifurcation point [DL192, Cañ98]. [DL192] first demonstrates computation of the voltage collapse loading margin sensitivity from the components of the normal vector to the bifurcation set in parameter space. Derivation of the normal vector to the saddle-node bifurcation set in parameter space is presented in [Dob92]. Analysis of the immediate instability precipitated by a generator reactive power limit is contained in [DL292]. [DAD92] concerns the sensitivity of Hopf bifurcations in power systems.

1.4 Summary

This thesis demonstrates that the sensitivity of the security margin to an event can be computed with respect to any system parameter, and that the sensitivities are practical and useful for control, computation, and contingency analysis.

This thesis considers security margins to events defined by voltage collapse and fold bifurcations, oscillatory instability and Hopf bifurcations, immediate instability due to generator reactive power limits, voltage limits and line flow limits. The usefulness of computing the sensitivities of these margins with respect to interarea transfers, load change and load model parameters, generator dispatch, transmission line parameters and line compensation, and VAR support is established for systems as large as 1500

buses.

Chapter 2 motivates and states the basic steady state modeling assumptions used in this thesis. Chapter 3 presents a thorough explanation of path following methods for power system security margin computations and improves and extends earlier work specific to voltage collapse. Established continuation methods for computing security margins can be improved to directly locate intermediate events of practical interest. The intermediate events are often points at which the equations that model the system change. Correct computation of security margins requires that these intermediate events be accounted for.

Chapter 4 describes how the sensitivity of security margins with respect to system parameters can be computed and used to estimate an operational boundary in parameter space. Sensitivity based estimates can be used to quickly assess the quantitative effectiveness of various control actions to maintain a sufficient security margin. The estimates are also useful in determining the importance of uncertainties in data or model assumptions. The evaluation of the estimates for large power system models is very efficient. Chapter 4 contains a rigorous and general derivation. It is also shown that the general sensitivity formulas can, in special cases, be reduced to yield established sensitivity formulas such as line distribution factors, outage distribution factors, participation factors and penalty factors.

Chapter 5 demonstrates the practical use of the sensitivity computations for a range of system parameters on a voltage collapse of the IEEE 118 bus system. The closeness of the estimates over a useful range of parameter variations and the ease of obtaining the linear estimate suggest that the sensitivity computations will be of practical value in avoiding voltage collapse. Chapter 5 contains a rigorous derivation of the linear and quadratic sensitivity of the loading margin to voltage collapse with respect to arbitrary parameters and includes material published in [GDA97] and noted in [VCK].

Chapter 6 extends the work of Chapter 5 to contingency analysis. Chapter 6 shows that effective contingency ranking for voltage collapse can be obtained by computing the loading margin sensitivities with respect to each line outage. This approach can take into account some of the effects of reactive power limits and easily handles multiple contingencies. The results show that the linear estimates are extremely fast and provide acceptable contingency ranking. Chapter 6 includes material published in [GDA98].

Chapter 7 tests the methods of Chapters 5 and 6 on a 40 bus model of the National Grid Company of the United Kingdom and introduces several new applications. It is shown that the methods applied to voltage collapse precipitated by fold bifurcation can be successfully adapted to voltage collapse precipitated by a generator VAR

limit. In addition, computation of the sensitivity of the loading margin to voltage collapse with respect to changes in generator VAR limits is demonstrated. Finally, the contingency computations of Chapter 6 that model a line outage as a change in the sparse bus admittance matrix are recomputed instead using changes in the dense bus impedance matrix (analogous to large deviation outage distribution factors). The results suggest that this approach is of questionable benefit.

Chapter 8 demonstrates how margin and sensitivity computations can be used to determine transfer capability margins. The methods are tested on a 1500 bus power system model. The sensitivity of the transfer margin with respect to area exports is used to obtain estimates of the effect of simultaneous transfers on transfers limited by both line flow limits and voltage limits. The results indicate that the methods should be useful in determining available transfer capabilities.

Chapter 9 describes applications concerning oscillatory instability margins and eigenvalue sensitivity. Chapter 9 demonstrates the computation of the transfer margins to oscillatory instability and the sensitivity of these margins with respect to import set points. If the difficulties attributable to very large system models can be addressed, the computation would be of practical value in assessing interarea transfer policies in a deregulated environment.

The conclusions of this thesis are discussed in Chapter 10 together with suggestions for future work.

Chapter 2

Assumptions

This chapter contains the basic assumptions that provide the foundation for the methods presented in this report. The mathematical model of a power system presented in this chapter is general and provides the basis for the computational methods presented in later chapters for computing security margins and sensitivities of margins.

A useful model accurately recreates some phenomena of the actual system and specifies which phenomena are ignored and the conditions for which the model is valid. The simplifying assumptions used to derive a model determine the phenomena that will be accurately portrayed and those that will be missed.

It is poor engineering practice to assume that an actual system will behave ideally. However, it is worse practice to operate an actual system in conditions in which even an ideal system could not properly function. The purpose of steady state stability analysis in power systems is to identify the operational limits of an ideal system. One objective of this chapter is to show how to locate the points at which the power system could not effectively operate subject even to small disturbances. Experience and judgment can be employed to determine a sufficient safety margin for the actual system. In the next section we describe the characteristics of the power system to be included in our model, and distinguish those that will be neglected.

2.1 Power system operation

The methods and assumptions of this thesis are motivated here by a brief description of power system operation. Power systems interconnect millions of electrical and mechanical devices. The variety of phenomena exhibited by an actual power system is immense. The following description includes only the relevant characteristics of which only a subset will be retained by our model.

One can view the power system as an enormous nonlinear electric circuit¹. The

¹Modeling a power system as an electric circuit may seem obvious to electrical engineers. However, models of power systems that greatly simplify or ignore the underlying circuit are common and useful for economic analysis. For modeling gross behavior like emissions or expenditures on a daily or monthly time scale, circuit descriptions of the system are not useful.

model should retain the fundamental characteristics of electric circuits and the dependence of state variables (voltages and currents) on circuit parameters.

Many power system phenomena are initiated by the aggregate effect of changing loads. The model should have the ability to partially account for the response of interconnected generators to fluctuating demands. As loads increase the rotational speed and hence frequency of individual generators decreases. A control system using frequency as a feedback increases the mechanical input to the generators which in turn results in increased electrical output and restoration of frequency. Another control system implements a dispatch among generators so that increased output is provided by those generators at which it is most economical to do so and so that interchange agreements for the transfer of power between areas and utilities are maintained.

With a cumulative increase in demand, system voltages can decline, initiating several activities. On load tap changing transformers adjust tap positions to maintain load side voltages. Shunt capacitors are switched in to provide reactive power support. Fast starting back-up generation may be brought on-line. The characteristic of changing system equipment and structure as a function of system state is a feature we wish to incorporate in our model.

While the demand and then generation increase, so do the flows and losses on the transmission lines, as well as the flows and losses in the circuits and devices that make up each generating unit.

When the flows on transmission lines increase, the temperature of the conductors increases resulting in a loss of mechanical strength and increased sag. The increased sag can cause a line to become dangerously close to ground increasing the possibility of flash over and faults. A faulted line can lead to momentary or prolonged outage of the line. Extended operation of a line beyond its thermal rating can permanently reduce the strength of the line. Once lines become overloaded, generation is redispatched to relieve the overloads, and in some cases the lines are interrupted to prevent permanent damage.

Generators can be damaged by overheating and over or under voltage conditions. Protective devices range from controls that remove the generator from the network (severe over or under voltage), to those that limit the output of the generator by controlling its operation. The latter include mechanical limits on the prime mover to fix the maximum power output, and control devices that limit the voltage or current in control circuits or generator windings to prevent overheating, shorting, and unit failure.

The model should account for the operation of protective devices and changes in system operation policy resulting from the condition of the system.

Every change in load or generation, switching of a device, or tap change at a

transformer is a disturbance to the power system. Disturbances may also be caused by random events like lightning strikes and short circuits. If the system is stable, the controls and dynamics will behave in such a way as to move the system state toward a new equilibrium after the disturbance. As the system becomes less stable, the rate at which the system approaches equilibrium after every disturbance decreases. The duration of time for which the transient effects of a disturbance dominate increases as the stability of the system decreases. Significantly large disturbances can cause the system state to diverge from the equilibrium or for the equilibrium to disappear.

When conditions are severe, several generators may reach operational limits and lines may trip due to shorts caused by steady overload, in turn further compromising the system security. The security of a system thus depends upon the accumulated effects of slow events (gradual demand increase and generation response) and discrete events (protective device operation), as well as the immediate effects of transients.

When the system is unstable or marginally stable, a small disturbance may propagate and grow, eventually causing cascading operation of protective devices. Even when the system is stable, large random disturbances such as lightning can propagate and trip protective devices. These phenomena, although of importance to power system operation, are not exhibited by our model.

We wish to include in our model as many of the operational parameters and characteristics that can reasonably be controlled or forecast, and neglect those that are beyond control or prediction. For instance, we account for the steady state evolution of a power system due to protective device and system operation including generator limits, but we ignore the transient effects caused by operation of the protective devices. We account for the long term effects of generator dispatch and interarea agreements but ignore the short time frame effects initiated by the systems that implement those policies.

We do not account for transient behavior, protective device coordination, or instantaneous limits. Hence we do not model power systems during periods when we know that transient effects are dominant. For example, we do not model the large disturbance response of a stable power system, or the dynamic evolution of an unstable power system. For this reason, the type of analysis emphasized in this thesis is classified as “steady-state” or “static” as opposed to “transient” or “dynamic”.

The purpose of the next section is to specify the assumptions for a model of a stable power system so that an unstable system can be detected from the model as a condition at which the assumptions are violated or become contradictory.

2.2 Assumptions

In this section we state the primary assumptions underlying the methods presented in this report for computing security margins and their sensitivities with respect to parameters. Our primary assumptions are qualitative and not dependent upon specific equations for the power system. However, secondary assumptions concerning the quantitative behavior of the power system are necessary for computation and simulation for any particular application. In this section we state primary assumptions essential to motivate the following chapters. In later sections that detail specific applications, the assumptions necessary for that application will be stated.

We assume that the dynamic behavior of the power system can be represented by parameterized differential equations,

$$\dot{z} = f(z, \lambda, u) \quad (1)$$

and difference equations

$$u^{k+1} = h(z, \lambda, u^k) \quad (2)$$

where

$z \in \mathbb{R}^n$ is the vector of state variables.

$\lambda \in \mathbb{R}^m$ is a vector of parameters.

u is a vector of discrete states.

f is continuously differentiable with respect to z, λ and p for every u .

The differential equations (1) account for the circuit behavior and evolution of state resulting from fluctuating demands. The difference equations (2) account for the evolution of state due to operation of protective devices, tap changes and other discrete events.

The distinction between variables and parameters is crucial. Parameters are active; they are directly set or assumed. Variables are passive; they assume the values imposed by solution of the equations. Perhaps the most important aspect of modeling is determining or assuming what is a parameter and what is a variable. The choice of variables and parameters can vary for each application.

Our primary assumptions are:

1. At every moment the power system has a state corresponding to a particular exponentially stable equilibrium solution of equation (1). This state is referred to as the *equilibrium state*.

2. The operation of state dependent devices can be considered to be dependent upon the equilibrium state.
3. The system state remains in the basin of attraction of the equilibrium solution of equation (1).

Fundamental to these assumptions is the distinction between the equilibrium state and the system state. The system state consists of the instantaneous values of the state variables. The equilibrium state however, is a theoretical point in state space that represents the fixed point of the differential equations that model the system at that moment. The equilibrium (z_0, λ_0, u_0) satisfies

$$0 = f(z_0, \lambda_0, u_0) \quad (3)$$

We do not require that the power system state be at equilibrium, only that the equations that model the system have an equilibrium.

One characteristic of power systems is that they include devices that reach particular states at which the equations that model the system change. This characteristic is independent of many of the other assumptions used to model the power system. For instance, the removal of a transmission line will require a change in the equations regardless of the assumptions concerning loads, or balanced three phase operation or sinusoidal currents. Assumption (2) means that the operation of a circuit breaker or relay is considered dependent upon the power system equilibrium, not the immediate system state. This assumption frees analysis from complicated time domain simulation.

Specifically, assumption (2) means that equation (2) has the characteristic that k is incremented only when the equilibrium solution of (1) violates a limit. In short, the equations that model the system change when the equilibrium solution of the system would violate a limit, not when the actual state violates a limit. The word “event” is used in this thesis to refer to a point at which the assumptions are violated or the difference equations (2) force a change in the differential equations (1).

The assumptions imply that the dynamic behavior of the power system is qualitatively the same as that of a linearized system at the equilibrium solution of equation (1). The stability of the power system with equilibrium state (z_0, λ_0) can thus be determined by the stability of the linear differential equation

$$\dot{z} = A\Delta z \quad (4)$$

where $A = f_z|_{(z_0, \lambda_0)}$. Since the power system equilibrium is assumed exponentially stable, all the eigenvalues of A have negative real parts.

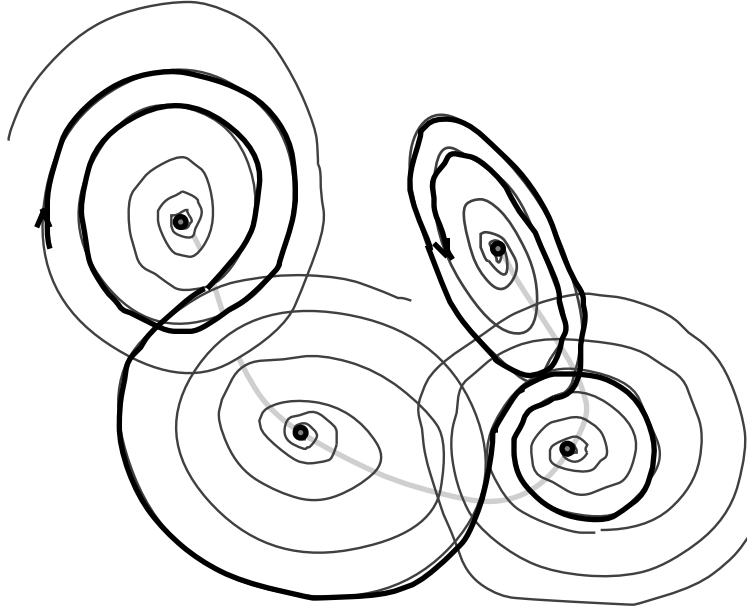


Figure 1: Phase portraits and equilibrium trajectory as parameter changes and state remains within each basin of attraction

One aspect of these assumptions is that transients and the events initiated by transients are ignored. A transient instability would result, for example, if a parameter change moved the system equilibrium so that the system state did not remain in the basin of attraction of the new stable equilibrium. However, since a system close to a steady state instability is usually more vulnerable to transient instability than a system farther from steady state instability, the distance to a steady state instability is an important indicator of relative system security.

Figures 1 and 2 present one way of visualizing these assumptions. The darkest curves represent the trajectory of the system state and the dots represent the equilibrium states corresponding to different parameter values. The evolution of the equilibrium state is shown by the broken curve joining the dots. A portion of a stable phase portrait is drawn about each equilibrium point. Each parameter change or event that moves the equilibrium of the differential equations (1) or causes the differential equations (1) to change as a result of the difference equations (2) incrementing u , alters the phase portrait and the trajectory of the system state. As the system parameters change smoothly or discontinuously, the system equilibrium state and phase portrait also change, but the system state changes continuously. The system state

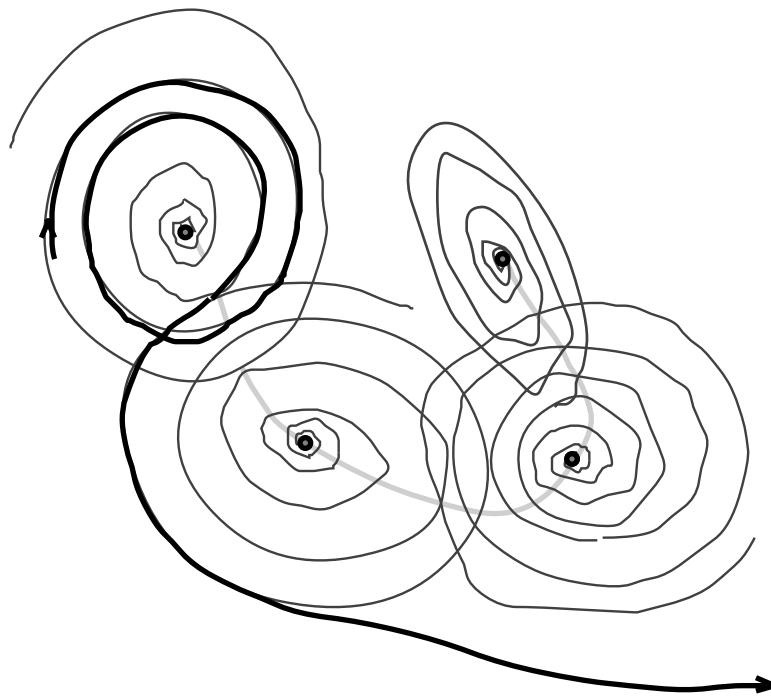


Figure 2: Phase portraits and equilibrium trajectory as parameter changes and state does not remain within each basin of attraction

in both figures initially spirals inward towards the top left equilibrium state. As the parameters of the system change the equilibrium state of the power system moves and the trajectory of the system state is altered. The trajectory of the system state is the transient response of the system to the parameter disturbances. In Figure 1, the system state remains in the basin of attraction of each equilibrium and traces a portion of the phase portrait corresponding to each equilibrium. The behavior illustrated in Figure 2 does not satisfy the assumptions since the system state does not remain in the basin of attraction of each equilibrium.

The main assumption required by the methods of this thesis is that the qualitative behavior of the system state can be determined by analysis of the equilibrium state.² The complicated trajectory of the system state is not modeled. The analysis of stability based on the equilibrium state is classified as static stability or steady-state stability analysis to distinguish it from transient or dynamic stability analysis. This classification has sometimes led to confusion since some researchers assume that if a dynamic phenomena is observed, a transient model must be required for analysis. However, the consequence of a static instability is dynamic. The distinction between static and dynamic analysis does not concern the consequences of the instability or phenomena observed but rather the nature of the assumptions employed for analysis.

By locating the parameters λ at which the assumptions break down, we identify not only the limits of the model but also a boundary at which reliable operation of the actual power system is unlikely. The model breaks down by only four generic mechanisms:

1. The stable equilibrium solution disappears as parameters change.
2. The stable equilibrium solution disappears as the difference equations change the differential equations.
3. The stable equilibrium solution becomes unstable as parameters change.
4. The stable equilibrium solution becomes unstable as the difference equations change the differential equations.

²These assumptions differ slightly from the often cited quasi-static steady state assumption [VC94, LöffPhD, DC89]. One common description of the quasi-static steady state assumption is that the parameter vector changes slowly compared to the dynamics of the system, so that the system state approximately traces a locus of stable equilibria. The quasi-static steady state assumptions satisfy our assumptions but are stronger. We also allow parameters to occupy discrete states and hence they change discretely, not necessarily slowly. However, we assume that the state remains in the basin of attraction of the new stable equilibrium. The term “quasi-static steady state” is also sometimes cited as justification for the standard load flow equations which assume that the power system voltages and currents are sinusoidal of constant frequency.

Mechanisms (1) and (2), characterized by the disappearance of the *equilibrium solution*, require only static equations for sensitivity and margin computations. In other words, any equilibrium equations with the same zero set as the correct differential equations will suffice.

Suppose that the power system is operating stably near an equilibrium (z_0, λ_0, u_0) . The parameters λ are forecast to change and occupy discrete values on a curve in parameter space $\Lambda(t)$. One objective is to compute the λ_* on Λ at which the system equilibrium (z_*, λ_*, u_*) first violates the assumptions. For instance, if the Jacobian matrix $f_z|_{(z_*, \lambda_*, u_*)}$ becomes singular the equilibrium solution is no longer exponentially stable violating assumption (1) and further change along $\Lambda(t)$ generally will lead to the disappearance of the equilibrium solution. Another possibility is that at (z_*, λ_*, u_*) equation (2) forces a change in u to u_{**} so that $f(z, \lambda_*, u_{**})$ has no equilibrium solution. The assumptions are also violated if the parameters change so that $f_z|_{(z_*, \lambda_*, u_*)}$ has a complex pair of eigenvalues in the left half plane.

Security and stability margins can be path dependent due to the discrete state variables and difference equations. For example, assume that from current parameters λ_0 , there are two different scenarios for progression to the eventual parameter values λ_2 . One forecast is λ_0 to λ_1 to λ_2 the other is λ_0 to λ_1' to λ_2 . Assume that the system encounters an irreversible limit as λ changes to λ_1 that does not occur as λ changes to λ_1' . The first forecast leads to a final equilibrium (z_2, λ_2, u_2) while the second to (z_2', λ_2, u_2') where $z_2 \neq z_2'$ and $u_2 \neq u_2'$. The equations that model the system at the two points can be different, $f(z, \lambda, u_2) \neq f(z, \lambda, u_2')$. This characteristic poses an obstacle for any computational methods aimed at determining security margins.

Modeling the system after the equilibrium has disappeared or is no longer stable is not an objective of this work. The emphasis of this thesis is preventative action.

Chapter 3

Margin Computations

This chapter contains a comprehensive explanation of methods to compute margins in electric power systems. Path following methods have found widespread use in power systems analysis; this chapter represents a synthesis of several different perspectives and suggests improvements and extensions to previous implementations. The presentation of the material in this chapter is original and is intended to give insight into the relation between the computational methods and the power system model.

3.1 Previous work

The practical use of path-following or continuation methods for tracing equilibrium solutions for power systems analysis most likely predates the first publication of such a method in the power systems literature. Continuation methods for locating the point of voltage collapse of power systems have been presented in [Iba, AC92, CA93, CFSB] and utilized in [GDA97, GDA98, RHSC, VC91]. [Seydel] includes a direct method for locating a saddle node bifurcation. Similar methods for computing the margin to voltage collapse are demonstrated in [AJ89, DL192].

The use of steady state continuation programs is now well established and explanation of the “continuation power flow” method appears in the recent power systems text [Kundur]. Continuation methods can be implemented with any set of power system equilibrium equations although common descriptions of the programs often assume the standard power flow equations. [VC94, VC96] use a continuation program with elaborate equilibrium equations. [DV93] and [LAH95] present other examples of more detailed equilibrium equations that could also be used in continuation methods. (See the discussion by Cañizares in [LAH95].)

The main ingredients of the material in this chapter are fundamental and well explained in the texts [Seydel] and [GZ].

3.2 Anatomy of margin computations

This section describes methods for computing security margins given a model that satisfies the assumptions stated in Chapter 2. The problem of computing a security margin to an event involves finding an equilibrium that satisfies a specific condition. For example, the condition can be that the equilibrium have a particular variable at a threshold value, or that the system Jacobian matrix be singular at that equilibrium.

The fundamental problem en route to establishing a security margin is the solution for a new equilibrium resulting from a specific change in the parameters. Typically, a forecast of the parameter values at a future time is available without an exact description of how the parameters progressed to those values. Ideally, the solution obtained is an equilibrium corresponding to the forecast parameter values that is connected by a curve of equilibria to the known solution for some reasonable pattern of parameter variation connecting the current and forecast parameter values. The solution must satisfy the equilibrium equations, not violate any limits, and lie on a curve that satisfies the equilibrium and limit conditions for some curve connecting the current and future parameter values. Unfortunately, even given two equilibrium points that satisfy the same limit constraints, it is not possible to verify that they are indeed solutions that satisfy these conditions without very specific restrictions on the equilibrium equations. See [GZ] for illustrations of what can go wrong. The situation is complicated even more by the inclusion of limits that can change the form of the equilibrium equations. We instead first address the solution to a simpler problem that ignores any limits.

Problem 1 (Simple)

$$\begin{array}{ll} \text{Given :} & \text{Find : } z_1 \text{ such that} \\ \left(\begin{array}{c} (z_0, \lambda_0) \\ F(z_0, \lambda_0) = 0 \\ \lambda_1 \end{array} \right) & \left(F(z_1, \lambda_1) = 0 \right) \end{array}$$

An effective and time-tested method for solving Problem (1) is Newton's method.

Method 1 (Newton) ¹

BEGIN: $z^1 \rightarrow z_0$

¹Notation: Several concepts in this chapter are illustrated with pseudo-code. Superscripts refer to iterations, so that z^k is the value stored for z after k iterations. Subscripts refer to either initial or final values corresponding to the problem statements. The \rightarrow should be read as "gets the value" so that $a \rightarrow b$ means a gets the value b . The expression $x \rightarrow Ax = b$ means that x gets the value that solves $Ax = b$.

WHILE: ($|F(z^k, \lambda_1)| > \text{TOLERANCE}$) AND ($\text{ITERATIONS} < \text{MAX}$)
 DO:

$$\Delta z \rightarrow F_z|_{(z^k, \lambda_1)} \Delta z = -F(z^k, \lambda_1)$$

$$z^{k+1} \rightarrow z^k + \Delta z$$

 IF ($|F(z^k, \lambda_1)| < \text{TOLERANCE}$) THEN $z_1 \rightarrow z^k$, ELSE WARNING

Many variants exist. For example, the elements of F_z can be updated only every few iterations (Very Dishonest Newton). In some cases F_z is approximated. There are many ways to solve the linear system in the iterative step [GV], some invented specifically for power systems applications [Sto74], like the popular fast decoupled load flow.

In general there is no guarantee that a solution exists or that the initial guess will be sufficiently close to it to get convergence within a reasonable number of iterations. The method may fail for several possible reasons:

1. A solution exists but the initial guess z_0 was not close enough to the solution for the method to converge, or converge fast enough.
2. There is no solution of $F(z, \lambda_1) = 0$ (previous fold bifurcation for $\lambda < \lambda_1$).
3. A solution exists but the method converged to the *wrong* solution, a solution on another branch of equilibria.

However, if a solution exists and F is continuously differentiable and regular in a neighborhood about the solution, the algorithm is guaranteed to converge to the solution for an initial guess in some neighborhood of that solution (see [GZ] for proof). Thus, it is prudent to modify Method (1) to improve the initial guess.

Method 2 (Newton with predictor) *This method uses a tangent linear approximation to start the Newton iteration. The initial step is often referred to as the predictor step. Variants exist that use quadratic predictors and predictors that require more than one previous solution [GZ].*

BEGIN:

$$Z_\lambda \rightarrow F_z|_{(z_0, \lambda_0)} Z_\lambda = -F_\lambda|_{(z_0, \lambda_0)}$$

$$z^1 \rightarrow z_0 + Z_\lambda(\lambda_1 - \lambda_0)$$

 WHILE: ($|F(z^k, \lambda_1)| > \text{TOLERANCE}$) AND ($\text{ITERATIONS} < \text{MAX}$)
 DO:

$$\Delta z \rightarrow F_z|_{(z^k, \lambda_1)} \Delta z = -F(z^k, \lambda_1)$$

$$z^{k+1} \rightarrow z^k + \Delta z$$

 IF ($|F(z^k, \lambda_1)| < \text{TOLERANCE}$) THEN $z_1 \rightarrow z^k$, ELSE WARNING

Note that for the case when λ appears linearly in F , this method is exactly equivalent to Method (1) except that the first iteration is performed outside of the loop.

As before, convergence is still not guaranteed and Method (2) can fail for all the same reasons as Method (1). If the method fails to converge we may restart it for a different choice of λ_1 closer to λ_0 . However, what if the method converged to the wrong solution? Can a wrong solution be detected?

In practice, power systems engineers believe that by inspecting the voltage magnitudes they can tell if a solution is reasonable². This suggests a simple way to improve the method so that convergence to a reasonable solution is more likely. Instead of solving $F(z, \lambda_1) = 0$, we solve an augmented set of equations $\begin{pmatrix} F(z, \lambda) \\ C(z, \lambda) \end{pmatrix} = 0$. The zero set of the map C specifies a desired characteristic of the solution. For example, if it was expected that the voltage at a particular bus would drop due to increases in loading, C can specify a voltage at that bus lower than its present voltage. Rather than solve for the state corresponding to a specified loading, the loading that corresponds to the specified characteristic of the state is found. Instead of being a fixed parameter of the solution method, λ is an unknown and λ_1 is an initial guess for λ . Hence, $C(z, \lambda)$ must include enough equations to allow for the solution of λ . When λ is multidimensional, λ_1 can define a direction from λ_0 and the step size in that direction then is an unknown.

Method 3 (Newton with predictor and corrector) *This example uses a particular corrector so that the state variable with the largest predicted change is fixed at its linearly predicted value. This method is the basic step employed by [AC92].*

BEGIN:

$$\begin{aligned} \Delta\lambda &\rightarrow (\lambda_1 - \lambda_0) \\ \hat{k} &\rightarrow \Delta\lambda/|\lambda| \\ Z_\lambda &\rightarrow F_z|_{(z_0, \lambda_0)} Z_\lambda = -F_\lambda|_{(z_0, \lambda_0)} \\ z^1 &\rightarrow z_0 + Z_\lambda \Delta\lambda \\ i &\rightarrow Z_\lambda \Delta\lambda(i) = \text{Max}_i (Z_\lambda \Delta\lambda) \end{aligned}$$

²The following discussion is from “Sparseness in Power Systems Equations” in [Reid]:

Larcombe: Power flow equations are nonlinear and so will in general have several solutions. How do you ensure that you have the correct solution?

Baumann: This is a difficulty and the analysis that is available is rarely helpful. We usually start with a solution having the same voltage value at each node in the hope of finding a solution with small voltage differences, a feature that the *engineers regard as desirable*.

WHILE: ($|F(z^k, \lambda^k)| > \text{TOLERANCE}$) AND (ITERATIONS $<$ MAX)

DO:

$$\begin{pmatrix} \Delta z \\ \Delta s \end{pmatrix} \rightarrow \begin{pmatrix} F_z|_{(z^k, \lambda^k)} & F_\lambda|_{(z^k, \lambda^k)} \hat{k} \\ e(i) & 0 \end{pmatrix} \begin{pmatrix} \Delta z \\ \Delta s \end{pmatrix} = \begin{pmatrix} -F(z^k, \lambda^k) \\ z^k(i) - z^1(i) \end{pmatrix}$$

$$s^{k+1} \rightarrow s^k + \Delta s$$

$$\lambda^{k+1} \rightarrow \lambda^k + \Delta s \hat{k}$$

IF($|F(z^k, \lambda^k)| < \text{TOLERANCE}$) THEN $(z_*, \lambda_*) \rightarrow (z^k, \lambda^k)$ ELSE WARNING

Note that since $z^k(i) - z^1(i) = 0 \forall k \geq 1$, the corrector fixes the i -th variable for all iterations. Essentially, the selected variable is treated as a parameter, and the original parameter is treated as a variable. This process of selecting a variable to fix is sometimes referred to as the parameterization step.

Since the predictor-corrector will converge to a solution for a λ_* different than the desired λ_1 , to solve problem (1) the method needs to be repeatedly run until λ_* is within tolerance of the desired λ_1 . However, most often the goal is to find the λ that corresponds to some particular event anyway, and λ_1 represents the first estimate of the parameters at that event.

When F_z is nearly singular evaluated at any point during the iteration, Methods (1) and (2) require solution of an ill conditioned linear system and are thus unstable and prone to generate numerical errors. However, the Jacobian matrix $\begin{pmatrix} F_z & F_\lambda \\ C_z & C_\lambda \end{pmatrix}$, not F_z , determines the condition of the predictor-corrector method. For a properly chosen (C_z, C_λ) numerical instabilities caused by a singular F_z are avoided.

Thus, the appended corrector equation has two beneficial effects. Not only does it decrease the chances of convergence to an unacceptable solution, but the appended row improves the conditioning of the Jacobian matrix used in the iterative step. To find equilibrium solutions very close to or at fold bifurcations of $F(z, \lambda) = 0$, a corrector should be used so that the linear system remains well conditioned even for F_z singular. It is possible then to avoid numerical instability associated with the singularity of F_z , and the trajectory of the equilibrium as a parameter is varied can be traced right around a fold bifurcation.

The process of selecting a corrector equation can be thought of as appending rows to the Jacobian matrix, not necessarily appending equations to be solved. For example, one popular option [CA93, DeM96] is to choose (C_z, C_λ) as the vector orthogonal to the initial tangent prediction, which is equivalent to selecting C so that (C_z, C_λ) is a vector in the null space of $(F_z, F_\lambda)^T$. Note that frequently it is advantageous to expand the number of state variables to improve sparsity [Alv97] or to locate a solution with a particular condition such as a bifurcation.

Sometimes the process of selecting the corrector equations is referred to as the parameterization step [CA93], and it can be performed after the predictor step [AC92] or after the corrector if another equilibrium is to be found [CA93]. The entire method is then the “predictor-corrector-parameterization” method.³ The predictor-corrector or predictor-corrector-parameterization method is the building block of path following methods for power systems. If the continuation parameter reflects the actual time evolving system parameters, the continuation method can be used as a “static simulator” of the power system, tracing the progression of the system equilibrium. Alternatively, continuation methods may also be used to trace a set of equilibria that satisfy some other characteristics such as an operational boundary. In either case, discrete device operation and limits, realistic parameter forecasts, and interarea and generator dispatch policy must be accounted for.

It is frequently the case that solution for an equilibrium after a discrete parameter change will force several limits to be violated. The most common solution then is to fix one limit at a time and resolve, starting with the most severely violated limit. Although this method is simple and well accepted, there is no guarantee that the solution obtained represents a realistic power system equilibrium. For some applications it is important to identify the order in which the limits are encountered.

The process of applying limits as the system equilibrium evolves needs careful attention. The operation of the power system changes in response to approaching and encountering limits. The response to one limit may affect which limits will occur next. The limits encountered and thus the equations that model the system at any point are dependent upon the path the system followed to reach that point. Thus, *security margins are path dependent*.

For some parameters and applications, it is reasonable to assume that λ evolves in a piecewise linear manner. For example, from λ_0 the parameters are forecast to change to λ_1 , and λ may successively occupy discrete values that lie on a ray connecting λ_0 to λ_1 . If the discrete values are close enough together, or if λ changes continuously, the order that limits are encountered under the assumptions is well defined⁴.

The repeated objective of a program to trace the equilibrium state of the system as parameters change in a quasi-continuous piecewise linear pattern is to find the relevant equilibrium corresponding to the next limit event. Method (3) requires adjustment for use in a continuation method that accounts for limit events. Essentially, the core problem to be solved is to find each λ that forces the equilibrium equations to change

³The term “corrector” is usually used to refer to the iterative loop itself, so that methods (1) and (2) are technically predictor-corrector methods as well.

⁴Of course, the assumptions may not reflect reality. Although we can compute a precise order of events under our assumptions, the actual timing may depend on transient effects.

due to a limit en route to finding a solution at some maximum forecast parameters.

Problem 2 (Find the next event) Z_{lim} is a vector of limits.

$$\begin{array}{l}
 \text{Given :} \\
 \left(\begin{array}{c} (z_0, \lambda_0, u_0) \\ f(z_0, \lambda_0, u_0) = 0 \\ F(z, \lambda) = f(z, \lambda, u_0) \\ z_0 < Z_{lim} \\ \lambda_1 \end{array} \right)
 \end{array}
 \qquad
 \begin{array}{l}
 \text{Find : } (z_*, \lambda_*) \text{ such that} \\
 \left(\begin{array}{c} z_* \leq Z_{lim} \\ z_*[i] = Z_{lim}[i] \\ F(z_*, \lambda_*) = 0 \end{array} \right) \\
 \text{OR} \\
 \left(\begin{array}{c} z_* < Z_{lim} \\ F(z_*, \lambda_1) = 0 \end{array} \right)
 \end{array}$$

One possible solution to problem (2) is to use method (3) with the orthogonal corrector or parameterization step in an interval halving approach. For an initial guess of λ_1 , method (3) is used to find another equilibrium. If a limit is not violated λ is increased and the process repeated until a solution that violates a limit is found or a solution at λ_1 is obtained. If a limit is violated before that, we can then decrease λ to the midpoint between the last no-limit solution and the first post-limit solution, eventually finding a point within tolerance of the exact point where the first limit is reached. The idea is that if you take small enough steps and find a pre-limit point that is reasonably similar to an acceptable starting point, and then a point with only one limit violated reasonably close to the pre-limit point, that one limit is likely to be the next limit. However, the interval halving approach may require an excessive number of solutions.

An improvement is made by modifying the predictor step of method (3) to predict the next limit, and then select a corrector to solve directly for the point at which that limit is reached. The resulting method will exactly locate the parameter and state corresponding to the next predicted event such as a line flow or bus voltage reaching an operational limit. For example, if I is the magnitude of a line current of interest and I_{max} the limit, the corrector equation would be $E(z, \lambda) = I - I_{max}$.

Method 4 (Direct method to locate the next event) Z_{lim} is a vector of the maximum limits of the z variables. The corrector is selected to be the linearly predicted next limit event. $E(z, \lambda, i) = z[i] - Z_{lim}[i]$

BEGIN:

$$\begin{aligned}
\Delta\lambda &\rightarrow (\lambda_1 - \lambda_0) \\
\hat{k} &\rightarrow \Delta\lambda/|\lambda| \\
Z_s &\rightarrow F_z|_{(z_0, \lambda_0)} Z_s = -F_\lambda|_{(z_0, \lambda_0)} \hat{k} \\
i &\rightarrow \text{Max}_i Z_s[i]/(Z_{lim}[i] - z_0[i]) \\
\Delta s &\rightarrow z_0[i] + Z_s[i]\Delta s = Z_{lim} \\
s^1 &\rightarrow \Delta s \\
z^1 &\rightarrow z_0 + Z_s\Delta s \\
\lambda^1 &\rightarrow \lambda_0 + \Delta s\hat{k}
\end{aligned}$$

$$\text{WHILE: } \left(\begin{array}{c} F(z^k, \lambda^k) \\ E(z^k, \lambda^k, i) \end{array} \right) > \text{TOLERANCE} \text{) AND (ITERATIONS } < \text{MAX) }$$

DO:

$$\begin{pmatrix} \Delta z \\ \Delta s \end{pmatrix} \rightarrow \begin{pmatrix} F_z|_{(z^k, \lambda^k)} & F_\lambda|_{(z^k, \lambda^k)} \hat{k} \\ E_z|_{(z^k, \lambda^k, i)} & E_\lambda|_{(z^k, \lambda^k, i)} \hat{k} \end{pmatrix} \begin{pmatrix} \Delta z \\ \Delta s \end{pmatrix} = - \begin{pmatrix} F(z^k, \lambda^k) \\ E(z^k, \lambda^k, i) \end{pmatrix}$$

$$\begin{aligned}
s^{k+1} &\rightarrow s^k + \Delta s \\
\lambda^{k+1} &\rightarrow \lambda^k + \Delta s\hat{k} \\
z^{k+1} &\rightarrow z^k + \Delta z
\end{aligned}$$

$$\text{IF} \left(\begin{array}{c} F(z^k, \lambda^k) \\ E(z^k, \lambda^k, i) \end{array} \right) < \text{TOLERANCE} \text{) THEN } (z_*, \lambda_*) \rightarrow (z^k, \lambda^k) \text{ ELSE WARNING}$$

The output of this method is a solution at the point where the next predicted limit is reached. Note that $E_z = e(i)$, so that the corrector forces the solution to have $z[i]$ at its limit value. [AJYB] and [RHSC] implement the predictor portion of this method, but use the corrector of Method (3). The results presented in Chapter 8 were computed using an implementation of this method that predicted voltage, line flow, and real or reactive power limits.

It is possible to revise the predictor so that it can select not only for limit events, but also fold bifurcations (Chapter 5) or Hopf bifurcations (Chapter 9). $E(z, \lambda)$ can be defined by the conditions for the fold bifurcation or a Hopf bifurcation or some other constraint. The following chapters make use of a direct method to locate a fold bifurcation once a continuation method locates a very near point and has determined the limits and equations that apply at the fold bifurcation.

Method 5 (Direct method to find a fold bifurcation point) *The corrector is the condition for the fold bifurcation. \hat{k} is the unit vector in the direction of parameter variation and (z_0, λ_0) is an equilibrium solution close to the exact bifurcation. μ is the real eigenvalue with smallest magnitude of $F_z|_{z_0, \lambda_0}$ and can be initially computed by inverse iteration, along with the corresponding left eigenvector w . Similar methods are demonstrated in [Seydel, AJ89]*

BEGIN:

$$\begin{aligned} z^1 &\rightarrow z_0 \\ \lambda^1 &\rightarrow \lambda_0 \\ (w^1, \mu^1) &\rightarrow w^1(F_z - \mu^1 I) = 0 \\ C(w, z, \lambda) &\rightarrow \begin{pmatrix} wF_z \\ w \cdot w^T - 1 \end{pmatrix} = 0 \end{aligned}$$

WHILE: ($|F(z^k, \lambda^k)| > \text{TOLERANCE}$) AND (ITERATIONS $<$ MAX)

DO:

$$\begin{pmatrix} 0 & F_z|_{(z^k, \lambda^k)} & F_\lambda|_{(z^k, \lambda^k)} \\ F_z^T|_{(z^k, \lambda^k)} & w^k F_{zz}|_{(z^k, \lambda^k)} & w^k F_{z\lambda}|_{(z^k, \lambda^k)} \\ w^k & 0 & 0 \end{pmatrix} \begin{pmatrix} \Delta w \\ \Delta z \\ \Delta \lambda \end{pmatrix} = \begin{pmatrix} -F(z^k, \lambda^k) \\ -C(w^k, z^k, \lambda^k) \end{pmatrix}$$

$$\begin{aligned} \lambda^{k+1} &\rightarrow \lambda^k + \Delta \lambda \\ z^{k+1} &\rightarrow z^k + \Delta z \\ w^{k+1} &\rightarrow w^k + \Delta w \end{aligned}$$

$$\text{IF} \left(\begin{vmatrix} -F(z^k, \lambda^k) \\ -C(w^k, z^k, \lambda^k) \end{vmatrix} < \text{TOLERANCE} \right) \text{ THEN} \begin{pmatrix} z_* \rightarrow z^k \\ \lambda_* \rightarrow \lambda^k \\ w_* \rightarrow w^k \end{pmatrix} \text{ ELSE WARNING}$$

Note that a linear predictor can be used to improve the initial guess. Alternatively, if equilibrium solutions are obtained for points on both sides of the fold, a point in between can be used as an initial guess. The method can also be modified to locate a Hopf bifurcation [Alv90].

3.2.1 Description of margin computation program

The previous methods can be included in a continuation program to locate the parameter values at an event and thus determine the margins to events. The basic idea is to successively find the equilibrium as the parameters vary, locate each equilibrium at which a limit event occurs and check the stability at each equilibrium. For example, assume that from the current operating equilibrium (z_0, λ_0, u_0) a forecast is made so that the demand on the system requires the parameter vector to successively assume the values $\lambda_1, \lambda_2, \dots, \lambda_j$. The λ parameter vector could include individual load and generator constant powers, generator participation factors, interchange set points, load model parameters or any system parameter that can be forecast or deduced. Each λ_{k+1} can depend on the solution corresponding to λ_k . For example, if at each λ it is assumed that the generation is re-dispatched according to an optimum power flow or the outcome of a bidding process, then the subsequent λ reflects the next forecast loading along with the transfers and participation factors derived from solution at the previous loading.

Assume that the forecast provides a piecewise linear estimate of the projected actual parameter change. In other words, the actual parameter change is forecast to successively occupy the discrete values λ_i as well as intermediate values that lie on lines connecting the λ_i . Each increment defines a direction of parameter change. The first direction is $\hat{k}_1 = (\lambda_1 - \lambda_0)/|(\lambda_1 - \lambda_0)|$. The first objective of the program is to find the equilibrium corresponding to λ_1 – the problem we have already addressed. Several intermediate equilibria corresponding to $\lambda = \lambda_0 + s\hat{k}_1$ for $s < 1$ may be found as well, especially when those parameter values correspond to limit events. The process is repeated to find the equilibrium corresponding to λ_2 and so on, until equilibria corresponding to each forecast λ are found, or until an equilibrium at which the system loses stability is found.

Method 6 (Generic power systems continuation method) *Continuation method to find steady state instability or security limits.*

BEGIN: OBTAIN STATE INCLUDING LIMITS, AND FORECAST PARAMETER CHANGES,
($\lambda_1, \lambda_2, \dots, \lambda_n$).

WHILE (STABLE AND SECURE) AND ($\lambda \neq \lambda_n$)

DO:

WHILE (STABLE AND SECURE) AND ($\lambda \neq \lambda_j$)

DO:

1. CALL PREDICTOR-CORRECTOR (CORRECTOR DETERMINED BY THE LINEAR ESTIMATE OF THE NEXT EVENT), RETURN NEW EQUILIBRIUM AND AT MOST ONE LIMIT.
2. CHECK STABILITY.
3. IF STABLE, APPLY LIMIT, CHECK STABILITY.

INCREMENT j

The output of the program is either the final state at the last forecast parameter values, or the state and parameters at which the system loses stability or violates a security constraint.

When the parameter forecast is based on a realistic time evolution of the actual parameters, the program can be viewed as a static simulator of the power system. However, there are good uses for parameter forecasts that do not reflect the time evolution of parameters. Chapter 6 uses this method to determine a theoretical post-contingency steady state, where λ represents line admittance. Similarly, λ may represent interchange set points and Method (6) can be used to determine the interarea transfer boundary at a specific loading level. Thus Method (6) is both a simulation tool and a computational tool.

This method has now been successfully implemented with a 1500 bus model for a major US utility, and used to determine the loading and transfer margins to events at which system costs increase discretely. The model predicts and finds real and reactive power output limits, line flow limits, and voltage limits initiating switching operation or violating security constraints. At each limit event, generation is redispatched according to a Constrained Economic Dispatch (CED) to determine the next direction of parameter variation.

Once method (6) has determined the point of instability or security limit violation, a nominal margin to that event can be defined by the norm of the difference in the parameter values at the current operating point and those at the event point. The choice of norm is arbitrary and should be based on convenience and ease of interpretation. If the current operating point is (z_0, λ_0, u_0) and the point of instability is (z_*, λ_*, u_*) , $\lambda_* - \lambda_0$ is a vector in parameter space. The length of the vector can be measured in any norm.

In some instances, the margin is best measured in state space, not parameter space. For example, assume that the instability is a Hopf bifurcation and that a detailed load model was employed so that expressions for the real and reactive power at a bus were dependent upon state variables (such as voltages and/or time derivatives of voltages). In this case, the real and reactive powers are state variables, not parameters, but operators may still wish to measure a margin to instability in real power since it is easily monitored. In this case the margin can be defined by a norm of $z_* - z_0$. Note that it may even be advantageous to measure norms in state and parameter space - the norm of $(z_*, \lambda_*) - (z_0, \lambda_0)$. One may even choose a measure in a discrete parameter space; for example, the number of discrete events encountered between the current operating point and loss of stability.

3.3 Summary

A conceptual continuation program for computing margins to events has been explained. The continuation program serves two purposes. On one hand, it is a computational tool for locating specific equilibrium solutions, such as fold bifurcations or limit violations. On the other hand, it is a system simulator, showing the evolution of the system equilibrium as conditions are altered. The program uses a predictor-corrector method to trace a curve of equilibria. The corrector serves two roles. First, it improves the likelihood of convergence to an acceptable solution or a specific type of solution. Second, it avoids problems due to a poorly conditioned or singular system Jacobian matrix. The predictor also has two roles. First, it improves the initial guess of the Newton step so that convergence to a correct solution is more likely. Second,

it determines which corrector to use by indicating what the likely next event is.

Suppose that the margin to some event has been computed. How would the margin change if some parameter was different than forecast? Will it be necessary to recompute another continuation to find the new margin? This question is answered in Chapter 4.

Chapter 4

Sensitivity Computations

Chapter 3 described how the security margin to an event boundary could be efficiently computed by using a corrector that specified the event condition. Once the solution at an event is obtained in this manner the sensitivity of the margin to that boundary with respect to almost every power system parameter can be obtained for very little additional computational cost. This chapter explains and derives the formula for the sensitivity of a margin with respect to an arbitrary parameter vector.

Suppose that we are interested in locating the point where the power system voltages become unacceptably low due to the gradual increase in demand along some forecast pattern. The continuation program can trace a curve of equilibria as demand increases, locating intermediate limits that initiate tap changing or generator protection, until the point where the first low voltage limit occurs is found. The continuation program may have assumed a particular interarea transfer or pattern of transfers. How much can the transfer be adjusted without significantly impacting the margin to a low voltage event? By how much will the load at which that limit is encountered change for a different transfer?

4.1 Methods of sensitivity analysis

The brute force way to answer the previous questions is as follows. At the initial operating point, we alter the interarea transfers as proposed and find the corresponding equilibrium. Next, the continuation method is used as before to locate the new first voltage limit. If several possible changes to the interarea transfer are under consideration, several continuations are run. This method is outlined below.

Method 7 (Multiple Continuations)

Brute force method to compute points on an event boundary.

```
BEGIN: OBTAIN INITIAL STATE, PARAMETERS, FORECAST, AND CONTROL  
PARAMETER VALUES  $(p_0, p_1, \dots, p_n)$ .  
WHILE  $(p \neq p_n)$   
DO:
```

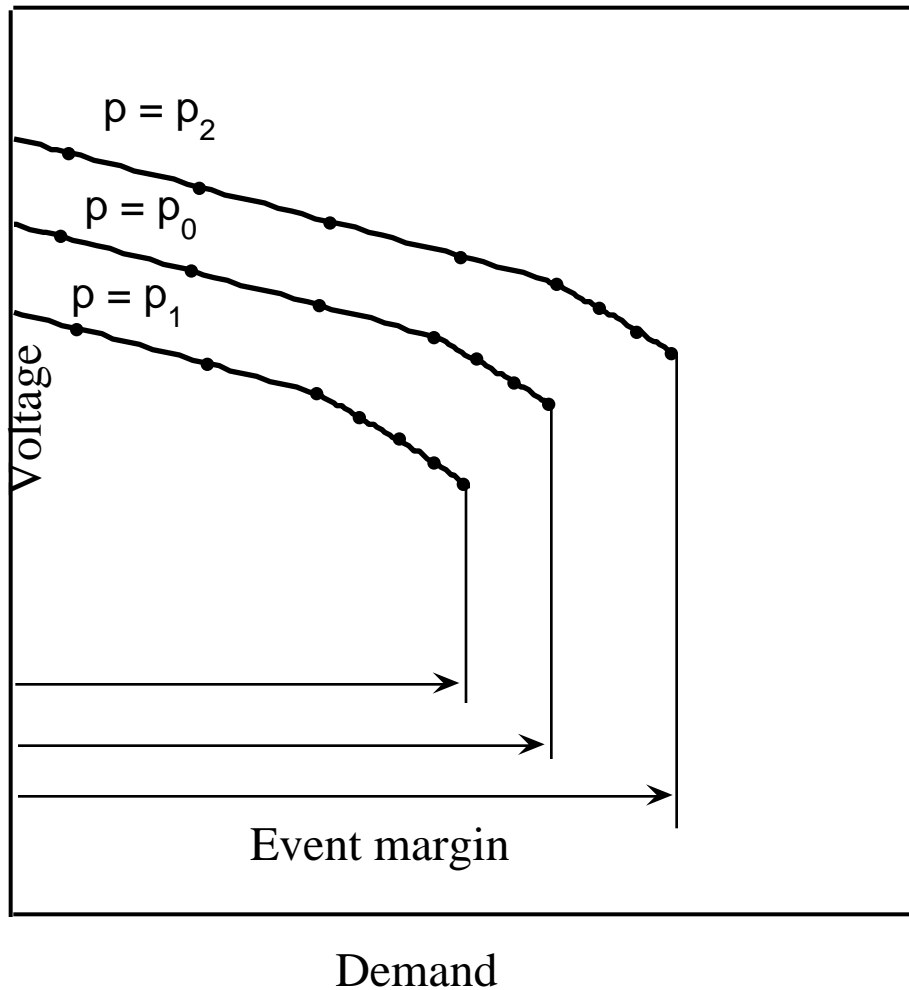


Figure 3: Equilibria trajectories for different values of the parameter p

- CALL CONTINUATION METHOD, TRACE EQUILIBRIUM TRAJECTORY, RETURN BOUNDARY POINT
- UPDATE p .

This program returns the boundary points and equilibrium trajectories approaching the boundary for each desired value of p .

Figure 3 shows a picture of several of the resulting curves. The dots represent points at which the equilibrium solutions are computed.

One alternative to Method (7) also uses the continuation Method (6). However, after locating a nominal point on the boundary, the continuation is used to trace

a portion of the boundary starting from the nominal boundary point. The control parameter becomes the continuation parameter and a locus of equilibria at which the limit voltage is encountered is traced. The method is outlined below. [HD95] implements this method for a small power system. (This method was also suggested by Cañizares in the discussion to [GDA97]).

Method 8 (Boundary Trace) *Use the continuation method to find points on a curve situated on the boundary around a nominal boundary point.*

BEGIN: OBTAIN INITIAL STATE, PARAMETERS, FORECAST, AND CONTROL PARAMETER p .

CALL CONTINUATION METHOD TO LOCATE NOMINAL BOUNDARY POINT AND CONDITION.

WHILE (STEP CHANGE > MIN) AND ($p \neq p_{max}$)

DO:

1. CALL PREDICTOR-CORRECTOR ROUTINE (CORRECTOR IS THE EVENT CONDITION AT THE NOMINAL POINT), RETURN NEW EQUILIBRIUM ON BOUNDARY.
2. CHECK LIMITS.
3. IF LIMITS, REDUCE STEP CHANGE, ELSE INCREASE STEP

The program ends with either the control parameter at its maximum value and the resulting change in the margin, or the maximum control parameter change and margin corresponding to a point on the boundary where the limits in effect change.

Figure 4 shows the sequence of equilibria computed by Method (8) and the initial continuation to find the nominal point on the boundary. This curve includes all the boundary points computed by the previous method.

There is an alternative to either Method (7) or (8). Instead of computing additional points on the boundary, a Taylor series evaluated at the nominal boundary point can be used to approximate the boundary. The first order Taylor series estimate is equivalent to the initial predictor step that would be implemented by Method (8). Second order and higher Taylor series approximations are possible, with the higher order derivatives computed explicitly at the nominal point, or approximated by computing one or more additional points on the curve. The Taylor series method is outlined below.

Method 9 (Taylor series approximation) *Compute one nominal boundary point, estimate curve on the boundary.*

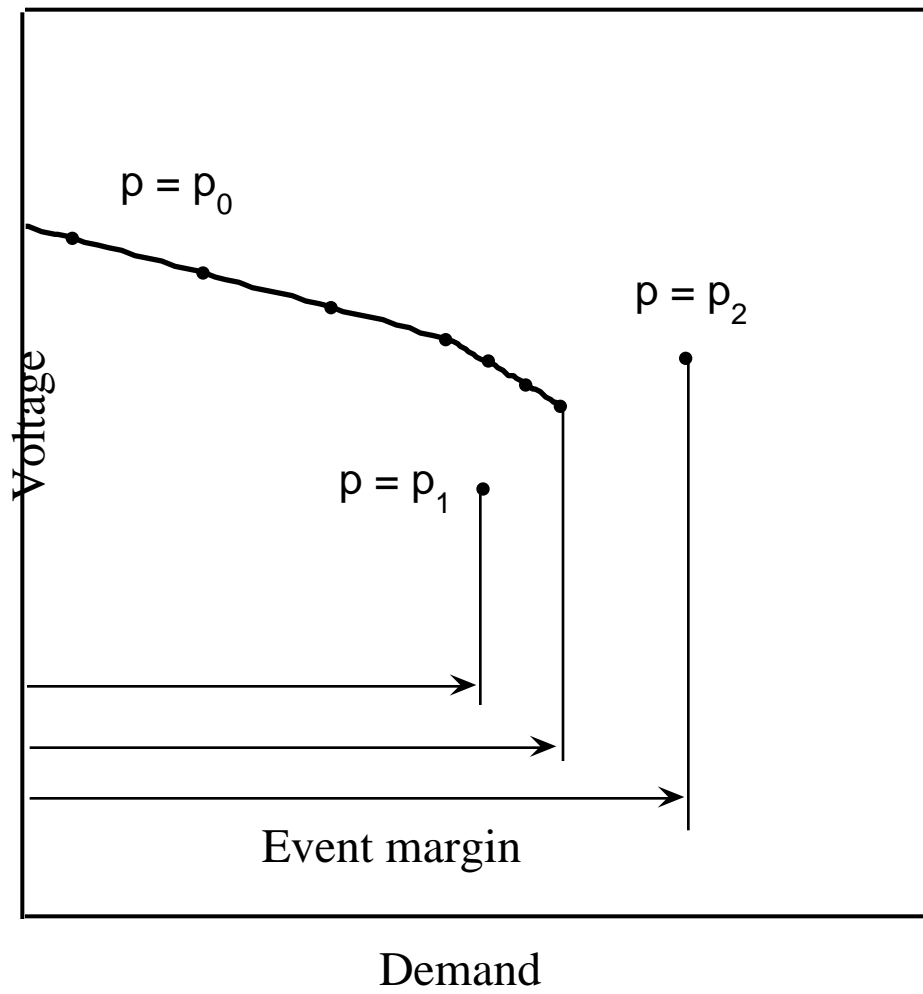


Figure 4: Nominal trajectory and boundary as function of the parameter p

BEGIN: OBTAIN INITIAL STATE, PARAMETERS, FORECAST, AND CONTROL PARAMETER p .

1. CALL CONTINUATION METHOD TO LOCATE NOMINAL BOUNDARY POINT.
2. COMPUTE DERIVATIVES OF EQUILIBRIUM AND CONDITION EQUATIONS WITH RESPECT TO p AT BOUNDARY POINT.
3. EVALUATE TAYLOR SERIES ESTIMATES.

The output of this program is a Taylor series approximation of a curve on the boundary evaluated for any value of p .

Figure 5 shows the Taylor series approximations to the boundary obtained from computation of the nominal boundary point.

The advantage of Method (7) is that events that occur that differ from those of the nominal continuation can be found en route to establishing the new margins. For example, if for a given change to the control parameter, a different limit is reached than for the nominal case, this will be detected. The disadvantage is that each continuation is time consuming. The advantage of the Method (8) is time savings; one computes exactly the equilibria of interest. The drawback is that if the change in parameters changes the events encountered en route to the boundary, the results will be incorrect and the computation a waste of time. Method (8) partially screens for this by examining the solutions for limit violations on the boundary¹. Method (9) is less accurate than either continuation approach, but offers the greatest time savings by many orders of magnitude. Approximate curves for many different parameters can be computed faster than the exact computation of one curve for one parameter. The first order Taylor series estimate is always much faster than the other methods since the first order term is essentially the same as one predictor step. The second order Taylor series is only worth computing if it is faster than computing a second point on the boundary (since it is simple to fit a quadratic with two points and a tangent vector).

Another advantage of Method (9) is that the sensitivity formulas are similar for any parameter. Thus, if the formulas are evaluated for one parameter they can be reevaluated for a different parameter at only a fraction of the cost to compute the first sensitivity. The greater the number of parameters of interest, the greater the computational savings of Method (9) over Method (8). In addition, the sensitivity formulas are also useful for determining immediate control action.

¹Note that this screening could only detect new limits violated on the boundary, not changes in the order of the limits encountered or limits that should no longer be enforced. For example, a change in the parameter p may cause a previous limit to not be encountered, and thus the equations used to trace the boundary may not be valid yet the solutions would appear to satisfy the limit conditions.

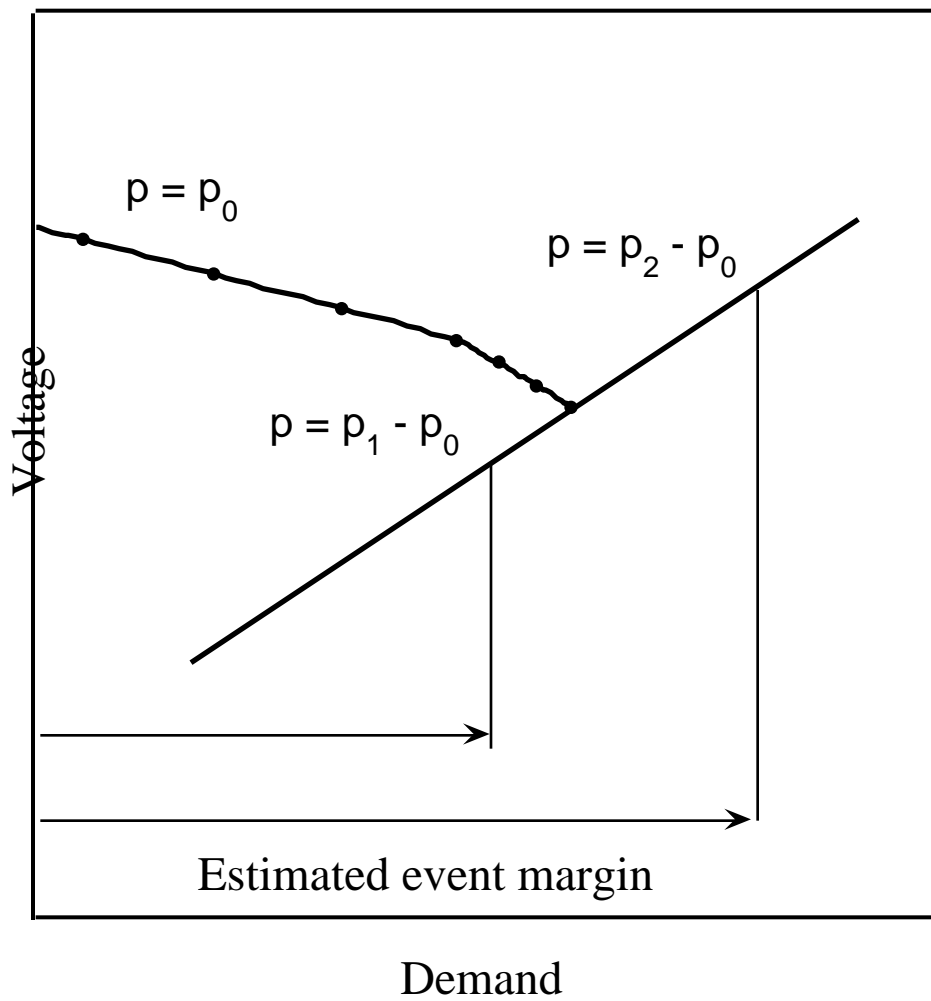


Figure 5: Nominal trajectory and estimated boundary

4.2 Sensitivity formulas

This section presents derivations of the formulas for the sensitivity of margins to events with respect to arbitrary parameters.

4.2.1 Derivation

Assume that (z_0, λ_0, u_0) is a stable operating point where $z \in \mathbb{R}^n$ and $\lambda \in \mathbb{R}^m$. The continuation program determines that the point (z_*, λ_*, u_*) corresponds to an event for variation of the λ parameters in the direction k . Let \hat{k} be a unit vector in the norm used to measure the margin.

$$\hat{k} = (\lambda_* - \lambda_0) / |\lambda_* - \lambda_0| \quad (5)$$

The security margin M to the event is $M = |\lambda_* - \lambda_0|$.

The equilibrium equations valid at (z_0, λ_0, u_0) are $\tilde{F}(z, \lambda) = f(z, \lambda, u_0)$. The equilibrium equations valid at (z_*, λ_*, u_*) are $F(z, \lambda) = f(z, \lambda, u_*)$. $E(z, \lambda)$ defines the event equation at (z_*, λ_*, u_*) . For many limits, including voltage, flow, and power limitations, defining the event equation E is simple. However, two events, the fold and Hopf bifurcations, require special consideration and are discussed in sections 4.2.4 and 4.2.5 and detailed in Chapters 5 and 9 respectively. In general the selection of the event equations E is analogous to selecting corrector equations C that allow for direct solution of a boundary point.

Suppose that it is of interest how changing a selected parameter p changes the state and remaining parameters at which the event described by E occurs. At the nominal event point $\begin{pmatrix} F(z_*, \lambda_*, p) \\ E(z_*, \lambda_*, p) \end{pmatrix} = 0$. Define the map H as

$$H(z, \lambda, p) = \begin{pmatrix} F(z, \lambda, p) \\ E(z, \lambda, p) \end{pmatrix} \quad (6)$$

The curve (if it exists) that Method (9) estimates is a subset of the set of equilibria that satisfy the event conditions in state and parameter space around the nominal boundary point. This set of equilibria, the preimage of the zero set of H , is denoted $H^{-1}(0)$. Using calculus on $H^{-1}(0)$ is defensible only when $H^{-1}(0)$ is a differentiable manifold. It turns out that for very general conditions this will indeed be true and we are justified in the assumption that there are curves on $H^{-1}(0)$ that describe the sets of interest to us. The conditions are

1. $H_z|_{(z_*, \lambda_*)}$ has rank n .

2. $\left(\begin{array}{cc} H_z & H_\lambda \hat{k} \end{array} \right) \Big|_{(z_*, \lambda_*)}$ has rank $n + 1$.

Condition (2) is a transversality condition stating that a vector through (z_*, λ_*) in the \hat{k} direction intersects $H^{-1}(0)$ transversally. Condition (1) can be interpreted as a condition of uniqueness. Simply stated, Condition (1) specifies that only one event occurs at a time. (Note that Condition 2 implies Condition 1. The redundancy here is intentional and serves to distinguish between the restrictions on E and the restrictions on \hat{k} .) The details and implications of these conditions are addressed in section 4.2.3. For now, assume that $H^{-1}(0)$ is a smooth manifold and a smooth curve on that manifold parameterized by p is $(Z(p), \Lambda(p))$ so that $(Z(p_0), \Lambda(p_0)) = (z_*, \lambda_*)$ and

$$\left(\begin{array}{c} F(Z(p), \Lambda(p), p) \\ E(Z(p), \Lambda(p), p) \end{array} \right) = 0 \quad (7)$$

Assume that p is not a component of λ . The more general case in which p is a component of λ or λ depends on p is addressed in sections (4.2.2) and (4.2.3).

Since the system is assumed stable at the nominal operating point, \tilde{F}_z is nonsingular as p is varied in a neighborhood about p_0 . Then as p is adjusted each new equilibrium $(\tilde{Z}(p), \lambda_0, p)$, satisfying $F(\tilde{Z}(p), \lambda_0, p) = 0$, can be associated with one corresponding point $(Z(p), \Lambda(p), p)$ satisfying $H((Z(p), \Lambda(p), p)) = 0$ that is the closest point on $H^{-1}(0)$ in the direction \hat{k} . The difference in parameter space between the operating point $(\tilde{Z}(p), \lambda_0, p)$ and the corresponding boundary point $(Z(p), \Lambda(p), p)$ is

$$\Lambda(p) - \lambda_0 = L(p)\hat{k} \quad (8)$$

where $L(p)$ is a scalar step in the \hat{k} direction as a function of p . The margin as a function of p is

$$M(p) = |\Lambda(p) - \lambda_0| = |L(p)\hat{k} + \lambda_0 - \lambda_0| = |L(p)\hat{k}| \quad (9)$$

Since \hat{k} is a unit vector in the norm used for the margin, the margin as a function of p is $M(p) = L(p)$. Write $\Lambda(p)$ in terms of the margin $L(p)$

$$\Lambda(p) = L(p)\hat{k} + \lambda_0 \quad (10)$$

Equation (7) can then be written

$$\left(\begin{array}{c} F(Z(p), L(p)\hat{k} + \lambda_0, p) \\ E(Z(p), L(p)\hat{k} + \lambda_0, p) \end{array} \right) = 0 \quad (11)$$

Differentiating (11) at (z_*, λ_*) with respect to p and applying the chain rule for derivatives yields a linear system

$$\left(\begin{array}{cc} F_z & F_\lambda \hat{k} \\ E_z & E_\lambda \hat{k} \end{array} \right) \Big|_* \left(\begin{array}{c} Z_p \\ L_p \end{array} \right) = - \left(\begin{array}{c} F_p \\ E_p \end{array} \right) \Big|_* \quad (12)$$

The matrix $\left(\begin{array}{cc} F_z & F_\lambda \hat{k} \\ E_z & E_\lambda \hat{k} \end{array} \right) \Big|_*$ is nonsingular by Condition 2.

Solution of (12) then yields L_p , the sensitivity of the security margin with respect to p . The first order estimate of the change in margin corresponding to the change in p of Δp is

$$\Delta L = L_p \Delta p \quad (13)$$

Solution of (12) additionally yields Z_p , the tangent vector at (z_*, λ_*, p_0) to the curve in state space that describes how the state variables change to satisfy the equilibrium and event conditions as p varies². Thus, $Z_p \Delta p$ is the first order Taylor series estimate of how the state changes on $H^{-1}(0)$ for a parameter change of Δp .

Since the matrix $\left(\begin{array}{cc} F_z & F_\lambda \hat{k} \\ E_z & E_\lambda \hat{k} \end{array} \right) \Big|_*$ is the same for any³ parameter p , once the matrix is factored and the sensitivities obtained for one parameter, computing the sensitivities for any additional parameters only requires obtaining the derivatives $\left(\begin{array}{c} F_p \\ E_p \end{array} \right) \Big|_*$ and one forward and backward substitution.

If obtaining L_p for many parameters is of primary interest, and there is no desire to obtain Z_p , then full solution of the linear system (12) is not necessary. Since any set of $n + 1$ vectors in \mathbb{R}^n are linearly dependent there is a non-zero vector w such that

$$w \left(\begin{array}{c} F_z \\ E_z \end{array} \right) \Big|_* = 0 \quad (14)$$

w is a vector orthogonal to the range of $\left(\begin{array}{c} F_z \\ E_z \end{array} \right) \Big|_*$ and w is unique up to a scalar multiplication when $\left(\begin{array}{c} F_z \\ E_z \end{array} \right) \Big|_*$ is full rank, which is guaranteed by condition (1). Pre-multiplying (12) by w yields

$$w \left(\begin{array}{c} F_\lambda \hat{k} \\ E_\lambda \hat{k} \end{array} \right) \Big|_* L_p = -w \left(\begin{array}{c} F_p \\ E_p \end{array} \right) \Big|_* \quad (15)$$

$w \left(\begin{array}{c} F_\lambda \hat{k} \\ E_\lambda \hat{k} \end{array} \right) \Big|_*$ is not zero since $\left(\begin{array}{cc} F_z & F_\lambda \hat{k} \\ E_z & E_\lambda \hat{k} \end{array} \right) \Big|_*$ is nonsingular, so (15) can be solved

² $Z_p \Delta p$ can thus be used to screen for cases where new limits would be violated ($Z_p \Delta p[i] > Z_{lim}[i]$)

³The presentation assumes that \hat{k} does not explicitly depend on p and that p is not a component of λ . The appropriate formulas for these special cases are simply obtained by applying the Chain Rule for derivatives (see Appendix 5.7.C).

to obtain the sensitivity with respect to p of the margin to the event.

$$L_p = - \frac{w \left(\begin{array}{c} F_p \\ E_p \end{array} \right) \Big|_*}{w \left(\begin{array}{c} F_{\lambda \hat{k}} \\ E_{\lambda \hat{k}} \end{array} \right) \Big|_*} \quad (16)$$

Note that regardless of the number of parameters under consideration, w needs to be computed only once.

Higher order sensitivities

Higher order sensitivities of the security margin with respect to p are computed by repeatedly differentiating (11) at (z_*, λ_*) with respect to p and solving linear systems of equations. Chapters 5, 6, and 7 use the quadratic sensitivity of the loading margin to voltage collapse with respect to transmission line parameters to estimate the effects of line outages. Quadratic sensitivities have found use in optimization routines. [OloPhD] uses quadratic sensitivities to improve the rate of convergence of an optimization process. Quadratic sensitivities are also used by [GSHT] for sensitivity analysis of optimal power flow solutions, and in [NorPhD] for operation of series compensators.

4.2.2 Normal vector to the event boundary in parameter space

The sensitivity of the security margin to changes in many parameters is effectively just an indexing operation once the scaled normal vector is obtained. The normal vector to the event boundary in parameter space defines to first order the proportions by which all the parameters must vary to keep the equilibrium at the security boundary. The normal vector is useful in determining the relative effectiveness of different parameters on the security margin. Note that if a point on the security boundary is obtained using a direct method that uses the E equations as corrector equations, obtaining the normal vector requires only one additional forward and backward substitution using the previously factored Jacobian matrix.

The vector w used to obtain the margin sensitivity formulas is used to define the normal vector to the hypersurface in parameter space that represents the surface on which parameters must vary so that the resulting equilibrium satisfies the event and equilibrium conditions.

Let $(Z(p), \Lambda(p))$ represent arbitrary smooth curves in state space and parameter space parameterized by p which satisfy

$$H(Z(p), \Lambda(p), p) = \begin{pmatrix} F(Z(p), \Lambda(p), p) \\ E(Z(p), \Lambda(p), p) \end{pmatrix} = 0 \quad (17)$$

and $(Z(p_0), \Lambda(p_0)) = (z_*, \lambda_*)$. The tangent vector $(\dot{Z}, \dot{\Lambda}, \dot{P})$ to the curve $(Z(p), \Lambda(p), p)$ at (z_*, λ_*, p_0) satisfies

$$\begin{pmatrix} F_z & F_\lambda & F_p \\ E_z & E_\lambda & E_p \end{pmatrix} \Big|_* \begin{pmatrix} \dot{Z} \\ \dot{\Lambda} \\ \dot{P} \end{pmatrix} = 0 \quad (18)$$

Pre-multiplying (18) by w yields

$$w \begin{pmatrix} F_\lambda & F_p \\ E_\lambda & E_p \end{pmatrix} \Big|_* \begin{pmatrix} \dot{\Lambda} \\ \dot{P} \end{pmatrix} = 0 \quad (19)$$

where w is found from (14). Equation (19) shows that the vector N

$$N = w \begin{pmatrix} F_\lambda & F_p \\ E_\lambda & E_p \end{pmatrix} \Big|_* \quad (20)$$

is orthogonal to the tangent vector $(\dot{\Lambda}, \dot{P})$ at (λ_*, p_0) for an arbitrary curve $(Z(p), \Lambda(p), p)$ satisfying (17).

4.2.3 General derivation

Preliminary Assumptions

Assume that (z_0, λ_0, p_0) is a stable operating point, and that $* = (z_*, \lambda_*, p_0)$ is the nominal event point where $z \in \mathbb{R}^n$ and $\lambda \in \mathbb{R}^m$. Let p represent the parameters of interest, with $p \in \mathbb{R}^\rho$.

The smooth map $Q : \mathbb{R}^\rho \rightarrow \mathbb{R}^m$ describes the explicit dependence of λ on p by $\lambda = Q(p)$. Note that $Q(p)$ can be a constant function. Assume that in a neighborhood V of (z_0, λ_0, p_0) , the map $\tilde{F} : V \rightarrow \mathbb{R}^n$ is smooth and

$$\tilde{F}(z_0, \lambda_0, p_0) = 0 \quad (21)$$

Since λ depends explicitly on p ,

$$\tilde{F}(z, Q(p), p) = 0 \quad (22)$$

As the p parameters change, the stable equilibrium moves to satisfy the \tilde{F} equilibrium equations. Since (z_0, λ_0, p_0) is asymptotically stable by the assumptions of Chapter

2, \tilde{F}_z is nonsingular in an open neighborhood of (z_0, λ_0, p_0) contained in V . By the Implicit Function Theorem there is a unique smooth map $\tilde{Z}(p)$ defined on a neighborhood of p_0 so that $\tilde{Z}(p_0) = z_0$ and

$$\tilde{F}(\tilde{Z}(p), Q(p), p) = 0 \quad (23)$$

We are interested in the point on the event boundary that corresponds to each stable operating point. The λ parameters at the stable operating point depend explicitly on the p parameters while the parameters corresponding to boundary points depend implicitly and explicitly on the parameters p . Defining a direction in which to measure the margin distinguishes between the proportions of each of the parameters that vary explicitly and those that vary implicitly.

The margin M to the event is the distance between the stable operating point and the nominal event point along a direction \hat{k} . It is practical then to represent λ in coordinates so that the margin to the event is the scalar difference in only one coordinate. This coordinate then varies implicitly with p while the remaining coordinates vary explicitly with p .

Let $T : \mathbb{R}^m \rightarrow \mathbb{R}^m$ represent a linear isomorphism from λ to (ℓ, s) , $\ell \in \mathbb{R}^1$ and $s \in \mathbb{R}^{m-1}$ where the columns of T form an orthogonal basis for \mathbb{R}^m and ℓ represents the projection of λ in the \hat{k} direction so that

$$\lambda = T \begin{pmatrix} \ell \\ s \end{pmatrix} = \begin{pmatrix} \hat{k} & K \end{pmatrix} \begin{pmatrix} \ell \\ s \end{pmatrix} \quad (24)$$

and

$$\begin{pmatrix} \ell \\ s \end{pmatrix} = T^{-1}\lambda \quad (25)$$

The nominal margin then is

$$M = |T^{-1}(\lambda_* - \lambda_0)| = \ell_* - \ell_0 \quad (26)$$

To emphasize the dependence on p we write

$$(\tilde{L}(p), \tilde{S}(p)) = T^{-1}Q(p) \quad (27)$$

In addition, assume F and E are smooth maps in a neighborhood U of (z_*, λ_*, p_0) and that at the nominal event point

$$\begin{pmatrix} F(z_*, \lambda_*, p_0) \\ E(z_*, \lambda_*, p_0) \end{pmatrix} = 0 \quad (28)$$

Define the smooth map $H : U \rightarrow \mathbb{R}^{n+1}$

$$H(z, \lambda, p) = \begin{pmatrix} F(z, \lambda, p) \\ E(z, \lambda, p) \end{pmatrix} \quad (29)$$

and $H(z_*, \lambda_*, p_0) = 0$

Assumptions

1. $H_z|_*$ has rank n .
2. $\left(\begin{array}{cc} H_z & H_\lambda \hat{k} \end{array} \right)|_*$ has rank $n + 1$.

Properties

1. $H^{-1}(0)$ is locally an $m + \rho - 1$ manifold in a neighborhood of (z_*, λ_*, p_0) and there exists a neighborhood U of p_0 and unique smooth maps $(Z(p), \Lambda(p))$ so that $(Z(p_0), \Lambda(p_0)) = (z_*, \lambda_*)$ and $p \in U$ implies that $H(Z(p), \Lambda(p), p) = 0$.
2. The set $\Sigma = \{(\Lambda(p), p) \mid p \in U\}$ is an $m + \rho - 1$ manifold in $\mathbb{R}^{m+\rho}$ that is diffeomorphic to $H^{-1}(0)$. The vector $N = (wH_\lambda, wH_p)|_*$, where w is given by $wH_z|_* = 0$, is in the direction normal to Σ at (λ_*, p_0) . N is unique up to scalar multiple.
3. The sensitivity of the margin M with respect to p is

$$M_p = L_p - \tilde{L}_p = - \left(\frac{wH_p + wH_\lambda Q_p}{wH_\lambda \hat{k}} \right) \Big|_* \quad (30)$$

Proof

Assumption (2) implies that H is surjective at (z_*, λ_*) and by the Preimage Theorem (pages 20 -21 [GP]) $H^{-1}(0)$ is locally an $m + \rho - 1$ manifold. Assumption (1) implies that there exists a nonzero row vector w such that $wH_z|_{(z_*, \lambda_*)} = 0$ and w is unique up to scalar multiple.

Define the smooth map $G : \mathbb{R}^n \times \mathbb{R}^1 \times \mathbb{R}^\rho \rightarrow \mathbb{R}^{n+1}$

$$G(z, \ell, p) = H(z, T(\ell, \tilde{S}(p)), p) \quad (31)$$

The derivative of G with respect to (z, ℓ) is $(H_z, H_\lambda \hat{k})$ and is nonsingular at (z_*, λ_*, p_0) by Assumption 2. By the Implicit Function Theorem there exists a neighborhood U of p_0 and unique smooth maps $(Z(p), L(p))$ so that $(Z(p_0), L(p_0)) = (z_*, \ell_*)$ and $p \in U$ implies

$$G(Z(p), L(p), p) = 0 \quad (32)$$

By the Preimage Theorem $G^{-1}(0)$ is a manifold. Since T is a diffeomorphism from λ to (l, s) coordinates, $H^{-1}(0)$ is diffeomorphic to $G^{-1}(0)$. Let $\Lambda(p) = T(L(p), \tilde{S}(p))$. Then

$$G(Z(p), L(p), p) = H(Z(p), \Lambda(p), p) = 0 \quad (33)$$

and Property 1 is proved.

Differentiating Equation (33) with respect to p yields

$$H_z Z_p + H_\lambda \Lambda_p + H_p = 0 \quad (34)$$

Pre-multiplying by w and evaluation at (z_*, λ_*, p_*) yields

$$wH_\lambda|_* \Lambda_p + wH_p|_* = 0 \quad (35)$$

showing that $N = (wH_\lambda, wH_p)|_*$ is normal to the manifold $\{(\Lambda(p), p) \mid p \in U\}$ at (λ_*, p_*) . N is nonzero by Assumption 2, so we can consider N a map from $\mathbb{R}^m \times \mathbb{R}^\rho$ to \mathbb{R}^1 with a kernel spanned by $m + \rho - 1$ basis vectors. Define the map $\Gamma : \mathbb{R}^m \times \mathbb{R}^\rho \rightarrow \mathbb{R}$

$$\Gamma(\lambda, p) = wH(Z(p), \lambda, p) \quad (36)$$

Assumption 2 implies that $(\Gamma_\lambda, \Gamma_p)|_* = (wH_\lambda, wH_p)|_*$ is surjective. By the Preimage Theorem, $\Sigma = \Gamma^{-1}(0)$ is an $m + \rho - 1$ manifold with codimension 1. In a neighborhood of (z_*, λ_*, p_*) Σ is diffeomorphic to $H^{-1}(0)$ since the map $\Pi : H^{-1}(0) \rightarrow \Gamma^{-1}(0)$ defined by

$$\Pi(z, \lambda, p) = (\lambda, p) \quad (37)$$

is one to one and onto and the inverse map

$$\Psi(\lambda, p) = (Z(p), \lambda, p) \quad (38)$$

is smooth. Since Γ is constant on Σ , differentiating (36) with respect to (λ, p) , evaluating at (λ_*, p_*) , and using $wH_z|_* = 0$ shows that $(wH_\lambda, wH_p)|_*$ is the normal vector to Σ at (λ_*, p_*) and Property 2 is proved.

Define the map $\tilde{G} : \mathbb{R}^n \times \mathbb{R}^\rho \rightarrow \mathbb{R}^n$ by

$$\tilde{G}(z, p) = \tilde{F}(z, Q(p), p) \quad (39)$$

Each point on $G^{-1}(0)$ is associated with one point on $\tilde{G}^{-1}(0)$ by change in the ℓ coordinates only. On $\tilde{G}^{-1}(0)$, ℓ and s depend explicitly on p .

On $G^{-1}(0)$, ℓ depends implicitly on p and s depends explicitly on p . Differentiating Equation (32) with respect to p yields

$$G_z Z_p + G_\ell L_p + G_p = 0 \quad (40)$$

The sensitivities with respect to p are found from the solution of the linear system

$$\left(\begin{array}{cc} G_z & G_\ell \end{array} \right) \Big|_* \left(\begin{array}{c} Z_p \\ L_p \end{array} \right) = -G_p|_* \quad (41)$$

Equation (41) can be written in terms of derivatives of H (see (31)) as

$$\left(\begin{array}{cc} H_z & H_{\lambda \hat{k}} \end{array} \right) \Big|_* \left(\begin{array}{c} Z_p \\ L_p \end{array} \right) = -H_{\lambda|_*} K \tilde{S}_p - H_p|_* \quad (42)$$

Pre-multiplication of (42) by w yields

$$w H_{\lambda \hat{k}}|_* L_p = -w H_{\lambda|_*} K \tilde{S}_p - w H_p|_* \quad (43)$$

Note that $w H_{\lambda \hat{k}}|_* \neq 0$ by Assumption (2). Rearranging (43) yields

$$L_p = - \frac{w H_{\lambda} K \tilde{S}_p + w H_p}{w H_{\lambda \hat{k}}} \Big|_* \quad (44)$$

The margin to the event as a function of p is

$$M(p) = L(p) - \tilde{L}(p) \quad (45)$$

The sensitivity of the margin with respect to the p parameters is found by differentiating (45) with respect to p .

$$M_p = L_p - \tilde{L}_p = - \frac{w H_{\lambda} K \tilde{S}_p + w H_p}{w H_{\lambda \hat{k}}} \Big|_* - \tilde{L}_p \quad (46)$$

Multiply \tilde{L}_p by unity as $w H_{\lambda \hat{k}}/w H_{\lambda \hat{k}}$ and rearranging yields

$$M_p = - \frac{w H_p + w H_{\lambda} (K \tilde{S}_p + \hat{k} \tilde{L}_p)}{w H_{\lambda \hat{k}}} \Big|_* = - \frac{w H_p + w H_{\lambda} Q_p}{w H_{\lambda \hat{k}}} \Big|_* \quad (47)$$

satisfying Property 3. Note that if the p parameters do not affect the components of λ , Equation (47) reduces to the previous formula (16)

$$M_p = L_p = - \frac{w H_p}{w H_{\lambda \hat{k}}} \Big|_* \quad (48)$$

[GP] presents and derives the Implicit Function Theorem and the Preimage Theorem in Section 4 of Chapter 1. In particular note the proposition concluding the section that shows that the kernel of the derivative of the submersion is the tangent space to the preimage manifold, which is related to the interpretation here of the normal vector N . A different construction is presented in [AMR] Section 5, Chapter 3. Of note in [AMR] is supplement 3.5A which discusses Lagrange multipliers.

4.2.4 Fold bifurcation

This section informally specifies the construction of E , the event equation for the fold bifurcation, so that the assumptions of the previous derivations are met. Chapter 5 presents a general and detailed derivation. The derivation here intends to show the connection between the assumptions used to derive the general results and the conditions of a generic fold bifurcation employed in Chapter 5 and 6.

In the previous section, Assumption (1) required that only one constraint occurred at a time. However, in power systems we are commonly concerned with locating the points at which the system equations F become singular. If F_z has rank $n - 1$, E_z must be orthogonal to the kernel of F_z or the matrix $\left(\begin{array}{c} F_z \\ E_z \end{array} \right) \Big|_*$ will not have maximum rank. One motivation for this section comes from the analysis of direct methods to locate fold bifurcations discussed in Chapter 3. The specification of E is analogous to selecting corrector equations for numerical solution.⁴

Generically, fold bifurcation of the system equations coincides with singularity of the system Jacobian matrix $F_z|_*$ due to a simple zero eigenvalue.⁵ An expression for a simple eigenvalue μ of $F_z|_*$ can be written in terms of its corresponding left and right eigenvectors.

$$\mu = wF_z|_*v \quad (49)$$

where the vectors w and v are normalized so that $|v| = 1$ and $wv = 1$. v and w are smooth functions of z and λ near (z_*, λ_*) . One choice for the E equations is

$$E^{\text{FOLD}}(z, \lambda) = wF_zv \quad (50)$$

and H is defined as

$$H(z, \lambda) = \left(\begin{array}{c} F(z, \lambda) \\ E(z, \lambda) \end{array} \right) \quad (51)$$

For this construction to satisfy Assumption (1), the matrix

$$\left(\begin{array}{c} F_z \\ E_z \end{array} \right) \Big|_* \quad (52)$$

⁴One requirement of computational methods for power systems is that sparsity be exploited whenever possible. For the purposes of deriving formulas, the sparsity of the equations is not relevant. However, practical application of any analytical results eventually requires a sparse implementation. In short, the computational procedures can differ from the theoretical derivations.

⁵The general derivation in the appendix of Chapter 5 also applies to certain cases of fold bifurcation corresponding to the system Jacobian matrix dropping rank due to the occurrence of a repeated zero eigenvalue of algebraic multiplicity two and geometric multiplicity one.

must have maximal rank which implies that

$$E_z|_*v \neq 0 \quad (53)$$

which can be written as

$$wF_{zz}|_*(v, v) \neq 0 \quad (54)$$

Not surprisingly, equation (54) is one condition for a generic fold bifurcation. The other transversality condition can be found by requiring assumption (2). Since w is the left eigenvector corresponding to the zero eigenvalue of $F_z|_*$, the vector $(w, 0)$ is the vector satisfying equation (14) and

$$(w \ 0) \begin{pmatrix} F_z \\ E_z \end{pmatrix} \Big|_* = 0 \quad (55)$$

Assumption (2) requires that

$$(w \ 0) \begin{pmatrix} F_\lambda \\ E_\lambda \end{pmatrix} \Big|_* \neq 0 \quad (56)$$

which is equivalent to the other generic fold bifurcation condition that

$$wF_\lambda|_* \neq 0 \quad (57)$$

Equations (54) and (57) are the transversality conditions for a generic fold bifurcation and identify the construction of E that satisfies the assumptions required by the derivations for the sensitivity formulas.

4.2.5 Hopf bifurcation and eigenvalue sensitivity

The fold bifurcation corresponds to one real eigenvalue of F_z being zero. The Hopf bifurcation corresponds to one complex eigenvalue pair with zero real part. Event equations for Hopf bifurcations can also be written in terms of the critical eigenvalue and corresponding eigenvectors.

Assume that F are differential equations that define the equilibrium and dynamic response of the system with z state variables.

$$E^{\text{HOPF}}(z, \lambda) = \text{Re}\{\mu(z, \lambda)\} = \text{Re}\{w(z, \lambda)F_z(z, \lambda)v(z, \lambda)\} \quad (58)$$

where the eigenvectors w and v corresponding to the critical eigenvalue μ of F_z are normalized so that $|v| = 1$ and $wv = 1$ (μ is assumed simple). Note that obtaining w , v and μ and locating a Hopf bifurcation point can require considerable computational effort for very large power systems. A more detailed analysis is presented in Chapter 9.

The Hopf condition satisfies assumption (1) when $F_z|_*$ is nonsingular, which is equivalent to assuming that we do not have a fold bifurcation at the same point as a Hopf bifurcation. One should be wary of situations when the two events do approach each other, and this is discussed in Chapter 9.

The derivatives of E are required for predictor steps for the continuation method, for the Jacobian matrix of a direct solution method to locate the Hopf point, and to compute the Taylor series estimates of margin to Hopf instability. The derivatives of E^{HOPF} are related to eigenvalue sensitivities as follows: Differentiating Equation (49) with respect to λ yields

$$\mu_\lambda = w(F_{zz}Z_\lambda + F_{z\lambda})|_*v \quad (59)$$

Z_λ is found by solving the linear system

$$F_z|_*Z_\lambda = -F_\lambda|_* \quad (60)$$

Evaluated at the equilibrium, Z_λ is a linear map which takes changes in the parameter and gives the corresponding first order change in the equilibrium state. The sensitivity of the eigenvalue with respect to λ is

$$\mu_\lambda = wF_{zz}|_*(Z_\lambda, v) + wF_{z\lambda}|_*v \quad (61)$$

This formula is derived differently in [DAD92]. $wF_{zz}|_*(Z_\lambda, v)$ is the portion of the sensitivity attributable to the implicit dependence of the equilibrium state on λ . $wF_{z\lambda}|_*v$ is the portion of the sensitivity due to the explicit dependence of the Jacobian matrix elements on λ .

Consider a symbolic formula for the system Jacobian matrix F_z . Each matrix element is a function of the state and parameters. Varying a parameter moves the equilibrium, and each matrix element can thus change as a result of the state variable equilibrium values implicitly depending upon the parameters as well as an explicit dependence on the parameter (i.e. the parameter appears in the symbolic formula for the matrix element). The eigenvalues of F_z are functions of the elements of F_z . Thus the eigenvalues can be thought of as affected by two distinct means: the explicit effect of the parameters on the elements of the Jacobian matrix, $wF_{z\lambda}v$, and the implicit effect of the parameters on the equilibrium at which the Jacobian matrix is evaluated, $wF_{zz}(Z_\lambda, v)$.

The matrix μ_λ can be thought of as a map from parameter space to the complex plane giving the tangent approximation to the eigenvalue locus as a function of the parameter changes. $\text{Real}\{\mu_\lambda\}$ is a vector of the same dimension as λ , and may be thought of as a vector normal to a hypersurface in parameter space. If $\Delta\lambda$ is a vector tangent to that surface, then $\text{Real}\{\mu_\lambda\}\Delta\lambda = 0$, which shows that $\text{Real}\{\mu_\lambda\}$ is

the normal vector to the set of parameters for which $Real\{\mu\}$ remains constant. If $Real\{\mu_\lambda\}$ is evaluated at a Hopf bifurcation, $Real\{\mu\} = 0$ and $Real\{\mu_\lambda\}$ is a normal vector to the Hopf bifurcation set in parameter space.

We expect that by applying the formulas of section (4.2.1) the same results should be obtained. Let $E(z, \lambda) = Real\{wF_z v\}$. The vector u satisfies

$$(u \ 1) \begin{pmatrix} F_z \\ Real\{wF_{zz}v\} \end{pmatrix} \Big|_* = 0 \quad (62)$$

implying that $u = (-Real\{wF_{zz}v\}F_z^{-1})|_*$ and

$$N = (u \ 1) \begin{pmatrix} F_\lambda \\ Real\{wF_{z\lambda}v\} \end{pmatrix} \Big|_* \quad (63)$$

The normal vector to the Hopf bifurcation set in parameter space is

$$N = -Real\{wF_{zz}v\}F_z^{-1}F_\lambda + Real\{wF_{z\lambda}v\} \quad (64)$$

evaluated at (z_*, λ_*) . Equation (64) agrees with the real part of (61) since $Z_\lambda = -F_z^{-1}F_\lambda$.

Participation factors

Note that the formulas for the eigenvalue sensitivity presented in the previous section can be reduced to yield participation factors. Participation factors have found widespread use in power systems [IEEE1, Kundur, WRPK, PAVS, PPAV].

Consider the case where F_z is a constant matrix and λ represents the (i, j) element of F_z . Then the formula for the eigenvalue sensitivity reduces to $w[i]v[j]$ which is referred to in power systems as the participation factor of the j - th variable in the i - th mode. In other words, participation factors are the first order eigenvalue sensitivities of the system Jacobian matrix with respect to the elements of the matrix. Participation factors do not account for either the explicit or implicit dependence of the Jacobian matrix on parameters. Participation factors have been found useful for a multitude of power system problems. It is interesting to consider what improvements can be made by using the complete eigenvalue sensitivity formulas.

4.3 Traditional sensitivity

Approximate sensitivity methods have found widespread use in power systems for many years. The two most generally accepted methods are termed ‘‘Distribution Factors’’ and ‘‘Outage Distribution Factors’’. This section shows the relationship

between distribution factors or outage distribution factors and the sensitivity formulas used for this thesis. In short, for a specific set of assumptions, the sensitivity formulas in this thesis will reduce to the distribution factors calculated by the methods such as those presented in [Debs, WW] and [Heydt]. That is, the formulas for distribution factors or linear sensitivity factors presented in most power systems texts are a special case of the exact sensitivity formulas used in this thesis. However, the formulas used in this thesis offer several advantages:

- The exact sensitivity formulas account for the dependence on the equilibrium point at which the linearization is made. The approximate formulas assume a constant Jacobian.
- The formulas are valid for any choice of equilibrium equations, and can be applied to find the sensitivity of any state variable or function of state variables to any parameter.
- The exact sensitivity formulas can be used to obtain the sensitivity of the margin to an event.
- Quadratic and higher order sensitivities can be obtained by differentiating (68) and solving additional linear equations as in Chapter 5 and [GDA97].
- The vector formulation of these sensitivity factors leads to efficient computation using sparse vectorized techniques.

One particular area of application for approximate methods is contingency analysis. Since many contingencies need to be considered, often in real time, it was necessary to find a way to predict the effects of contingencies without actually solving for the post contingency equilibrium. The most common objective of contingency analysis is to estimate the effects of contingencies on line flows. Overloaded lines can sag, short, and trip, increasing the flows on other lines and leading to cascading outages.

- *Distribution factors* measure the sensitivity of line flows to bus power injections. They are used for predicting the effects of altering the generation dispatch or interchanges on line flows.
- *Outage distribution factors* measure the sensitivity of line flows to line outages.

Distribution factors are essentially the predictions of line flows resulting from the first iteration of a fast decoupled load flow solution for the predicted generation pattern. Distribution factors represent the approximate sensitivity of line flows to

changes in power injections. Since, to first order, a line outage can be represented by power injections, distribution factors can be used to derive outage distribution factors that estimate the change in flows resulting from line outages. Outage distribution factors are often referred to as “non-linear” sensitivities, that exploit the constant Jacobian assumption of the fast decoupled load flow and the nonlinear dependence of the bus impedance matrix on the line parameters.

We first derive a formula for the sensitivity of the flow to an arbitrary parameter for general assumptions, and then show that for specific assumptions the formula reduces to a standard expression for a distribution factor. The derivation is a special case of the derivations presented in Section 4.2, and follows that of Section 4.2.1 closely.

Assume an equilibrium model of the power system that yields static equations

$$0 = F(\theta, p) \quad (65)$$

where θ is the vector of equilibrium states, and p a vector of parameters.

If F represents the loadflow equations then θ is a vector that includes voltages, angles, and power output at the slack generator or a distributed slack. Alternatively, F can also include more detail such as equations modeling the voltage regulators at generators, area interchange, or FACTS devices.

Let G represent the equation for flow γ on some line so that

$$0 = G(\theta, p) - \gamma \quad (66)$$

Our derivation is simplified if we let ψ represent the expanded state vector including the line flow, so that $\psi = (\theta, \gamma)$ and (65) and (66) can be combined as

$$0 = H(\psi, p) \quad (67)$$

Assume that an equilibrium (ψ_*, p_*) is a solution to (67) and $H_{\psi}|_{(\psi_*, p_*)}$ is not singular (true exactly when F_{θ} is non-singular). By the implicit function theorem there is a unique curve in state space parameterized by p that passes through (ψ_*, p_*) so that every point on the curve in some neighborhood of (ψ_*, p_*) is a solution to (67) and (65) and the curve is differentiable at (ψ_*, p_*) . Denote this curve by the map $\Psi(p)$. Then differentiating with respect to p at (ψ_*, p_*) yields

$$0 = H_{\psi}|_{(\psi_*, p_*)} \Psi_p + H_p|_{(\psi_*, p_*)} \quad (68)$$

The vector Ψ_p is the tangent vector at (ψ_*, p_*) to the curve $\Psi(p)$ in state space. The elements of Ψ_p are the sensitivities of the state variables to the parameter p at (ψ_*, p_*) . (68) is a linear system of equations that can be efficiently solved to obtain

all the sensitivities of the state variables to the parameter p . However, assume that we are only interested in obtaining the sensitivity of the line flow, Γ_p . We rewrite (68) as

$$0 = \begin{pmatrix} F_\theta & 0 \\ G_\theta & -1 \end{pmatrix} \Big|_{(\theta_*, p_*)} \begin{pmatrix} \Theta_p \\ \Gamma_p \end{pmatrix} + \begin{pmatrix} F_p \\ G_p \end{pmatrix} \Big|_{(\theta_*, p_*)} \quad (69)$$

The matrix $\begin{pmatrix} F_\theta \\ G_\theta \end{pmatrix} \Big|_{(\theta_*, p_*)}$ has n columns and $n + 1$ rows. Since every set of $n + 1$ vectors in \mathbb{R}^n is linearly dependent, there is always a nonzero vector w so that

$$0 = w \begin{pmatrix} F_\theta \\ G_\theta \end{pmatrix} \Big|_{(\theta_*, p_*)} \quad (70)$$

Normalize w so that the last component is unity. Pre-multiplying (69) by w and solving (69) for Γ_p yields:

$$\Gamma_p = w \begin{pmatrix} F_p \\ G_p \end{pmatrix} \Big|_{(\theta_*, p_*)} \quad (71)$$

Equation (71) is the sensitivity of the line flow with respect to the parameter p . Note that p can be any parameter, and γ does not need to be a line flow, but could for example be the sum of tie flows on an interface, or a generator VAR output, or a voltage. Computing w requires solution of one sparse linear equation and is essentially equivalent to solving one iteration of the loadflow. Equation (71) can be compared to another expression for Γ_p obtained from solving the linear system (69)

$$\Gamma_p = G_\theta \Theta_p = (G_\theta [F_\theta]^{-1} F_p) \Big|_{(\theta_*, p_*)} \quad (72)$$

It is much quicker to compute either the row vector w or the column vector $[F_\theta]^{-1} F_p$ than it is to compute the inverse Jacobian matrix $[F_\theta]^{-1}$. However, equation (72) provides a useful insight. When the flow sensitivities are used to compute estimates of the change in flow by a Taylor series,

$$\Delta\gamma = \Gamma_p \Delta p = G_\theta \Theta_p \Delta p \quad (73)$$

the right hand side is the product of the derivative of the flow to the state multiplied by the derivative of the state to the parameter, multiplied by the change in parameter. $\Theta_p \Delta p$ is then just the estimate for the change in state corresponding to a change in the parameter. Large deviation sensitivity formulas can be derived from (73) by replacing $\Theta_p \Delta p$ with a better estimate for $\Delta\theta$. The better estimate results

from evaluating some of the terms in (72) at the post-event equilibrium.⁶ Large deviation sensitivity formulas also result from choosing different parameterizations. For example, let the parameter vector p be the vector of line resistance, reactance, and charging capacitance of the line to be outaged and write the equilibrium equations F explicitly in terms of the bus impedance matrix Z . F then corresponds to voltage balance equations instead of power balance equations. Since the Z matrix does not vary linearly with changes in a line parameter, large deviation sensitivity formulas result from replacing $[F_\theta]^{-1}F_p\Delta p$ in (73) with $[F_\theta]^{-1}F_Z\Delta Z$ where ΔZ is the matrix $Z_{new} - Z_{old}$ and F_Z (a tensor) is the derivative of the equilibrium equations with respect to the Z matrix. Another way to see this is to think of the impedance matrix as a function of the parameter, $Z(p)$. The linear sensitivity uses $F_p\Delta p = F_Z Z_p \Delta p$. The large deviation sensitivity uses $F_Z\Delta Z(p)$ where $\Delta Z(p)$ is an explicit function of p . Other large deviation sensitivity formulas can also be derived using higher order Taylor series estimates. The higher order terms can be exactly computed or approximated.

Now it remains to show that for the assumptions of [Heydt] or [Debs, WW] the quantity on the right hand side of (71) is exactly the distribution factor. The derivation of distribution factors presented in [Debs, WW] assumes that the bus voltage magnitudes are unity and the line resistances can be ignored (the DC loadflow assumptions). Only the assumption of unity bus voltage magnitudes is required to derive the formulas in [Heydt].

The approximate real power balance equations for the DC loadflow assumptions can be written

$$F(\theta, s) = P - B\theta \quad (74)$$

where B is the susceptance matrix. The θ variables consist of the vector of bus angles not including the reference bus, and the scalar variable s represents the slack generation. For a single slack bus, s is one element of the vector P or real power injections. Note that equilibrium equations can also be written

$$\tilde{F}(\theta, s) = XP - \theta \quad (75)$$

where X is the reactance only portion of the bus impedance matrix Z and $X = B^{-1}$.

Let the flow of interest be on the line connecting bus i and bus j ,

$$\gamma = G(\theta, s) = -b_{ij}(\theta_i - \theta_j) \quad (76)$$

⁶The post-event equilibrium point most likely is not known, but some of the derivatives in (72) might not depend on the equilibrium or the higher order dependence of those derivatives on the parameter might be known explicitly.

Since the equilibrium equations are linear, F_θ is a constant complex matrix where each column corresponding to a bus angle is exactly a column of the B matrix and the single column corresponding to the slack generation is zero except for a one in the row (assume the s row) corresponding to the slack power balance equation. G_θ is a row vector of all zeros except in the columns corresponding to the buses connected by the line, which contain the line susceptance; denote this vector b where

$$b = (0, \dots, -b_{ij}, 0, \dots, b_{ij}, 0, \dots, 0) \quad (77)$$

and $b_{ij} = 1/x_{ij}$. Assume that the parameter p is a complex power injection at bus k , so that G_p is zero and $F_p = e(k)$ is a column vector of all zeros except a one in the k -th row corresponding to the bus injection. Equation (69) becomes

$$0 = \begin{pmatrix} B & e(s) & 0 \\ b & 0 & -1 \end{pmatrix} \begin{pmatrix} \Theta_p \\ S_p \\ G_p \end{pmatrix} + \begin{pmatrix} e(k) \\ 0 \end{pmatrix} \quad (78)$$

Equation (70) becomes

$$0 = w \begin{pmatrix} B & e(s) \\ b & 0 \end{pmatrix} \quad (79)$$

If neither bus i or j is the slack bus, $w = (bX, -1)$, and equation (71) becomes

$$\Gamma_p = -bXe(k) \quad (80)$$

The b row vector “hits” only the i and j rows of X and the $e(k)$ column vector “hits” only the k -th column of X . Equation (80) can be written

$$\Gamma_p = \frac{X_{ik} - X_{jk}}{x_{ij}} = \rho_{ij,k} \quad (81)$$

which is the commonly accepted formula for the distribution factors. Note that if Equation (75) was used instead of Equation (74) to define the equilibrium condition the same result is obtained. The steps follow in the same manner except that F_θ is an identity matrix and F_p is the X matrix multiplied by $e(k)$.

The [Heydt] assumption implies approximate complex equilibrium equations

$$0 = \text{diag}(\theta^*)S^* - Y^*\theta^* \quad (82)$$

where θ is complex and “diag” is the map of a vector to a diagonal matrix with the vector entries in the same order on the diagonal. To get the distribution factor formulas in [Heydt] simply use the full impedance and admittance matrices (replace Y with B and Z with X using common notation). Equation (81) becomes

$$\Gamma_p = \frac{Z_{ik} - Z_{jk}}{z_{ij}} = \rho_{ij,k} \quad (83)$$

The estimates of line flows computed from these distribution factors are equivalent to the updates of line flows resulting from one iteration of the fast decoupled loadflow.

Outage distribution factors are traditionally obtained by applying the distribution factor formula for (complex) power injections that cancel the flow on the outaged line (compensation). This corresponds to selecting p as a vector of power injections at the connected buses and can also be derived by assuming that the parameter p represents the outaged line parameter vector as in [GDA98]. Finally, large deviation sensitivity formulas should be used for outage distribution factors. This is accomplished by using the post outage Z bus (or X) bus quantities in the formula, which can be computed from the Y bus (or B bus) changes using the matrix inversion lemma [Debs, Bergen]. This is justified since the approximations yield linear models with constant Jacobian matrices. For example, to derive the large sensitivity outage distribution factors, replace the $\Theta_p \Delta p$ term from (73) with $\Delta \Theta = P \Delta X$. Note that different large sensitivity outage distribution factors can be derived from the general formula (71) without the fast decoupled loadflow assumptions.

4.4 Penalty factors, β coefficients, and normal vectors

The effectiveness of each generator in a power system in servicing load depends upon the location of that generator relative to the loads in the network. Due to transmission losses, a generator that produces power inexpensively but is located a great distance from loads might not be any more economical than an expensive generator located close to major loads. The penalty factor associated with a generation bus indicates the extent to which that generator is hindered by transmission losses. The β coefficients are the reciprocals of the penalty factors. In this section we derive an expression for the penalty factors and β coefficients based on the normal vector formula. The formula is general and applies to many possible models of the power system.

If the cost to generate power at two buses is equal, then the bus with the higher β (or lower penalty factor) will be most economical. Similarly, a load with a higher β is more costly to service. In the recent jargon of the California ISO, the β coefficients are referred to as “meter-multipliers”. The penalty factors and “betas” are usually derived in power systems texts in a chapter concerning economic dispatch and optimum power flow. The product of each generator’s β coefficient and incremental cost is shown to be equal to the system Lagrange multiplier, referred to as “system lambda”. In short, total cost is minimized when the product of each generator’s loss

adjusted incremental cost is the same. [Alv78] shows how to compute the β coefficients from the loadflow Jacobian matrix.⁷ Unfortunately, most power system texts do not correctly reproduce or reference the proof. [Bergen] comes the closest but the proof is flawed by a typographical error. In [Kusic], the author states

A major problem of economic dispatch is to determine the penalty factors, or equivalently the loss partial derivatives $\frac{\partial PL}{\partial P_i}$, as dependent on the output power of each of the M generation units. A large number of researchers have contributed to the solution of this problem, usually with assumptions concerning the behavior of loads on the system and the reactive power flow.

Let F represent the system equilibrium equations with state variables $z = (x, s)$. x includes bus voltages and angles and generator reactive power outputs but not generation real power outputs; the scalar s represents the system losses or slack generation and can be distributed in any manner so that F_z is non-singular. λ can be any system parameters. F can include an explicit equation for the total system line losses in which case the total losses is a variable in x . However, an explicit loss equation causes a dense row in the Jacobian matrix used for computations and there is no advantage to including one.

Assume that (x_0, s_0, λ_0) is the present stable operating point satisfying the equilibrium equations $F(x, s, \lambda) = 0$ and assume that $F_z|_{(x_0, s_0, \lambda_0)}$ is nonsingular. Then the matrix F_x is a full rank matrix with one more row than column and there exists a row vector β such that

$$\beta F_x|_{(z_0, \lambda_0)} = 0 \quad (84)$$

β is unique up to a scalar multiple. The sensitivity of the losses to a change in the parameter vector in the direction \hat{k} is found from (16)

$$S_\lambda = -\frac{\beta F_s|_{(z_0, \lambda_0)}}{\beta F_\lambda|_{(z_0, \lambda_0)} \hat{k}} \quad (85)$$

The components of β are the “betas” or reciprocals of the penalty factors. This can be seen as follows. Select s to correspond to a single slack generator output so that F_s is a column vector of all zeros except a one in the row corresponding to real power balance at the slack bus. Then select λ to represent real or reactive power injection at each bus so that F_λ is a matrix with a single one in each column, positioned in

⁷Prior to Alvarado’s publication, these factors were often approximated by means of the B-coefficient matrix and referred to as “loss factors” or B-factors. Now, the exact coefficients are commonly referred to as “betas” after the notation adopted in the paper. However, reference to [Alv78] is sparse.

the rows corresponding to real or reactive power balance at a bus. If \hat{k} is a vector with only one nonzero entry for load increase at one bus, Equation (85) computes the sensitivity of the required power output of the slack bus with respect to increase in demand at one bus. If there is one slack generator or marginal generator, it is convenient to normalize β so that the component corresponding to that generator is one.

Another interpretation is that the β vector determines the normal vector in parameter space to the surface on which the parameters must change to maintain an equilibrium solution. Consider a formulation without a specific slack generator or slack distribution. Let $X(t)$ represent a curve in state space and $\Lambda(t)$ a curve in parameter space as functions of a scalar t so that

$$F(X(t), \Lambda(t)) = 0 \quad (86)$$

Then the tangent vector $(\dot{X}, \dot{\Lambda})$ to the curve $(X(t), \Lambda(t))$ at (x_0, λ_0) satisfies

$$\left(\begin{array}{cc} F_x & F_\lambda \end{array} \right) \Big|_{(x_0, \lambda_0)} \begin{pmatrix} \dot{X} \\ \dot{\Lambda} \end{pmatrix} = 0 \quad (87)$$

Pre-multiply (87) by β to obtain the normal vector, N to $\Lambda(t)$ at λ_0 is

$$N = \beta F_\lambda \Big|_{(x_0, \lambda_0)} \quad (88)$$

where β is found from (84).

The concept of penalty factors has been generalized. By appropriate choice of the vector λ the penalty factor or “beta” corresponding to real or reactive power injection at any bus can be computed. However, there is no reason to limit the parameters to bus injections or the equations to the standard loadflow equations. For example, if interchange equations are appended with additional variables to maintain the set interchanges, the penalty factor associated with each interchange can be computed and thus the value of power at each interchange. This allows the optimum interchange set points to be determined within the economic dispatch solution. In addition, linear and quadratic estimates of the changes in losses resulting from interarea transactions could be computed efficiently.

4.5 Example: line overload

We conclude this chapter with a simple illustration that uses the sensitivity formulas. Assume that the critical event located by the continuation program for the forecast parameter change was a line overload. It is desired to move away from the overload

by adjusting the generator dispatch. Let P represent the vector of generator real power outputs. The state variables z include a slack variable that distributes losses to all generators on AGC. Let λ represent a vector of area export set points and \hat{k} the forecast direction of change in area exports corresponding to a transaction between multiple areas. \hat{k} is normalized so that a margin is measured in total real power exports from one area.

For the line overload (and events such as generator VAR limits and under or over voltage limits) E takes a particularly simple form

$$E(z, \lambda, p) = z[i] - Z_{lim}[i] \quad (89)$$

where the line current is the i th component of the state variable z . Thus,

$$E_z = e(i) \quad (90)$$

$$E_p = 0 \quad (91)$$

and $F_z|_{(z_*, \lambda_*)}$ is non-singular.

Alternatively, one can consider the line flow not an element of z , in which case $E_z|_{(z_*, \lambda_*)}$ is the derivative of the flow with respect to the state variables and is a simple formula to compute. Depending on the rating used, the flow can be measured in MVA, MW, or Amp; the form of E and E_z is different for each.

The first step is to compute w , a vector in the null space of $(F_z|_{(z_*, \lambda_*)}^T, e(i)^T)$. The derivative of the equilibrium equations with respect to the generator real power outputs is F_p and is a diagonal matrix with non-zero entries only in the rows corresponding to the generator real power balance equations. By formula (88), the direction to change the dispatch that increases the transfer margin to the line overload the most is $N = w \begin{pmatrix} F_p \\ 0 \end{pmatrix} \Big|_{(z_*, \lambda_*)}$.

Now suppose that it is not reasonable to change the dispatch in that manner, but another dispatch, p_1 is proposed so that $p_0 + \Delta p = p_1$. The linear estimate of the change in transfer margin then is

$$\Delta M = \frac{-w \begin{pmatrix} F_p \\ 0 \end{pmatrix} \Big|_{(z_*, \lambda_*)}}{w \begin{pmatrix} F \lambda \hat{k}_* \\ 0 \end{pmatrix} \Big|_{(z_*, \lambda_*)}} \Delta p \quad (92)$$

Alternatively, or if it is desired to check for other possible limit violations, equation (12) can be employed to also estimate how the equilibrium state changes at the projected overload. In this case, the linear system (12) has multiple right hand side

since F_p is a matrix so it is best to parameterize p by a scalar t so that (12) is computed using the vector right hand side $F_p \dot{p}$, yielding \dot{Z} so that $\Delta Z = \dot{Z} \Delta t$ where $\Delta p = F_p \dot{p} \Delta t$.

Finally, the most economical direction to dispatch generation and not cause overload can be found by solving a linear program minimizing the cost of generation subject to the constraint that equilibrium is met and the line rating is not exceeded. If $\Theta(p)$ is the generator cost function, and β the reciprocals of the penalty factors, the linear program minimizes $\Theta_p \Delta p$ subject to the constraints that

$$\beta \Delta p = 0 \tag{93}$$

and

$$N \Delta p \leq 0 \tag{94}$$

The next two chapters detail the case where the critical event is a fold bifurcation of the equilibrium equations.

Chapter 5

Margin and Sensitivity Methods for Voltage Collapse

This chapter concerns computing and exploiting the sensitivity of the loading margin to voltage collapse with respect to various parameters. The main idea of this chapter is that after the loading margin has been computed for nominal parameters, the effect on the loading margin of altering the parameters can be predicted by Taylor series estimates. [GDA97] is a concise version of this chapter.

Loading margin is a fundamental measure of proximity to voltage collapse. Linear and quadratic estimates to the variation of the loading margin with respect to any system parameter or control are derived. Tests with a 118 bus system indicate that the estimates accurately predict the quantitative effect on the loading margin of altering the system loading, reactive power support, wheeling, load model parameters, line susceptance, and generator dispatch. The accuracy of the estimates over a useful range and the ease of obtaining the linear estimate suggest that this method will be of practical value in avoiding voltage collapse.

5.1 Introduction

Voltage collapse is an instability of heavily loaded electric power systems characterized by monotonically decreasing voltages and blackout [DCL, Davos]. Secure operation of a power system requires appropriate planning and control actions to avoid voltage collapse. This chapter describes and illustrates the use of loading margin sensitivities for the avoidance of voltage collapse.

For a particular operating point, the amount of additional load in a specific pattern of load increase that would cause a voltage collapse is called the loading margin. We are interested in how the loading margin of a power system changes as system parameters or controls are altered. This chapter describes how to compute linear and quadratic Taylor series estimates for the variation of the loading margin with respect to *any power system parameter or control*. The effects on the loading margin of changing the following controls and parameters is estimated:

- Emergency load shedding
- Reactive power support, shunt capacitance
- Variation in the direction of load increase
- Interarea redispatch, wheeling
- Changes to load model and load composition
- Varying line susceptance, FACTS device
- Generator redispatch

Loading margin sensitivities have a simple geometric meaning. Figure 6 shows nose curves of a large power system for three values of a power system parameter. The loading margin is the change in loading between the stable operating point and the nose of the curve corresponding to each parameter setting. The nose corresponds to a saddle-node bifurcation point of the power system when it is parameterized by loading, and is often referred to as the “point of collapse” or “bifurcation point”. A similar set of curves results for varying any other system parameter, such as the line impedance or powerfactor of the load. As the parameter increases, the nose of the curve occurs at a higher loading and the loading margin increases. Figure 7 shows the loading margin as a function of the parameter value. Each nose curve in Figure 6 contributes one point to Figure 7. The sensitivity of the loading margin with respect to the parameter at the nominal parameter value is given by the tangent linear approximation to the curve in Figure 7. *Once the loading margin has been computed for nominal parameters, the effect on the loading margin of altering the parameters can be predicted by using linear or quadratic estimates.* Exhaustively recomputing the nose for each parameter change is avoided.

Loading margin is an accurate measure of proximity to voltage collapse which takes full account of system limits and nonlinearities. Moreover, loading margin estimates can be directly associated with costs, allowing for economic comparison of different strategies [Alv91]. Methods to compute the nose and hence the loading margin are presented in [CA93, CFSB, AC92, VC91, Iba] and are discussed in Chapter 2.

Another approach to assessing proximity to voltage collapse uses fast time-domain simulation to predict whether the system will collapse (e.g. [Kur93, DS93]). This approach has the advantage of better representing the potentially complex series of time dependent events which can influence voltage collapse. For example, the time dependence of generator reactive power limits can be represented. However, sensitivity information is difficult to obtain from time-domain simulations and requires

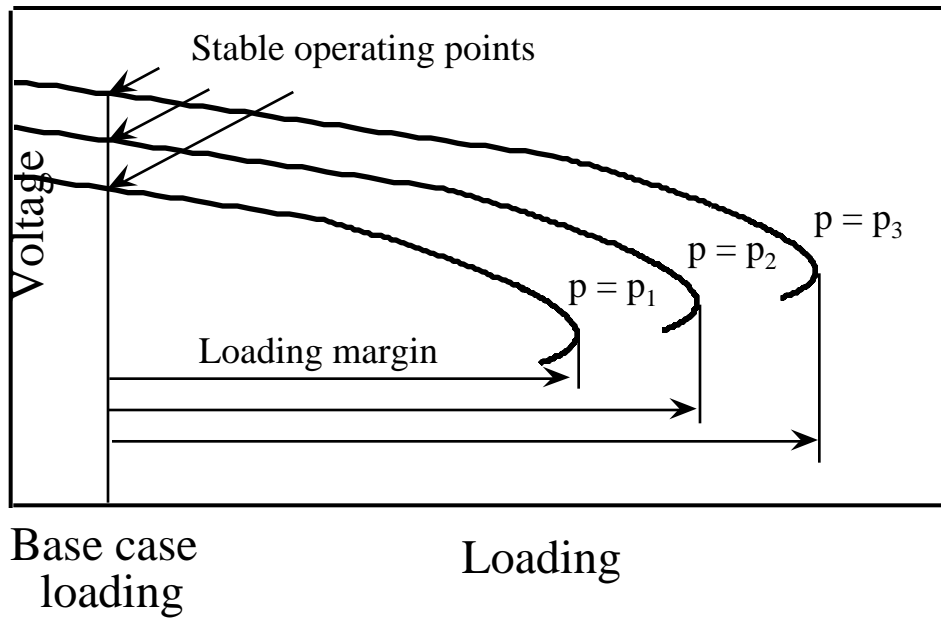


Figure 6: Nose curves as parameter p varies

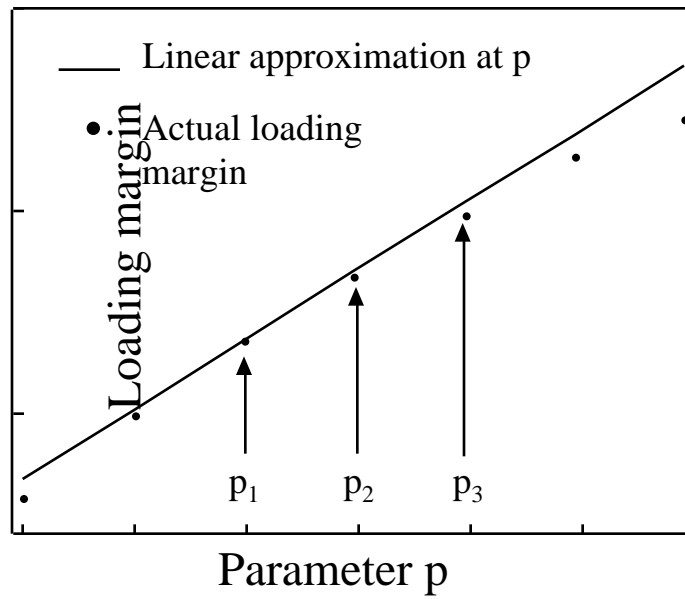


Figure 7: Loading margin as parameter p varies

a new simulation for each parameter variation considered. A single computation of a loading margin uses a power system model with some approximations but can yield a wealth of useful sensitivity information. The loading margin and time-domain simulation approaches are complementary. Recent work combines aspects of both approaches [VC94].

There has been previous work on the sensitivity of various indices for voltage collapse. Tiranuchit and Thomas [TT88] computed the sensitivity of the minimum singular value of the system Jacobian and Overbye and DeMarco [OD91] computed the sensitivity of an energy function index. The first order sensitivity of the loading margin was derived by Dobson and Lu [DL192]. This chapter is an extension and application of [DL192].

In a discussion to [GDA97], Wu, Fischl, and Nwankpa reference [WF93] which uses an optimization formulation (or regularization method) to derive sensitivity formulas similar to those here and in [GDA97]. The first order sensitivity formula of [WF93] can be shown to be equivalent to the first order sensitivity formula derived in this report and in [GDA97]. However, the second order sensitivity formula of [WF93] does not agree with the second order sensitivity formula of [GDA97] and this report. The reason for the discrepancy is an error in the derivation of [WF93]. Wu, Fischl, and Nwankpa raise several topics motivating the work in Chapter 6 and [GDA98]. The complete discussion and closure to [GDA97] appears in the IEEE Transactions [GDA97].

5.2 Theoretical background and assumptions

One influential theory of voltage collapse [DC89] models the power system as differential equations with slowly moving parameters and describes voltage collapse as the dynamic consequence of a saddle node bifurcation. In a saddle node bifurcation, the stable operating equilibrium coalesces with an unstable equilibrium and disappears. The dynamic consequence of a generic saddle node bifurcation is a monotonic decline in system variables.

Although differential equations are the proper setting for understanding voltage collapse and are necessary for explaining why voltages dynamically decrease as a consequence of a saddle node bifurcation, it is possible and very advantageous to compute loading margins to voltage collapse and their sensitivities using static equations [Dob94]. These static equations are equivalent to equations derived from the differential equations by setting all the derivatives to zero. Usually the exact dynamic equations of the power system are poorly known. For example, both the form and data for dynamic load models for voltage collapse studies are controversial. However,

static models of the power system are much better known. The idea is to use the static models for computations, while supposing there to be underlying dynamics of a sensible form whose equilibrium equations reduce to the static models. Dobson [Dob94] proves that there is no loss of accuracy in using static models in place of the underlying dynamic models when computing loading margins and their sensitivities.

The derivations and application of the sensitivity formulas require the choice of a nominal stable operating point at which parameters or controls are to be adjusted, and a projected pattern of load increase. The pattern of load increase determines the nominal bifurcation point (nose) and also defines the direction in which the loading margin is measured. *The bifurcation point should be computed by a method that takes into account system limits such as generator reactive power limits as they are encountered.* In general, the limits enforced at the bifurcation are different than those at the stable operating point. The derivation of the sensitivity formulas requires that the system equations remain the same as parameters are varied. In particular, the limits enforced at the bifurcation are assumed to stay the same as parameters are varied.

5.3 Informal derivation

This section informally derives the first order sensitivity of the loading margin L with respect to any parameter p . See Chapter 4 and the appendices of this chapter for a rigorous derivation of this and the quadratic sensitivity formulas.

Suppose that the equilibria of the power system satisfy the equations

$$f(x, \lambda, p) = 0 \quad (95)$$

where x is the vector of state variables and λ is the vector of real and reactive load powers. Let λ_0 be the real and reactive powers at the operating equilibrium. We specify a pattern of load increase with a unit vector \hat{k} . Then the load powers at the saddle node bifurcation causing voltage collapse are

$$\lambda = \lambda_0 + \hat{k}L \quad (96)$$

where L is the loading margin. The choice of norm is arbitrary, \hat{k} is a unit vector in whatever norm is used to measure the loading margin L . Since \hat{k} is a unit vector, it also follows that $L = |\lambda - \lambda_0|$.

At a saddle node bifurcation, the Jacobian matrix f_x is singular. For each (x, λ, p) corresponding to a bifurcation, there is a left eigenvector $w(x, \lambda, p)$ (a row vector) corresponding to the zero eigenvalue of f_x such that

$$w(x, \lambda, p)f_x(x, \lambda, p) = 0 \quad (97)$$

The points (x, λ, p) satisfying (95) and (97) correspond to bifurcations and a curve of such points can be obtained by varying p about its nominal value p_* . Linearization of this curve about the bifurcation (x_*, λ_*, p_*) yields

$$f_x|_* \Delta x + f_\lambda|_* \Delta \lambda + f_p|_* \Delta p = 0 \quad (98)$$

where f_λ is the derivative of f with respect to the load powers λ and f_p is the derivative of f with respect to the parameter p . ‘ $|_*$ ’ means ‘evaluated at (x_*, λ_*, p_*) ’. Pre-multiplication by $w = w(x_*, \lambda_*, p_*)$ yields

$$w f_\lambda|_* \Delta \lambda + w f_p|_* \Delta p = 0 \quad (99)$$

since (97) implies that $w f_x|_* = 0$. Equation (99) can be interpreted as stating that $(w f_\lambda|_*, w f_p|_*)$ is the normal vector at (λ_*, p_*) to the bifurcation set in a load power and parameter space [DL192].

Using the parameterization of λ by L from (96) yields $\Delta \lambda = \hat{k} \Delta L$ and substitution in (99) gives

$$w f_\lambda \hat{k} \Delta L + w f_p \Delta p = 0 \quad (100)$$

and hence the sensitivity of the loading margin to the change in parameters is

$$L_p|_* = \frac{-w f_p|_*}{w f_\lambda|_* \hat{k}} \quad (101)$$

For the linear estimate we use (101) and

$$\Delta L = L_p|_* \Delta p \quad (102)$$

The same formula holds for multiple parameters p , in which case $w f_p|_*$ is a vector (see appendices). This is useful when approximating the combined effects of changes in several parameters or when comparing the effects of various parameters on the loading margin.

For the quadratic approximation we use (101), (113) and

$$\Delta L = L_p|_* \Delta p + \frac{1}{2} L_{pp}|_* (\Delta p)^2 \quad (103)$$

5.4 Application to test system

The practical use of the sensitivity formulas derived in the previous section and the appendices is illustrated using a particular voltage collapse of the 118 bus IEEE standard test system [wahoo]. (Refer to [wahoo] to reproduce the results. Also area

numbers and bus numbers correspond to those in [wahoo].) The system loading and loading margin is measured by the sum of all real load powers (an L^1 norm). The stable operating point at which we test parameter variation has a total system loading of 5677 MW. Buses critical to the voltage collapse are in area two. The generator dispatch distributes the slack so that generators in each area provide additional real power roughly in proportion to their size. The loads increase proportionally from the base case loading and the voltage collapse occurs for a total load of 7443 MW and a loading margin of 1766 MW. Seven generators reach reactive power limits between the stable operating point and the voltage collapse. (Note that the reactive power limit for generator 4 is increased to avoid complications caused by an immediate instability that would have occurred just prior to the voltage collapse. An immediate instability [DL292] can be caused by a generator reaching a reactive power limit.)

The sensitivity formulas evaluated at the voltage collapse yield linear and quadratic estimates of the loading margin as a function of any parameter. The performance of these estimates is tested for seven different parameters representative of a range of control actions or system uncertainties. The solid lines and dotted curves in Figures 8 thru 14 are the respective linear and quadratic estimates for the loading margin variation as a function of the chosen parameter.

The dots in Figures 8 thru 14 represent the actual values of the loading margin as computed by combined continuation and direct methods [CA93]. The large dots represent the loading margin computed assuming that the reactive power limits which apply *at the voltage collapse* remain the same when the parameters are varied. (This assumption was used in deriving our sensitivity formulas.) The small dots represent the actual loading margin allowing different reactive power limits to apply at the voltage collapse. The small dots are computed by enforcing generator reactive power limits as the loading is increased from the stable operating point.

Both the small and large dots take into account limits as the loading is increased from the base case, but changes in the limits due to parameter variations are only accounted for by the small dots. The small dots test the practicality of using the estimates in a setting where the limits can vary. In Figures 8 thru 13, the assumptions about limits make little difference and the large dots cover the small dots. The effects of limits will be addressed as future work in later chapters.

5.4.1 Emergency load shedding

Bus 3 is a strong candidate for load shedding based on the magnitude of the components of the left zero eigenvector at the bifurcation. At the stable operating point, bus 3 has a load of 60 MW and 15 MVARs and a voltage of .95 p.u. Figure 8 shows the results for shedding up to 60 MW of base load at constant power factor. Each MW

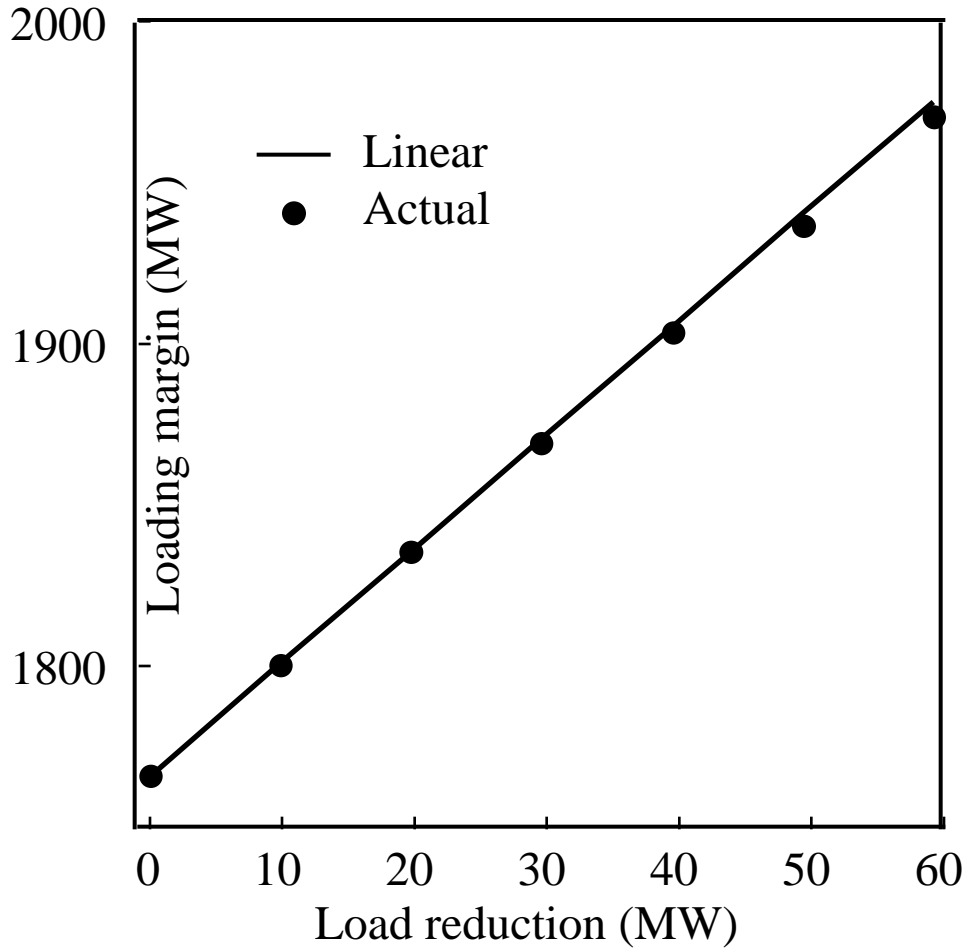


Figure 8: Effect of load shedding on voltage collapse margin

of load reduction increases the loading margin by 3.5 MW, and the relation remains almost linear over the entire range of load shed.

Note that “load shedding” could refer to several distinct situations requiring different use of the Taylor series formulas. For the example shown here, we shed a specific amount of real and reactive power at the base loading at one bus. However, the load at that bus still increases from the base case at the same power factor and at the same rate as assumed for the nominal case. If one wishes instead to estimate the effect of shedding base load *and* not increasing the load at this bus, then one must account for changes to all the system parameters effected. Specifically, the change in the direction of load increase \hat{k} , and the change in base load must both be accounted for. An example of changing the direction of load increase follows.

5.4.2 Direction of load increase

Computing the loading margin requires a direction of load increase to be assumed. Variation in the direction of load increase can result from temperature dependence of the loads or inaccuracies in forecasting. Thus it is useful to estimate the sensitivity of the loading margin to the direction of load increase.

The direction of load increase is multi-dimensional, so that not every conceivable variation can be parameterized in such a way that a 2-dimensional graph is comprehensible. To ease visualization, we choose to parameterize the change in direction by a scalar. For this example, the direction of load increase is varied by transferring load increase from the critical bus 1 to a less critical bus in the same area, bus 23. For a particular loading factor, the total load remains the same but the proportion of load at bus 23 increases and the proportion at bus 1 decreases. Figure 9 shows that a linear estimate for the change in the loading margin performs well over the full range of variation.

5.4.3 Reactive power support

The largest generator in area two is at bus 10, which is connected by a long transmission line to the high voltage side of the network. At the stable operating point, the generator at bus 10 is near its reactive power limit. Bus 9 represents the midpoint of the transmission line, and is a logical place to consider adding reactive power to alleviate the voltage collapse. The addition of shunt capacitance at bus 9 could represent operation of switched capacitors or SVC. Figure 10 shows that the linear estimate is accurate and quantifies the effectiveness of reactive power support at bus 9.

5.4.4 Area interchange

Recent trends in deregulation are expected to increase wheeling which can affect system security.

Figure 11 shows the effects on the loading margin of adjusting the flows between area 2 and the main area. The nominal interchange between the main area and area 2 is 103 MW. Importing an additional 100 MW results in an increase in loading margin of over 200 MW, which is well predicted by the linear estimate.

The adjustment of the interarea flows caused the number of generators reaching reactive power limits to change, yet these changes did not significantly affect the accuracy of the estimates. Most of the additional generators that reached limits were not at critical buses. The linear estimates were accurate for varying the interarea flow by plus or minus 100 percent.

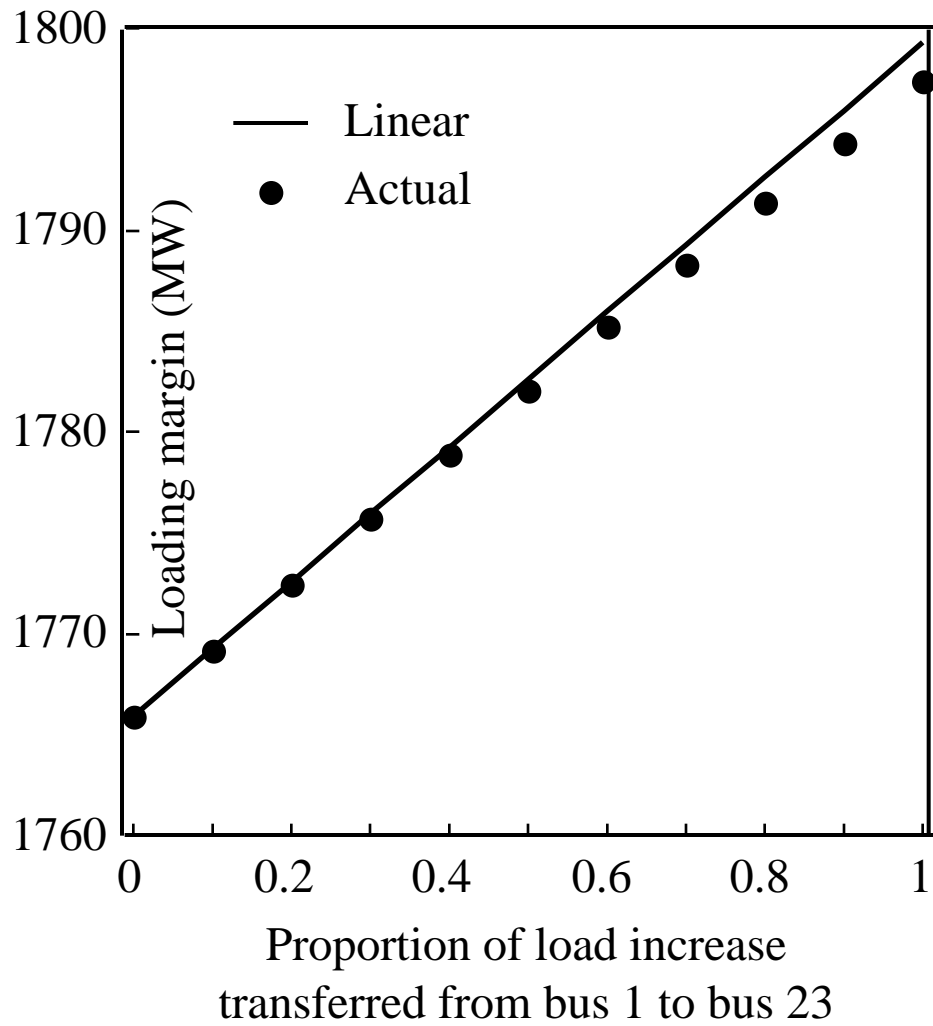


Figure 9: Effect of assumed loading direction on voltage collapse margin

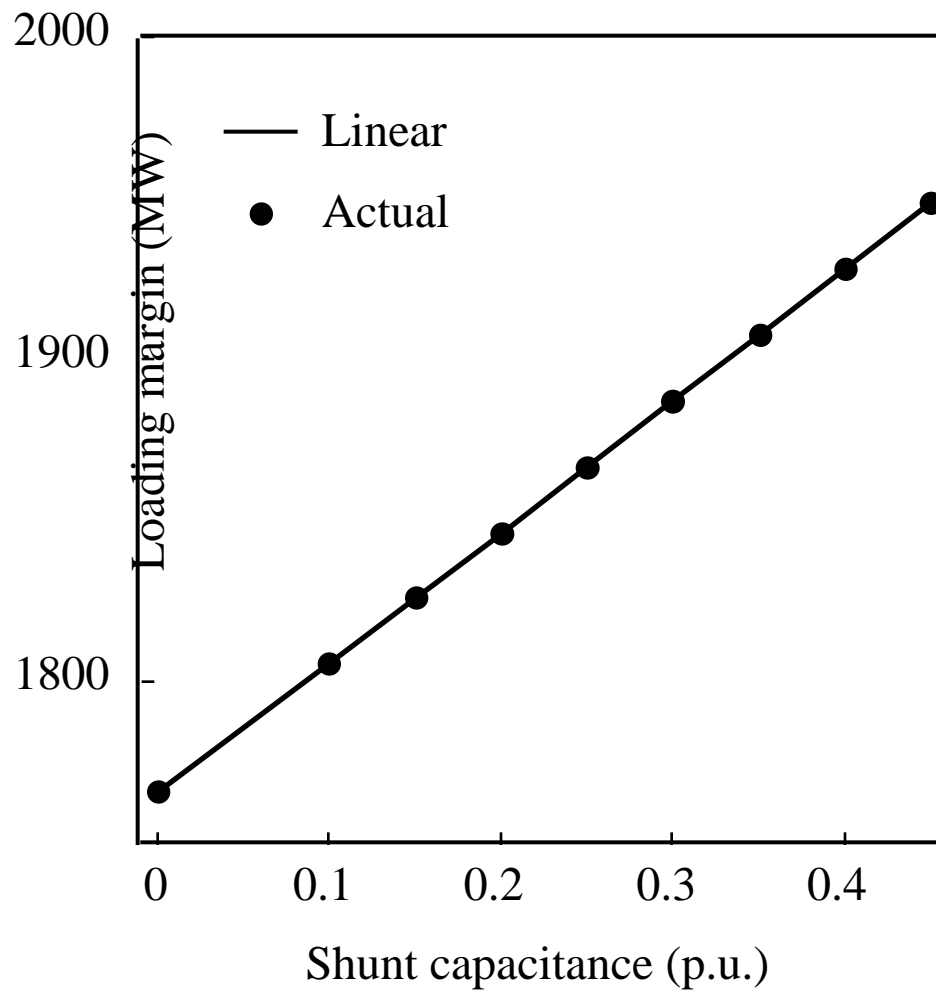


Figure 10: Effect of shunt capacitance on voltage collapse margin

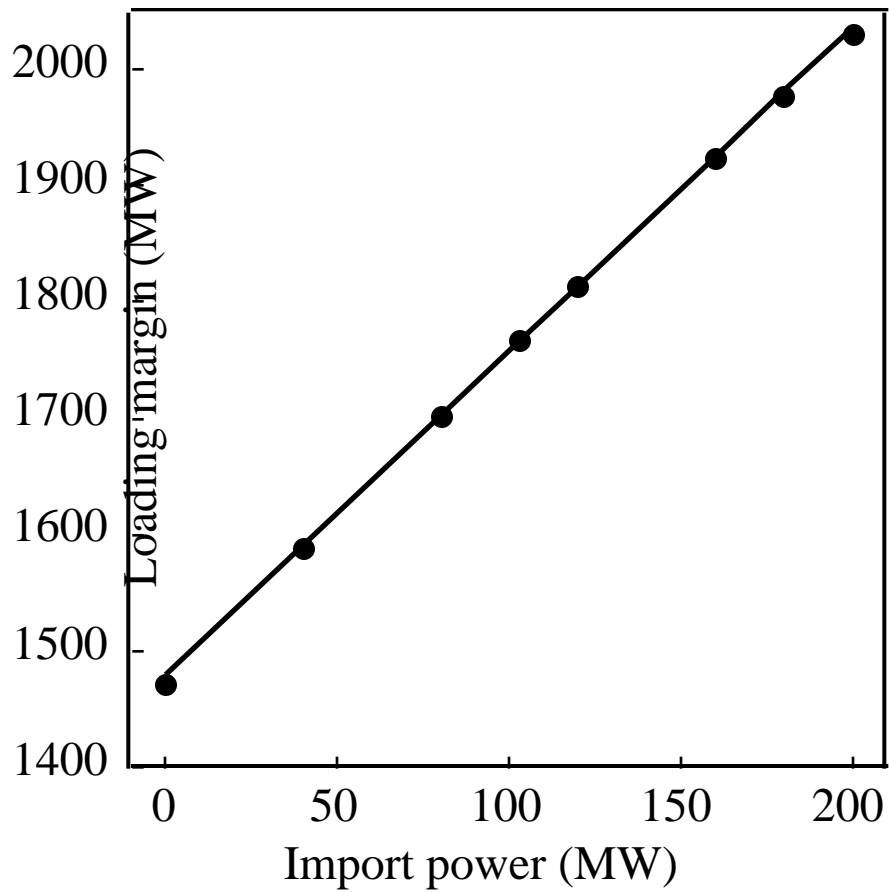


Figure 11: Effect of import into critical area on voltage collapse margin

5.4.5 Load model

Load models are important in voltage collapse studies. The sensitivity of the loading margin with respect to parameters of a load model can be used to estimate the effect on the loading margin of using more detailed models. Figure 12 shows the effect on the loading margin of an additional reactive load Q at bus 3 linearly dependent upon the bus voltage V so that $Q = KV$. K can be interpreted as MVARs at 1 p.u. voltage.

For this case we add voltage dependent load at bus 3, we do not change the constant power factor base load or change the rate of constant power factor load increase. If instead we were to assume that the original base load was voltage dependent, then a different computation would be performed taking account changes to all the parameters affected. In addition, one must specify how the direction of load increase and the loading margin measure are affected by any parameter changes. It is certainly possible to have either or both the direction of load increase or the measure of the loading margin dependent upon some load model parameters. The formulas presented in this chapter are general and can be applied to these cases, but care must be taken in computing the derivatives and applying the chain rule correctly.

5.4.6 Line susceptance

Variations in a line susceptance could represent the operation of a FACTS device or could reflect uncertainty in the network data. Figure 13 shows the effect of altering the susceptance of the line connecting bus 9 to bus 10.

For this example, the quadratic estimate is required to obtain accurate results over the full range of variation and the effects of changing limits are noticeable but not significant.

5.4.7 Generator dispatch

Generators 10 and 12 together assume 50% of the slack for area 2 with generator 10 alone picking up 42% for the nominal dispatch. Figure 14 shows the effect of shifting slack from generator 10 to generator 12. The two generators participate equally in the dispatch when 17% of the total area slack is moved from generator 10 to generator 12.

Figure 14 shows that the distribution of real power can greatly affect the loading margin and that the quadratic estimate is accurate over a much larger range than the linear estimate. Moreover, the effects of limits can be significant. In this case, shifting more than 15% of the total area slack to generator 12 prevents generator 10 from reaching its reactive power limit; additional transfer past this point has little

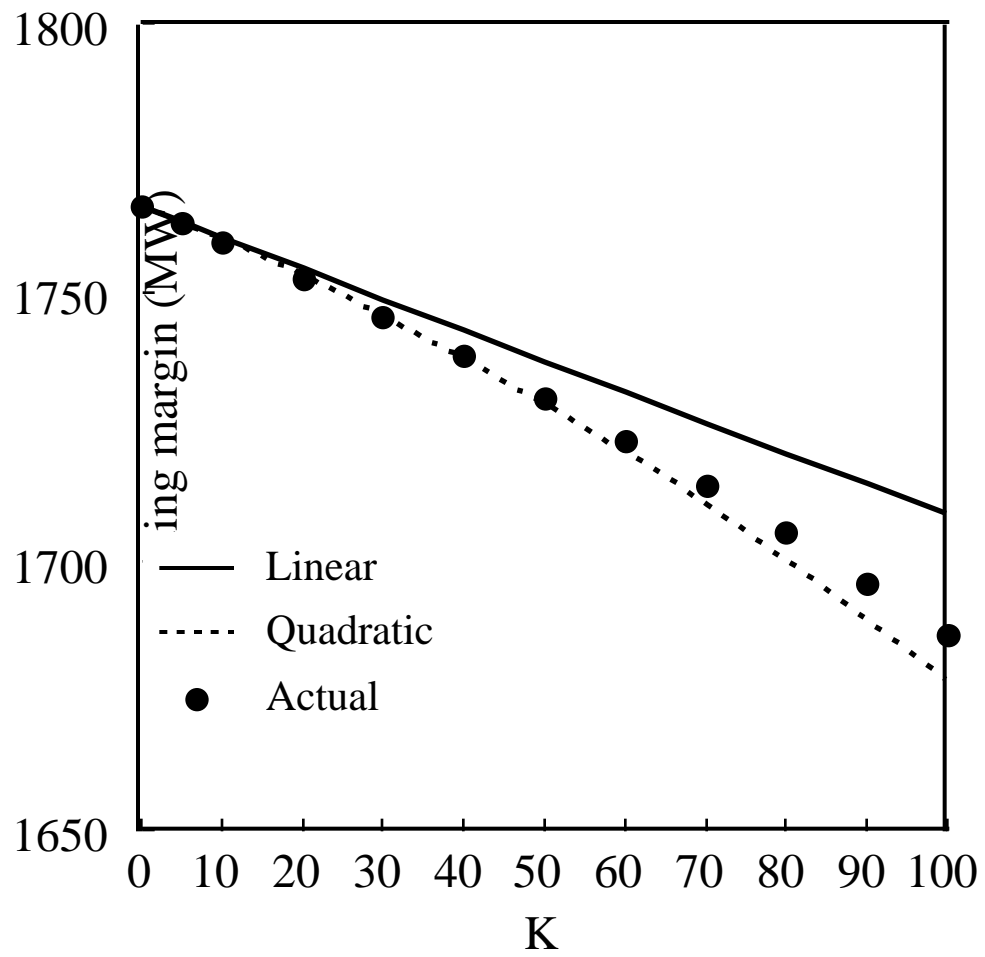


Figure 12: Effect of composition of load model on voltage collapse margin

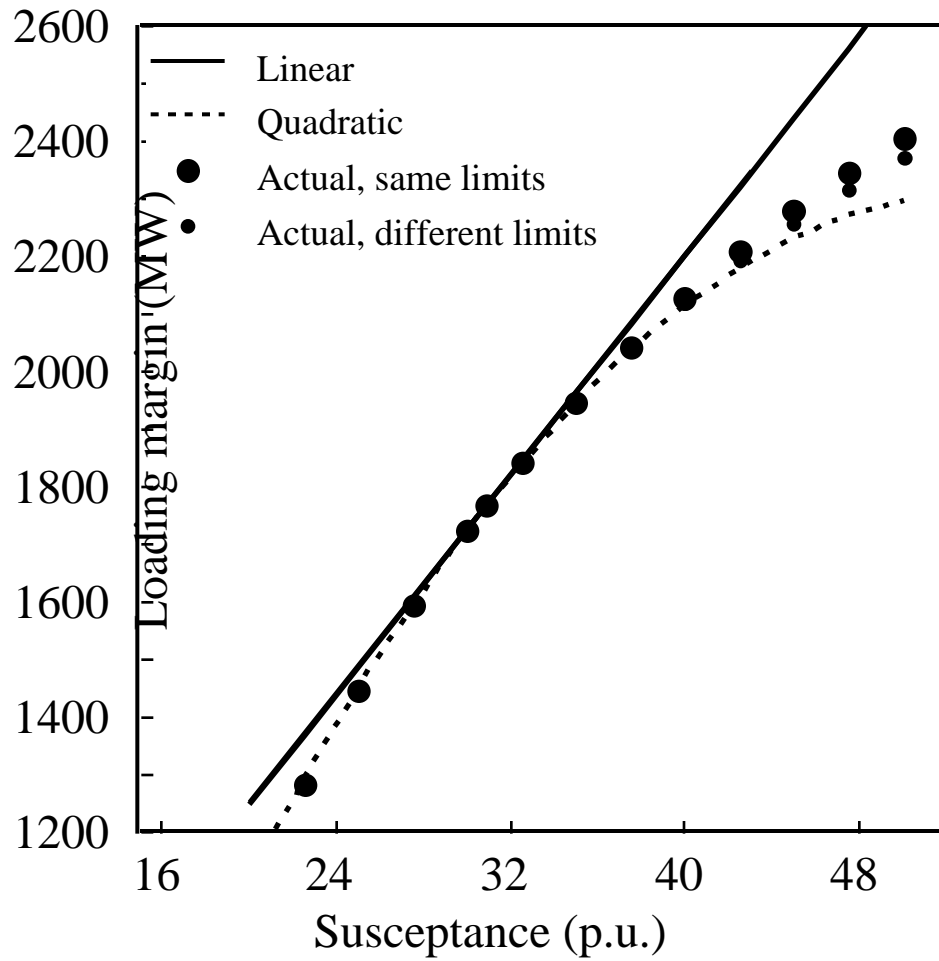


Figure 13: Effect of susceptance on voltage collapse margin

effect on the loading margin.

5.5 Discussion

The loading margin sensitivities only depend on quantities evaluated at the nominal bifurcation point. Evaluation of the linear sensitivity is particularly simple. Once the nominal bifurcation point is computed, the linear sensitivity requires computation of the left eigenvector w and the derivative $f_p|_*$ of the power system equations with respect to the parameter. In many cases $f_p|_*$ has only one or two nonzero entries. w can be found by inverse power methods or as a byproduct of a direct method used to refine location of the bifurcation point [DL192]. Since w is the same regardless of the parameter chosen, it is very quick to compute the sensitivity to any additional parameters.

The quadratic estimate additionally requires solution of a sparse set of linear equations (109,111), the right eigenvector v and some second order derivatives. The second order derivatives include the matrix $wf_{xx}|_*$, where $f_{xx}|_*$ is the Hessian tensor. $wf_{xx}|_*$ can be obtained as a byproduct of a direct method that uses a Newton iteration. The other higher order derivatives are more easily obtained and often evaluate to zero. When the quadratic term is small, it increases confidence in the accuracy of the linear estimate. When the quadratic term is not small, it serves as a more accurate estimate.

One source of inaccuracy is the neglect of higher order terms in the estimates. When the computed bifurcation is near a different bifurcation corresponding to voltage collapse of another area of the system, movement of the parameter can cause the voltage collapse to ‘shift’ from one area to the other. Since the set of critical parameters and loadings could have significant variations in curvature in this case, the linear and quadratic estimates would be useful only over a small parameter range. (The area of the power system corresponding to a bifurcation is described by the right eigenvector v corresponding to the Jacobian singularity since the components of v specify the relative participation of bus voltages and angles in the voltage collapse [DC89, Dob92].)

Another source of inaccuracy is that the estimates assume a fixed set of equations whereas the form of the equations can change discretely whenever a parameter variation causes power system limits to change. The 118 bus system results are examples in which this does not significantly impair the usefulness of the estimates. However, this source of inaccuracy has the potential to be significant and requires awareness when using the estimates. Future work could address the effect of limits on loading margin sensitivities, perhaps by representing the effect of the limits using homotopy methods [GreMS].

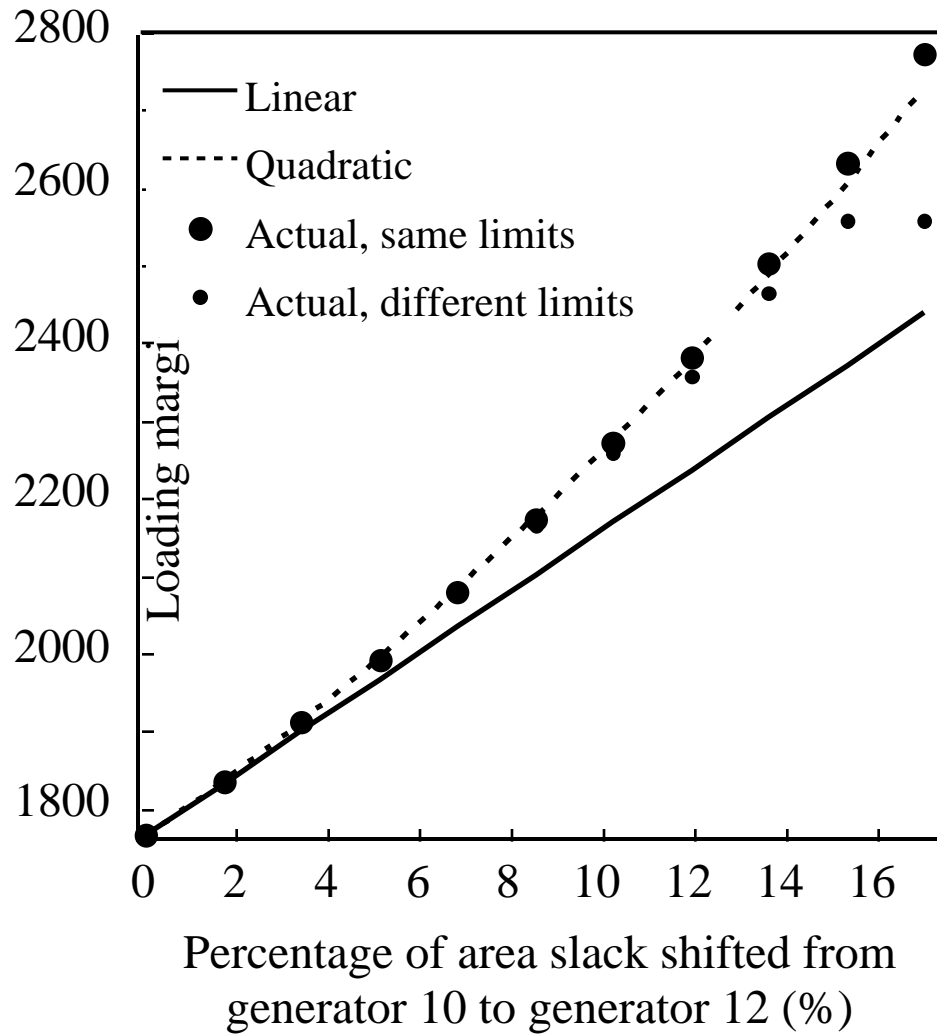


Figure 14: Effect of generator dispatch on voltage collapse margin

The loading margin and sensitivity computations require only static power systems equations but accurately reflect the proximity to voltage collapse of the dynamic power system. In particular, explicit knowledge of load dynamics is not needed.

5.6 Conclusions

In this chapter linear and quadratic Taylor series estimates for the variation of the loading margin with respect to any power system parameter or control are presented. These estimates can be used to quickly assess the quantitative effectiveness of various control actions to maintain a sufficient loading margin to voltage collapse. That is, the computations approximate the change in loading margin for a given change in each control. The estimates are also useful in determining the sensitivity of the loading margin to uncertainties in data. Evaluation of the estimates is efficient; calculation of any number of estimates requires only computation of a single nose or bifurcation point of the power system.

The sensitivity formulas are more rigorously derived in the following appendix. The quadratic estimate is new and the derivation of the linear estimate improves on previous work in [DL192]. The derivation is independent of the norm chosen to measure the loading margin.

The practical use of the sensitivity computations is illustrated for a range of system parameters on a voltage collapse of the IEEE 118 bus system. The likely sources of inaccuracy discussed in the previous section include variations in the generator reactive power limits enforced at the nose. The results suggest that the linear estimate is good for many parameters and can sometimes be improved with the quadratic estimate. Direct comparison of different control actions can be made in terms of their effect on the loading margin. The closeness of the estimates over a useful range of parameter variations and the ease of obtaining the linear estimate suggest that the sensitivity computations will be of practical value in avoiding voltage collapse.

5.7 Appendices

Appendix 5.7.A Derivation of sensitivity formulas

Let $f : \mathbb{R}^n \times \mathbb{R}^m \times \mathbb{R}^l \rightarrow \mathbb{R}^n$ be a smooth function such that the solutions of

$$0 = f(x, \lambda, p) \quad (104)$$

are the equilibria of the power system near (x_*, λ_*, p_*) . We assume that f has a fold bifurcation at (x_*, λ_*, p_*) satisfying:

- F(a) $f(x_*, \lambda_*, p_*) = 0$
- F(b) $f_x|_*$ has rank $n - 1$
- F(c) $w f_\lambda|_* \hat{k} \neq 0$
- F(d) $w f_{xx}|_*(v, v) \neq 0$, where v and w are nonzero vectors satisfying $f_x|_* v = 0$ and $w f_x|_* = 0$.

These are the generic conditions for a fold bifurcation [CH]. (They differ slightly from the conditions for a saddle node bifurcation and the distinction between the two bifurcations is discussed in [Dob94]. The fold bifurcation is more appropriate when working with static equations.)

Let λ_0 be the base case loading and let the unit vector $\hat{k} \in \mathbb{R}^m$ be a given direction in loading space. The loading is parameterized by $\ell \in \mathbb{R}$:

$$\lambda(\ell, \hat{k}, \lambda_0) = \lambda_0 + \ell \hat{k} \quad (105)$$

The loading may be measured with any norm, but different norms lead to different unit vectors \hat{k} . Let

$$g(x, \ell, p) = f(x, \lambda_0 + \ell \hat{k}, p) \quad (106)$$

Since $g_x = f_x$, $g_{xx} = f_{xx}$, and $g_\ell = f_\lambda \hat{k}$, g also has a fold bifurcation at (x_*, ℓ_*, p_*) and the corresponding conditions F(a)-(d) are satisfied with g written for f except that F(c) becomes $w g_\ell|_* \neq 0$.

Appendix 5.7.B proves that near (x_*, ℓ_*, p_*) there is a smooth surface Ψ parameterized by p so that each point on Ψ corresponds to a fold bifurcation. Points on Ψ are of the form $(X(p), L(p), p)$ where $X(p)$ defines the variation of the bifurcating equilibrium with parameter p and $L(p)$ defines the variation of the loading margin with parameter p . In the useful case of one dimensional p , Ψ is a curve. Points of Ψ satisfy

$$g(X(p), L(p), p) = 0 \quad (107)$$

$$\mu(X(p), L(p), p) = 0 \quad (108)$$

(107) states that $(X(p), L(p), p)$ is an equilibrium and (108) is the condition for bifurcation (μ is defined in Appendix 5.7.B).

Differentiation of (107) with respect to p yields

$$g_x X_p + g_\ell L_p + g_p = 0 \quad (109)$$

Evaluation at (x_*, ℓ_*, p_*) and pre-multiplication by w leads to $wg_\ell|_* L_p|_* + wg_p|_* = 0$ and the desired first order result

$$L_p|_* = -\frac{wg_p|_*}{wg_\ell|_*} = -\frac{wf_p|_*}{wf_\lambda|_* \hat{k}} \quad (110)$$

The second order term $L_{pp}|_*$ may be found as follows. Differentiation of (108) (obtained by differentiating (116)) and evaluation at (x_*, ℓ_*, p_*) yields

$$wg_{xx}|_*(v, X_p|_*) + wg_{x\ell}|_* v L_p|_* + wg_{xp}|_* v = 0 \quad (111)$$

which, with (109) evaluated at (x_*, ℓ_*, p_*) , is a set of $n + 1$ linear equations we may solve for $X_p|_*$. F(b) and F(d) imply that these $n + 1$ equations have rank n and are uniquely solvable for $X_p|_*$.

Differentiation of (109) gives

$$\begin{aligned} g_x X_{pp} + 2g_{x\ell} X_p L_p + g_{xx}(X_p, X_p) + 2g_{xp} X_p \\ + g_{\ell\ell} L_p L_p + g_\ell L_{pp} + 2g_{\ell p} L_p + g_{pp} = 0 \end{aligned} \quad (112)$$

Evaluation at (x_*, ℓ_*, p_*) , pre-multiplication by w , and solving for $L_{pp}|_*$ gives

$$\begin{aligned} L_{pp}|_* = \frac{-1}{wg_\ell|_*} \left[2wg_{x\ell} X_p L_p + wg_{xx}(X_p, X_p) + 2wg_{xp} X_p \right. \\ \left. + wg_{\ell\ell} L_p L_p + 2wg_{\ell p} L_p + wg_{pp} \right] \Big|_* \end{aligned} \quad (113)$$

All terms on the right hand side are known and can easily be expressed in terms of f . If the loading λ appears only linearly in (104) then (113) simplifies to

$$L_{pp}|_* = \frac{-1}{wg_\ell|_*} \left[wg_{xx}(X_p, X_p) + 2wg_{xp} X_p + wg_{pp} \right] \Big|_* \quad (114)$$

If, in addition, the parameters p also appear in (104) as linear terms, then $g_{xp} = g_{pp} = 0$ and the last two terms of the bracket in (114) vanish.

Appendix 5.7.B Construction of Ψ .

The surface Ψ of bifurcation points is constructed as the zero section of a smooth function U . Write B^{ij} for the cofactor of the (i, j) element of a matrix $B \in \mathbb{R}^{n \times n}$.

Since condition F(b) states that $g_x|_*$ has rank $n - 1$, we can find i and j such that $(g_x|_*)^{ij} \neq 0$. Since the cofactors of a matrix are smooth functions of the entries of the matrix, there is a neighborhood $S \subset \mathbb{R}^{n \times n}$ of $g_x|_*$ such that $B^{ij} \neq 0$ for $B \in S$. Define the smooth functions $\tilde{w}(B) = (B^{1j}, B^{2j}, \dots, B^{nj})$ and $\tilde{v}(B) = (B^{i1}, B^{i2}, \dots, B^{in})^T$. Then

$$\tilde{w}(B)B = \det B e_j^T \quad \text{and} \quad B\tilde{v}(B) = \det B e_i \quad (115)$$

where e_i is a column vector of all zeros except that the i th position has value one. $\tilde{w}(B)$ and $\tilde{v}(B)$ are non-zero vectors for $B \in S$. Define $w = \tilde{w}(g_x|_*)$ and $v = \tilde{v}(g_x|_*)$. It follows from (115) and $\det g_x|_* = 0$ that $w g_x|_* = 0$ and $g_x|_* v = 0$ so that w and v are nonzero vectors satisfying the conditions in the definition of the fold bifurcation.

Define the smooth map $\beta : S \rightarrow \mathbb{R}$ by $\beta(B) = \tilde{w}(B)B\tilde{v}(B)$. It follows from (115) that $\beta(B) = B^{ij} \det B$. Since g_x is smooth, there is a neighborhood N about (x_*, ℓ_*, p_*) such that $(x, \ell, p) \in N$ implies $g_x|_{(x, \ell, p)} \in S$. Define $\mu : N \rightarrow \mathbb{R}$ by

$$\begin{aligned} \mu(x, \ell, p) &= \beta(g_x(x, \ell, p)) \\ &= \tilde{w}(g_x(x, \ell, p))g_x(x, \ell, p)\tilde{v}(g_x(x, \ell, p)) \end{aligned} \quad (116)$$

and define $U : N \rightarrow \mathbb{R}^n \times \mathbb{R}$ by $U(x, \ell, p) = \begin{pmatrix} g(x, \ell, p) \\ \mu(x, \ell, p) \end{pmatrix}$. Then Ψ is defined as the zero section of U : $\Psi = U^{-1}(0)$.

The matrix $(U_x, U_\ell)|_* = \begin{pmatrix} g_x|_* & g_\ell|_* \\ w g_{xx}|_* v & w g_{x\ell}|_* v \end{pmatrix}$ is invertible if $a = b = 0$ is the only solution to $(U_x, U_\ell)|_* \begin{pmatrix} a \\ b \end{pmatrix} = 0$, or, equivalently,

$$g_x|_* a + g_\ell|_* b = 0 \quad (117)$$

$$w g_{xx}|_* v a + w g_{x\ell}|_* v b = 0 \quad (118)$$

Since F(c) implies that $g_\ell|_*$ is not in the range of $g_x|_*$, to satisfy (117), $b = 0$ and then F(b) implies that $a = \alpha v$ for some scalar α . Then (118) with $b = 0$ yields $\alpha w g_{xx}|_*(v, v) = 0$ and F(d) implies $\alpha = 0$ and $a = 0$. Thus $(U_x, U_\ell)|_*$ is invertible.

It then follows from the implicit function theorem that there is a neighborhood P of p_* and smooth functions $X : P \rightarrow \mathbb{R}^n$ and $L : P \rightarrow \mathbb{R}$ such that $\{(X(p), L(p), p) \mid p \in P\} \subset \Psi$ and $U(X(p), L(p), p) = 0$, which can be rewritten as (107) and (108).

Appendix 5.7.C Sensitivity of the margin to the locally closest fold bifurcation.

In the discussion to [GDA97], Cañizares inquires about sensitivity of the margin when we do not assume a particular direction of load increase but instead allow the direction

of load increase to vary. For example, one may be interested in the sensitivity of the margin to a locally closest bifurcation [Dob93], and thus \hat{k} would not be a constant but must vary to satisfy the conditions of a locally closest bifurcation. Similarly, the example given in this chapter for changing the direction of load increase requires that \hat{k} be considered as a function of the parameter being varied. Specifically, equation (106) could be written

$$g(x, \ell, p) = f(x, \lambda_0 + \ell \hat{k}(p), p) \quad (119)$$

to emphasize the dependence of \hat{k} on p . Equation (110) then becomes

$$L_p|_* = -\frac{wg_p|_* + wg_\ell|_* \hat{k}_p L_0}{wg_\ell|_*} = -\frac{wf_p|_* + wf_\lambda|_* \hat{k}_p L_0}{wf_\lambda|_* \hat{k}} \quad (120)$$

Now we consider the case of the sensitivity of the margin to the locally closest bifurcation. In this case L_0 is the margin from the base loading to the nominal closest bifurcation in the direction \hat{k} . At a locally closest bifurcation,

$$wf_\lambda|_* - \left| wf_\lambda|_* \right| \hat{k}^T = 0 \quad (121)$$

where $|wf_\lambda|_*$ is the norm of $wf_\lambda|_*$. Substituting for $wf_\lambda|_*$ in the numerator of (120) yields

$$L_p|_* = -\frac{wf_p|_* + \left| wf_\lambda|_* \right| \hat{k}^T \hat{k}_p L_0}{wf_\lambda|_* \hat{k}} \quad (122)$$

In general, to find k_p one must specify the norm for \hat{k} as well as the normalization of the eigenvectors. However, for the common case where \hat{k} is a unit vector in an L^2 norm, $\hat{k}^T \hat{k}_p = 0$ and (122) reduces to

$$L_p|_* = -\frac{wf_p|_*}{wf_\lambda|_* \hat{k}} \quad (123)$$

which is exactly the first order sensitivity formula used for the less general parameterizations of λ . This result is also obtained in [Dob93]. The derivation of higher order terms can also be generalized for the case where \hat{k} changes to identify a locally closest bifurcation. However, the formulas will be dependent upon the normalizations assumed and can additionally require computation of the eigenvector sensitivities.

Chapter 6

Contingency Analysis for Voltage Collapse

This chapter presents a contingency ranking method for voltage collapse. The change in the loading margin to voltage collapse when line outages occur is estimated. First a single nose curve is computed by continuation to obtain a nominal loading margin. Then linear and quadratic sensitivities of the loading margin to each contingency are computed and used to estimate the resulting change in the loading margin. The method is tested on a critical area of a 1390 bus system and all the line outages of the IEEE 118 bus system. The results show the effective ranking of contingencies and the very fast computation of the linear estimates. This chapter contains the material presented in [GDA98].

6.1 Introduction

Contingencies such as unexpected line outages often contribute to voltage collapse blackouts. These contingencies generally reduce or even eliminate the voltage stability margin. To maintain security against voltage collapse, it is desirable to estimate the effect of contingencies on the voltage stability margin. Action can then be taken to increase the margin so that likely contingencies do not cause blackout.

Suppose the power system is operating stably at a certain loading level referred to as the “base case loading”. By means of a short term load forecast or otherwise, assume a particular pattern of load increase. The amount of additional load in this direction that would cause a voltage collapse is called the loading margin to voltage collapse. The curve marked “nominal” in Figure 15 shows a specific bus voltage as a function of total system loading. The nose of the curve is associated with voltage collapse [IEEE1, DCL, Davos] and the nominal loading margin is the megawatt distance between the base case loading and the loading at the nose.

Suppose that a contingency such as loss of a line occurs at the base case loading. Assuming that the system stabilizes after the transient, the voltage as a function of loading changes to the curve marked “contingency” in Figure 15. Since the contingency causes the nose to move to a lower loading, the loading margin is reduced. The

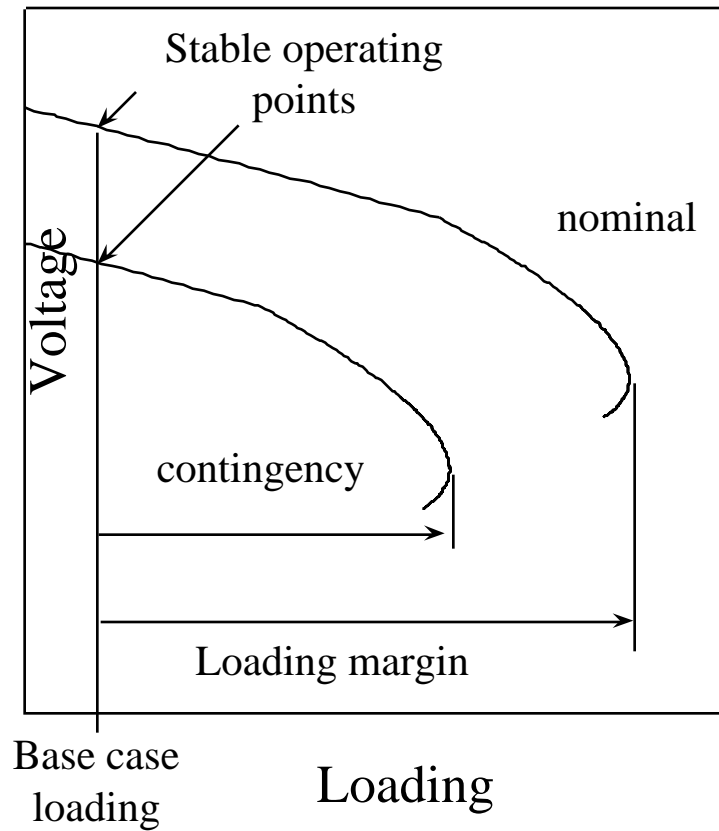


Figure 15: Nominal and contingency nose curves

line outage can be modeled by discretely changing the admittance of the line. The loading margin can then be recomputed. However, the recomputation of the loading margin can be avoided: if the loading margin is thought of as a smooth function of the line admittance, then the sensitivity of the loading margin with respect to changes in the admittance can be calculated and used to estimate the change in the loading margin due to the line outage.

The main idea of this chapter is to compute a single nose curve and associated sensitivities and to use these to quickly estimate the change in the loading margin to voltage collapse for any line outage. This approach uses the general loading margin sensitivity formulas derived in the previous chapters and in [GDA97].

The computations are summarized:

1. A pattern of load increase, generator dispatch policy, and area interchange schedule are forecast or assumed.
2. A continuation method such as [Iba, AC92, CA93, RHSC, CFSB] is used to locate the nose and hence determine the nominal loading margin.
3. Quantities needed for the sensitivity formulas are evaluated at the nose point. Then, for each contingency, the change in loading margin is estimated by evaluating the sensitivity formulas presented in section 4.5.

The accuracy of the estimate can be significantly improved by using quadratic sensitivities.

This chapter only addresses security with respect to voltage collapse; security concerns such as under voltages, thermal overloads, oscillations and transient stability are not addressed.

6.2 Previous work

The overall approach of this chapter is similar to and inspired by [WF93]. [WF93] use quadratic estimates to approximate the effect of contingencies on interarea transfer margins for an 11 bus system. An interarea transfer margin can be viewed as a particular and useful choice of a loading margin and the linear estimate of [WF93] is then equivalent to the linear estimate of this chapter and [GDA97]. The derivation in [WF93] uses an optimization formulation while the derivation in [GDA97] is geometric in nature. However, the formula of [WF93] for the quadratic estimate neglects the implicit dependence of the Jacobian on the operating equilibrium and is different than that used in here (see closure of [GDA97]). The idea of treating a discrete parameter such as line admittance as a continuous parameter has also been presented in [AlvPhD]. Second order sensitivities have been used for power system optimization problems in [PPTT] and [OloPhD].

Contingency screening and analysis concerning line flow and voltage limit violations, as well as transient stability, have been an active research area for several

decades. References [MTK96, SenPhD, Gal84] describe methods of contingency analysis for several operating criteria such as line overloads and voltage limits. A comprehensive bibliography is contained in the recent work [MTK96]. [SenPhD] provides an excellent synopsis of earlier work, and serves as a useful resource and introduction to steady state contingency analysis.

The effect of contingencies on long term voltage stability is addressed in [ABH82, NTSCO, EVMW, FFOCH, FFHH, RAUPG, EIMORT, Weh95, CWF97]. References [FFOCH, FFHH, EIMORT, CWF97] specifically address the effect of contingencies on the margin to voltage collapse. Reference [ZGOY] presents a method of estimating the loading margin to voltage collapse that is applicable to contingency analysis.

[FFOCH] describes a sensitivity based method to estimate the margin to voltage instability, and proposes performing contingency selection by computing an index dependent upon the post-contingency sensitivity of voltage to reactive power. [FFHH] compares the method of [FFOCH] to an optimization method and a curve fit method to determine the margin to voltage instability. [EIMORT], motivated by [FFHH], demonstrates computing three load flows per contingency and fitting a curve to determine the loading margin. [CWF97] perform a similar curve fit with only 2 load flows per contingency. [ZGOY] explains a similar approach and concludes that good results can be obtained with 5 load flow solutions.

The method presented in this chapter differs from [FFHH, EIMORT, CWF97, ZGOY] in that no curve fitting is used, and that post-contingency loading margins are estimated by sensitivity analysis as deviations from a nominal loading margin. The curve fit methods produce voltage profiles so that contingencies can also be screened for voltage magnitude problems as well as stability margin. However, it is difficult to properly account for changes in reactive power limits by fitting curves to only a few equilibrium solutions. The sensitivity method can take account of reactive power limits when the initial continuation computes the nominal nose. The curve fit methods require several load flows to be computed per contingency. The sensitivity methods require a single continuation to find the nominal nose (10 to 100 loadflow solutions) and then require much less computation per contingency. The linear estimate for each contingency is at least three orders of magnitude faster than one load flow solution. The quadratic estimate for each contingency is about equivalent in computational expense to one load flow solution, and thus is faster than any method requiring multiple loadflow solutions per contingency.

The next section describes the test results and is followed by a discussion; the computations are detailed in section 4.5.

6.3 Results

The contingency analysis is tested on two systems. A 1390 bus system is used to assess the computation time and practicality of the method. The 118 bus system tests the effects of encountering generator VAR limits and evaluates all possible line outages on a system vulnerable in multiple areas.

For each system, a base case operating point at which the outages are assumed to occur is identified, a given pattern of load increase is assumed, and a nominal loading margin is obtained by locating the nose point with a continuation method. The system loading and loading margin are measured by the sum of all real load powers. The estimates for each contingency are evaluated at the nominal nose point.

To test the accuracy of the estimates, the actual loading margins are computed for each outage as follows: A post-contingency operating point at the base case loading is obtained by solving several load flows, each for a gradually decreased line admittance until the line is completely outaged. This procedure does not necessarily reflect the settling of the actual system transient, but it is a sensible way to identify a plausible post-contingency operating point [RHSC] (the procedure is needed to avoid convergence to a nearby unstable equilibrium). Then a continuation starting from the post-contingency operating point is used to find the nose as the load is increased in the specified direction. All load flow and continuation computations are performed using the PFLOW package [PFLOW]. The estimates are computed using [MATLAB] and the Sparse Matrix Manipulation System [Alv90, SMMS].

6.3.1 1390 bus system

The estimates are tested on all non-radial 500kV line outages in an area of a 1390 bus system thought to be prone to voltage collapse. The 1390 bus system includes more than 2000 transmission lines and more than 200 transformers.

The base case operating point at which the outages are assumed to occur has a total system loading of 94097 MW and reflects a very heavily loaded system. Both real and reactive power increase from the base case loading at 5 critical buses. The dispatch distributes slack to 25 generators.

For this test, transformer taps are assumed fixed at the base case loading and generator VAR limits encountered above the base case loading are ignored. The total system loading at the nominal point of collapse is 95548 MW corresponding to a loading margin of 1451 MW.

The results ordered by severity are shown in Table 1. The quadratic estimate selects the top 5 and top 12 of the most severe outages. The linear estimate selects 3 of the top 5 and 11 of the top 12. In general, the magnitude of the error increases

with the severity of the outages and the actual loading margins are less than the estimates. The result highlighted with *slanted* typeface indicates a case for which the quadratic estimate captures a critical outage that the linear estimate misses.

The following approximate timings were obtained on a Hewlett Packard 9000 series 700 workstation:

- 1000 linear estimates require 1 CPU second.
- One quadratic estimate requires 15 CPU seconds.
- One iteration of a loadflow requires 2 CPU seconds.
- One loadflow solution requires 5 to 25 CPU seconds.

Thus each linear estimate takes negligible time compared to a loadflow iteration whereas each quadratic estimate takes about the same time as a loadflow solution (several loadflow iterations).

6.3.2 All single contingencies of the 118 bus system

The contingency analysis is next tested using a particular base case and voltage collapse of the 118 bus IEEE test system [GDA97, wahoo]. The base case operating point at which the outages are assumed to occur has a total system loading of 5677 MW. Both real and reactive loads at 91 buses increase proportionally from the base case loading. 17 generators participate in the dispatch with the slack distributed so that generators in each area provide additional real power roughly in proportion to their size. There are 9 fixed tap transformers. A continuation method is used to obtain the nominal loading margin and generator VAR limits apply as demand increases. The nominal voltage collapse occurs for a total load of 7443 MW and a loading margin of 1766 MW. The area interchange is enforced for the entire continuation and the appropriate area interchange equations are included in the computation of the estimates. This case is intended to provide a challenging test for the sensitivity based formulas since the system is stressed in every area, increasing the possibility that some outages may cause a voltage collapse in a different area than that of the nominal collapse. Changes in generator VAR limits were computed during both the procedure to find the post-contingency operating point and the subsequent continuation.

Linear and quadratic estimates for the post-contingency loading margins are evaluated for *all* of the possible line outages (177 outages). Two of the contingencies are so severe that a post-contingency operating point does not exist.

For the 175 survivable line outages, the mean post-contingency loading margin is 1738 MW, 28 MW less than the nominal loading margin of 1766 MW. The mean

Table 1: Estimated loading margins for all 500kV line outages in a critical area of the 1390 bus system.

nominal loading margin = 1451 MW

Linear estimate MW (rank)	Quadratic estimate MW (rank)	Exact MW (rank)
1124 (3)	791 (2)	323 (1)
1083 (2)	864 (3)	706 (2)
1072 (1)	870 (4)	772 (3)
1258 (11)	1078 (5)	866 (4)
1462 (29)	439 (1)	902 (5)
1197 (6)	1195 (9)	973 (6)
1197 (7)	1195 (10)	974 (7)
1219 (9)	1194 (8)	1018 (8)
1219 (10)	1195 (11)	1020 (9)
1216 (8)	1206 (12)	1024 (10)
1184 (4)	1170 (6)	1047 (11)
1185 (5)	1172 (7)	1051 (12)
1393 (16)	1339 (14)	1172 (13)
1416 (19)	1405 (20)	1209 (14)
1348 (12)	1338 (13)	1306 (15)
1366 (13)	1363 (15)	1310 (16)
1366 (14)	1363 (16)	1311 (17)
1398 (17)	1370 (17)	1330 (18)
1398 (18)	1370 (18)	1331 (19)
1379 (15)	1377 (19)	1369 (20)
1442 (25)	1439 (28)	1382 (21)
1421 (20)	1420 (23)	1392 (22)
1436 (21)	1417 (22)	1393 (23)
1437 (22)	1407 (21)	1394 (24)
1441 (23)	1424 (24)	1407 (25)
1441 (24)	1425 (25)	1407 (26)
1445 (26)	1432 (26)	1408 (27)
1446 (27)	1433 (27)	1409 (28)
1450 (28)	1448 (29)	1428 (29)

absolute error of the linear estimate is 20 MW and the mean absolute error of the quadratic estimate is 16 MW. The median error for both the linear and quadratic estimates is less than 1 MW.

In order to determine how assumptions concerning generator VAR limits affect the accuracy of the estimates, actual loading margins were also computed enforcing a fixed set of generator limits, determined by those generators that were at VAR limits at the nominal nose point. (The formulas assume that a fixed set of equations model the equilibrium, i.e. that those generators limited at the nominal nose and only those generators are limited at the post-contingency nose.) The estimates perform better with the set of generators at VAR limits fixed, although for most outages the assumption makes little difference: The mean absolute errors reduce to 13 MW and 10 MW for the linear and quadratic estimates respectively; while the mean actual change in the margin is 21 MW.

The majority of line outages do not significantly affect the loading margin and these are adequately screened by the estimates. Of the 126 outages causing less than a 10 MW change in the loading margin, the mean absolute errors of both the linear and quadratic estimates are less than 1 MW. Only 6 of the 126 outages have an error greater than 3 MW and the maximum error is 10 MW.

Of the 26 outages that cause between a 10 MW and 50 MW change in margin (mean change of 22 MW), the mean absolute errors of the linear and quadratic estimates are 14 MW and 11 MW respectively. The median absolute errors of the linear and quadratic estimates for these outages are 12 MW and 8 MW respectively.

The 25 worst outages resulting in at least a 50 MW change in the margin are shown in Table 2. Estimates of a negative loading margin indicate that the formulas predict that no post-contingency solution exists for the base case loading at which the outage occurs. Both the linear and quadratic estimates select 20 of the 25 most severe outages and 10 of the worst 12. Fifteen of the 25 most severe outages involve lines terminating at a transformer bus. Four of the 25 worst cases can be attributed to the effects of changing generator VAR limits (highlighted with *slanted* typeface). Of these four cases, only one could be somewhat anticipated from the quadratic estimates. With the exception of these four cases, both the quadratic and linear estimates perform well in ranking and grouping the outages.

6.3.3 Multiple contingencies of 118 bus system

Estimates of the effects of multiple contingencies are easily obtained. Linear estimates of multiple contingencies are simply sums of the linear estimates of the single contingencies making up the multiple contingency. Quadratic estimates of multiple contingencies include the sum of the quadratic estimates of the single contingencies

Table 2: Estimated loading margins for the 25 worst outages of the 118 bus system.

nominal loading margin = 1766 MW

Line Outage Bus No.	Linear Estimate MW (rank)	Quadratic Estimate MW (rank)	Exact ¹ MW (rank)	Exact ² MW(rank)
9 10	-376	-1635	fatal	fatal
8 9	93	-962	fatal	fatal
26 30	1502 (1)	1394 (1)	1318 (2)	1029 (1)
4 5	1641 (2)	1545 (2)	1246 (1)	1224 (2)
100 103	1766 (132)	1766 (141)	1766 (139)	1356 (3)
25 27	1646 (3)	1571 (3)	1477 (3)	1468 (4)
23 25	1691 (5)	1636 (5)	1493 (4)	1488 (5)
69 75	1764 (50)	1762 (48)	1768 (163)	1582 (6)
38 65	1664 (4)	1626 (4)	1603 (5)	1591 (7)
22 23	1734 (11)	1710 (10)	1638 (7)	1620 (8)
17 113	1702 (6)	1669 (6)	1633 (6)	1633 (9)
3 5	1731 (8)	1709 (8)	1664 (8)	1664 (10)
11 13	1757 (25)	1750 (19)	1684 (13)	1664 (11)
8 30	1739 (12)	1751 (23)	1668 (9)	1667 (12)
88 89	1766 (113)	1766 (121)	1766 (119)	1669 (13)
17 18	1742 (14)	1724 (12)	1670 (10)	1670 (14)
64 65	1762 (39)	1758 (38)	1740 (26)	1671 (15)
15 17	1731 (10)	1710 (9)	1676 (11)	1676 (16)
30 38	1740 (13)	1742 (17)	1683 (12)	1683 (17)
21 22	1753 (19)	1742 (16)	1689 (16)	1684 (18)
4 11	1716 (7)	1697 (7)	1686 (14)	1686 (19)
23 32	1731 (9)	1712 (11)	1688 (15)	1687 (20)
5 6	1745 (15)	1732 (13)	1704 (17)	1704 (21)
1 3	1760 (31)	1754 (27)	1707 (18)	1707 (22)
2 12	1757 (24)	1750 (18)	1711 (19)	1711 (23)

1. VAR limited generators same as those at nominal nose.
2. VAR limited generators can differ from those at nominal nose.

together with cross terms accounting for interaction between the contingencies.

The quadratic estimate is tested on the 118 bus system with 21 double line outages composed of combinations of 7 single line outages involving 8 buses. (The mean change in the loading margin of these 7 single line outages is 30 MW, and the mean absolute error in the quadratic estimates for these 7 single outages is 13 MW.) The mean change in the loading margin for the 21 double outages is 63 MW. The mean absolute error in the quadratic estimate is 32 MW. If the cross term is neglected, and the estimate found by simply summing the single line quadratic estimates, the mean absolute error is unchanged. For these contingencies, including the cross term of the quadratic estimate has a negligible effect on the accuracy of the estimates.

6.4 Discussion

The 1390 bus results show that the sensitivity formulas are practical for ranking the severity of line outages in large power systems. In particular, the linear estimate takes very little time. Once the nominal point of collapse is found and the zero left eigenvector obtained, 2000 single contingencies could be screened in less time than it takes to solve an average loadflow. The quadratic estimate could then be used to refine the estimates for those cases with the largest linear estimates. The computation time required for the quadratic estimate is approximately equal to the computation time required for an average loadflow.

The linear estimate identifies most severe contingencies. The quadratic term can significantly improve the linear estimate, and occasionally identifies a severe contingency missed by the linear estimate. Significant second order effects seem to be correlated to the outages of lines terminating at transformers, tie lines and their neighbors. Interarea flows are particularly sensitive to outages of tie lines and the flows from the high voltage networks to the low voltage networks are particularly sensitive to outages of lines terminating at transformers. These outages cause large power disturbances and would also be of concern for security issues other than voltage collapse.

The test results with both systems suggest that estimates whose quadratic term is small relative to the linear term are often closer approximations of the actual post-contingency loading margin than those for which the quadratic estimate is large compared to the linear estimate. The estimates almost always underestimate the severity of outages. The 118 bus results demonstrate that although in most cases assumptions regarding changes in limits have little effect, in some cases changes in limits are significant.

It might be desirable to establish more than one nominal collapse by running

continuations from the base case for more than one pattern of loading or different assumptions concerning system operation. For example, since it may be possible to temporarily violate interarea agreements in emergencies, one might want to compute nominal noses both with and without the area interchange enforced. This way, contingencies that cause problems under one set of assumptions but not others could be identified. Also, the nominal nose might be computed for different generator dispatches or load models. The parameter sensitivity methods in [GDA97] and the previous chapters can be used to select scenarios for which the loading margin is likely to vary significantly.

6.5 Computations

For the computations of this chapter, it is sufficient [Dob94] to model the power system with static equations

$$0 = F(x, \lambda, p) \quad (124)$$

where x is the vector of equilibrium states, λ a vector of load parameters, and p a vector of parameters such as line admittances. F should include area interchange, generator dispatch, and any other static controls. If a differential-algebraic or differential equation model of the power system is available then F can be chosen as the right hand side of those equations.

For each single non-radial line outage the parameter vector p is a vector with only three components – one each for conductance, susceptance, and shunt capacitance of the outaged line.

The first step in the computation is to obtain the projected direction of load increase from the short term load forecast. For λ_0 the current vector of load parameters and λ_1 the forecasted short term load, the vector

$$\hat{k} = \frac{\lambda_1 - \lambda_0}{|\lambda_1 - \lambda_0|} \quad (125)$$

defines a unit vector in the direction of load increase.

The second step is to compute the nominal nose by a continuation method. During the continuation, the system equations will change as limits such as reactive power limits apply.

The third step is to evaluate quantities at the nose and then, for each contingency, to evaluate the sensitivity formulas. For the rest of this section, (124) are the power system equations that apply at the nose. In particular, (124) accounts for the power system limits enforced at the nose. The linear and quadratic formulas are derived for general parameter changes in [GDA97] and the previous chapters.

6.5.1 Linear estimate formula

The linear estimate requires that the following quantities be computed at the nose:

- w , the left eigenvector corresponding to the zero eigenvalue of the system Jacobian F_x (F_x evaluated at the nose is singular). It is practical and time saving to compute w simultaneously with locating the nose.
- F_λ , the derivative of F with respect to the load parameters. For constant power load models F_λ is a diagonal matrix with ones in the rows corresponding to load buses.
- F_p , the derivative of F with respect to the line parameters evaluated at the nominal nose point. For a single line outage in any size system F_p has three columns and only four (five for outage of a tie line) nonzero rows in the rows corresponding to the power balance equations at the buses connected by the line. Since the p components appear linearly in F , the nonzero elements of F_p are simply the coefficients of p in F .

Let Δp be the negative of the admittance vector for the line(s) to be outaged. From Chapter 3, equations (101,102), the linear estimate for the change in margin then is:

$$\Delta L = L_p \Delta p = \frac{-w F_p \Delta p}{w F_\lambda \hat{k}} \quad (126)$$

The denominator of (126) is a scaling factor that is the same for all contingencies. The numerator of (126) contains the vector $F_p \Delta p$ which, since p appears linearly in F , is just the terms in F that contain p . For F representing real and reactive power balance, $F_p \Delta p$ is the vector of the pre-contingency real and reactive power injections on the outaged line. The linear formula is simply the power injections from the outaged lines scaled by the normalized left eigenvector $\tilde{w} = -w/w F_\lambda \hat{k}$:

$$\Delta L = \tilde{w}^{P_i} P_i + \tilde{w}^{Q_i} Q_i + \tilde{w}^{P_j} P_j + \tilde{w}^{Q_j} Q_j \quad (127)$$

where P and Q are the pre-contingency real and reactive power injections to the outaged line, i and j indicate the buses connected by the outaged line, and \tilde{w}^{P_i} represents the scaled left eigenvector component corresponding to real power balance at bus i . Formula (127) implies that lines with small flows are guaranteed to have small linear estimates.

Radial line outages that isolate a portion of the network are a special case in which the power balance equations of the isolated bus should be deleted from F . Thus, for a radial line outage F_p has only 2 nonzero rows corresponding to power balance at the connected bus.

6.5.2 Quadratic estimate formula

The quadratic estimate additionally requires the following quantities evaluated at the nose:

- v , the right eigenvector corresponding to the zero eigenvalue of F_x .
- wF_{xx} , the matrix formed by product of w with the Hessian tensor F_{xx} . F_{xx} does not need to be found independently since wF_{xx} can be obtained as a by-product of simultaneously solving for the exact nose point and w with a direct method.
- F_{xp} , the derivative of the Jacobian with respect to the line parameters. For a typical single line outage F_{xp} has at most 34 nonzero elements (16 each for the matrices corresponding to conductance and susceptance and 2 for the matrix corresponding to shunt capacitance). Since the line parameters appear linearly in the equilibrium equations, the nonzero elements are simple expressions of the voltages and angles at the buses connected by the outaged line.
- X_p , the sensitivity of the nose equilibrium with respect to p . (X is the position of the nose equilibrium; it varies with line parameters p .)

From Chapter 3, equations (101,102), the quadratic estimate of the change in loading margin is

$$\Delta L = L_p \Delta p + \frac{1}{2} \Delta p^T L_{pp} \Delta p \quad (128)$$

where

$$L_{pp} = -\frac{X_p^T w F_{xx} X_p + 2w F_{xp} X_p}{w F_{\lambda} \hat{k}} \quad (129)$$

and X_p is found by solving a sparse linear system with multiple right hand side:

$$\begin{pmatrix} F_x \\ w F_{xx} v \end{pmatrix} X_p = \begin{pmatrix} -F_p - F_{\lambda} \hat{k} L_p \\ -w F_{xp} v \end{pmatrix} \quad (130)$$

($w F_{xx} v$ is a row vector). Note that the linear estimate for the resulting change in the nose equilibrium is

$$\Delta X = X_p \Delta p \quad (131)$$

and may be used to identify those contingencies likely to violate additional generator VAR or voltage limits prior to voltage collapse. (Generator reactive power outputs are components of X .)

When formulas (128) and (129) are applied to a double contingency, the number of parameters in p and the dimensions of the vectors and matrices L_p , L_{pp} double. The quadratic estimate for a double contingency takes into account interaction between the two contingencies and is different from the sum of the quadratic estimates for the corresponding two single contingencies.

6.5.3 Computational efficiency

This section analyzes the computational expense of the contingency analysis. For comparison, each step of the computations will be likened to one loadflow solution or one iteration of a loadflow solution. Generally, any technique used to speed the process of computing a loadflow solution or loadflow iteration could also be used to speed up the computation of the estimates.

The slowest step in the procedure is the initial continuation to find the nominal nose. This continuation is only performed once, and any number of linear and quadratic estimates can be subsequently computed. The computational effort required for this continuation depends strongly on the system, the loading margin, the continuation algorithm, the desired accuracy, and assumptions about limits, and can range from several loadflow solutions to hundreds of loadflow solutions.

Quantities to be computed at the nominal nose only once are the left eigenvector w and the scaling factor $wF_\lambda \hat{k}$ (the quadratic estimate also requires the right eigenvector v). The cost of computing each eigenvector is roughly equivalent to one loadflow iteration.

The only computation required for each linear contingency estimate is finding the numerator of (126), and this just requires evaluating $F_p \Delta p$ at the nose and multiplying it by w . $F_p \Delta p$ could be obtained directly from the nominal loadflow computation (the pre-contingency flows on the outaged line), but computing it by sparse multiplying F_p and Δp is also very fast. The computational effort to obtain $wF_p \Delta p$ for one contingency is less than 10 flops if $F_p \Delta p$ is found directly from the loadflow solution and at most 25 flops if $F_p \Delta p$ needs to be recomputed. This expense is independent of system size since F_p always has only four or five nonzero rows. For an N bus system with $2N$ lines, obtaining all the linear estimates requires less than $20N$ flops – less than one iteration of the loadflow for any system with more than just 20 buses (a load flow iteration requires approximately N^2 flops). *On a practical system, once a nominal nose and the left eigenvector have been found, linear estimates for all the line outages can be obtained in less time than needed to obtain one loadflow solution.*

The quadratic estimate requires the one time computation of v , wF_{xx} , and the factoring of the matrix $\begin{pmatrix} F_x \\ wF_{xx}v \end{pmatrix}$ of (130). The quantities v and wF_{xx} are obtained from solution of the nominal nose at negligible cost. The cost of factoring $\begin{pmatrix} F_x \\ wF_{xx}v \end{pmatrix}$ is less than one iteration of a loadflow, and in practice this may require only a partial refactoring since F_x must be already factored for solution of the nominal nose.

The dominant step in the evaluation of each quadratic estimate is obtaining X_p , which is found by solving the sparse linear system (130). The cost of setting up

(130) for each contingency is just several sparse multiplications, less than N flops. Solving for X_p is roughly equivalent to three loadflow iterations. The remaining multiplications to establish the quadratic estimate require less than N flops, so that each quadratic estimate is roughly as expensive as several iterations of the loadflow and costs on the order of N^2 flops. The additional cost to compute any double contingency is negligible. The cost to compute one quadratic estimate for any single or double contingency is about equal to the cost of obtaining one loadflow solution.

6.6 Conclusion

This chapter demonstrates that effective contingency analysis for voltage collapse can be done by computing the loading margin sensitivities for a single nominal nose curve computation. This approach can take into account some of the effects of reactive power limits and easily handles multiple contingencies. The results show that the linear estimates are extremely fast and provide acceptable contingency ranking. For example, after the single nose curve and a left eigenvector are computed, the linear estimates of *all* single line outages for a practical system are computed in less time than is typically required for one load flow solution. The quadratic estimates refine the linear estimates and are more costly but are still faster than previous methods. The sensitivity calculations in the previous chapters and [GDA97] exploit the same single nose curve and can be used to quickly select corrective actions to improve the loading margin to voltage collapse if the contingency analysis indicates a need for this.

Chapter 7

Margin sensitivity methods applied to the power system of Southwest England

This chapter applies the sensitivity methods developed in the previous two chapters to a model of the Southwest of England electric power system to determine their effectiveness in operating the system sufficiently far from voltage collapse blackouts. The system data was graciously provided by the National Grid Company, plc.

The National Grid Company currently employs path following and sensitivity techniques for margin determination that are presented in [HSS, HawPhD, ECSW] based on the methods of [FFOCH]. The margin computation used here is practically the same, in that a predictor corrector path following method is used to establish the margin to events. However, the sensitivity computation differs from that presented in [ECSW]. The computation used in [ECSW] and described in detail in [LöfPhD] is the sensitivity of the smallest singular value of the system Jacobian matrix to system parameters, and is computed at a nominal stable operating point. The sensitivity computation used in this chapter is described in Chapters 4, 5, and 6, and [GDA97, GDA98] and reflects the sensitivity of the margin to the event with respect to any system parameters. One key difference is that the sensitivity computations tested here are evaluated at the event point, not the nominal stable operating point.

The two main uses of the sensitivity methods are

1. Quickly quantify the effect of varying power system controls or parameters on the proximity to voltage collapse
2. Quickly rank the severity of contingencies with respect to voltage collapse

The results confirm that the sensitivity methods perform well on the Southwest of England model for these uses. This chapter also examines the effect of generator VAR limits and presents a sensitivity computation for cases in which instability is directly precipitated by a VAR limit.

7.1 Introduction

For a particular operating point, the amount of additional load in a specific pattern of load increase that would cause a voltage collapse is called the loading margin. This chapter describes computing and exploiting the sensitivity of the loading margin to voltage collapse with respect to various parameters. The main idea is that after the loading margin has been computed for nominal parameters, the effect on the loading margin of altering the parameters can be predicted by Taylor series estimates. The linear Taylor series estimates are extremely quick and easy and allow many variations on the nominal case to be quickly explored. Exhaustively recomputing the point of voltage collapse instability for each parameter change is avoided.

7.2 Nominal voltage collapse margin

Computing the nominal voltage collapse

The nominal point of voltage collapse is the theoretical limit of the steady state model of the power system and is not a reasonable point at which to operate the actual power system. However, by computing the nominal point of collapse, and thus the loading margin to collapse, one can assess the security of the actual system operated at a nominal stable operating point. In addition, the effects of contingencies and events on the security of the actual system can be analyzed by computing the effects of the contingencies and events on the loading margin to collapse.

The test system consists of 40 buses representing a portion of the South West Peninsula power grid and is described in [HawPhD]. For this study, transformer taps and switched compensation devices were assumed fixed. The branch and transformer parameters are shown in Tables 3 and 4 respectively.

The derivations and application of the sensitivity formulas [GDA97] require the choice of a nominal stable operating point at which parameters or controls are to be adjusted, and a projected pattern of load increase. The nominal stable operating point is shown in Table 5. Bus types are differentiated as:

- ‘PQ’, bus voltage and angle vary to maintain specified real and reactive power injections.
- ‘PV’, reactive power output and bus angle vary to maintain specified real power injection and voltage.
- ‘VA’, real and reactive power output vary to maintain specified bus voltage and angle.

Table 3: Transformer data

Tap Bus	Impedance Bus	Circuit Number	Resistance p.u.	Reactance p.u.	Charging p.u.	nominal tap
1	29	1	0.001418	0.083418	0	1.111
1	29	2	0.00123	0.079708	0	1.111
2	30	1	0.001809	0.08	0	1.001
2	30	2	0.001473	0.079666	0	1.001
3	31	1	0.001628	0.084166	0	0.958
4	31	1	0.001614	0.083541	0	0.958
5	32	1	0.001701	0.083125	0	1.102
5	32	2	0.001743	0.083041	0	1.102
9	35	1	0.00075	0.0388	0	1.038
10	33	1	0.00073	0.0412	0	1.056
11	34	1	0.0004	0.02056	0	1.024
8	36	1	0.001458	0.080458	0	1.169
27	37	1	0.001859	0.08	0	0.94
28	37	1	0.001697	0.080875	0	0.94
39	38	1	0.000108	0.006375	0	1.0
20	19	1	0.00205	0.0805	0	1.0
22	21	1	0.00205	0.0805	0	1.0
13	12	1	0	0.033333	0	1.0
6	5	1	0	0.033333	0	1.0

Table 4: Branch data

Tap Bus	Impedance Bus	Circuit Number	Resistance p.u.	Reactance p.u.	Charging p.u.
29	30	1	0	0.11721	0
31	32	1	0	0.034641	0
31	30	1	0	0.07906	0
32	36	1	0	0.1038	0
37	36	1	0	0.022255	0
27	19	1	0.000944	0.00759	0.12472
28	21	1	0.000943	0.007571	0.11711
1	2	1	0.001173	0.009338	0.28787
1	3	1	0.002284	0.018398	0.5546
2	4	1	0.001106	0.009019	0.26562
3	5	1	0.00118	0.009832	0.2772
4	5	1	0.001173	0.009776	0.27568
5	9	1	0.000436	0.005956	0.2473
7	17	1	0.000641	0.005102	0.15718
8	17	1	0.000641	0.005102	0.15718
9	11	1	0.001122	0.015332	0.63657
5	10	1	0.000909	0.012123	0.50235
10	11	1	0.000645	0.008821	0.36627
11	12	1	0.000963	0.013157	0.54617
11	38	1	0.000728	0.009951	0.4129
12	14	1	0.000483	0.006598	0.27397
12	38	1	0.000306	0.003964	0.7604
12	15	1	0.000936	0.007448	0.22967
12	15	2	0.000936	0.007448	0.2297
12	25	1	0.000779	0.010648	0.44213
12	25	2	0.000779	0.010648	0.4421
14	38	1	0.000246	0.003362	0.13961
15	16	1	0.000211	0.002885	0.11979
15	16	2	0.000211	0.002885	0.11979
16	23	1	0.001964	0.015628	0.48192
16	23	2	0.001964	0.015628	0.48192
16	24	1	0.000523	0.00713	0.7547
17	19	1	0.00035	0.024146	0.058978
17	21	1	0.00035	0.024146	0.058978
17	23	1	0.002077	0.016536	0.5098
17	23	2	0.002077	0.016536	0.5098
25	26	1	0.000617	0.008432	0.35012
25	26	1	0.000617	0.008432	0.3501
26	40	1	0.000523	0.00715	0.29655
26	40	2	0.00052	0.00711	0.295
1	7	1	0.00409	0.034082	0.96111
1	8	1	0.00409	0.034082	0.9611
5	7	1	0.000918	0.007305	0.22515
5	8	1	0.000918	0.007305	0.22515
18	17	1	0.000115	0.01055	0
12	38	1	0.000306	0.003964	0.7604
16	24	2	0.000523	0.00713	0.7547

Table 5: Nominal stable operating point

Bus No.	Bus Name	Bus Type	Voltage (p.u.)	Angle (degrees)	Load (MW)	Load (MVAR)	Generation (MW)	Generation (MVAR)
1	INDQ4	PQ	1.014	-1.437	-	-	-	-
2	LAND4	PQ	1.007	-1.648	-	-	-	-
3	ABHA4T	PQ	1.011	-0.852	-	-	-	-
4	ABHA4U	PQ	1.008	-1.097	-	-	-	-
5	EXET4	PQ	1.016	-0.142	-	-	-	-
6	EXET0	PV	1.020	-0.142	-	-	-	12.9
7	TAUN4J	PQ	1.016	0.956	-	-	-	-
8	TAUN4K	PQ	1.018	0.865	-	-	-	-
9	AXMI4	PQ	1.014	-0.317	-	-	-	-
10	CHIC4	PQ	1.013	-0.201	-	-	-	-
11	MANN4	PQ	1.008	-0.033	-	-	-	-
12	LOVE4	PQ	1.006	0.721	422.0	-63.8	-	-
13	LOVE0	PV	1.010	0.721	-	-	-	11.1
14	NURS4	PQ	1.005	1.212	200.4	48.4	-	-
15	FLEE4	PQ	1.006	-0.416	469.1	96.5	-	-60.0
16	BRLE4	PQ	1.009	-0.478	-	-	-108.8	86.3
17	HINP4	PQ	1.014	2.109	-	-	-	-
18	HINP0	PV	1.000	8.683	-	-	1099.1	-77.7
19	HINP2J	PQ	0.994	3.476	-	-	-	-
20	HINP0J	PV	1.000	13.140	-	-	207.8	19.6
21	HINP2K	PQ	0.994	3.488	-	-	-	-
22	HINP0K	PV	1.000	13.153	-	-	207.8	19.7
23	MELK4	PQ	1.015	-0.140	-	-	-392.6	42.5
24	DIDC4	PV	1.005	-0.541	-	-	-38.6	-177.0
25	BOLN4	PQ	0.998	0.573	518.5	117.3	-	-
26	NINF4	PQ	0.994	1.710	358.4	153.1	-	-
27	BRWA2Q	PQ	0.987	3.036	-	-	-	-
28	BRWA2R	PQ	0.987	3.054	-	-	-	-
29	INDQ1	PQ	0.898	-8.621	294.8	63.7	-	-
30	LAND1	PQ	0.969	-5.284	131.6	39.1	-	-
31	ABHA1	PQ	0.984	-4.412	157.9	46.9	-	-
32	EXET1	PQ	0.951	-3.881	142.2	22.4	-	-
33	CHIC1	PQ	0.956	-1.228	40.0	5.6	-	-
34	MANN1	PQ	0.960	-4.609	368.5	91.6	-	-
35	AXMI1	PQ	0.967	-2.289	84.2	22.4	-	-
36	TAUN1	PQ	0.962	-1.860	31.6	6.7	-	-
37	BRWA1	PQ	0.992	-1.658	200.1	-	-	-
38	FAWL4	PQ	1.005	1.841	156.0	57.4	-	-
39	FAWL0	PV	1.000	8.420	-	-	1806.5	-9.5
40	DUNG4	VA	0.996	3.400	-	-	819.1	-26.4

Table 6: Reactive power limits

Bus No.	Bus Name	Maximum (MVAR)	Minimum (MVAR)
6	EXET0	150	-75
13	LOVE0	150	-75
18	HINP0	660	-9999
20	HINP0J	150	-9999
22	HINP0K	150	-90
24	DIDC4	9999	-9999
39	FAWL0	470	-9999

Table 7: Direction of load increase

Bus No.	Bus Name	Real Power	Reactive Power
29	INDQ1	0.2032	0.0439
30	LAND1	0.0907	0.0270
31	ABHA1	0.1089	0.0324
32	EXET1	0.0980	0.0154
33	CHIC1	0.0276	0.0039
34	MANN1	0.2540	0.0632
35	AXMI1	0.0581	0.0154
36	TAUN1	0.0218	0.0046
37	BRWA1	0.1379	0.0000

The pattern of load increase is a direction in loading space along which the loading margin is measured. The direction of load increase is shown in Table 7. Note that the sum of the real power components of the load direction is unity. Thus the direction of load increase is a unit vector using the L^1 norm.

The nominal point of collapse must be computed by a method that takes into account system limits such as generator reactive power limits as they are encountered. In general, the limits enforced at the point of collapse are different than those at the stable operating point.

The nominal voltage collapse was established as follows: From the base case equilibrium point (Table 5) representing a total load of 3575 MW, the loading was gradually increased at the specified buses in the proportions shown in Table 7. The effect of generators reaching VAR limits listed in Table 6 was modeled by replacing ‘PV’

buses with ‘PQ’ buses at the loading at which VAR limits were reached. Transformer taps were held fixed at the starting ratios. No other changes to the network parameters were implemented. In particular, no shunts were adjusted as the loading was increased. The base case system encountered a voltage collapse at a total load of 5380 MW, and thus the nominal margin is 1805 MW. Prior to voltage collapse, the PV buses at EXET0, FAWL0, and LOVE0 encountered VAR limits, and the PV bus at HINP0 was very close to reaching its VAR limit. Table 8 shows the solution at the nominal point of collapse. Generators that have reached reactive power limits are indicated in **bold face** as is the VAR output at HINP0 which is precariously close to a VAR limit.

The Jacobian of the equilibrium equations with respect to the state variables at the nominal point of collapse is singular (fold bifurcation). The left eigenvector corresponding to the zero eigenvalue of the system Jacobian matrix evaluated at the nominal point of collapse is shown in Table 9, normalized so that the largest component is unity. This left eigenvector is the normal vector to the set of real and reactive power injections that correspond to a fold bifurcation of the equilibrium equations. The left eigenvector indicates that the bus with the greatest influence on the loading margin is the Indian Queens 132kV bus.

7.3 Loading margin sensitivity

Introduction

This section describes and illustrates the use of loading margin sensitivities to avoid voltage collapse. The nominal stable operating point and the nominal point of collapse are described in the previous section.

The derivation of the sensitivity formulas assumes that the system equations remain fixed as parameters are varied. In particular, the limits enforced at the point of collapse are assumed to stay the same as parameters are varied. (A change in the system limits corresponds to a change in the system equations and the sensitivity based estimates using the equations valid at the nominal nose can become inaccurate when the parameters change sufficiently so that the equations change.)

For this study, when a generator represented by a ‘PV’ bus reaches a reactive power limit, it is converted to a ‘PQ’ bus, effectively changing the equilibrium equations modeling the system. In [GDA97] and [GDA98], the major cause for inaccuracies of the sensitivity based estimates is shown to be generator reactive power limits changing as parameters are varied.

The case studied here is indeed challenging since the generator at HINP0 is very

Table 8: Nominal point of collapse

Bus No.	Bus Name	Bus Type	Voltage (p.u.)	Angle (degrees)	Load (MW)	Load (MVAR)	Generation (MW)	Generation (MVAR)
1	INDQ4	PQ	0.832	-29.32	-	-	-	-
2	LAND4	PQ	0.826	-29.88	-	-	-	-
3	ABHA4T	PQ	0.863	-27.28	-	-	-	-
4	ABHA4U	PQ	0.851	-28.03	-	-	-	-
5	EXET4	PQ	0.895	-25.03	-	-	-	-
6	EXETO	PQ	0.948	-25.03	-	-	-	150.0
7	TAUN4J	PQ	0.914	-23.43	-	-	-	-
8	TAUN4K	PQ	0.915	-23.71	-	-	-	-
9	AXMI4	PQ	0.899	-24.20	-	-	-	-
10	CHIC4	PQ	0.907	-22.47	-	-	-	-
11	MANN4	PQ	0.916	-20.09	-	-	-	-
12	LOVE4	PQ	0.958	-14.54	422.0	-63.8	-	-
13	LOVEO	PQ	1.008	-14.54	-	-	-	150.0
14	NURS4	PQ	0.957	-14.44	200.4	48.4	-	-
15	FLEE4	PQ	0.972	-17.45	469.1	96.5	-	-60.0
16	BRLE4	PQ	0.982	-18.12	-	-	-108.8	86.3
17	HINP4	PQ	0.937	-21.56	-	-	-	-
18	HINP0	PV	1.000	-14.50	-	-	1099.1	650.0
19	HINP2J	PQ	0.924	-21.67	-	-	-	-
20	HINP0J	PV	1.000	-11.38	-	-	207.8	107.7
21	HINP2K	PQ	0.924	-21.65	-	-	-	-
22	HINP0K	PV	1.000	-11.35	-	-	207.8	107.6
23	MELK4	PQ	0.963	-20.77	-	-	-392.6	42.5
24	DIDC4	PV	1.005	-18.30	-	-	-38.6	582.1
25	BOLN4	PQ	0.958	-8.433	518.5	117.3	-	-
26	NINF4	PQ	0.971	-2.317	358.4	153.1	-	-
27	BRWA2Q	PQ	0.912	-22.70	-	-	-	-
28	BRWA2R	PQ	0.912	-22.66	-	-	-	-
29	INDQ1	PQ	0.569	-61.26	661.6	142.9	-	-
30	LAND1	PQ	0.717	-43.48	295.4	87.8	-	-
31	ABHA1	PQ	0.786	-39.44	354.4	105.3	-	-
32	EXET1	PQ	0.787	-37.56	319.0	50.2	-	-
33	CHIC1	PQ	0.852	-25.36	89.8	12.5	-	-
34	MANN1	PQ	0.821	-33.42	827.0	205.7	-	-
35	AXMI1	PQ	0.839	-29.97	189.0	50.2	-	-
36	TAUN1	PQ	0.845	-33.64	70.9	15.1	-	-
37	BRWA1	PQ	0.883	-34.07	449.0	-	-	-
38	FAWL4	PQ	0.957	-13.97	156.0	57.4	-	-
39	FAWLO	PQ	0.983	-6.965	-	-	1806.5	470.0
40	DUNG4	AV	0.996	3.400	-	-	2748.7	601.2

Table 9: Left eigenvector corresponding to the zero eigenvalue of the system Jacobian at the nominal point of collapse

Bus No.	Bus Name	Real Power	Reactive Power
1	INDQ4	0.1172	0.3041
2	LAND4	0.1227	0.2936
3	ABHA4T	0.0899	0.2240
4	ABHA4U	0.0984	0.2386
5	EXET4	0.0683	0.1710
6	EXET0	0.0683	0.1530
7	TAUN4J	0.0552	0.1439
8	TAUN4K	0.0568	0.1445
9	AXMI4	0.0625	0.1545
10	CHIC4	0.0522	0.1337
11	MANN4	0.0404	0.1056
12	LOVE4	0.0206	0.0542
13	LOVE0	0.0206	0.0491
14	NURS4	0.0207	0.0593
15	FLEE4	0.0238	0.0373
16	BRLE4	0.0242	0.0307
17	HINP4	0.0421	0.1031
18	HINP0	0.0281	0.0000
19	HINP2J	0.0450	0.0916
20	HINP0J	0.0258	0.0000
21	HINP2K	0.0449	0.0915
22	HINP0K	0.0257	0.0000
23	MELK4	0.0341	0.0651
24	DIDC4	0.0221	0.0000
25	BOLN4	0.0094	0.0337
26	NINF4	0.0027	0.0157
27	BRWA2Q	0.0502	0.0967
28	BRWA2R	0.0500	0.0966
29	INDQ1	0.9086	1.0000
30	LAND1	0.3177	0.4820
31	ABHA1	0.2107	0.3091
32	EXET1	0.1730	0.2479
33	CHIC1	0.0660	0.1364
34	MANN1	0.0988	0.1357
35	AXMI1	0.0955	0.1670
36	TAUN1	0.1122	0.1572
37	BRWA1	0.1085	0.1385
38	FAWL4	0.0198	0.0617
39	FAWL0	0.0048	0.0597
40	DUNG4	0.0000	0.0000

close to a limit at the nominal point of collapse. It is likely that for changes in some parameters, the maximum VAR limit at HINP0 will be reached prior to the new collapse point.

Computation of linear sensitivity

The linear estimate of the change in loading margin (ΔL) resulting from a change to an arbitrary parameter (Δp) is:

$$\Delta L = L_p \Delta p = \frac{-w F_p \Delta p}{w F_\lambda \hat{k}} \quad (132)$$

where :

- L_p is the sensitivity of the loading margin with respect to the parameter.
- F are the power system equilibrium equations (real and reactive power balance at each bus) that apply at the nose. In particular, F accounts for the power system limits enforced at the nose.
- F_λ , the derivative of F with respect to the load parameters. For constant power load models F_λ is a diagonal matrix with ones in the rows corresponding to buses with loads.
- F_p , the derivative of the equilibrium equations with respect to the parameter p at the nominal nose point. The parameter can be a vector and then F_p is a matrix.
- w , the left eigenvector corresponding to the zero eigenvalue of the system Jacobian F_x (F_x evaluated at a fold bifurcation is singular [IEEE1, DCL, Davos]).
- \hat{k} , the unit vector in the direction of load increase. \hat{k} also defines the direction in which the loading margin is measured. The direction of load increase is shown in Table 7.

The denominator of (132) is a scaling factor that is the same for all parameter changes. The linear sensitivity can be improved with a quadratic estimate, derived and explained in [GDA97].

Sensitivity with respect to load variation

Table 9 shows the left eigenvector corresponding to the zero eigenvalue of the system Jacobian evaluated at the nominal fold point. This left eigenvector indicates that the

voltage collapse is most affected by the load at the 132 KV Indian Queens bus. There are several situations in which the sensitivity of the margin to voltage collapse with respect to the load would be of interest.

There is usually uncertainty in the metering or forecast of loads. By computing the sensitivity to the load, one can estimate the effects of inaccuracy in the nominal values used. Secondly, it might be possible to interrupt load at a bus, and it would be useful to know how much margin can be gained for each MW of load shed. Finally, the sensitivity computation identifies buses that are good candidates for planned improvements. For example, load margin sensitivity can specify good locations for VAR support or areas where interruptible contracts can be most profitable.

Methods

The loading margin corresponding to various loads of the same power factor at the 132KV Indian Queens Bus is computed by the same continuation method used to obtain the nominal fold bifurcation. The results are compared to those obtained using the linear sensitivity formulas evaluated at the nominal fold bifurcation.

There is 294 MW of 0.98 power factor load at the Indian Queens 132KV bus at the nominal stable operating point. Results are obtained for variation of ± 50 MW, or ($\pm 17\%$) of the base load.

Results

The solid lines in Figures 16 and 17 are the linear estimates for the loading margin variation as a function of the load shed. The dots in Figures 16 and 17 represent the actual values of the loading margin as computed by the continuation method.

Figure 16 shows the effects on the loading margin for increasing the load at INDQ0 by 10 MW increments at power factor 0.98. The dots represent the collapse points as computed by continuation, and the line represents the linear estimate. Figure 17 shows the effects on the loading margin for decreasing the load at INDQ0 by 10 MW increments at power factor of 0.98.

The agreement between the linear estimates and the actual margins is excellent over the entire range, but better for the increase in load than the reduction of load. Closer inspection showed that a reduction of any more than 3 MW caused the generator at HINP0 to reach its reactive power limit prior to voltage collapse. The nearby VAR limit at HINP0 affected the accuracy of the estimates as speculated. Although the effect is recognizable as a deviation from the linear estimate, the magnitude of the error is insignificant. (In fact, the HINP0 VAR limit causes an immediate instability (see section 7.5). The immediate instability occurs closer to the estimate point of

collapse than the fold point computed and is shown by the circles in Figure 18.)

Sensitivity with respect to VAR limits

Computation of the nominal voltage collapse point showed that Buses EXET0, FAWL0, and LOVE0 all encounter VAR limits. We find out from sensitivities how the loading margin to voltage collapse would change if these limits were different.

Methods

The magnitude of the components of the zero left eigenvector (Table 9) corresponding to reactive power injection indicates that of the three generators that encounter VAR limits between the nominal stable operating point and the point of collapse, the generator at the 132 KV bus at Exeter has the greatest influence on the margin to collapse. The loading margin corresponding to various maximum reactive power limits at the 132KV Exeter Bus is computed by the same continuation method used to obtain the nominal fold bifurcation. The results are compared to those obtained using the linear sensitivity formula evaluated at the nominal fold bifurcation.

The nominal maximum reactive power limit at the Exeter 132KV bus is 150 MVARs. Results are obtained for a variation of 30 MVARs, or ($\pm 20\%$) of the nominal limit.

Results

The solid lines in Figure 19 shows the linear estimate for the loading margin variation as a function of the maximum reactive power limit at the 132 KV Exeter bus. The dots in Figure 19 represent the actual values of the loading margin as computed by the continuation method. The agreement between the linear estimates and the actual margins is excellent over the entire range.

7.4 Contingency ranking for voltage collapse

The sensitivity formulas (132) of the previous section can be used to estimate the effects of contingencies on the margin to voltage collapse. In this case the parameter p is a vector representing the line admittance, and instead of looking at the effect of small deviations, the change in the parameter is 100%.

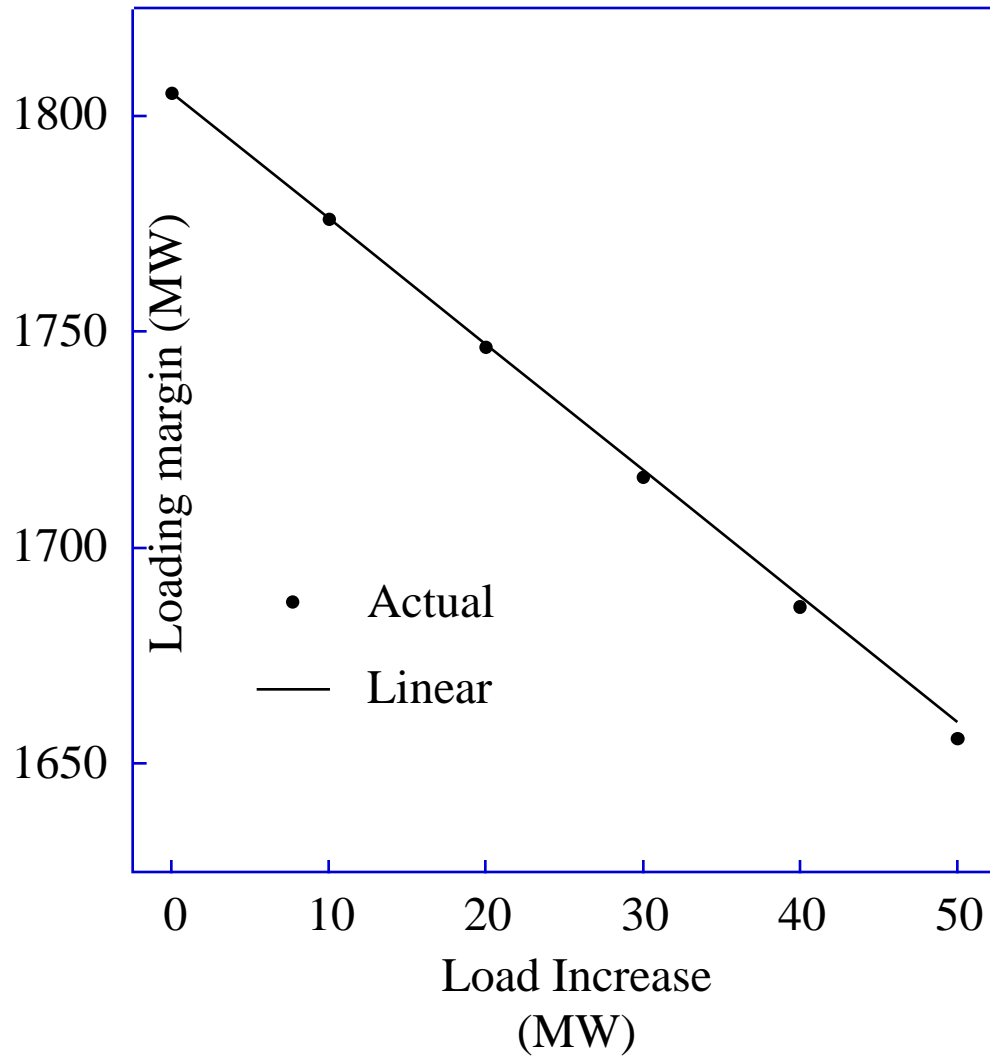


Figure 16: Effect of load increase at Indian Queens on the loading margin to voltage collapse

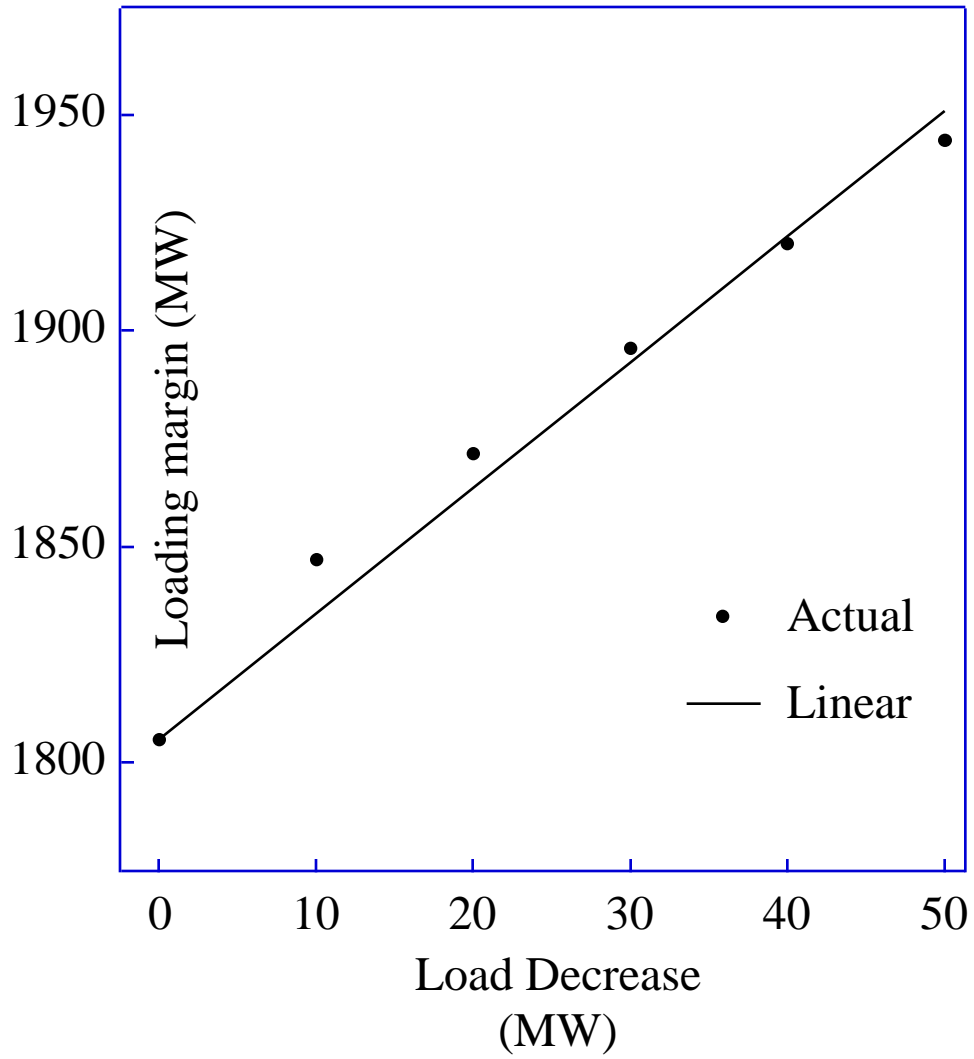


Figure 17: Effect of load decrease at Indian Queens on the loading margin to voltage collapse

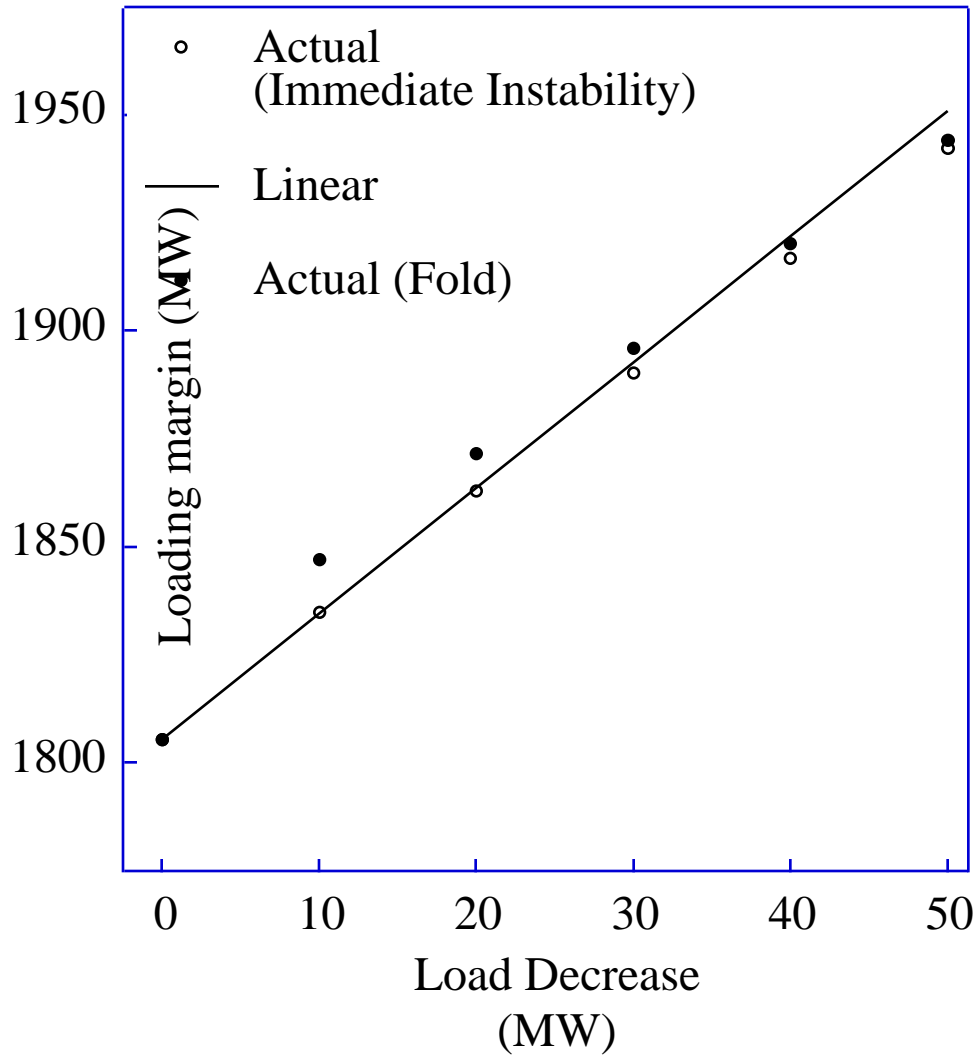


Figure 18: Effect of load decrease at Indian Queens on the loading margin to voltage collapse and critical VAR limit

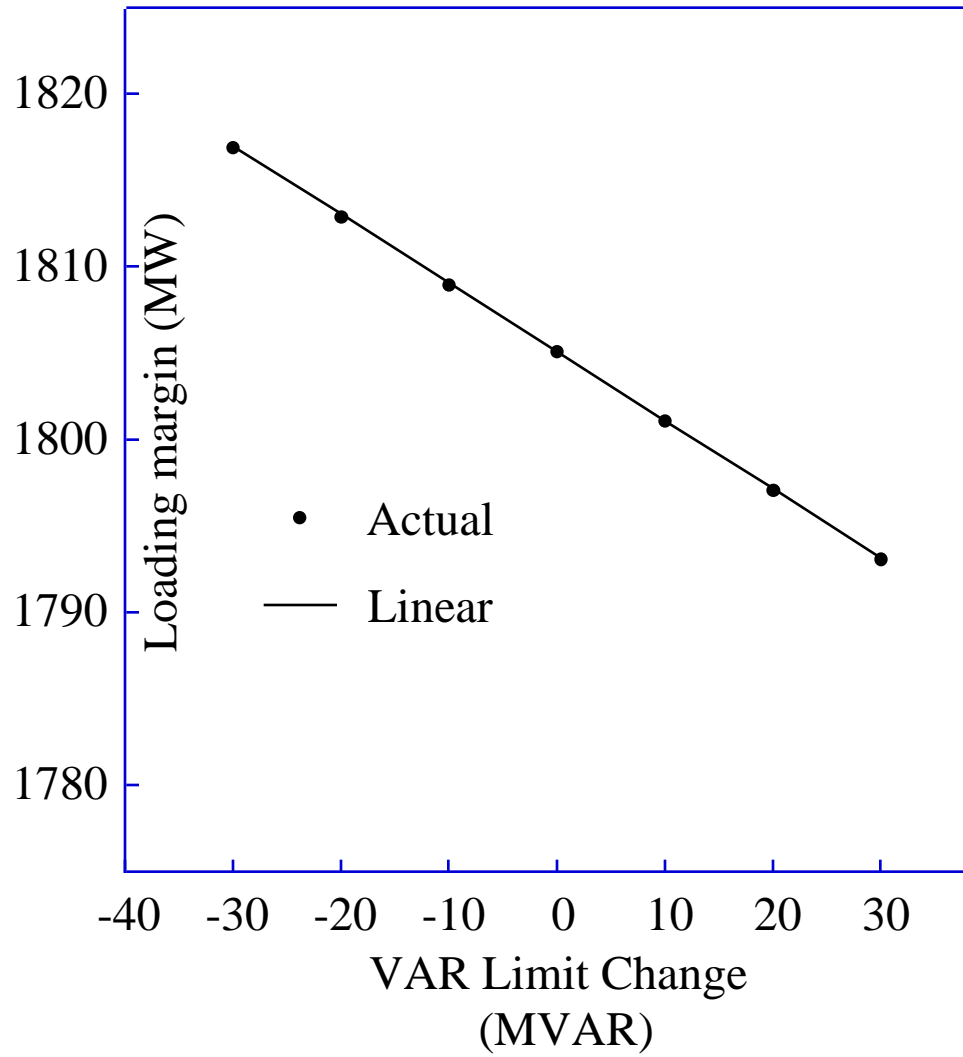


Figure 19: Effect of variation in VAR limits at Exeter on the loading margin to voltage collapse

Method

The estimates for the effects of contingencies were computed as described in [GDA98]. The actual margins resulting from the contingencies were computed by first identifying a stable post contingency equilibrium at the base case loading and then gradually increasing the load and accounting for VAR limits until a voltage collapse due to fold bifurcation of the equilibrium equations was found.

Radial line outages are a special case in which the derived formulas do not strictly apply since the post outage network will not be connected. We suggest that the contingency list be first screened to identify radial lines, and that these outages be analyzed and ranked separately from the other contingencies.¹

Results

Table 10 compares the estimates to the actual margins for all non-radial line outages resulting in at least a 75 MW reduction in loading margin. The ranks correspond to the rank of each outage among all other non-radial line outages. Table 11 compares the estimates to the actual margins for all radial line outages, with ranking shown among only radial lines. The two most critical radial line outages are among the most critical line outages and are identified as so. However, the estimates for the radial line outages tend to be better than the estimates for non-radial outages, and so the moderate radial outages tend to be ranked too high when included with all line outages. Table 12 shows the remaining line outages. Outages mis-grouped by the estimates are shown in bold face. The radial outages were all ranked correctly.

For the four outages causing less than a 10 MW change in margin, the mean error for the linear estimate was 3.0 MW and the maximum error was 4 MW. For the ten outages causing between a 10 MW and 20 MW change in margin, the mean error was 3.9 MW and the maximum error was 13 MW. For the thirteen outages causing between a 20 MW and 45 MW change in margin, the mean error was 10.4 MW and the maximum error was 26 MW. The estimates captured the thirteen worst non-radial line outages, all causing greater than 60 MW change in the margin. The worst results pertained to the outages between BRWA2Q and HINP2J (27.19.1) and BRWA2R and HINP2K (28.21.1).

As noted in [GDA98], the major cause for inaccuracy was due to changes in the

¹For the system used for this report, all radial line outages result in isolation of a single bus. The estimates were then obtained by assuming a reduced system in which the flows on the outaged line appear as loads at the bus still connected to the network following the outage, and the left eigenvector components for that bus adjusted to include the components corresponding to the isolated bus. The outage estimates then correspond to the case of adding load at a bus.

Table 10: Estimated and actual changes in the loading margin to fold bifurcation resulting from severe non-radial line outages
(nominal loading margin = 1805 MW)

Line Outage	Actual		Estimate		VAR
	Margin MW	Change	Linear MW (rank)	Quadratic	Limited Generators
29.30.1	1464	-341 (1)	-172 (1)	-266 (1)	EXET0
4.5.1	1555	-250 (2)	-82 (4)	-133 (4)	EXET0,FAWLO
7.17.1	1635	-170 (3)	-52 (9)	-87 (7)	EXET0,FAWLO,LOVE0
8.17.1	1637	-168 (4)	-54 (8)	-89 (6)	EXET0,FAWLO,LOVE0
1.7.1	1643	-162 (5)	-129 (2)	-154 (2)	EXET0,FAWLO
1.8.1	1643	-162 (6)	-129 (3)	-154 (3)	EXET0,FAWLO
11.38.1	1650	-155 (7)	-70 (5)	-101 (5)	EXET0,FAWLO,HINP0
2.4.1	1653	-152 (8)	-48 (11)	-75 (10)	EXET0,FAWLO
3.5.1	1653	-152 (9)	-51 (10)	-80 (9)	EXET0,FAWLO
11.12.1	1700	-105 (10)	-61 (6)	-83 (8)	EXET0,FAWLO,HINP0
1.3.1	1718	-87 (11)	-56 (7)	-71 (11)	EXET0,FAWLO

set of limits that apply at the point of collapse. This system proved to be a most challenging case, since all but nine outages forced a change in the limits applied at the nose.

As expected, often the change in VAR limits involved the HINP0 bus precariously close to a limit at the nominal point of collapse. In many instances, encountering this limit caused an immediate instability and this is addressed in section 7.5.

7.5 Voltage collapse due to VAR limits

The previous sections and the theory presented in [GDA97, GDA98] associate voltage collapse of the electric power system with a fold bifurcation of the equilibrium equations used to model the system. Experience [DCL, Davos, FOC90, FFOCH, HSS, HawPhD] has shown that the VAR limitations of generators are associated with voltage instability, and computational experience shows that the effect of changing PV buses in the equilibrium model of the power system to PQ buses often reduces the loading margin to voltage collapse.

In some cases, when the system loading is high, the effect of changing a PV bus to a PQ bus causes the margin to the fold bifurcation to increase. Upon application

Table 11: Estimated and actual changes in the loading margin to fold bifurcation resulting from radial line outages
(nominal loading margin = 1805 MW)

Line Outage	Actual		Estimate		VAR Limited Generators
	Margin MW	Change	Linear MW (rank)	Quadratic	
18.17.1	1367	-438 (1)	-265 (1)	-366 (1)	
39.38.1	1568	-237 (2)	-167 (2)	-203 (2)	EXET0,LOVE0,HINP0
6.5.1	1738	-67 (3)	-60 (3)	-62 (3)	
20.19.1	1752	-53 (4)	-46 (4)	-57 (4)	EXET0,FAWL0, LOVE0,HINP0
22.21.1	1752	-53 (5)	-46 (5)	-57 (5)	EXET0,FAWL0, LOVE0,HINP0
13.12.1	1792	-13 (6)	-19 (6)	-20 (6)	

of the limit, the equilibrium point appears on the bottom half of the nose curve, and voltages increase upon increase in load [HSS].

The points at which changing a PV bus to a PQ bus alter the system nose curve so that the equilibrium solution is on the lower voltage branch of the new nose curve represent points at which the power system may become immediately unstable. We refer to these points as points of immediate instability, to distinguish them from fold bifurcation points. However, either a fold bifurcation point or point of immediate instability can lead to a dynamic voltage collapse.

Tables 13,14, and 15 show the same results as in section 7.4 except that the actual margins are adjusted to reflect the cases in which an immediate instability was encountered before the fold bifurcation at the nose of the curve. In all cases, the VAR limit was caused by the generator at HINP0. Those cases for which a change in margin occurs are highlighted in bold. The immediate instability caused only minor changes in ranking between outages within 5 MW of each other. The outages are listed in the same rankings as in section 7.4.

For nearly half of the outages, instability was due to fold bifurcation, not immediate instability. All of the most serious outages were due to fold bifurcation. When the actual margin represents the distance to immediate instability and not to fold bifurcation, the margin to fold bifurcation is noted in parentheses. In all cases, fold bifurcation occurs within 11 MW of immediate instability. Table 16 compares the

Table 12: Estimated and actual changes in the loading margin to fold bifurcation resulting from less severe non-radial line outages
(nominal loading margin = 1805 MW)

Line Outage	Actual		Estimate		VAR
	Margin	Change MW	Linear	Quadratic	Limited Generators
31.30.1	1735	-70	-33	-51	EXET0,FAWL0
9.11.1	1739	-66	-39	-51	EXET0,FAWL0,HINP0
27.19.1	1747	-58	-6	-8	EXET0,FAWL0,LOVE0,HINP0
28.21.1	1748	-57	-5	-8	EXET0,FAWL0,LOVE0,HINP0
5.7.1	1752	-53	-27	-37	EXET0,FAWL0,LOVE0
5.8.1	1755	-50	-26	-36	EXET0,FAWL0,LOVE0
10.11.1	1757	-48	-21	-29	EXET0,FAWL0,HINP0
5.10.1	1759	-46	-29	-37	EXET0,FAWL0,HINP0
16.24.1	1764	-41	-28	-39	EXET0,FAWL0,LOVE0,HINP0
16.24.2	1764	-41	-28	-39	EXET0,FAWL0,LOVE0,HINP0
12.38.1	1767	-38	-12	-12	EXET0,FAWL0,LOVE0,HINP0
12.38.2	1767	-3	-12	-12	EXET0,FAWL0,LOVE0,HINP0
17.23.1	1771	-34	-24	-29	EXET0,FAWL0,HINP0
17.23.2	1771	-34	-24	-29	EXET0,FAWL0,HINP0
26.40.2	1775	-30	-17	-27	EXET0,FAWL0,LOVE0,HINP0
26.40.1	1775	-30	-17	-27	EXET0,FAWL0,LOVE0,HINP0
37.36.1	1777	-28	-4	-8	EXET0,FAWL0,LOVE0
25.26.1	1778	-27	-17	-25	EXET0,FAWL0,LOVE0,HINP0
25.26.2	1778	-27	-17	-25	EXET0,FAWL0,LOVE0,HINP0
5.9.1	1778	-27	-12	-14	EXET0,FAWL0,HINP0
32.36.1	1779	-26	-14	-21	EXET0,FAWL0,LOVE0
16.23.1	1785	-20	-18	-23	EXET0,FAWL0,LOVE0,HINP0
16.23.2	1785	-20	-18	-23	EXET0,FAWL0,LOVE0,HINP0
12.25.1	1787	-18	-16	-22	EXET0,FAWL0,LOVE0,HINP0
12.25.2	1787	-18	-16	-22	EXET0,FAWL0,LOVE0,HINP0
31.32.1	1787	-18	-5	-8	EXET0,FAWL0,LOVE0
1.2.1	1791	-14	-14	-13	EXET0,FAWL0,LOVE0,HINP0
15.16.1	1791	-14	-7	-9	EXET0,FAWL0,LOVE0,HINP0
15.16.2	1791	-14	-7	-9	EXET0,FAWL0,LOVE0,HINP0
12.15.1	1793	-12	-14	-20	EXET0,FAWL0,LOVE0,HINP0
12.15.2	1793	-12	-14	-20	EXET0,FAWL0,LOVE0,HINP0
12.14.1	1800	-5	-4	-4	EXET0,FAWL0,LOVE0,HINP0
14.38.1	1800	-5	-2	-2	EXET0,FAWL0,LOVE0,HINP0
17.19.1	1809	4	0	2	EXET0,FAWL0,LOVE0
17.21.1	1809	4	0	2	EXET0,FAWL0,LOVE0

Table 13: Estimated and actual changes in the loading margin to voltage collapse resulting from severe non-radial line outages
(nominal loading margin = 1805 MW)

Line Outage	Actual Margin MW	Change	Estimate		VAR Limited Generators
			Linear MW (rank)	Quadratic	
29.30.1	1464	-341 (1)	-172 (1)	-266 (1)	EXET0
4.5.1	1555	-250 (2)	-82 (4)	-133 (4)	EXET0,FAWLO
7.17.1	1635	-170 (3)	-52 (9)	-87 (7)	EXET0,FAWLO,LOVE0
8.17.1	1637	-168 (4)	-54 (8)	-89 (6)	EXET0,FAWLO,LOVE0
1.7.1	1643	-162 (5)	-129 (2)	-154 (2)	EXET0,FAWLO
1.8.1	1643	-162 (6)	-129 (3)	-154 (3)	EXET0,FAWLO
11.38.1	1650	-155 (7)	-70 (5)	-101 (5)	EXET0,FAWLO,HINP0
2.4.1	1653	-152 (8)	-48 (11)	-75 (10)	EXET0,FAWLO
3.5.1	1653	-152 (9)	-51 (10)	-80 (9)	EXET0,FAWLO
11.12.1	1699 (1700)	-106 (10)	-61 (6)	-83 (8)	EXET0,FAWLO,HINP0
1.3.1	1718	-87 (11)	-56 (7)	-71 (11)	EXET0,FAWLO

loading margins to fold bifurcation with the loading margins to immediate instability for each outage at which an immediate instability was observed prior to voltage collapse due to fold bifurcation.

Since all cases of immediate instability resulted from the generator at HINP0 hitting a VAR limit (although this did not always result in an immediate instability) it is natural to ask how the contingencies affect the loading margin to the HINP0 VAR limit, as opposed to the loading margin to the fold bifurcation. This topic is addressed in section 7.6.

7.6 Contingency ranking for voltage collapse due to VAR limits

The sensitivity computations can be easily extended to the case where the voltage collapse is an immediate instability due to a VAR limit rather than a fold bifurcation. The derivations of the sensitivity formulas in [GDA97] required the description of a manifold in which each point on the manifold corresponded to a point of fold bifurcation. The normal vector to this surface is defined by the zero left eigenvector

Table 14: Estimated and actual changes in the loading margin to voltage collapse resulting from radial line outages
(nominal loading margin = 1805 MW)

Line Outage	Actual Margin MW	Change	Estimate		VAR Limited Generators
			Linear MW (rank)	Quadratic	
18.17.1	1367	-438 (1)	-265 (1)	-366 (1)	
39.38.1	1568	-237 (2)	-167 (2)	-203 (2)	EXET0,LOVE0,HINP0
6.5.1	1738	-67 (3)	-60 (3)	-62 (3)	
20.19.1	1750 (1752)	-55 (4)	-46 (4)	-57 (4)	EXET0,FAWL0, LOVE0,HINP0
22.21.1	1750 (1752)	-55 (5)	-46 (5)	-57 (5)	EXET0,FAWL0, LOVE0,HINP0
13.12.1	1792	-13 (6)	-19 (6)	-20 (6)	

of the system Jacobian. Similarly we can construct a manifold in which each point corresponds to the point at which a particular generator is at a VAR limit. The normal vector to this surface can then be used in the sensitivity formulas to compute the sensitivity of the margin to encountering a VAR limit.

Computation of nominal point of instability

Computation of the point of immediate instability is similar to computation of a fold bifurcation point. The same continuation method can be used, and the point of collapse is the point at which a VAR limit is encountered and upon further increase in load the system voltages increase. Thus, the immediate instability can be detected by computing the sensitivity of the bus voltages to the loading factor after application of the limit. (Note that the software described in [HSS] performs this check to detect voltage collapse due to fold bifurcation or immediate instability.) It is in general easier to locate the exact point of encountering a VAR limit than it is to locate the exact fold bifurcation point. The equations are sparser, a good initial guess for the eigenvectors is unnecessary, and the Jacobian is less likely to be poorly conditioned since the power balance equations are not evaluated at a point of singularity.

For this study, the maximum VAR limit at HINP0 was changed from 660 MVAR to 630 MVAR. The continuation program was run as before, and again, VAR limits were reached at EXET0, FAWL0, and LOVE0. However, at a loading 5379 MW,

Table 15: Estimated and actual changes in the loading margin to voltage collapse resulting from less severe non-radial line outages
(nominal loading margin = 1805 MW)

Line Outage	Actual		Estimate		VAR
	Margin	Change MW	Linear	Quadratic	Limited Generators
31.30.1	1735	-70	-33	-51	EXET0,FAWL0
9.11.1	1735 (1739)	-66	-39	-51	EXET0,FAWL0,HINP0
27.19.1	1741 (1747)	-64	-6	-8	EXET0,FAWL0,LOVE0,HINP0
28.21.1	1742 (1748)	-63	-5	-8	EXET0,FAWL0,LOVE0,HINP0
5.7.1	1752	-53	-27	-37	EXET0,FAWL0,LOVE0
5.8.1	1755	-50	-26	-36	EXET0,FAWL0,LOVE0
10.11.1	1750 (1757)	-55	-21	-29	EXET0,FAWL0,HINP0
5.10.1	1753 (1759)	-52	-29	-37	EXET0,FAWL0,HINP0
16.24.1	1757 (1764)	-48	-28	-39	EXET0,FAWL0,LOVE0,HINP0
16.24.2	1757 (1764)	-48	-28	-39	EXET0,FAWL0,LOVE0,HINP0
12.38.1	1767 (1767)	-38	-12	-12	EXET0,FAWL0,LOVE0,HINP0
12.38.2	1767 (1767)	-38	-12	-12	EXET0,FAWL0,LOVE0,HINP0
17.23.1	1769 (1771)	-36	-24	-29	EXET0,FAWL0,HINP0
17.23.2	1769 (1771)	-36	-24	-29	EXET0,FAWL0,HINP0
26.40.2	1769 (1775)	-36	-17	-27	EXET0,FAWL0,LOVE0,HINP0
26.40.1	1770 (1775)	-35	-17	-27	EXET0,FAWL0,LOVE0,HINP0
37.36.1	1777	-28	-4	-8	EXET0,FAWL0,LOVE0
25.26.1	1771 (1778)	-34	-17	-25	EXET0,FAWL0,LOVE0,HINP0
25.26.2	1771 (1778)	-34	-17	-25	EXET0,FAWL0,LOVE0,HINP0
5.9.1	1780 (1778)	-29	-12	-14	EXET0,FAWL0,HINP0
32.36.1	1779	-26	-14	-21	EXET0,FAWL0,LOVE0
16.23.1	1778 (1785)	-27	-18	-23	EXET0,FAWL0,LOVE0,HINP0
16.23.2	1778 (1785)	-27	-18	-23	EXET0,FAWL0,LOVE0,HINP0
12.25.1	1779 (1787)	-26	-16	-22	EXET0,FAWL0,LOVE0,HINP0
12.25.2	1779 (1787)	-26	-16	-22	EXET0,FAWL0,LOVE0,HINP0
31.32.1	1787	-18	-5	-8	EXET0,FAWL0,LOVE0
1.2.1	1791	-14	-14	-13	EXET0,FAWL0,LOVE0,HINP0
15.16.1	1791	-14	-7	-9	EXET0,FAWL0,LOVE0,HINP0
15.16.2	1791	-14	-7	-9	EXET0,FAWL0,LOVE0,HINP0
12.15.1	1782 (1793)	-23	-14	-20	EXET0,FAWL0,LOVE0,HINP0
12.15.2	1782 (1793)	-23	-14	-20	EXET0,FAWL0,LOVE0,HINP0
12.14.1	1800	-5	-4	-4	EXET0,FAWL0,LOVE0,HINP0
14.38.1	1800	-5	-2	-2	EXET0,FAWL0,LOVE0,HINP0
17.19.1	1809	4	0	2	EXET0,FAWL0,LOVE0
17.21.1	1809	4	0	2	EXET0,FAWL0,LOVE0

Table 16: The loading margins to fold bifurcation and voltage collapse for all line outages causing an immediate instability prior to fold bifurcation
(nominal loading margin = 1805 MW)

Line Outage	Margin to Immediate Instability MW	Margin to Fold Bifurcation MW
11.12.1	1699	1700
9.11.1	1735	1739
27.19.1	1741	1747
28.21.1	1742	1748
10.11.1	1750	1757
20.19.1	1750	1752
22.21.1	1750	1752
5.10.1	1753	1759
16.24.1	1757	1764
16.24.2	1757	1764
12.38.1	1767	1767
12.38.2	1767	1767
17.23.1	1769	1771
17.23.2	1769	1771
26.40.2	1769	1775
26.40.1	1770	1775
25.26.1	1771	1778
25.26.2	1771	1778
5.9.1	1778	1780
16.23.1	1778	1785
16.23.2	1778	1785
12.25.1	1779	1787
12.25.2	1779	1787
12.15.1	1782	1793
12.15.2	1782	1793

HINP0 reaches its VAR limit of 630 MVARs, and the system becomes unstable once the PV bus is converted to a PQ bus. (A fold bifurcation of the post limit system occurs at 5385 MW. Note that the point of collapse for the original system occurred at a loading of 5380 MW due to fold bifurcation.)

Computation of sensitivity

When the voltage collapse is identified with the fold bifurcation of the equilibrium model, the left zero eigenvector can be used to compute the normal vector to the surface of bifurcation points in parameter space. Similarly, when the voltage collapse is identified with the immediate instability due to application of a VAR limit, there is a normal vector in parameter space to the surface of points at which the critical Q limit is reached. Chapter 4 details the computation of this vector for general limits. In short, when equation (132) is evaluated with the vector w computed at the critical VAR limit point (as opposed to at the fold bifurcation point), ΔL reflects the linear estimate of the change in margin to the VAR limit for the change in parameter Δp . Table 17 compares the VAR limit normal vector N to the zero left eigenvector W . The angle between N and W is 4.6 degrees. Note that it is considerably easier to compute N than W . There is no need to compute a Hessian term and computation of N does not require a good initial guess.

When the sensitivity computations and contingency rankings were repeated using N in place of W , no significant changes were observed. Tables 18 and 19 compare the linear estimates for the change in margin resulting from the lines outages computed with both the left zero eigenvector, W , at the original fold bifurcation point, and the normal vector to the VAR limit set, N , with the actual margins to instability for the original system. Note that there is very little difference in the estimates, and the top twelve contingencies are ranked the same except for two contingencies with a difference of less than 1 MW are switched. In each case limited by fold bifurcation, the estimate computed with the zero left eigenvector is better than the estimate computed with the normal vector. For the one contingency of the top twelve limited by immediate instability, the VAR limit normal vector is superior.

Table 19 shows the less critical contingencies which tend to be limited by immediate instability as opposed to fold bifurcation. The estimates are very similar, seldom differing by more than 5 MW. However, the estimates computed with the normal vector to the VAR limit set are better than those computed with the zero left eigenvector for the cases that were limited by immediate instability.

Table 17: Comparison of the normal vectors to the parameter set corresponding to fold bifurcation (W) and immediate instability (N)

Bus No.	Bus Name	Real Power		Reactive Power	
		W	N	W	N
1	INDQ4	0.1172	0.1357	0.3041	0.3351
2	LAND4	0.1227	0.1417	0.2936	0.3253
3	ABHA4T	0.0899	0.1061	0.224	0.2555
4	ABHA4U	0.0984	0.1153	0.2386	0.2703
5	EXET4	0.0683	0.0819	0.171	0.2018
6	EXET0	0.0683	0.0819	0.153	0.1806
7	TAUN4J	0.0552	0.0674	0.1439	0.1769
8	TAUN4K	0.0568	0.0693	0.1445	0.1776
9	AXMI4	0.0625	0.0749	0.1545	0.1826
10	CHIC4	0.0522	0.0627	0.1337	0.1584
11	MANN4	0.0404	0.0486	0.1056	0.1257
12	LOVE4	0.0206	0.0249	0.0542	0.0655
13	LOVE0	0.0206	0.0249	0.0491	0.0594
14	NURS4	0.0207	0.025	0.0593	0.0715
15	FLEE4	0.0238	0.0287	0.0373	0.0462
16	BRLE4	0.0242	0.0293	0.0307	0.0387
17	HINP4	0.0421	0.0522	0.1031	0.1376
18	HINP0	0.0281	0.0268	0	0.0608
19	HINP2J	0.045	0.0552	0.0916	0.1197
20	HINP0J	0.0258	0.0301	0	0
21	HINP2K	0.0449	0.0551	0.0915	0.1196
22	HINP0K	0.0257	0.03	0	0
23	MELK4	0.0341	0.0419	0.0651	0.0857
24	DIDC4	0.0221	0.0266	0	0
25	BOLN4	0.0094	0.0114	0.0337	0.0408
26	NINF4	0.0027	0.0033	0.0157	0.019
27	BRWA2Q	0.0502	0.0615	0.0967	0.1256
28	BRWA2R	0.05	0.0613	0.0966	0.1254
29	INDQ1	0.9086	0.9176	1	1
30	LAND1	0.3177	0.3473	0.482	0.5128
31	ABHA1	0.2107	0.2394	0.3091	0.3449
32	EXET1	0.173	0.2002	0.2479	0.2835
33	CHIC1	0.066	0.0789	0.1364	0.1615
34	MANN1	0.0988	0.1176	0.1357	0.1611
35	AXMI1	0.0955	0.1137	0.167	0.1971
36	TAUN1	0.1122	0.1355	0.1572	0.191
37	BRWA1	0.1085	0.1323	0.1385	0.1713
38	FAWL4	0.0198	0.0239	0.0617	0.0743
39	FAWL0	0.0048	0.0059	0.0597	0.0719
40	DUNG4	0	0	0	0

Table 18: Comparison of linear estimated changes in the loading margin to voltage collapse resulting from severe non-radial line outages
(nominal loading margin = 1805 MW)

Line Outage	Actual Margin MW	Estimate			VAR Limited Generators
		Change	VAR (N) MW (rank)	Fold (W)	
29.30.1	1464	-341 (1)	-172 (1)	-148 (1)	EXET0
4.5.1	1555	-250 (2)	-82 (4)	-80 (4)	EXET0,FAWL0
7.17.1	1635	-170 (3)	-52 (9)	-49 (10)	EXET0,FAWL0,LOVE0
8.17.1	1637	-168 (4)	-54 (8)	-51 (8)	EXET0,FAWL0,LOVE0
1.7.1	1643	-162 (5)	-129 (2)	-127 (2)	EXET0,FAWL0
1.8.1	1643	-162 (6)	-129 (3)	-126 (3)	EXET0,FAWL0
11.38.1	1650	-155 (7)	-70 (5)	-77 (5)	EXET0,FAWL0,HINP0
2.4.1	1653	-152 (8)	-48 (11)	-47 (11)	EXET0,FAWL0
3.5.1	1653	-152 (9)	-51 (10)	-51 (9)	EXET0,FAWL0
11.12.1	1699 (1700)	-106 (10)	-61 (6)	-69 (6)	EXET0,FAWL0,HINP0
1.3.1	1718	-87 (11)	-56 (7)	-56 (7)	EXET0,FAWL0

7.7 Large deviation sensitivity based contingency analysis

This section examines application of the margin sensitivity formula (132) for the case when F represents node voltage equations and the parameter p is the matrix of changes in the impedance bus matrix resulting from each line outage. This formulation is analogous to what is traditionally referred to as large deviation sensitivity and is explained in section (4.3) of this thesis.

The formulas used for the contingency analysis are general and do not depend upon the form of the F equations used to model the system. Usually the F equations include power balance equations at every node in the system. The F equations can also be formulated with node voltage equations instead of power balance equations. The equilibrium solution of the two forms of the equations does not differ. The power balance equations can be written in terms of the bus admittance matrix which is sparse. The node voltage equations instead use the inverse of the bus admittance matrix, the bus impedance matrix, and this matrix is generally dense. For most computations, the power balance form is preferred since the resulting Jacobian matrix is very sparse, retaining the structure of the original connection matrix. The Jacobian

Table 19: Comparison of linear estimated changes in the loading margin to voltage collapse resulting from less severe non-radial line outages
(nominal loading margin = 1805 MW)

Line Outage	Actual	Change MW	Estimate		VAR
	Margin		VAR (N)	Fold (W)	Limited Generators
31.30.1	1735	-70	-33	-30	EXET0,FAWL0
9.11.1	1735 (1739)	-66	-39	-44	EXET0,FAWL0,HINP0
27.19.1	1741 (1747)	-64	-6	-6	EXET0,FAWL0,LOVE0,HINP0
28.21.1	1742 (1748)	-63	-5	-6	EXET0,FAWL0,LOVE0,HINP0
5.7.1	1752	-53	-27	-25	EXET0,FAWL0,LOVE0
5.8.1	1755	-50	-26	-24	EXET0,FAWL0,LOVE0
10.11.1	1750 (1757)	-55	-21	-23	EXET0,FAWL0,HINP0
5.10.1	1753 (1759)	-52	-29	-32	EXET0,FAWL0,HINP0
16.24.1	1757 (1764)	-48	-28	-33	EXET0,FAWL0,LOVE0,HINP0
16.24.2	1757 (1764)	-48	-28	-33	EXET0,FAWL0,LOVE0,HINP0
12.38.1	1767 (1767)	-38	-12	-13	EXET0,FAWL0,LOVE0,HINP0
12.38.2	1767 (1767)	-38	-12	-13	EXET0,FAWL0,LOVE0,HINP0
17.23.1	1769 (1771)	-36	-24	-31	EXET0,FAWL0,HINP0
17.23.2	1769 (1771)	-36	-24	-31	EXET0,FAWL0,HINP0
26.40.2	1769 (1775)	-36	-17	-20	EXET0,FAWL0,LOVE0,HINP0
26.40.1	1770 (1775)	-35	-17	-20	EXET0,FAWL0,LOVE0,HINP0
37.36.1	1777	-28	-4	-4	EXET0,FAWL0,LOVE0
25.26.1	1771 (1778)	-34	-17	-20	EXET0,FAWL0,LOVE0,HINP0
25.26.2	1771 (1778)	-34	-17	-20	EXET0,FAWL0,LOVE0,HINP0
5.9.1	1780 (1778)	-29	-12	-13	EXET0,FAWL0,HINP0
32.36.1	1779	-26	-14	-14	EXET0,FAWL0,LOVE0
16.23.1	1778 (1785)	-27	-18	-22	EXET0,FAWL0,LOVE0,HINP0
16.23.2	1778 (1785)	-27	-18	-22	EXET0,FAWL0,LOVE0,HINP0
12.25.1	1779 (1787)	-26	-16	-18	EXET0,FAWL0,LOVE0,HINP0
12.25.2	1779 (1787)	-26	-16	-18	EXET0,FAWL0,LOVE0,HINP0
31.32.1	1787	-18	-5	-5	EXET0,FAWL0,LOVE0
1.2.1	1791	-14	-14	-15	EXET0,FAWL0,LOVE0,HINP0
15.16.1	1791	-14	-7	-7	EXET0,FAWL0,LOVE0,HINP0
15.16.2	1791	-14	-7	-7	EXET0,FAWL0,LOVE0,HINP0
12.15.1	1782 (1793)	-23	-14	-16	EXET0,FAWL0,LOVE0,HINP0
12.15.2	1782 (1793)	-23	-14	-16	EXET0,FAWL0,LOVE0,HINP0
12.14.1	1800	-5	-4	-5	EXET0,FAWL0,LOVE0,HINP0
14.38.1	1800	-5	-2	-2	EXET0,FAWL0,LOVE0,HINP0
17.19.1	1809	4	0	1	EXET0,FAWL0,LOVE0
17.21.1	1809	4	0	1	EXET0,FAWL0,LOVE0

matrix resulting from the node voltage equations is dense.

Note that evaluating the sensitivity formulas assuming the node voltage model does not require that the equilibrium points or bifurcation points be computed using those equations. Since the zero set of either the node voltage or power balance equations is the same, the sparser power balance equations should be used for computing the nominal boundary point and the normal vectors. The formulas are evaluated as before, except that a linear transformation is applied to w . The quantity F_p represents the change in the node voltage equations resulting from a change in the line impedance p , and is computed using a rank one update of the bus impedance matrix.

The results of the large deviation analysis are compared with those of the previous analysis for all non-radial line outages. The large deviation sensitivity based estimates do in general provide bigger estimates and often over estimates for the changes in margin. However, though of greater magnitude they are no more accurate than the quadratic estimate, and they appear no better at ranking than the linear estimate. The large deviation estimates appear more erratic; although the large deviation estimate captures 10 of the top 11 contingencies, it mis-ranks a negligible outage (31.32.1) in the top 11.

The large deviation method utilizes sparse matrix techniques [AST83, SAA85] to compute the update of the impedance bus matrix and is faster than the quadratic estimate but not as fast as the linear estimate.

7.8 Conclusions

The methods presented in Chapters 5 and 6 were tested on a small but challenging case. The nominal voltage collapse occurred at an equilibrium at which a critical VAR output was precariously close to a limit. It was expected that line outages as well as small changes in parameters would cause the system to encounter the limit prior to voltage collapse. This phenomena had previously been associated with inaccuracies in the estimates and rankings.

For this case, it was shown that the VAR limited changes produced a noticeable but negligible effect on the estimates. In addition, the formulas were shown to perform well estimating the effect on the loading margin of altering a generator maximum VAR limit, illustrating a new application for the methods.

This chapter also tested a new implementation of the sensitivity formulas derived in Chapter 4 using the node voltage form of the equilibrium equations. Contingency analysis was performed by evaluating the sensitivity formulas for changes in the impedance matrix resulting from line outages. The initial tests indicate that the

Table 20: Comparison of linear, quadratic, and large deviation estimates for changes in the loading margin to voltage collapse resulting from severe non-radial line outages (nominal loading margin = 1805 MW)

Line Outage	Actual	Estimate		
	Change	Linear	Quadratic	Large Deviation
		MW (rank)		
29.30.1	-341 (1)	-172 (1)	-266 (1)	-187 (6)
4.5.1	-250 (2)	-82 (4)	-133 (4)	-211 (4)
7.17.1	-170 (3)	-52 (9)	-87 (7)	-231 (2)
8.17.1	-168 (4)	-54 (8)	-89 (6)	-285 (1)
1.7.1	-162 (5)	-129 (2)	-154 (2)	-221 (3)
1.8.1	-162 (6)	-129 (3)	-154 (3)	-208 (5)
11.38.1	-155 (7)	-69 (5)	-101 (5)	-119 (10)
2.4.1	-152 (8)	-48 (11)	-75 (10)	-178 (7)
3.5.1	-152 (9)	-51 (10)	-80 (9)	-125 (9)
11.12.1	-105 (10)	-62 (6)	-83 (8)	-98 (12)
1.3.1	-87 (11)	-56 (7)	-71 (11)	-131 (8)

power balance form of the equilibrium equations used in Chapter 6, where line outages are reflected by changes in the admittance matrix, perform more consistently, are faster, and provide better ranking.

Finally, since voltage collapse can be precipitated by generator power limits, a new estimate was tested using the normal vector to the critical VAR limit in place of the zero left eigenvector at a fold bifurcation. The results were comparable. However, the VAR normal vector is easier to compute than the left zero eigenvector and also does not require that a continuation method locate an exact fold bifurcation point.

Table 21: Comparison of linear, quadratic, and large deviation estimates for changes in the loading margin to voltage collapse resulting from less severe non-radial line outages

(nominal loading margin = 1805 MW)

Line Outage	Actual	Estimate		
	Change	Linear	Quadratic MW	Large Deviation
31.30.1	-70	-34	-51	-54
9.11.1	-66	-39	-51	-79
27.19.1	-58	-6	-8	-21
28.21.1	-57	-5	-8	-21
5.7.1	-53	-27	-37	-82
5.8.1	-50	-26	-36	-60
10.11.1	-48	-21	-29	-55
5.10.1	-46	-29	-37	-67
16.24.1	-41	-28	-39	-60
16.24.2	-41	-28	-39	-60
12.38.1	-38	-12	-12	-25
12.38.2	-38	-12	-12	-25
17.23.1	-34	-24	-29	-45
17.23.2	-34	-24	-29	-45
26.40.2	-30	-17	-27	-34
26.40.1	-30	-17	-27	-35
37.36.1	-28	-4	-8	11
25.26.1	-27	-17	-25	-37
25.26.1	-27	-17	-25	-37
5.9.1	-27	-11	-14	-37
32.36.1	-26	-14	-21	-23
16.23.1	-20	-18	-23	-26
16.23.1	-20	-18	-23	-26
12.25.1	-18	-16	-22	-39
12.25.2	-18	-16	-22	-39
31.32.1	-18	-5	-8	-114
1.2.1	-14	-14	-13	-33
15.16.1	-14	-7	-9	-13
15.16.2	-14	-7	-9	-13
12.15.1	-12	-14	-20	-30
12.15.2	-12	-14	-20	-30
12.14.1	-5	-4	-4	-9
14.38.1	-5	-2	-2	-4
17.19.1	4	0	2	-19
17.21.1	4	0	2	-19

Chapter 8

Sensitivity of Transfer Capability Margins

This chapter applies the margin and sensitivity methods to the problem of computing the transfer capability margin and determining the effect of varying simultaneous transfers, loading, generation, and reactive power support.

8.1 Introduction

Open access to transmission services requires continual determination of the available transfer capability (ATC) for each interface of a region or area of the power network. The ATC indicates how much interarea power transfers can be increased without compromising system security at a particular moment and for a prescribed interval in time. The ATC is vital information for the bulk power market. The available transfer capability is the total transfer capability (TTC) minus existing transfer commitments together with adjustments to allow some margin of safety. Essentially, transmission capacity can only be reserved when there is capacity available. While there exists general agreement concerning the fundamental requirements of the ATC, computational procedures vary. In addition, once the ATC or TTC is computed under one set of operating conditions, it is important to determine the effects of varying conditions and assumptions. It is desirable to understand the effect of increased transfer on each interface on the ATC of every other interface. This chapter illustrates the use of sensitivities for estimating the effect on the transfer capability of varying simultaneous transfer directions, loading, generation, and reactive power support. The results apply to the case of transfer limited by line flow limits, voltage limits, generator real and reactive power limits, and voltage collapse. The computations are illustrated on a 40 bus, 3 area model and performance is tested with a 1500 bus, twenty area system. Both systems are derived from a portion of the US grid.

Previous Work

A concise analysis of ATC computations and current terminology, along with a comprehensive bibliography is contained in [Sau97]. Foundational work regarding transmission transfer capability determination is represented in [DGM79, GVHW, LTA72, LA73, StC53], and, concerning sensitivity and optimal power flow, in [SM79, PPTT, DT68]. NERC documents [NERC95, NERC96] contain useful terminology and descriptions. The most current information can be found at the OASIS web sites for each operating region.

Path following methods are used in this chapter to obtain nominal transfer margins. The details of these methods are explained in Chapter 3 of this thesis. Previous use of continuation methods for margin determination includes [CA93, CFSB, RHSC, VC91]. In particular, [RHSC, VC91] illustrate the combined use of continuation methods and sensitivity analysis for security margin computation. Chapter 1 references fundamental work in this area.

[GDA97] presents exact analytical margin sensitivity formulas with illustrative examples including the effect of variation in interarea transfers on the loading margin to voltage collapse. [WF93] applies sensitivity analysis to the determination of the contingencies that most limit transfer capability, and motivates the work on contingency analysis presented in [GDA98]. [RAMCJ] demonstrates the use of sensitivity formulas for locating series compensation to increase power transfer capability.

This chapter continues a research direction in available transfer capability indicated in [Sau97] by applying the margin sensitivity ideas to transfer capability. This chapter is an extension of the work reported in [GDAS]. This chapter tests the application of the methods reported in [GDAS] on a realistic power system example.

8.2 Overview of transfer capability determination

For this chapter we use the main features of the NERC 1995 and 1996 definitions [NERC95, NERC96]: The power system is judged to be secure for the purpose of interarea transfer if “all facility loadings are within normal ratings and all voltages are within normal limits”, the system “remains stable following a disturbance that results in the loss of any single element”, “the post-contingency system ... has all facility loadings within emergency ratings and all voltages within emergency limits” [Sau97]. While there exists general agreement concerning the fundamental requirements of posted transfer capabilities, computational procedures are currently in the process of refinement. Implementation varies regionally as well as by projected time period (criteria for next day analysis can differ from seven days ahead). The most current

information can be found at the OASIS web sites for each operating region. This section outlines the components common to many transfer capability computations [Sau97].

- **Specify Operating Horizon.** The time period, or operating horizon, for the transfer capability computations must be specified. The assumptions used to establish a base case as well as security criteria can depend upon the operating horizon.
- **Establish Base Case.** The base case reflects the most likely condition of the power system for some point in the (possibly very near) future. Obtaining a credible base case is not a trivial task since there is always uncertainty with forecasting the future. The base case must account for the forecast loading in each area and all scheduled and forced transmission and generator outages for the identified operating horizon. In addition, transmission reservations and energy schedules (existing transmission commitments) must be accounted for in a manner consistent with the operating horizon. Generation dispatch in each area must be specified along with a stacking order and some criteria to distribute additional demand arising from deviations to the base case. Normal and emergency limits for all lines and transformers need to be specified.
- **Capacity Benefit Margin Determination** Reliability criteria require that a portion of the total transfer capability be reserved to meet generation reliability requirements. The reliability criteria can be based on historical analysis, the result of a Loss of Load Expectation computation, or based on the size of the largest plant or two largest units in the area.
- **Transfer Specification** A list of possible transfer directions to consider must be obtained, along with specification of participation factors for generation and source and sink for each transfer.
- **Contingency Incremental Transfer Capability Computation** A list of contingencies must be obtained and some system of contingency analysis and incremental transfer adjustment for each transfer direction computed. This step often makes use of sensitivity and DC loadflow assumptions. The point of this computation is to establish the limiting contingency and event (usually assumed to be a flow limit) for each transfer direction.
- **Transmission Reliability Margin Determination** The transmission reliability margin is determined from the contingency incremental transfer capabilities. The TRM is intended to provide a safety margin for the posted transfer

capability in view of credible contingencies.

The available transfer capability is defined as

$$\begin{aligned} \text{Available Transfer Capability (ATC)} = & \\ & \text{Total Transfer Capability (TTC)} \\ & - \text{Existing Transmission Commitments (ETC)} \\ & - \text{Transmission Reliability Margin (TRM)} \\ & - \text{Capacity Benefit Margin (CBM)} \end{aligned}$$

There is considerable flexibility within the framework described by [NERC95, NERC96]. Significant variation in implementation exists between regions and areas. For example, the list of credible contingencies considered and the weighting applied to each, or the conditions which merit full AC solution and which can be adequately screened with DC or sensitivity methods can influence the transfer capability computations. In addition, the existing transactions considered in the computation might only include firm transactions or they may include non-firm transactions or projections. In some respects the process of posting available transfer capability is similar to booking seats on an airplane; each individual airline can decide for each flight how many tickets should be sold, even if they sell more or less than the number of seats on the capacity for. However, they most certainly do know exactly what the capacity of each plane is! Essentially, transfer capability computation involves forecasting, contingency analysis and ranking, multiple AC power flow solutions, and engineering judgment based on system experience.

Path following methods

Path following methods are a useful tool for accurately computing transfer capabilities. Path following or continuation methods work by tracing equilibrium solutions from a known operating point as some parameter is adjusted. The problem of computing a transfer margin to a security violation involves finding an equilibrium that satisfies a specific condition such as a variable reaching a limit.

Continuation methods can be implemented with any set of power system equilibrium equations, although common descriptions of the programs often assume the standard power flow equations. The continuation program used to establish the transfer capabilities must take into account the effects of limits that change the equilibrium equations and the sequence in which the limits are encountered. In particular, the continuation program should use a predictor-corrector method so that equilibrium solutions are found at successive limit events.

The transfer for a particular transfer direction is gradually increased starting at the base case transfer, and several equilibria computed corresponding to different transfer levels until the critical security violation is encountered. The real power transfer at the first security violation is the total transfer capability.

System modeling

This section details the modeling required to compute the transfer capability. The continuation program used to establish the nominal transfer capability traces equilibrium solutions, not transient trajectories of the state. Thus, detailed equations that model the dynamic response of the system yield the same results as steady state equations provided that they have the same equilibrium solutions [Dob94].

The model must include the following:

- Static equilibrium equations. The equilibrium equations can be standard or elaborate power balance equations, or the the right hand side of the system differential, or differential algebraic equations.
- Equilibrium equations that model the interarea transfers. Appending to the power balance equations equation (133) for each area is sufficient:

$$\text{Area Export Set Point} = \Sigma(\text{area tie line MW flows}) \quad (133)$$

A transfer between two areas is enforced by raising the export set point of the sending area and lowering the export set point of the receiving area by the amount of the transfer.

- Static generator dispatch equations. As the transfers are altered, the dispatch equations should distribute area slack to the area generators proportionally according to the generator participation factors. For example, if the generator participation factor of the i th generator in the area is α_i , the dispatch equation can take the form

$$(\text{generator } i \text{ output}) = \alpha_i P_{\text{area slack}} \quad (134)$$

A more detailed representation of the voltage control system and governor equations is probably not necessary because of the time frame appropriate for ATC computations.

8.3 Sensitivity

Once the capability for one transfer direction has been determined, it is useful to estimate the effect on the transfer capability of adjusting simultaneous transfers, and of modifying the assumptions used for the initial transfer capability determination. This section states the sensitivity formulas and outlines the computations. The formulas are derived and further explained in Chapter 4.

8.3.1 Assumptions

We assume that the transfer capability (CBM, TRM, ATC and TTC) for an interface has been obtained and also a critical limit and corresponding solved case (the critical case) at which the limit is encountered has been identified by a continuation method. For example, DC loadflow methods, transfer distribution factors and outage sensitivities can be used to find the approximate TTC for many cases and identify a critical contingency and TRM, then a continuation of AC loadflow solutions could be used to refine the capability computation and screen for voltage and VAR limits likely to be encountered between the base case and the critical case. The critical case may then reflect a post-contingency system, and the system equations at the critical case could differ from that of the base case. Changes in the equations might reflect a line contingency or application of generator real and reactive power limits and emergency dispatch policies.

We assume that the static equations that model the power system just before encountering the critical event can be written in the form

$$0 = F(z, \lambda, p) \tag{135}$$

where

- z is the vector of n equilibrium states, which can include individual line flows as well as total flows across each interface.
- λ is a parameter vector of area export set points.
- p is a vector of parameters such as bus power injections, load parameters or generator participation factors [GDA97]. p can also be considered elements of λ for computation of the sensitivity of a transfer margin to simultaneous transfer.
- F should include area interchange, generator dispatch, and any other static controls. If a differential-algebraic or differential equation model of the power system is available then F can be chosen as the right hand side of those equations.

Note that it is useful to distinguish between the equations used for computations and the equations assumed to model the system. For example, it would be inefficient to compute all line flows or generator VAR outputs with each iteration of a loadflow solution, but it is convenient to assume that they are state variables of the model.

The security requirements are reflected by inequalities in the equilibrium states:

$$z_i^{\min} \leq z_i \leq z_i^{\max}, \quad i = 1 \cdots n \quad (136)$$

When a limit is encountered, one of the following equations holds for some i :

$$z_i = z_i^{\min} \quad (137)$$

$$z_i = z_i^{\max} \quad (138)$$

and we write the applicable equation in the general form

$$0 = z_i - z_{lim} = E(z, \lambda, p) \quad (139)$$

Suppose that at transfer λ_* the critical limit is encountered. The vector of state, transfers, and parameters at the limit is (z_*, λ_*, p_*) and

$$F(z_*, \lambda_*, p_*) = 0 \quad (140)$$

$$E(z_*, \lambda_*, p_*) = 0 \quad (141)$$

(z_*, λ_*, p_*) is the critical point identified by the ATC computation.

8.3.2 Sensitivity formulas

The sensitivity of the transfer capability T to the parameter p , denoted T_p , is computed applying the methods detailed in Chapter 4:

$$T_p = - \frac{w \begin{pmatrix} F_p \\ E_p \end{pmatrix} \Big|_{(z_*, \lambda_*, p_*)}}{w \begin{pmatrix} F_{\lambda} \hat{k} \\ E_{\lambda} \hat{k} \end{pmatrix} \Big|_{(z_*, \lambda_*, p_*)}} \quad (142)$$

where

- \hat{k} is a unit vector describing the transfer direction. For the simple case of imports across one interface matched by exports across another interface, \hat{k} is a column vector with a one in the row corresponding to one interface equation and a negative one in the row corresponding to the other interface equation.

- F_p and E_p are the derivatives of the equilibrium and limit equations with respect to parameter p .
- $F_\lambda \hat{k}$ and $E_\lambda \hat{k}$ are the vectors representing the derivatives of the equilibrium and limit equations with respect to the interarea transfers in the direction of scheduled interchange.
- w is a nonzero row vector orthogonal to the range of the Jacobian matrix J of the equilibrium and limit equations, where

$$J = \left(\begin{array}{c} F_z \\ E_z \end{array} \right) \Big|_{(z_*, \lambda_*, p_*)} \quad (143)$$

The row vector w is found by solving the linear system

$$wJ = 0 \quad (144)$$

The Jacobian matrix J has n columns and $n+1$ rows. Since every set of $n+1$ vectors in \mathbf{R}^n is linearly dependent, there is always a nonzero vector w that solves (144). J generically has rank n , so that w is unique up to a scalar multiple. This scalar multiple does not affect (142).

The first order estimate of the change in transfer capability corresponding to the change in p of Δp is

$$\Delta T = T_p \Delta p \quad (145)$$

The estimate of the transfers at the critical limit for a change in p is

$$\lambda_*(p) = \lambda_0 + \hat{k} \Delta T \quad (146)$$

Note that established sensitivity methods such as outage distribution factors and transfer distribution factors can be derived using equation (142) as shown in Chapter 4. The derivation of these sensitivities in a general framework is useful since it extends their application to voltage and VAR limitations.

If the security limit is due to voltage collapse or oscillatory instability, slightly different sensitivity formulas apply, and these formulas are presented in Chapter 4. Details concerning the formulas applicable to voltage collapse are presented in Chapter 5. The formulas applicable to oscillatory instability are detailed in Chapter 9.

8.4 Example

The methods are first illustrated with a 40 bus test system to motivate the important concepts. The methods are then tested on a realistic 1500 bus model and placed in context of the ATC evaluation.

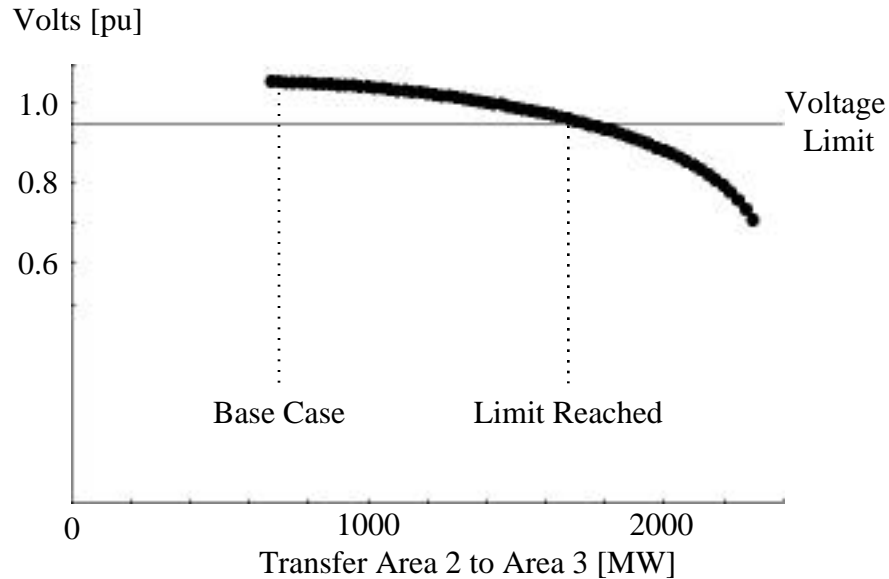


Figure 20: Critical bus voltage versus transfer to Area 3

8.4.1 40 bus system

The 40 bus system represents an equivalent network for roughly 40,000 MW of generation. There are three areas and 2 interfaces. Area 2 is modeled in the greatest detail and reflects 24,500 MW of generation. Area 1 and Area 3 are modeled in less detail. The entire system represents 36,570 MW of generation. At the base case operating point, 430 MW flow from Area 1 to Area 2 and 675 MW flow from Area 2 to Area 3.

Initial transfer computation

The initial transfer capability is computed by increasing the export set point for Area 2 and decreasing the export set point for Area 3 while holding the exports from Area 1 constant. As the transfer is increased, the first security violation is a low voltage limit corresponding to a transfer of 1734 MW across the Area 2 - Area 3 interface. If the transfer is further increased, eventually voltage collapse occurs for a transfer of 2280 MW.

Figure 20 shows the voltage profile at the bus most affected by the transfer.

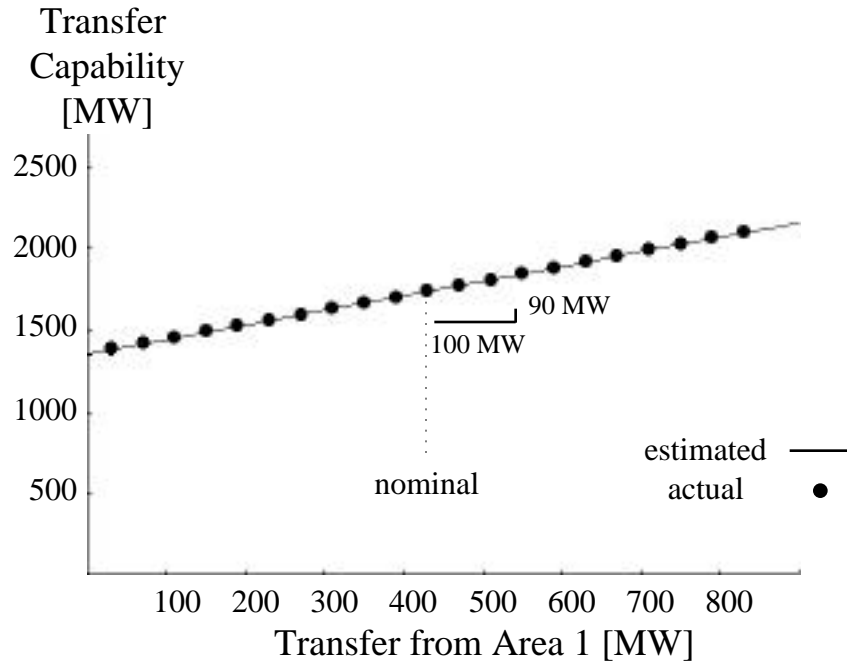


Figure 21: Effect of simultaneous transfer on transfer capability limited by low voltage

Simultaneous transfer

Formula (142) is evaluated to determine the sensitivity of the transfer capability with respect to export from Area 1 at both the low voltage limit and the voltage collapse limit. The sensitivities were used to obtain first order estimates of the transfer capability from Area 2 to Area 3 as a function of the transfer from Area 1 to Area 2. Figure 21 shows the estimates of the transfer capability limited by the low voltage limit and the actual computed transfer capability for a range of transfer from Area 1. Figure 22 shows the estimates of the transfer capability limited by voltage collapse and the actual computed transfer capability for the same range of transfer from Area 1. The dots in Figures 21 and 22 represent the actual computed boundary points and the line represents the linear estimates. Agreement between estimates and actual transfer capability is excellent.

Generator Dispatch

Assumptions concerning which generators back off or increase output to satisfy transfers can influence the transfer capability computation. In addition, unplanned generator outages can cause previously computed transfer margins to be inaccurate.

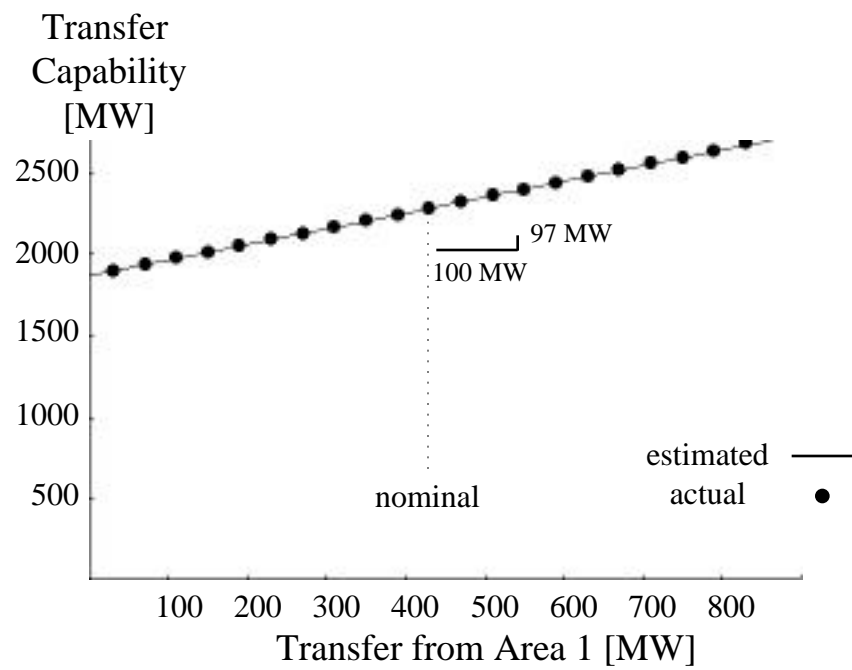


Figure 22: Effect of simultaneous transfer on transfer capability limited by voltage collapse

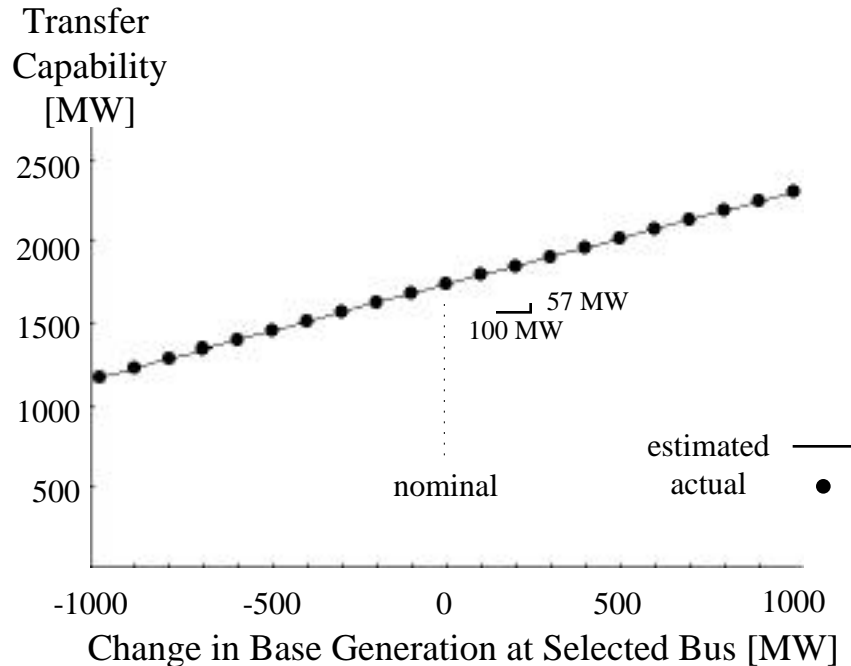


Figure 23: Effect of generator dispatch on transfer capability limited by low voltage

The largest plant in Area 2 consists of two 1000 MW generator units. The initial transfer computation assumed that only one unit was operational. The sensitivity formulas were evaluated for variation of ± 1000 MW to model the effects of either outage of the remaining unit or additional maximum output provided by the second unit. Figure 23 compares the estimates for the resulting transfer capability with the transfer capability computed by full continuation. Agreement is excellent over the entire range.

Load variation

The variation of individual or aggregate loads can affect the transfer capability. Figure 24 compares the linear estimates and the actual computations of the transfer capability resulting from changing the load level at the critical bus. The critical bus is the bus that reached the initial low voltage limit.

Reactive power support

The sensitivity formulas could prove useful determining the effects of control actions or planned improvements on the transfer capabilities. Figure 25 shows the effect of

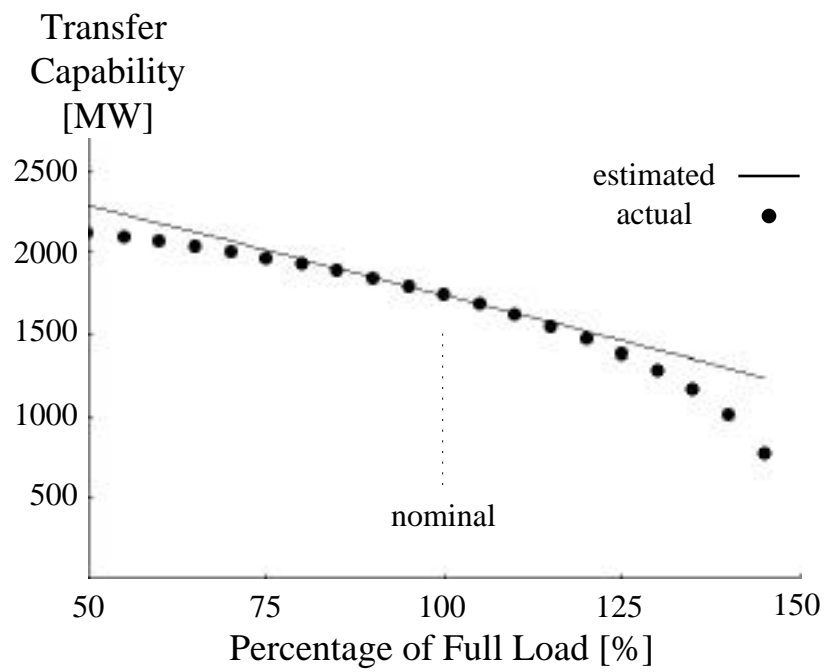


Figure 24: Effect of load variation at a critical bus on transfer capability limited by low voltage

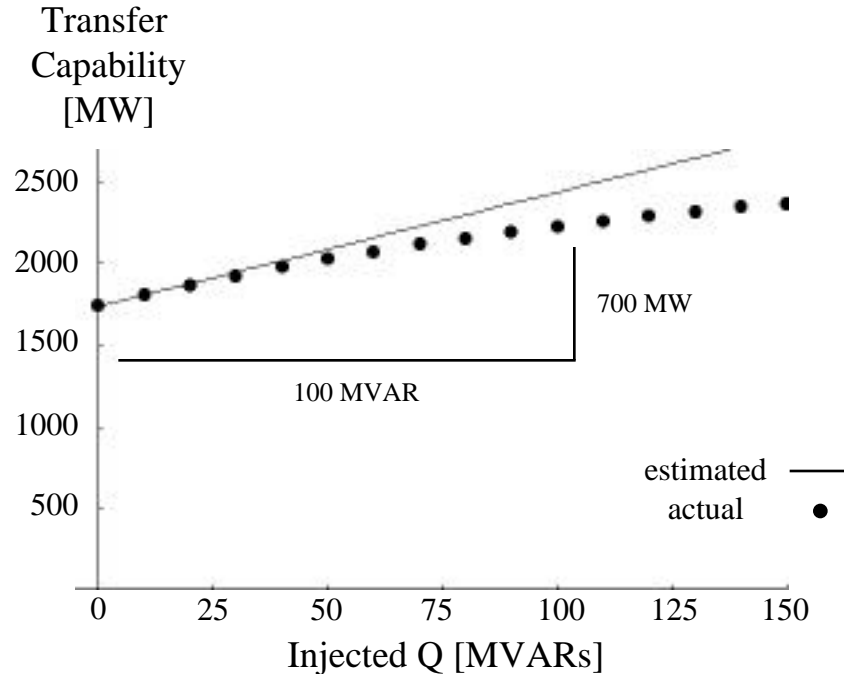


Figure 25: Effect of reactive power support on transfer capability limited by low voltage

adding reactive power support at the critical bus.

8.4.2 1500 bus system

The sensitivity formulas are tested on a 1500 bus power system partitioned into 20 areas and derived from a portion of the US grid. The main area is modeled in detail (1200 buses), and the other areas are represented by equivalents that retain all tie buses and tie bus neighbors. The transfer capability computation for one transfer direction is computed and the sensitivity formulas tested. The transfer margin for one transfer direction can be used to determine the transfer capability of several interfaces. However, the computation of the ATC for all interfaces of the main area requires that the nominal transfer capability be determined from several transfer directions. The ATC for each interface is determined by the most limiting transfer capability for that interface. Several interfaces might be limited by transfer in the same direction.

Base Case. The base case reflects a solution at which all voltages and line flows are within limits. There are 235 generators in the main area representing a capacity of

Table 22: Area exports at base case, nominal transfer limit, and contingency transfer limit

Area	Net Export Base Case	Net Export Flow limit	Net Export Voltage Limit
Main	506 MW	506 MW	506 MW
A	621 MW	1597 MW	1876 MW
G	-5402 MW	-6378 MW	-6657 MW
N	1330 MW	1330 MW	1330 MW

more than 30,000 MW. The base case main area load is 24,000 MW and the total load in the entire system is 105,000 MW. The base case existing exports for the main area and areas A,G, and N are shown in the first column of Table 22. (Note that the sum of these exports does not equal zero because not all areas are shown.)

The generator incremental dispatch within the main area is determined by a constrained economic dispatch using quadratic cost curves for each dispatchable unit. The incremental dispatch of the other areas is assumed in proportion to the size of each generator in that area. The assumption concerning which buses act as sources or sinks for each transfer direction can influence the transfer capability computation. The relative participation of individual generators depends upon the economics of each generator. In a competitive environment utilities might be reluctant to share data that indicates the relative profitability of each of their units.

Transfer Specification. Transfer across the Area A - Main Area interface is increased by increasing import from Area A and increasing export to Area G.

Capacity Benefit Margin For this case, the CBM is selected to be twice the capacity of the largest unit in the main area. The largest unit in the main area has a maximum output of 900 MW and the CBM is thus 1800 MW. The 1800 MW is then allocated among six interfaces based on the results of an off-line analysis.

Transfer Reliability Margin. The critical contingency is known to be the loss of a 500kV tie line to Area G. The transfer margin is computed for the base case as well as the critical contingency (CITC).

Nominal and Contingency Incremental Transfer Capability The results in this Chapter were computed using an implementation of the program described in Chapter 3 that uses linear sensitivity to predict the next switching, MW, VAR, or flow limit and then directly computes a full AC solution corresponding to that limiting event. For the base case the limiting event is an overload on one 500KV line. For the CITC computation, the limiting event is a bus voltage reaching an emergency low voltage rating. Table 22 shows the area exports for four of the twenty areas at both

Table 23: Sensitivities of the transfer margin with respect to area exports

Area	Nominal Flow Limit [MW/MW]	Contingency Voltage limit [MW/MW]
Main	-1.003	-0.961
A	-1.000	-1.000
B	-0.945	-0.984
C	-0.929	-0.980
D	-0.989	-0.993
E	-0.997	-0.981
F	-0.989	-0.992
G	0.000	0.000
H	-0.074	0.169
I	-0.886	-0.240
J	-0.992	-0.950
K	-0.995	-0.971
L	-0.036	0.098
M	0.022	-0.455
N	-0.003	-0.050
O	-0.033	0.066
P	-0.149	0.487
Q	0.005	-0.254
R	-0.946	-0.959
S	-0.977	-0.984

the nominal and contingency transfer limits. The incremental transfer margin for the nominal transfer is 976 MW and the incremental transfer margin for the contingency case is 1255 MW.

8.4.3 Sensitivity of the transfer capability to transactions

Table 23 shows the sensitivities of the transfer margins with respect to every area export. These sensitivities are essentially the components of the normal vector to the event boundary, and are computed simultaneously with the direct method that computes the margin. The first column of Table 23 shows the sensitivities of the line flow limited transfer capability with respect to all area export set points, normalized so that Area G is the slack area. The second column of Table 23 shows the relative sensitivity of the voltage limited contingency incremental transfer capability with

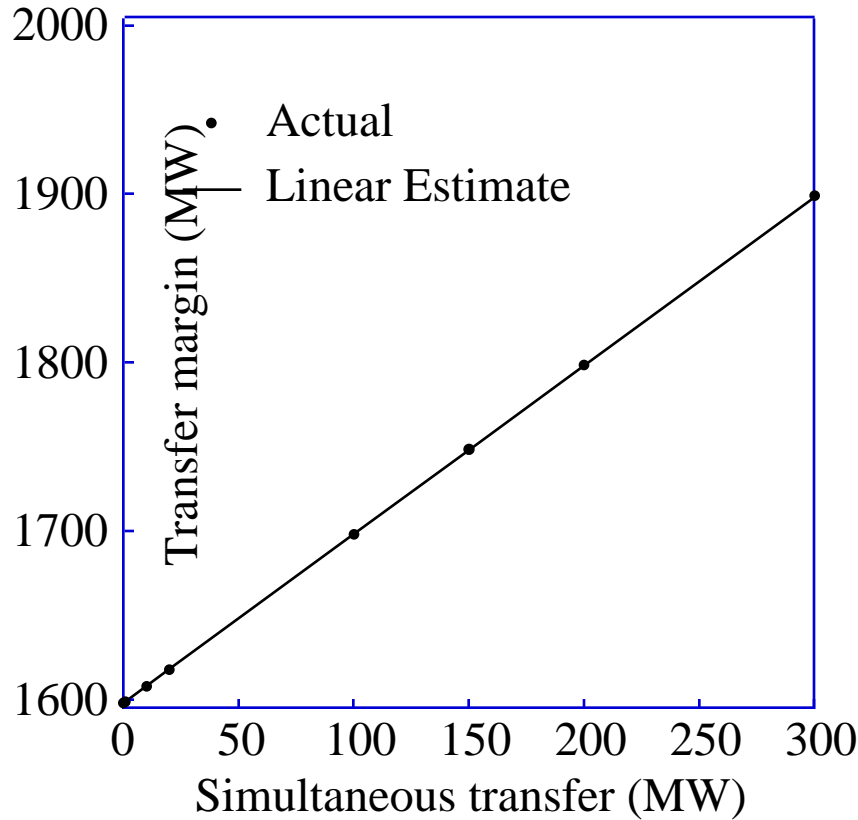


Figure 26: Effect of simultaneous transfer on margin to first flow limit

respect to the area export set points. To compute the sensitivity of the margin with respect to a transaction between two areas, simply subtract the component corresponding to the receiving area from the component of the sending area. These sensitivities indicate that transfer from Area M to the main area should be the most effective in reducing the overload. The sensitivities also indicate that transfer from Area P to Area A best relieves the voltage constraint.

Equation (142) is used to compute estimates for the change in the nominal transfer capability, as limited by the line overload, resulting from transactions between Area N and the main area. Figure 26 shows the linear estimate for the change in transfer margin as a function of the simultaneous transfer from Area N to the main area. The estimates are compared with actual values computed by continuation represented by the dots in Figure 26. Figure 27 compares the linear estimate with actual values computed by continuation for the change in the voltage limited contingency incremental transfer margin.

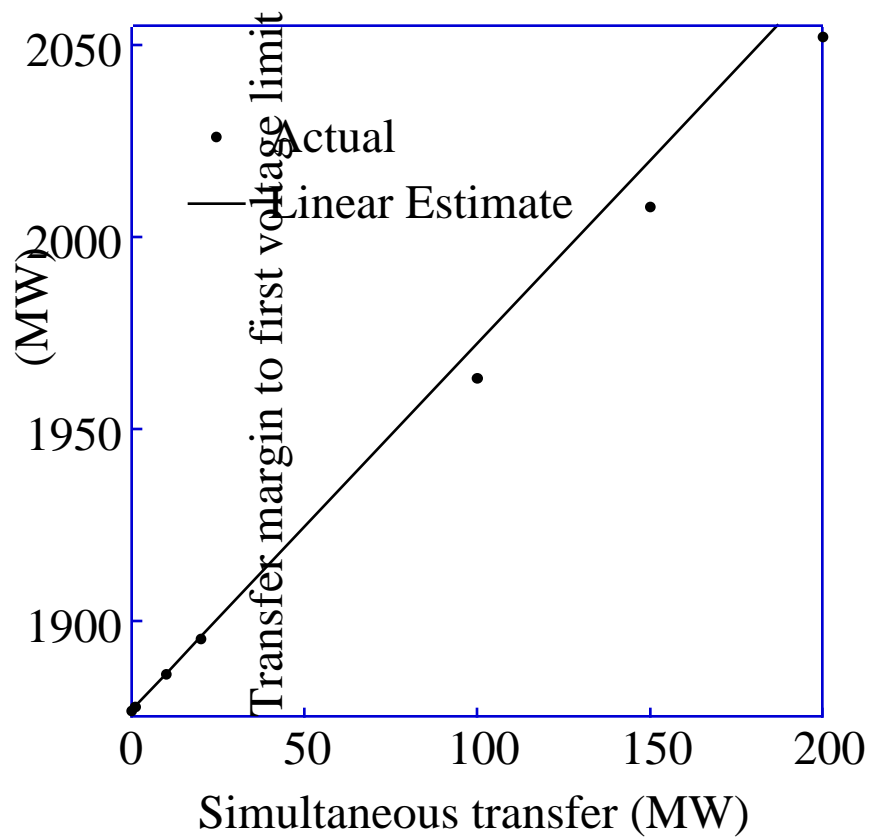


Figure 27: Effect of simultaneous transfer on margin to voltage limit

8.4.4 Computational efficiency

Results were obtained running MATLAB version 5 uncompiled on a 200 MHz Pentium based computer with 96 MB of RAM.

The continuation program uses exact first order sensitivities at each solved equilibrium point to compute estimates of the transfer margins to the following events:

- generator maximum and minimum real power limits
- generator minimum reactive power limits
- line and transformer flow limits
- shunt switching events initiated by high and low voltage limits
- low bus voltage limits

Testing the program on several scenarios using the 1500 bus system indicates that the method is effective and reduces the total number of loadflow solutions required by each continuation. The program forces a maximum 250 MW step increase. The average transfer step between event solutions is 120 MW, and the median step is 136 MW. The maximum step size predicted a flow limit for a 227 MW transfer with less than a .1 MW error. 85% of solutions required 2 loadflow iterations or less and no solutions required more than 3 iterations. (Note that in all cases maximum transfer was limited by voltage collapse precipitated by VAR limits causing immediate instability as indicated by the voltage sensitivity computation after application of the limit. Direct solution of fold bifurcation solutions most likely would require more loadflow iterations.) The mean error for the predictor step was 4.8% and the median error was 3.7%. The majority of events are generator VAR limits and voltage limits. Voltage and VAR limits tend to yield larger errors than real power or flow limits. Larger step sizes were correlated with large errors.

The continuation method to establish the limiting event for a transfer direction usually requires less than one minute. However, depending upon the initial operating point, one continuation can take from several seconds to several minutes. From a typical operating point, increasing the largest transfers past several limiting events to establish the point of maximum transfer (fold bifurcation or immediate instability) requires about 10 minutes. The method is slowed by the large number of voltage and VAR limits that are encountered near points of extreme transfer or loading.

Computation of the event normal vector once the event point is found is about equivalent to one iteration of the loadflow, and required less than one second. Computation of the derivatives with respect to varying transfer directions is a simple index

operation requiring virtually no time once the normal vector is computed. Thus, once the limiting event is found, the sensitivity of the transfer margin to that event with respect to thousands of simultaneous changes in load, generation, interarea transfers or line status can be obtained in less than one second.

8.5 Discussion

The results show that the computation of transfer margins by continuation methods is efficient and yields important sensitivity information. The sensitivity information is obtained as a by-product of the computation to obtain the transfer margins. The sensitivities prove accurate at estimating the effect on the margins of simultaneous transfer not considered by the continuation.

The example is representative of only a portion of a complete ATC computation. The transfer margins would need to be computed for several other transfer directions. However, the sensitivity of the margins to the area exports indicate which transfer directions are likely to affect the margin to each event. In addition, the transfer margins are used to determine the limiting flows on each interface. Once the incremental transfer margins for enough nominal and contingency transfer directions have been computed, the minimum flows on each interface corresponding to limiting transfers are established. Then a portion of the CBM is allocated to each interface and the ATC of each interface is posted for that operating horizon. The entire ATC computation needs to be repeated for each operating horizon in which the conditions and assumptions have changed. The practical use of accurate sensitivity information could ease the computational burden of this process.

8.6 Conclusions and Future Work

This chapter suggests how the sensitivity of the transfer capability can be computed and used to estimate the effect on the transfer capability of variations in parameters such as those describing other transfers, operating conditions or assumptions. A continuation method is used to find the nominal and contingency incremental transfer capability. The first order sensitivity of this transfer capability to a wide range of parameters can then be quickly computed. The objective is to use these sensitivities to quickly extract the maximum possible engineering information from each continuation. The sensitivity methods could contribute to the quick update of transfer capabilities when operating conditions or other transfers change. The sensitivity information should greatly reduce the computational burden of computing the available transfer capability and the transfer reliability margin.

Chapter 9

Eigenvalue and margin sensitivities for the avoidance of interarea oscillations

The loss of system stability due to voltage collapse associated with the saddle node or fold bifurcation was addressed in previous chapters. This chapter concerns oscillatory instability which is associated with Hopf bifurcation. The fold bifurcation is characterized by a simple zero eigenvalue of the Jacobian matrix of the system *equilibrium* equations. The Hopf bifurcation is characterized by an undamped complex pair of eigenvalues of the Jacobian matrix of the system *dynamic* equations. Since detection of Hopf bifurcations requires dynamic equations, not just equilibrium equations, the analysis is different from that of the previous chapters but still follows the same general framework.

9.1 Introduction

Interarea oscillations are often observed as oscillations of real power flow between regions of a power system or groups of generators [IEEE1]. Voltages and current oscillate with the power swings. If the oscillations are undamped, voltages may exceed limits causing protective devices to trip and forcing equipment outages. Cascading outages can lead to blackouts.

Established methods of preventing and controlling interarea oscillations require the linearization of the system dynamic model about an operating equilibrium point [IEEE1, Kundur, SauPai, Bergen]. The eigenvalues, and thus qualitative behavior, of the linearized system depend upon the equilibrium point at which the system is linearized. Standard linear control system techniques can be applied to the parameters of the linearized model. However, when the gross operating conditions of the system change, a new equilibrium point must be calculated and the control techniques applied to the linearized system at that new equilibrium.

Many of the parameters that influence the system equilibrium point, such as interarea transfers, do not appear as parameters of the linearized equations and thus

the effects of changing these parameters on the dynamic behavior of the power system can not be ascertained from the linearized equations. In addition, the power system can be modeled by separate equations for different time scales. The equations that are used to detect an oscillation (transient time scale) are different than those used to trace the long time slow evolution of the system (steady state time scale).

This chapter presents a method for avoiding interarea oscillations by determining the effects of controls and parameters that move the steady state system equilibrium of the power system. The methods in this chapter can be used to analyze the effect on an oscillation of varying *interarea transfers* and wheeling agreements, generator dispatch, load shedding, and direction of load growth.

Previous Work

References [SauPai, Kundur] include both contemporary and classical approaches to power system dynamic stability and machine modeling. The texts [WW, Bergen, Kusic] all contain informative descriptions of the Automatic Generation Control (AGC) and tie line bias control. The working group paper [Jal92] and its many discussions provide an accurate assessment of current AGC practices and emphasize the time scale appropriate for AGC. Anderson and Fouad [AF] is the classic text for power system control and stability.

The basic mathematical analysis of the Hopf bifurcation is well covered in [GH] and computational methods to locate Hopf bifurcations are presented in [Seydel] and [Alv90]. Eigenvalue parametric sensitivity and generalized eigenvalue computation is addressed in [GV]. Previous work concerning Hopf bifurcations in power systems includes [AV84], [DAD92] and [MMH95]. [Cañ95] and [HH91] address saddle node bifurcation in systems of differential-algebraic equations. Applicable work regarding small signal stability and eigensensitivity includes [IEEE1], [Mar86], [Sme93]. [DC91] considers the computational complexity and cost of parametric robust stability determination for power system dynamic models. Methods for computing eigenvalues and eigenvectors for power systems are presented in [Mar86, WS90, WRPK, AS96] and for general sparse unsymmetric matrices in [DS93].

9.2 Assumptions and model

In this section we state the primary assumptions underlying the methods presented in this chapter. The primary assumptions are implied by standard power systems practice and are qualitative and not dependent upon specific equations for the power system. However, secondary assumptions regarding the explicit system equations are

necessary for computation and quantitative analysis.

Over transient time periods (less than one second to tens of seconds), disturbances and fluctuating demands result in the system frequency varying about synchronous speed. Generators respond to frequency fluctuations according to their governor characteristics and the interarea flows vary around the scheduled transfers. The dynamic behavior of the power system over transient time periods is assumed to be represented by parameterized differential equations,

$$\dot{z} = F(z, r, \lambda) \quad (147)$$

where

F is smooth with respect to z, r and λ .

z is the vector of state variables.

r is the vector of load reference set points for each generator.

λ is a vector of parameters.

The system (147) is often modeled by a differential-algebraic system of equations

$$\begin{aligned} \dot{x} &= f(x, y, r, \lambda) \\ 0 &= g(x, y, r, \lambda) \end{aligned} \quad (148)$$

where

$z = (x, y)$ is the vector of state variables.

f and g are smooth with respect to z, r and λ .

The derivative of g with respect to the y variables, denoted g_y is nonsingular evaluated over the range of interest.

The distinction between variables and parameters is crucial. Parameters are active; they are directly set or assumed. Variables are passive; they assume the values imposed by solution of the equations. The choice of variable and parameter is time scale dependent. The differential-algebraic system of equations (147) account for the transient behavior of the power system for which the vector load reference set points is considered a parameter of (147). A perturbation to the parameters cause the state to move from equilibrium and the system frequency to change.

The steady state behavior of the power system over longer time periods is assumed to be represented by static equations,

$$0 = H(z, r, \lambda) \quad (149)$$

where

z and r are variables.

$\lambda \in \mathbf{R}^m$ is a vector of parameters.

H is smooth with respect to z, λ and r .

$$H(z_0, r_0, \lambda_0) = 0 \Rightarrow F(z_0, r_0, \lambda_0) = 0$$

Note that in (147) or (148) r is a parameter, but in (149) r is a variable. The equations (149) consider the time scale in which generation is economically dispatched to meet the slowly evolving component of load fluctuation and the Automatic Generation Control (AGC) acts to maintain scheduled interchanges and restore system frequency. Equations (147) or (148) represent the behavior of the system as the loads and the state fluctuate about nominal equilibrium values and system frequency can deviate from synchronous speed. Equilibria of H are equilibria of F , but H includes equations that describe how r changes over extended periods of time to account for economic dispatch, interarea schedules, and AGC, and assumes that system frequency is synchronous speed.

The electrical output of a generator is controlled by two inputs, the governor droop and the load reference set point. The governor droop determines how the generator responds to a change in frequency. The governor droop is a constant parameter, not a control parameter. The load reference set point determines the steady state power output of the generator. The load reference set point is a control input that can be revised according to an economic dispatch and permits control through the AGC.

Immediately following a disturbance the transient response of each generator is determined by its electrical proximity to the disturbance. The system frequency a short time (a few seconds) after a disturbance, and the proportion of the disturbance “picked-up” by each generator, is determined by each generator’s rotating inertia. Several seconds after a disturbance the system frequency and generator response is affected by each generator’s governor and droop. The relative outputs of the generators when the system frequency is restored to synchronous speed is determined by each generator’s load reference set point. The load reference set point is adjusted only every few minutes, not seconds [Jal92]. Over transient time periods then, the load reference is a parameter. Over longer time periods that assume steady state operation at synchronous speed, the load reference set points are variables determined by the system conditions and dispatch policy. At steady state the load reference set points equal the generator power outputs.

Although the separation of the power system model into separate equations for different time scales is not usually explicitly stated, this corresponds to the standard practice of solving a loadflow to determine an operating point (solving (149)) but using a detailed dynamic model (147) to either estimate the stability via eigenvalue computation, or the transient trajectory following some disturbance. Note that the

load reference set points are not always the only quantities that are a variable in one time scale and a parameter for the other. For instance, it is common to model loads differently for steady state time scales than for transient time scales. The key differences between the transient and steady state models are:

- System frequency is a variable for the transient time frame and a constant for the steady state time frame.
- Economic dispatch and area interchange occur over the steady state time frame but not the transient time frame.

The time scale separation of the power system model is not an artifact of approximate equations but a reflection of intentional control design. The decoupling of the transient control from the operational control provides for the secure operation of the power system during severe disturbances.

The steady state power system model is valid for some particular parameter value λ_0 if:

1. The steady state equations (149) have an equilibrium solution (z_0, r_0, λ_0) . (z_0, r_0) is referred to as the *equilibrium state*.
2. (z_0, r_0) is an exponentially stable equilibrium solution of the differential equations (147).
3. The system state remains in the basin of attraction of the equilibrium solution of the differential equations (147).

Fundamental to these assumptions is the distinction between the equilibrium state and the system state. The system state consists of the instantaneous values of the state variables. The equilibrium state however, is a theoretical point in state space that represents the fixed point of the differential equations (147) that model the system at that moment. We do not require that the power system state be at equilibrium, only that the equations that model the system have an equilibrium.

The assumptions imply that the dynamic behavior of the power system is qualitatively the same as that of a linearized system at the equilibrium solution of the differential equations (147). The stability of the power system with equilibrium state (z_0, r_0) can thus be determined by the stability of the linear differential equation

$$\dot{z} = A\Delta z \tag{150}$$

where $A = F_z|_{(z_0, r_0)}$. Since the power system equilibrium is assumed exponentially stable, all the eigenvalues of A have negative real part.

By locating the parameters λ at which the assumptions break down, we identify not only the limits of the model but also a boundary at which reliable operation of the actual power system is unlikely. The model breaks down by two generic mechanisms:

1. The stable equilibrium solution disappears as parameters change.
2. The stable equilibrium solution becomes unstable as parameters change.

Mechanism (1) is characterized by the disappearance of the *equilibrium solution* and is associated with voltage collapse. Mechanism (2) is characterized by a complex pair of eigenvalues of the linearized equation (150) with zero real part corresponding to Hopf bifurcation of the differential equations (147) and the occurrence of undamped oscillations in the actual system. Lightly damped oscillations are problematic in the actual power system, and correspond to eigenvalues of (150) approaching but not necessarily crossing the imaginary axes. This chapter presents methods of predicting and avoiding oscillations by changing λ , the parameters of the equilibrium equations (149).

9.3 Motivation

Suppose that as a transfer increases on a power system a lightly damped mode appears. If the transfer further increases will an oscillation occur? If another transfer is adjusted will the damping of the mode become worse or better?

One approach to answer these questions involves gathering empirical sensitivity information from repeated computations. Several equilibrium solutions of (149) corresponding to different transfer levels (λ) are computed and then the eigenvalues of (150) corresponding to each equilibrium are found. If several possible changes to the interarea transfer are under consideration, equilibrium solutions and eigenvalues are computed for each case. If results are needed for several different load levels, then for each set of transfers, equilibrium and eigenvalue computations must be repeated at each loading. This empirical sensitivity analysis is computationally burdensome.

An alternative to empirically determining sensitivity requires evaluating analytical formulas for the sensitivities of interest. In particular, we are interested in the sensitivity of the damping of the least damped mode, and the sensitivity of the margin to onset of oscillations (or unacceptably low damping). Instead of computing many equilibrium solutions of (149) and corresponding eigenvalues of (150) for each, one or only a few equilibrium solutions are obtained and the sensitivity with respect to any parameter evaluated. The damping or margin resulting from changes to parameters can then be approximated by a Taylor series.

The advantage of empirical sensitivity determination is accuracy. The disadvantage is computing time. Analytical sensitivity evaluation offers great time savings by many orders of magnitude.

9.4 Computations

In this section we present the formulas for the sensitivity of an eigenvalue and the sensitivity of the margin to oscillations, with respect to any parameter.

Eigenvalue sensitivity

Assume that (z_0, r_0, λ_0) is the present stable operating point with a lightly damped semisimple eigenvalue μ . Let $A = F_z|_{(z_0, r_0, \lambda_0)}$ represent the Jacobian matrix of (147) evaluated at (z_0, r_0, λ_0) . Then an equation for μ in terms of its corresponding eigenvectors is

$$\mu = wAv \quad (151)$$

where w is the left (row) eigenvector of A corresponding to μ and v is the right (column) eigenvector of A corresponding to μ . Choose w and v normalized so that $|v| = 1$ and $wv = 1$. We are interested in how μ changes as λ varies. For instance, λ represents the scheduled interchange transfers. As λ varies, z and r vary to satisfy (149) and thus μ changes as A is evaluated at a different equilibrium.

$$\mu(z, r, \lambda) = wF_z(z, r, \lambda) \quad (152)$$

Thus, computing the sensitivity of μ is a two step process: first the sensitivity of the equilibrium state to changing λ is computed, and then the sensitivity of μ found by application of the chain rule. The sensitivity of the equilibrium state with respect to λ is found by solving the linear system

$$\left(\begin{array}{cc} H_z & H_r \end{array} \right) \Big|_o \begin{pmatrix} Z_\lambda \\ R_\lambda \end{pmatrix} = \left(\begin{array}{c} -H_\lambda \end{array} \right) \Big|_o \quad (153)$$

where $0 = (z_0, r_0, \lambda_0)$. The vector Z_λ represents the sensitivity of the equilibrium state with respect to λ . The vector R_λ represents the sensitivity of the load reference set points (or mechanical inputs) to the generators with respect to λ . The sensitivity of the eigenvalue with respect to λ is then found by evaluating

$$\mu_\lambda = \left(\begin{array}{cc} wF_{zz}v & wF_{zr}v \end{array} \right) \begin{pmatrix} Z_\lambda \\ R_\lambda \end{pmatrix} + wF_{z\lambda}v \quad (154)$$

Note that since w and v are also functions of the equilibrium state, computing second order and higher sensitivity terms requires solving for the derivatives of the eigenvectors [GV]. In typical system models $F_{zr} = 0$ and for most of the parameters we are considering, $F_{z\lambda} = 0$ since λ and r do not appear in F_z . Estimates for the change in the damping as λ changes by $\Delta\lambda$ are found from

$$Re\{\Delta\mu\} = Re\{\mu_\lambda\}\Delta\lambda \quad (155)$$

The steps in the computation then are :

1. obtain F_z evaluated at (z_0, r_0, λ_0)
2. find the eigenvalue μ and corresponding eigenvectors w and v of the critical mode.
3. obtain the Jacobian matrices H_z, H_r, H_λ at (z_0, r_0, λ_0)
4. solve the linear system (153) for Z_λ and R_λ .
5. obtain the Hessian tensors F_{zz} and $F_{z\lambda}$ at (z_0, r_0, λ_0)
6. evaluate (154)
7. evaluate (155) for proposed changes $\Delta\lambda$

The computation generalizes to the case when λ is a vector.

Sensitivity of the margin to onset of oscillations

Again let (z_0, r_0, λ_0) represent the stable operating point with an eigenvalue μ . We are concerned with how much the scalar parameter λ can vary before the damping of μ becomes unacceptably low or zero. Several equilibrium solutions of (149) are found for varying λ until one with unacceptable damping is located. (Alternatively, consider a present operating point of unacceptable damping.) Let $(z_*, r_*, \lambda_*) = *$ represent this critical equilibrium point. Then $\lambda_* - \lambda_0$ is the nominal margin to oscillation. Now we ask how altering another scalar parameter, p , can influence the margin. For instance, if λ represents the transfer to one area, p might represent the transfer to another area. The margin to oscillation is denoted Λ , and is an implicit function of p .

Computing the sensitivity of Λ with respect to p involves solving the linear system

$$\begin{aligned} & \left(\begin{array}{ccc} H_z & H_r & H_\lambda \\ wF_{zz}v & wF_{zr}v & wF_{z\lambda}v \end{array} \right) \Big|_* \begin{pmatrix} Z_p \\ R_p \\ \Lambda_p \end{pmatrix} \\ & = \left(\begin{array}{c} -H_p \\ -wF_{zp}v \end{array} \right) \Big|_* \end{aligned} \quad (156)$$

The vector (Z_p, R_p) represents the sensitivity of the equilibrium state and mechanical power inputs on the boundary of constant damping of μ as p and λ vary. Again, note that commonly $F_{z\lambda} = F_{zr} = F_{zp} = 0$. Estimates for the change in the margin as p changes by Δp are found by

$$\Delta\Lambda = \Lambda_p \Delta p \quad (157)$$

The steps in the computation are :

1. obtain the critical equilibrium (z_*, r_*, λ_*)
2. find the eigenvalue μ and corresponding eigenvectors w and v of the critical mode at the critical equilibrium.
3. obtain the Jacobian matrices H_z, H_r, H_λ, H_p at (z_*, r_*, λ_*)
4. obtain the Hessian tensors $F_{zz}, F_{z\lambda}$ and F_{zp} at (z_*, r_*, λ_*)
5. solve the linear system (156) for Z_p, R_p , and Λ_p .
6. evaluate (157) for proposed changes Δp

Solution of (156) can be simplified as follows. Compute the vector η satisfying

$$\eta \left(\begin{array}{cc} H_z & H_m \\ wF_{zz}v & wF_{zr}v \end{array} \right) \Big|_* = 0 \quad (158)$$

Since $\left(\begin{array}{cc} H_z & H_r \\ wF_{zz}v & wF_{zr}v \end{array} \right) \Big|_*$ has one more row than column, there is always a vector satisfying (70). Pre-multiplication of equation 156 by η and rearranging yields

$$\Lambda_p = - \frac{\eta \left(\begin{array}{c} H_p \\ wF_{zp}v \end{array} \right) \Big|_*}{\eta \left(\begin{array}{c} H_\lambda \\ wF_{z\lambda}v \end{array} \right) \Big|_*} \quad (159)$$

The sensitivity of the margin with respect to p is then found by evaluating (159).

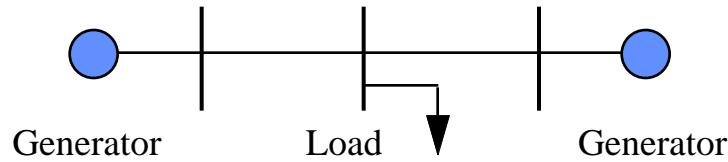


Figure 28: One line diagram of 3 bus test system

9.5 Results

This section presents results concerning measuring distances to instabilities in terms of interarea flows, tie line flows, or flows on particular lines. Adjusting the dispatch of generation to maintain specific line flows is one type of power system control that can not be well represented by the classical approach of linearizing about an operating point. Adjusting the dispatch or interchange moves the equilibrium without any change to the parameters that appear explicitly in the linearized model.

3 bus system

The first example involves a three bus, two line system. There is a load bus connected to two generator buses. Figure 28 shows a one line diagram of the system. From a nominal stable operating point, increasing the load at the load bus at a constant power factor causes a Hopf bifurcation to occur. Thus, from the stable operating point, it is possible to measure the distance to instability with a loading margin. The loading margin to oscillation instability can be affected by adjusting the generator dispatch. Figure 29 shows the results for varying the proportion of load assumed by Generator 2 from 0% to 20%. The nominal percentage is assumed to be 10%. The dots represent the actual computed bifurcation points, and the solid line is the estimate computed by evaluating equation (157). Note that the range for which the sensitivity gives an accurate prediction depends on the location of the nominal instability at which computations are evaluated (Figure 30).

Eigenvalue interaction

Figures 31,32,and 33 illustrate the interaction of two complex pairs of eigenvalues for the 3 bus power system model as the generator dispatch is varied. Each figure corresponds to a different setting for the voltage reference set point at one of the generator buses. Observe that a naive application of linear eigenvalue sensitivity techniques would yield little useful information. (Imagine tangent vectors to the

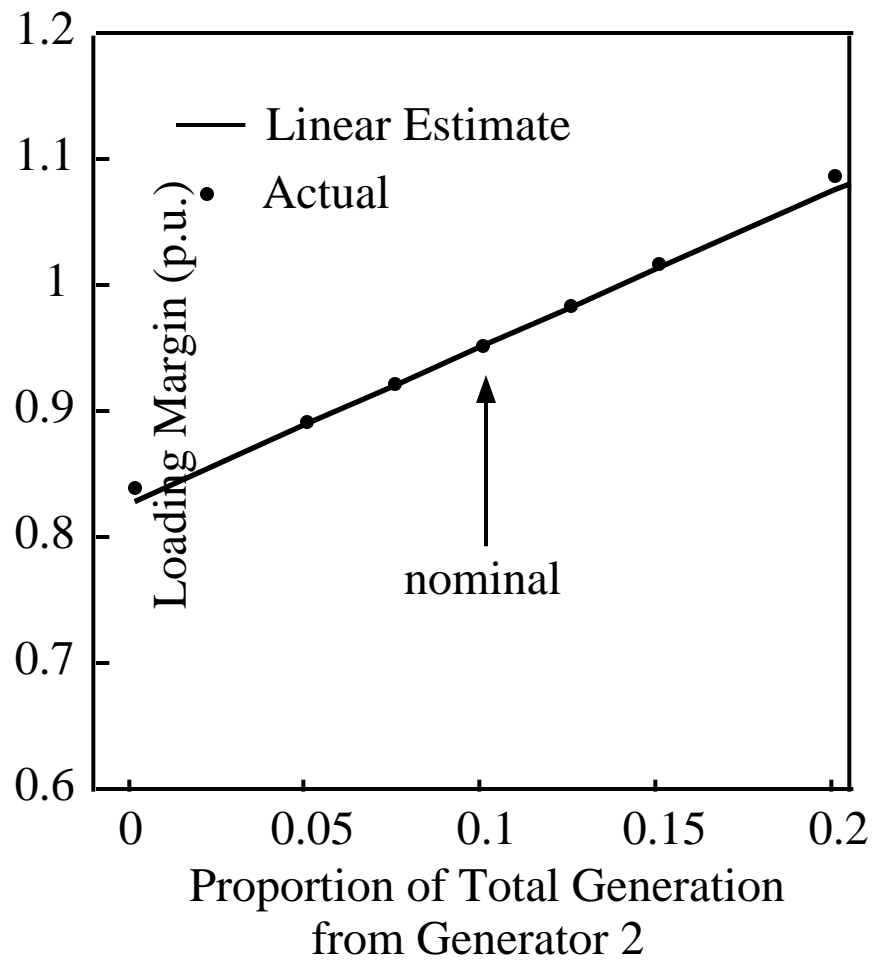


Figure 29: Effect of generation dispatch on Hopf margin

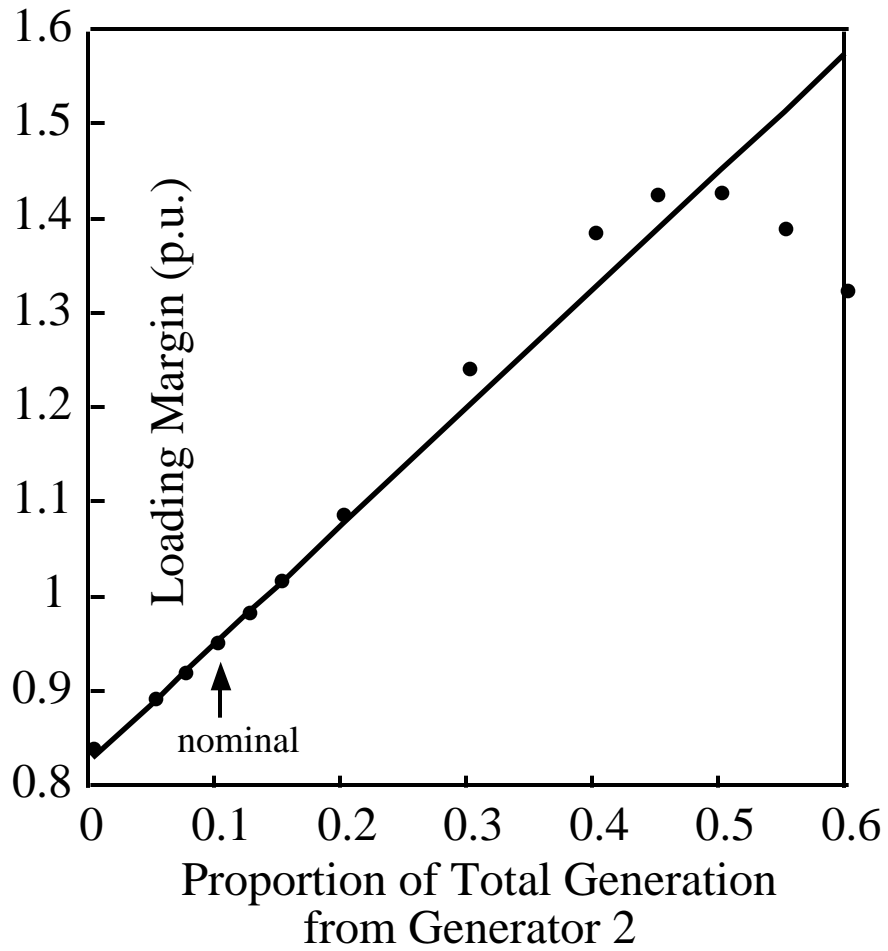


Figure 30: Effect of generation dispatch on Hopf margin, extended variation

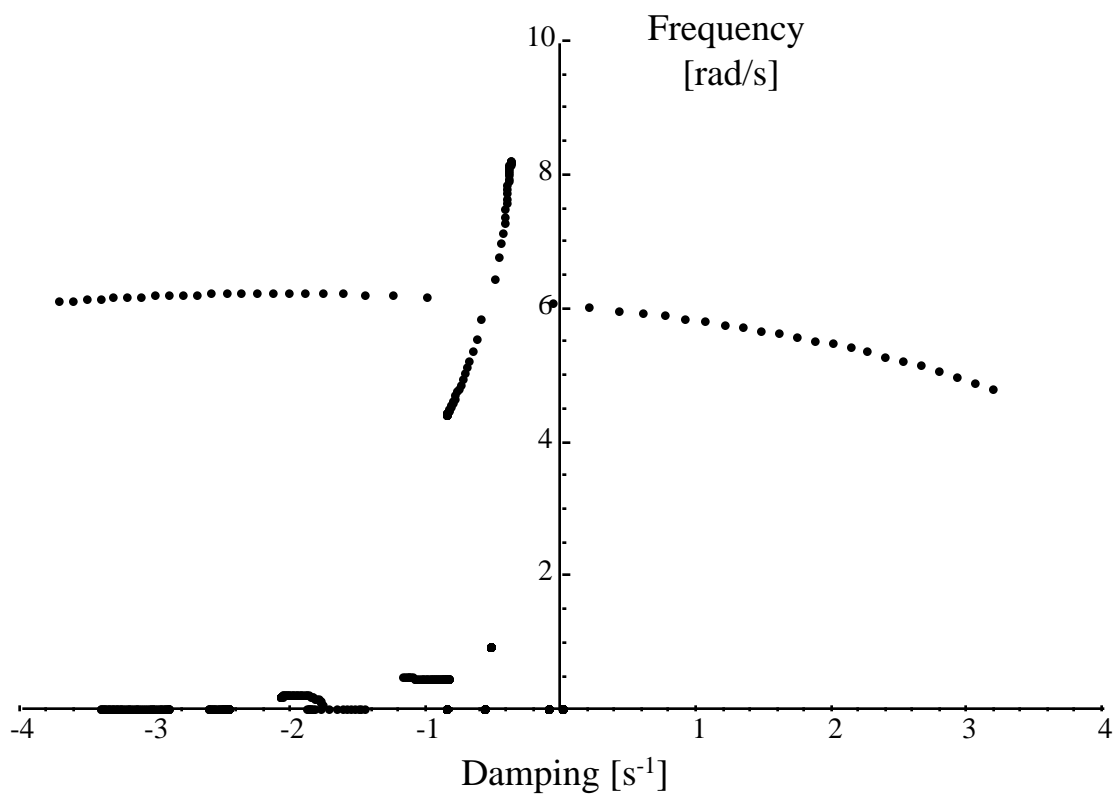


Figure 32: Trajectory of critical eigenvalues as generator dispatch is varied for generator terminal voltage of 1.05 p.u.

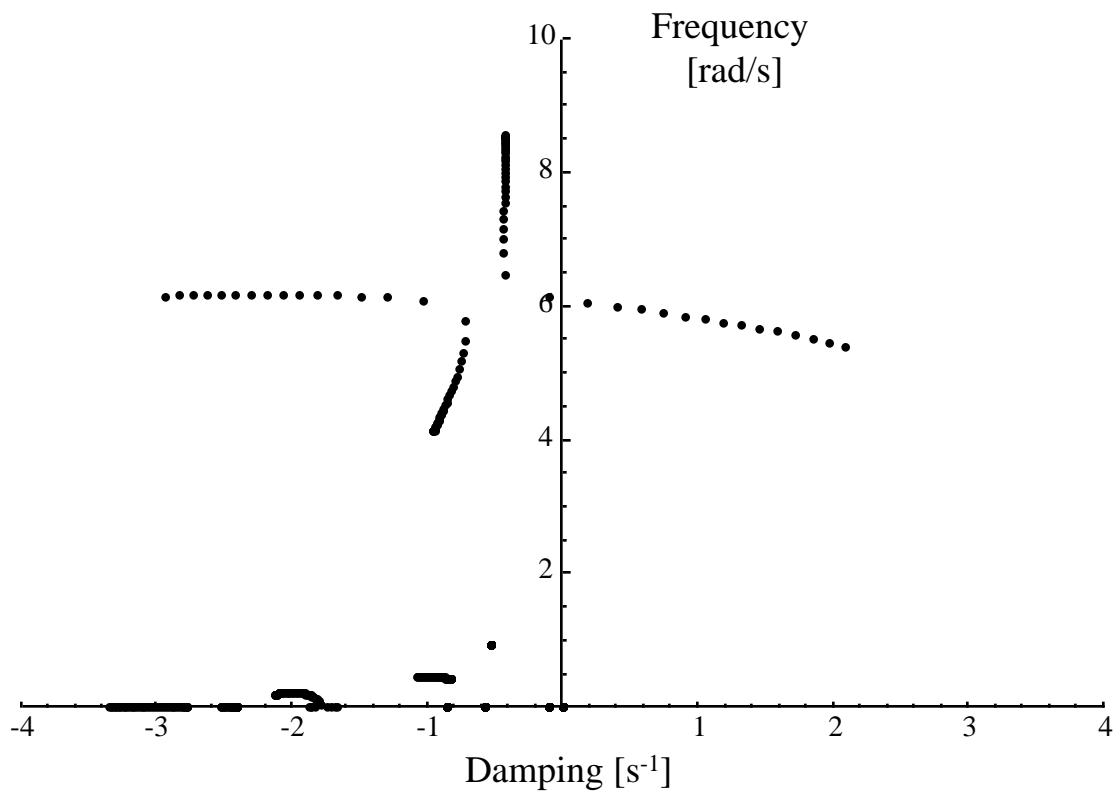


Figure 33: Trajectory of critical eigenvalues as generator dispatch is varied for generator terminal voltage of 1.10 p.u.

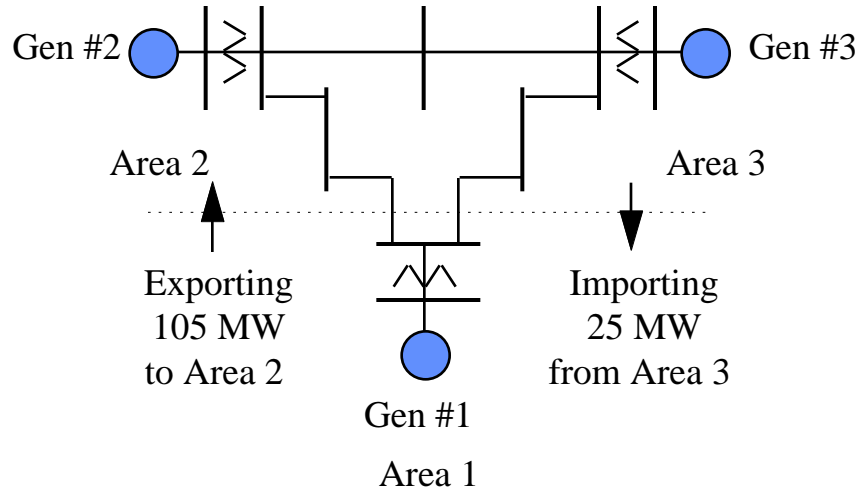


Figure 34: One line diagram of 9 bus test system

trajectories with magnitudes inversely proportional to the distances between dots). If the sensitivities are evaluated near the bends in the trajectories, they would provide useful approximations only for very small changes to the parameter. In addition, the very nature of the movement can be dramatically changed by a small change in the parameters. Note that the interaction shown in Figures 31 leads to a qualitatively different result than the interaction shown in Figure 33. Which of the two interacting eigenvalues becomes unstable as the dispatch is adjusted switches when the generator voltage reference set point moves through 1.50 p.u. This phenomena is discussed in detail in [EngMS].

9 bus system

The second example uses the 9 bus WSCC system in [SauPai] with some modifications. Consider this as a three area system with one generator per area and each area tied to the other two areas. Figure 34 shows a one line diagram of the system. Each generator is modeled by a ninth order dynamic model including an IEEE type I exciter and a third order governor model. For the transient differential equations (148) the real power portions of the loads are modeled as fifty percent constant voltage and fifty percent constant current and the reactive power portions of the loads are modeled as sixty percent constant voltage and forty percent constant current. For the steady state equations 149 the loads are modeled as constant power. The least damped eigenvalues at the base case are shown in Figure 35. Figure 36 shows the movement of the least damped modes as transfer from Area 1 to Area 3 increases

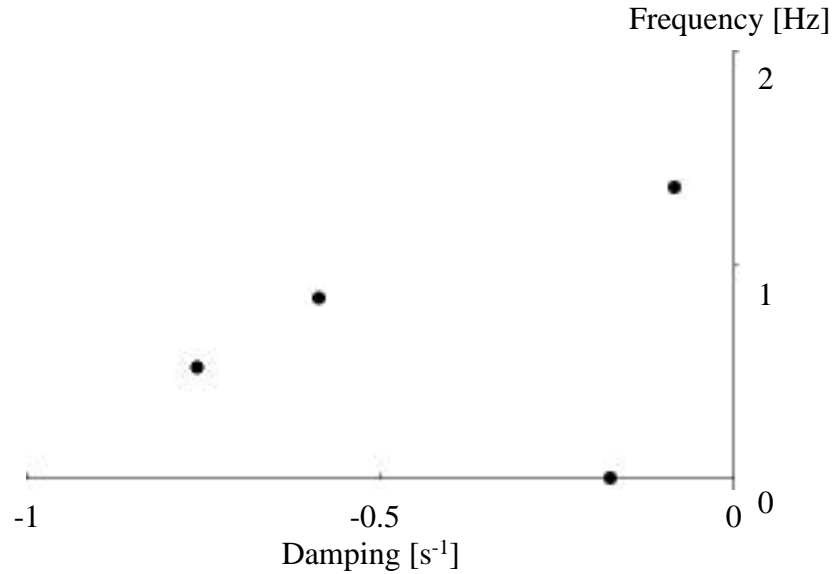


Figure 35: Least damped eigenvalues at base case of 9 bus system.

and transfer from Area 1 to Area 2 is held constant. Figure 37 shows the movement of the critical mode as a function of the transfer. Figure 38 shows the damping of the critical mode as a function of the transfer and the linear estimate of the behavior computed at the base case. We are interested in how adjusting the interchange with one area can affect the margin to instability as measured by the interchange with another area. We examine how adjusting the flow between Area 1 and Area 2 influences the margin to instability as measured by the flow on the tie line connecting Area 1 to Area 3, and how well this behavior is predicted by the sensitivity formulas.

Figure 39 shows the effect of varying the flow between Areas 1 and 2 on the margin to instability as measured by the flow between Areas 1 and 3. The dots are the actual bifurcation points for each interchange; the solid line is the Taylor series estimate computed by evaluating equation (157).

37 bus system

The 37 bus system has 3 generators represented with tenth order models and 25 generators represented with 2nd order models. Loads are considered constant power. There are three areas represented. At the base case, Area 1 is importing about 70 MW from Area 2 and exporting about 700 MW to Area 3. As the interchange is adjusted, generators pick up slack proportional to their size.

We are interested in the maximum amount of power that Area 1 can wheel from

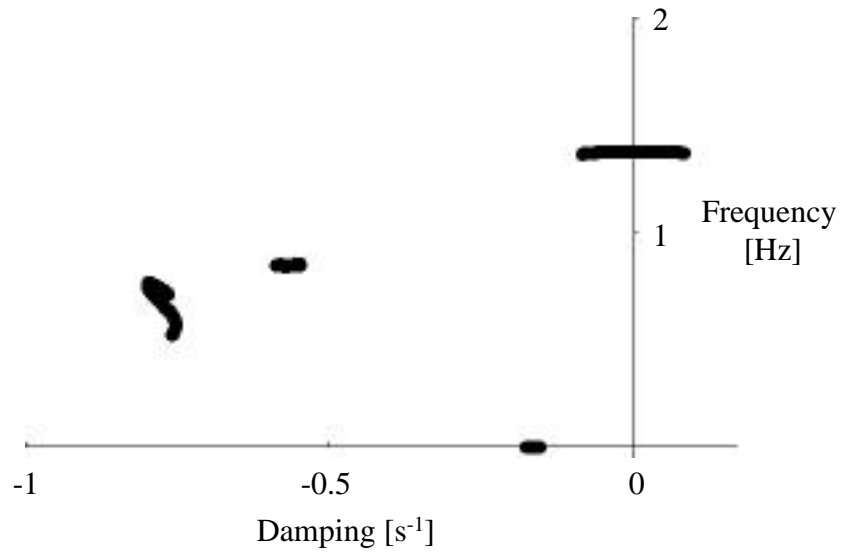


Figure 36: Movement of least damped eigenvalues as transfer to Area 3 increases.

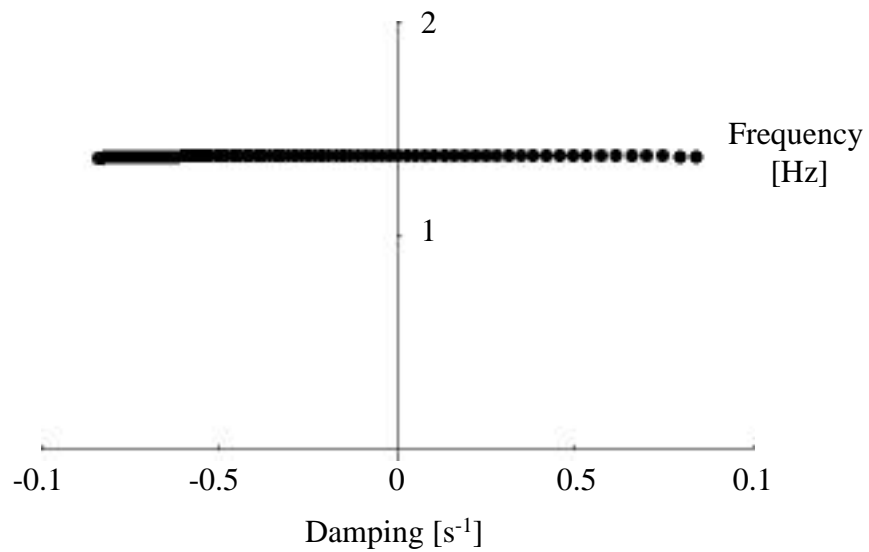


Figure 37: Movement of critical eigenvalue as transfer to Area 3 increases.

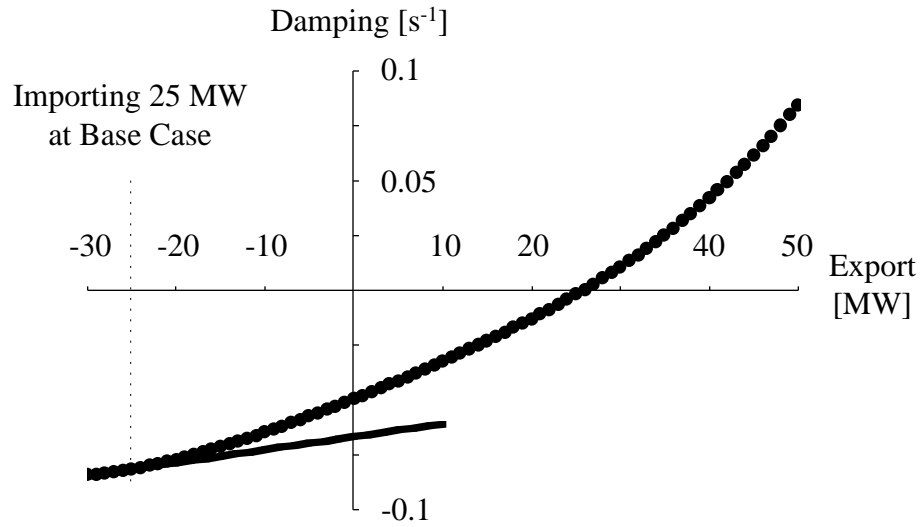


Figure 38: Damping of critical mode versus linear estimate as function of transfer to Area 3 in 9 bus system.

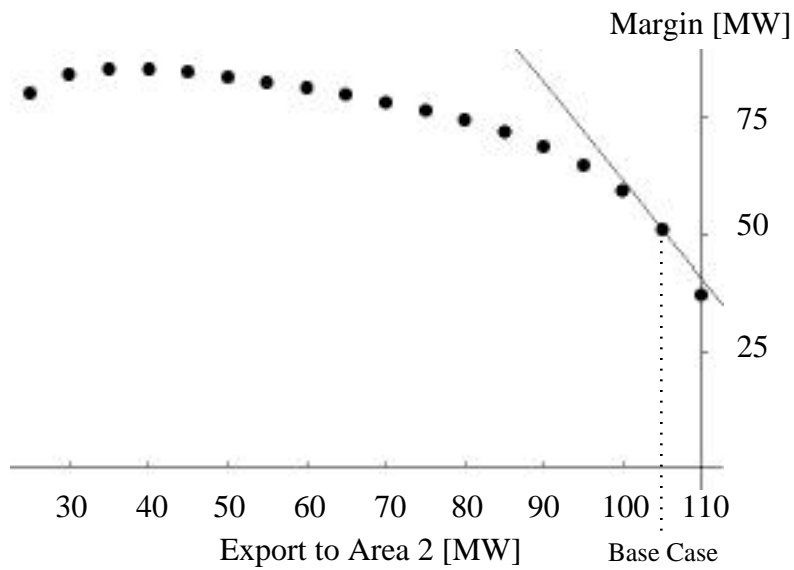


Figure 39: Linear estimate and actual margin to oscillations as function of export to Area 2 in 9 bus system.

Area 2 to Area 3 without interarea oscillation. Eigenanalysis at the base case shows two modes (of 80 eigenvalues) that are considerably less damped than all others. Using the sensitivity formulas, the sensitivities of these eigenvalues are computed with respect to the export set points for each area. These parameters appear in area interchange equations appended to the equilibrium equations and dispatch equations. The area interchange equations are just the sum of the real power flows on the tie lines for each area. The area interchange parameters do not appear in the linearized small signal equations, and hence are a prime example of the versatility of the sensitivity formulas derived in this chapter versus classical linearization techniques that can not account for variation of these parameters.

The computed sensitivities indicate that only one of the two modes is affected by transfers. A succession of equilibrium points as the wheeling is increased and decreased between zero MW and 1500 MW is computed using a continuation method coded in Mathematica.

Figure 40 shows the damping of the sensitive eigenvalue versus the real power wheeling. The solid line in Figure 40 represents the linear sensitivity of the damping with respect to transfer from Area 2 to Area 3 computed at the base case. The sensitivity computation suggests that the transfer would be limited to near 1000 MW due to oscillation. However, the damping does not vary linearly with the transfer and the mode never becomes unstable. If more than 1500 MW is wheeled, the system experiences voltage stability problems.

9.6 Discussion and conclusions

This chapter illustrates the use of eigenvalue and margin sensitivities for estimating the effects of adjusting parameters of the steady state model on the transient behavior of the power system. These parameters, such as area export set points, do not appear in the transient models that determine the oscillatory stability of the system and can not be studied with traditional linearized techniques. This chapter identifies eigenvalue interaction as a precursor to oscillatory instability. Future work could address the possibility of avoiding oscillatory instability by detecting and controlling eigenvalue interaction.

Several obstacles exist to successfully implementing the continuation methods to locate Hopf bifurcations in realistic power system models. The most obvious obstacle is computing all the eigenvalues of very large and possibly ill conditioned systems [AS96, DS93]. This obstacle can be partially circumvented if measured data or experience can help to identify a critical mode. Possibly only one or several eigenvalues and eigenvectors would then need to be computed and tracked. However, unlike the

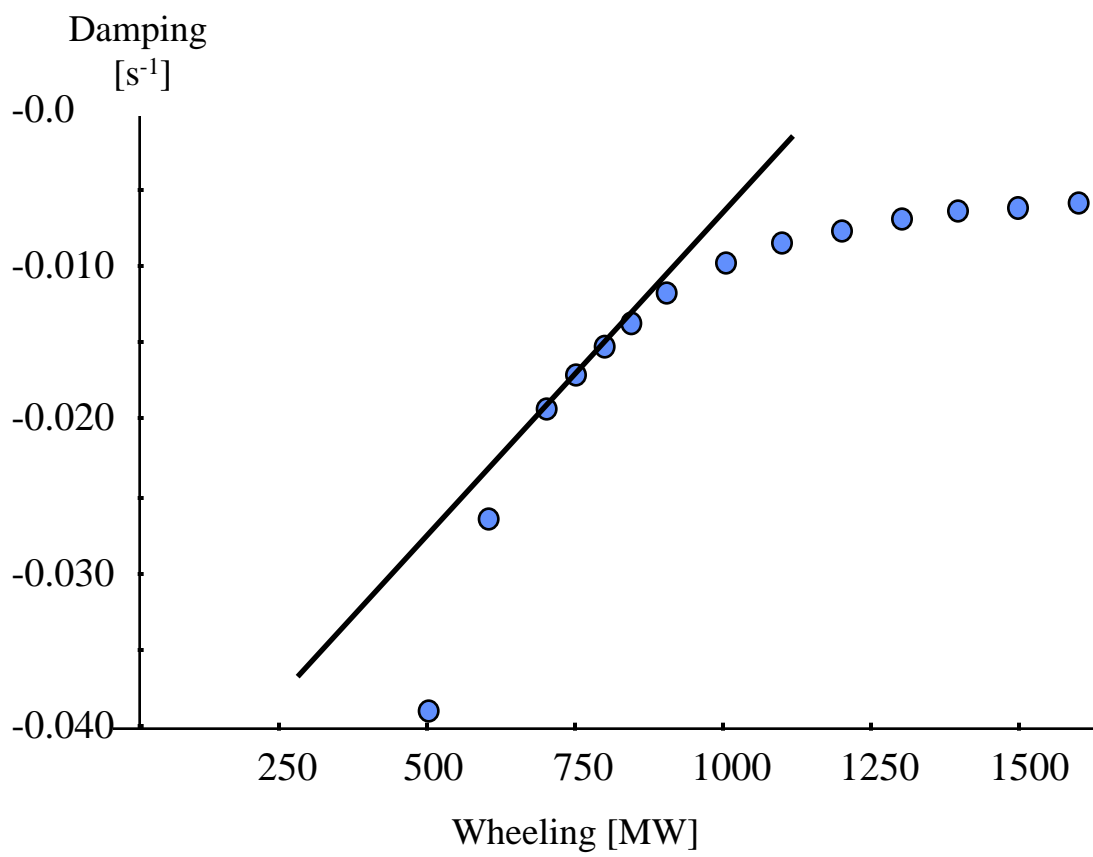


Figure 40: Effect of interarea exchange on damping of 37 bus system

case of fold bifurcation or simple limit constraints, there is no guarantee that a lightly damped mode will go unstable even as transfer or loading is increased. This point is illustrated by the 37 bus system results.

Very large power system models not only contain large numbers of dynamic variables and modes, but even larger numbers of parameters, many of which are poorly known. Even with a reduced set of important eigenvalues and a small system, eigenvalue behavior and interaction can create numerical challenges as shown by Figures 31, 32, and 33 for the three bus system. The eigenvalues of the system Jacobian matrix can be sensitive to the uncertain parameters, and robust stability determination for variation in these parameters is computationally infeasible [DC91].

9.7 Appendix

Sensitivity computations for the differential-algebraic model

Accepted practice is to model the power system with differential-algebraic equations of the form

$$\begin{aligned}\dot{x} &= f(x, y, \lambda) \\ 0 &= g(x, y, \lambda)\end{aligned}$$

Essentially, the “dynamic” variables, x , are those variables for which a differential equation exists. For example x includes machine rotor speeds and angle deviations. The “algebraic variables” y are those variables that do not appear explicitly as time derivatives in the model equations. For example, the direct and quadrature axis currents of a synchronous machine do not appear as time derivatives in the model equations. Note that this is not to say that algebraic variables do not have dynamics, it is simply that the time derivatives of the algebraic variables do not appear explicitly in the equations.

For illustration, the f equations include the swing dynamics for each modeled machine and may also include equations for voltage regulators and governor equations for each generator. The g equations include the stator algebraic equations at each machine as well as the power balance equations at each bus.

The distinction between algebraic and dynamic variables is a time scale separation. The algebraic variables may be thought of as those variables with stable dynamics much faster than those of the dynamic variables.

The parameters, λ , can include everything that is not a variable; there is no distinction between parameters that appear in the dynamic or static equations. For example, machine moments of inertia, damping, and control gains, are parameters

that appear in f while transmission line parameters and generator participation factors appear in g . λ may include any or all of these.

The maps f and g define another system as follows. Where the derivative of g with respect to y is nonsingular, by the implicit function theorem there is locally a map h such that

$$0 = g(x, h(x, \lambda), \lambda) \quad (160)$$

The map h describes how the algebraic variables depend upon the state variables to satisfy the algebraic constraints. We can describe the complete system then by the composition of f with h

$$\dot{x} = F(x, \lambda) = f(x, h(x, \lambda), \lambda) \quad (161)$$

which is valid where h is defined. The equilibria of the system satisfy $0 = F(x, \lambda)$ and the stability of the equilibrium (x_0, λ_0) is determined by the eigenvalues of the derivative of F with respect to the state variables x . The remainder of this appendix assumes that all derivatives are evaluated at (x_0, λ_0) . By the Chain Rule:

$$F_x = f_x + f_y h_x \quad (162)$$

where h_x is found from the algebraic equations.

$$0 = g(x, h(x), \lambda) \Rightarrow 0 = g_x + g_y h_x \Rightarrow h_x = -[g_y]^{-1} g_x \quad (163)$$

and

$$F_x = f_x - f_y [g_y]^{-1} g_x \quad (164)$$

There is no need to distinguish between the static and dynamic equations as far as locating equilibrium solutions and fold bifurcations. However, detection of the Hopf bifurcation requires attention to the Jacobian matrix F_x , not $\begin{pmatrix} f_x & f_y \\ g_x & g_y \end{pmatrix}$. The formulas from the previous section can be applied to the eigenvalues or Hopf bifurcation of F_x . However, computing the inverse of g_y is costly. It is more intuitive and computationally simpler to approach the problem of locating the eigenvalues of F_x as a “generalized eigenvalue problem”.

If A and B are two square matrices of the same dimension, the pencil of A and B is the set of all matrices that can be represented as $A - \mu B$ for μ a complex number. Each eigenvalue, μ , of the pencil satisfies

$$\det(A - \mu B) = 0 \quad (165)$$

and the eigenvectors corresponding to the each eigenvalue satisfy

$$Av = \mu Bv \quad (166)$$

The problem of finding μ and v that satisfy equation (166) is called the generalized eigenproblem.

In power systems, B is simply the diagonal matrix with ones on the rows corresponding to the dynamic variables, denoted E .

$$E = \begin{pmatrix} I_{n \times n} & 0 \\ 0 & 0 \end{pmatrix} \quad (167)$$

For $z = (x, y)$ and $F(z, \lambda) = \begin{pmatrix} f(z, \lambda) \\ g(z, \lambda) \end{pmatrix}$, the generalized eigenvalue-eigenvector equations can be written

$$(F_z - \mu E)\tilde{v} = 0 \quad (168)$$

$$\tilde{w}(F_z - \mu E) = 0 \quad (169)$$

$$\tilde{w}(F_z - \mu E)\tilde{v} = 0 \quad (170)$$

where μ is an eigenvalue of the pencil of F_z and E , and \tilde{w} and \tilde{v} the corresponding left and right eigenvectors respectively. Rewrite equation (170) as

$$\begin{pmatrix} w & w' \end{pmatrix} \left(\begin{pmatrix} f_x & f_y \\ g_x & g_y \end{pmatrix} - \begin{pmatrix} \mu I_{n \times n} & 0 \\ 0 & 0 \end{pmatrix} \right) \begin{pmatrix} v \\ v' \end{pmatrix} = 0 \quad (171)$$

Solution of equations (169,169,171) implies that

$$wf_y = -w'g_y \quad (172)$$

$$g_x v = -g_y v' \quad (173)$$

$$wf_x + w'g_x - w\mu I = 0 \quad (174)$$

$$f_x v + f_y v' - \mu I v = 0 \quad (175)$$

The left eigenvalue-eigenvector equation for F_x can be written

$$0 = w(F_x - \mu I) = w(f_x - f_y[g_y]^{-1}g_x - \mu I) = wf_x + w'g_x - w\mu I \quad (176)$$

Similarly the right eigenvalue-eigenvector equation for F_x can be written

$$0 = (F_x - \mu I)v = (f_x - f_y[g_y]^{-1}g_x - \mu I)v = f_x v + f_y v' - \mu I v \quad (177)$$

It follows that μ is an eigenvalue of F_x and partitions w of \tilde{w} and v of \tilde{v} are the corresponding eigenvectors. (This observation is also made in [Sme93] and [Cañ95], except that [Sme93] does not consider parameters that move the equilibrium and [Cañ95] concerns finding the left eigenvector corresponding to the zero eigenvalue of a system at saddle node bifurcation.)

The eigenvalue sensitivity formula is found as in Chapter 4, differentiating equation (170) with respect to the parameter.

$$\tilde{w}(F_{zz}Z_\lambda + F_{z\lambda} - \mu_\lambda E)\tilde{v} = 0 \quad (178)$$

$$\tilde{w}\mu_\lambda E\tilde{v} = \tilde{w}(F_{zz}Z_\lambda + F_{z\lambda})\tilde{v} \quad (179)$$

$$\mu_\lambda = \frac{\tilde{w}(F_{zz}Z_\lambda + F_{z\lambda})\tilde{v}}{\tilde{w}E\tilde{v}} \quad (180)$$

$$= \frac{\tilde{w}(F_{zz}Z_\lambda + F_{z\lambda})\tilde{v}}{wv} \quad (181)$$

where Z_λ is found from solution of the linear system

$$F_z Z_\lambda = -F_\lambda \quad (182)$$

Note that the desired normalization is still $wv = 1$ *not* $\tilde{w}\tilde{v} = 1$.

Computational methods for the eigenvector-eigenvalue problem can be converted to the generalized eigenvalue approach by simply substituting the matrix μE everywhere the matrix μI is found and partitioning the eigenvectors accordingly. The formulation of the eigenproblem for the differential-algebraic equations as a generalized eigenproblem allows for the application of well established computational methods. In addition, some routines exist specifically for generalized eigenproblems [GV, MS73]. Note that the error analysis of the generalized eigenproblem differs from that of the standard eigenproblem. This is particularly apparent for power systems applications that involve nearly singular g_y . Although the inverse of g_y does not need to be computed, as g_y approaches singularity the eigenvectors become very sensitive and the sensitivity computations become poorly conditioned. This behavior can be associated with singularity of the equilibrium equations and proximity to voltage collapse. Essentially, the time scale separation implicit in constructing the differential-algebraic model is not justified when g_y approaches singularity. Future analysis is required concerning the power system model when the algebraic variables are singular (see [VSZ91]).

Chapter 10

Conclusions and Future Research

10.1 Conclusions

This thesis demonstrates that the computation of security margins and the sensitivity of the security margins with respect to parameters yields practical information useful for the control and planning of large electric power systems. The security margin reflects the amount by which parameters can change before a security violation is reached, and the sensitivity of that margin indicates how that margin is affected by other parameters. The thesis establishes a coherent, consistent, and general framework for margin and sensitivity analysis applicable to a variety of security criteria. The thesis shows how to efficiently compute the security margins defined by limiting events and instabilities, and the sensitivity of those margins with respect to any model parameter.

Applications

This thesis forwards the application of margin and sensitivity methods in the areas of voltage stability, contingency analysis, oscillatory instability, and transfer capability.

The methods of this thesis find considerable service in the area of voltage stability and voltage collapse. The loading margin to voltage collapse is a fundamental index of relative voltage stability and system security. We show that the sensitivity of the loading margin to voltage collapse with respect to arbitrary parameters can be computed efficiently and used to obtain quantitative estimates of the effects of varying parameters and assumptions. The effective use of the estimates is illustrated for a range of system parameters including interarea transfers, load model parameters, shunt compensation, the direction of load increase, generator dispatch, and line parameters. The closeness of the estimates over a useful range of parameter variations and the ease of obtaining the linear estimate suggest that the sensitivity computations will be of practical value in avoiding voltage collapse.

Generator reactive power limits have a significant influence on voltage stability and generators reaching maximum reactive power limits can precipitate immediate voltage collapse. The sensitivity based estimates are shown to be useful for approximating

the change in loading margin corresponding to changes in generator reactive power limits. This thesis introduces the use of the normal vector to the boundary of a critical generator reactive power limit and shows that the margin sensitivity methods work effectively for voltage collapse caused by either saddle node bifurcation of equilibria or immediate instability due to generator reactive power limits.

This thesis also demonstrates that effective contingency analysis for voltage collapse can be done by computing the loading margin sensitivities from a single nominal nose curve. The results show that the linear estimates are extremely fast and provide acceptable contingency ranking. For example, after the single nose curve and a left eigenvector are computed, the linear estimates of *all* single line outages for a practical 1390 bus system are computed in less time than is typically required for one load flow solution. The quadratic estimates refine the linear estimates and are more costly but are still faster than previous methods.

The margin and sensitivity methods are also shown to be useful for determining transfer capabilities. Interarea transfer can be limited by several security criteria such as low voltage limits, line flow limits, or voltage stability. The general sensitivity formulas presented in this thesis are applicable to security margins defined by any limit criteria. The sensitivity based estimates of the effect of simultaneous transfers on the transfer margins are computed and agree well with the exact computations for a 1500 bus model of a portion of the US grid. A method to compute transfer margins by directly locating intermediate limit events reduces the total number of loadflow iterations required by each margin computation and provides sensitivity information for minimal additional cost.

The use of margin sensitivities for estimating the effects of adjusting steady state model parameters on the oscillatory stability of the power system is demonstrated. The steady state parameters such as area export set points do not appear in the transient time scale models, but do implicitly affect the oscillatory stability. These eigenvalue and margin sensitivities can not be computed with traditional methods based on the linearization of the transient time scale equations. Application of the margin and sensitivity methods to interarea oscillations has identified eigenvalue interaction as a potential mechanism for instability.

Theory

This thesis extends the understanding of security margins and sensitivity computations for power systems.

This thesis defines admissible power system models based on the fundamental assumptions of steady state analysis implied by accepted engineering practice. The sensitivity formulas derived are valid for any power system equations that satisfy the

assumptions and are independent of any approximations used to derive the equations. It is demonstrated that the general sensitivity formulas derived in this thesis can be reduced in special cases to yield traditional approximate sensitivity formulas such as line distribution factors, outage distribution factors, participation factors and penalty factors. For example, it is shown that large deviation sensitivity formulas result from reparameterization of the system equations, that participation factors are eigenvalue sensitivities that neglect the implicit dependence of the system Jacobian matrix on the equilibrium point, and that exact penalty factors are the components of the normal vector to the hypersurface in parameter space that describes how system parameters must change to satisfy equilibrium conditions.

This thesis provides an explanation of established methods for computation of security margins synthesized from basic principles of numerical analysis. Improvements to accepted techniques are suggested and applied. For example, by adapting the corrector step to directly locate intermediate events of practical interest, the normal vector to each event can be obtained at negligible cost and used to obtain sensitivities of the security margin with respect to any parameters. In addition, the total number of solutions required to compute the security margin are minimized.

10.2 Future work

There are several avenues for future research.

Reliability

There is growing concern over the effect of deregulation on the reliability of electric power systems. Utilities are in need of a reliability indicator that can be tracked over time and used to quantitatively assess system reliability. Security margins seem well suited for this role. The loading margin to the first limit violation could be used to compare the relative security of different systems or of the same system at different times. In addition, the sensitivity of the reliability margin can be computed to any parameter and used to forecast the reliability margin resulting from contingencies and transactions.

Contingency analysis

The methods of Chapter 6 and 7 considered contingency analysis for voltage collapse precipitated by either saddle node bifurcation of equilibria or immediate instability due to reactive power limitations. However, the methods could be extended to any

security criteria or performance index. The normal vector to each event boundary could be computed in route to establishing the nominal point of collapse, and the contingencies ranked according to each criteria. For instance, the contingencies ranked the highest due to their effect on the margin to voltage collapse may not be the worst contingencies with respect to flow limits or economic cost. Chapter 6 and the discussion to [GDA98] by Anjan Bose and Hang Liu suggest that the contingency methods might be improved by computing more than one nominal point of collapse. For instance, it might prove beneficial to compute the point of collapse corresponding to different area export schedules, varying assumptions about VAR limits, or by changing the nominal loading patterns in hopes of capturing contingencies masked by the nominal continuation.

Constrained economic dispatch

Direct computation of the security margin and the normal vector to the event boundary permits inclusion of security margin constraints in the constrained economic dispatch problem. Essentially, the normal vector to the boundary could be used to define an inequality constraint in an iterative step of the optimization process. Inclusion of security constraints in the optimization problem allows for the computation of the components of the nodal prices attributable to reliability. This information could be used to identify the most profitable locations to offer interruptible contracts or to locate peaking generation.

Oscillations

Many of the difficulties encountered applying margin sensitivity methods to the problem of oscillatory instability were attributable to the large number of states represented by even modest sized power system models. In addition, the behavior of eigenvalues is notoriously complicated. The possibility of avoiding oscillatory instability by detecting and controlling eigenvalue interaction should be investigated. One goal for future research in the area of power system oscillations is the development of fundamental understanding and heuristic rules for avoiding oscillations. The eigenvalue sensitivity formulas coupled with conjectures regarding power system behavior may lead to general rules for avoiding oscillations. Approximate information concerning the frequency of an oscillation and the mode shape coupled with knowledge that increasing a particular parameter always increases the equilibrium value of a particular state variable could be used to show that changing the parameter in general will damp that oscillation. For example, if decreasing the interarea transfer between two areas has the effect of decreasing the angle difference between two buses, and that in

general the damping of an eigenvalue associated with oscillation between those two areas increases with the decreasing angle difference, then decreasing the interarea transfer between the two areas would be a general guideline for suppressing oscillation between those two areas. It is possible that the eigenvalue and eigenvector sensitivity formulas may indicate that only a subset of the generator equations are required to determine interarea oscillatory modes.

Bibliography

- [AV84] E.H. Abed, P.P. Varaiya, "Nonlinear oscillations in power systems", *International Journal of Electric Energy and Power Systems*, vol. 6, no. 1, Jan. 1984, pp. 37-43.
- [AMR] R. Abraham, J.E. Marsden, T. Ratiu, *Manifolds, Tensor Analysis, and Applications*, Springer-Verlag, New York, 1988.
- [AF] P.M. Anderson, A.A. Fouad, *Power System Control and Stability*, Iowa State University Press, Ames Iowa, 1977.
- [AC92] V. Ajjarapu, C. Christy, "The continuation power flow: a tool for steady state voltage stability analysis", *IEEE Trans. Power Systems*, vol.7, no.1, Feb.1992, pp. 416-423.
- [AJYB] V. Ajjarapu, N. Jain, Z. Yu, S. Battula "Recent developments to the continuation power flow", Proceedings 1993 North American Power Symposium, Washington D.C., Oct. 11-12, 1993, pp. 205-214.
- [ABH82] F. Albuyeh, A. Bose, B. Heath, "Reactive power considerations in automatic contingency selection", *IEEE Trans. Power Apparatus and Systems*, vol PAS-101, no. 1, Jan. 1982, pp. 107-111.
- [AST83] O. Alsac, B. Stott, W.F. Tinney, Sparsity oriented compensation methods for modified network solutions, *IEEE Trans. Power Apparatus and Systems*, vol. PAS-102, May 1983, pp. 1050-1060.
- [Alv78] F. L. Alvarado, "Penalty factors from Newton's method", *IEEE Trans. Power Apparatus and Systems*, vol. PAS-97, no. 6, Nov/Dec 1978, pp. 2031-2040.
- [Alv90] F. Alvarado, "Bifurcations in nonlinear systems: computational issues", Proceedings of the 1990 IEEE/ISCAS, New Orleans LA, May 1-3, 1990, IEEE publication CH2868-8, Vol. 2, pp. 1268-1271.
- [Alv97] F. L. Alvarado, "Matrix enlarging methods and their application", *BIT*, vol. 37, no. 3, 1997, pp. 473-505.

- [Alv91] F. Alvarado et al., “Engineering foundations for the determination of security costs”, *IEEE Trans. Power Systems*, vol. 6, no. 3, Aug. 1991, pp. 1175-1182.
- [ADH94] F. Alvarado, I. Dobson, Yi Hu, “Computation of closest bifurcations in power systems”, *IEEE Trans. Power Systems*, vol. 9, no. 2, May 1994, pp. 918-928.
- [AJ89] F.L. Alvarado, T.H. Jung, “Direct detection of voltage collapse conditions”, Proceedings: Bulk Power System Voltage Phenomena – Voltage Stability and Security, EPRI-6183, Jan. 1989, pp. 523-538.
- [Alv90] F.L. Alvarado, “Manipulation and visualization of sparse matrices”, *ORSA (Operations Research Society of America) Journal on Computing*, 2(2):186-207, Spring 1990.
- [AlvPhD] F.L. Alvarado, *Optimal planning of power systems*, PhD Thesis, University of Michigan, 1972.
- [SMMS] *Sparse Matrix Manipulation System* : Users manual and software available via anonymous ftp at eceserv0.ece.wisc.edu in subdirectory pub/smms93
- [AS96] G. Angelidis, A. Semlyen, “Improved methodologies for the calculation of critical eigenvalues in small signal stability analysis”, *IEEE Trans. Power Systems*, vol. 11, no. 3, Aug 1996, pp. 1209-1217.
- [Bergen] A.R. Bergen, *Power Systems Analysis*, Prentice-Hall, Englewood Cliffs NJ, 1986.
- [BN] F. Brauer, J. Nohel, *The Qualitative Theory of Ordinary Differential Equations*, Dover, NY, 1969.
- [CA93] C.A. Cañizares, F.L. Alvarado, “Point of collapse and continuation methods for large AC/DC systems”, *IEEE Trans. Power Systems*, vol.7, no.1, Feb.1993, pp. 1-8.
- [CA91] C.A. Cañizares, F.L. Alvarado, “Computational experience with the point of collapse method on very large AC/DC systems”, in [DCL].
- [Cañ98] C.A. Cañizares, “Calculating optimal system parameters to maximize the distance to saddle-node bifurcations”, *IEEE Trans. Circuits and Systems — I:Fundamental Theory and Applications*, vol. 45, no. 3, March 1998, pp.225-237.

- [Cañ95] C.A. Cañizares, “Conditions for saddle-node bifurcations in AC/DC power systems”, *Electrical Power & Energy Systems*, vol.17, no.1, 1995, pp. 61-68.
- [CañPhD] C.A. Cañizares, *Voltage Collapse and Transient Energy Function Analyses of AC/DC Systems*, PhD. Thesis, University of Wisconsin–Madison, 1991.
- [PFLOW] *PFLOW* : Software available via anonymous ftp at [iliniza.uwaterloo.ca](ftp://iliniza.uwaterloo.ca) in subdirectory `pub/pflow`
- [CFSB] H.-D. Chiang, A. Flueck, K.S. Shah, N. Balu, “CPFLOW: A practical tool for tracing power system steady-state stationary behavior due to load and generation variations”, *IEEE Trans. Power Systems*, vol. 10, no. 2, May 1995, pp. 623-634.
- [CWF97] H-D Chiang, C-S Wang, A.J. Flueck, “Look-ahead voltage and load margin contingency selection functions for Large-Scale Power Systems”, vol. 12, no. 1, Feb. 1997, pp. 173-180.
- [CH] S.N. Chow, J. Hale, *Methods of bifurcation theory*, section 6.2, Springer Verlag, NY, 1982.
- [CA95] M. L.Crow, J. Ayyagari, “The effect of excitation limits on voltage stability”, *IEEE Trans. Circuits and Systems — I:Fundamental Theory and Applications*, vol. 42, no. 12, Dec. 1995, pp. 1022-1026.
- [Davos] L.H. Fink, ed., Proceedings: Bulk power system voltage phenomena III, voltage stability, security & control, ECC/NSF workshop, Davos, Switzerland, Aug. 1994.
- [DCL] L.H. Fink, ed., Proceedings: Bulk power system voltage phenomena, voltage stability and security, ECC/NSF workshop, Deep Creek Lake, MD, Aug. 1991, ECC Inc., 4400 Fair Lakes Court, Fairfax, VA 22033-3899.
- [Debs] A.S. Debs, *Modern Power Systems Control and Operation*, Kluwer Academic, Boston, 1988.
- [DV93] C. L. DeMarco, G. C. Verghese, “Bringing phasor dynamics into the power system load flow”, Proceedings 1993 North American Power Symposium, Washington D.C., Oct. 11-12, 1993, pp. 463-471.

- [DeM96] C. L. DeMarco, "A novel continuation method for computing alternate power flow solutions", Proceedings 1996 North American Power Symposium, Cambridge, MA, Nov. 1996.
- [DC91] C. L. DeMarco, G. E. Coxson, "Computational complexity results in parametric robust stability analysis with power system applications", in *Systems and Control Theory for Power Systems*, Springer-Verlag, NY, 1991.
- [DS93] J. Deuse, M. Stubbe, "Dynamic simulation of voltage collapses, *IEEE Trans. Power Systems*, vol.8, no.3, Aug.1993, pp. 894-904.
- [DAD92] I. Dobson, Fernando Alvarado and C. L. DeMarco, "Sensitivity of Hopf bifurcations to power system parameters", Proceedings of the 31st Conference on Decision and Control, Tucson, Arizona, Dec. 1992, pp. 2928-2933.
- [DC89] I. Dobson, H.-D. Chiang, "Towards a theory of voltage collapse in electric power systems, *Systems and Control Letters*, vol. 13, 1989, pp. 253-262.
- [Dob94] I. Dobson, "The irrelevance of load dynamics for the loading margin to voltage collapse and its sensitivities", in [Davos].
- [Dob92] I. Dobson, "Observations on the geometry of saddle node bifurcation and voltage collapse in electric power systems", *IEEE Trans.Circuits & Systems,Part 1*, vol.39, no.3, Mar.1992, pp. 240-243.
- [Dob93] I. Dobson, "Computing a closest bifurcation instability in multidimensional parameter space", *Journal of Nonlinear Science*, vol. 3, no. 3, 1993, pp. 307-327.
- [DL192] I. Dobson, L. Lu, "Computing an optimum direction in control space to avoid saddle node bifurcation and voltage collapse in electric power systems", *IEEE Trans. Automatic Control*, vol 37, no. 10, Oct. 1992, pp. 1616-1620.
- [DL292] I. Dobson, L. Lu, "Voltage collapse precipitated by the immediate change in stability when generator reactive power limits are encountered", *IEEE Trans. Circuits and Systems, Part 1*, vol. 39, no. 9, Sept. 1992, pp. 762-766.
- [DL93] I. Dobson, L. Lu, "New methods for computing a closest saddle node bifurcation and worst case load power margin for voltage collapse", *IEEE Trans. Power Systems*, vol.8, no.3, Aug.1993, pp. 905-913.

- [DT68] H. W. Dommel, W. F. Tinney, "Optimal power flow solutions", *IEEE Trans. on Power Apparatus and Systems*, vol. PAS-87, no.3, Oct. 1968, pp. 1866-1876.
- [DGM79] R. D. Dunlop, R. Gutman and P. P. Marchenko, "Analytical Development of Loadability Characteristics for EHV and UHV Transmission Lines," *IEEE Trans. Power Apparatus and Systems*, Vol. PAS-98, No. 2, March/April 1979, pp. 606-617.
- [DS93] I. S. Duff, J. A. Scott, "Computing selected eigenvalues of sparse unsymmetric matrices using subspace iteration", *ACM Transactions on Mathematical Software*, vol. 19, No. 2, June 1993.
- [EngMS] H. Engdahl, *Simulation evidence for interacting pairs of eigenvalues causing oscillations in electric power systems*, MS. Thesis, Royal Institute of Technology, Stockholm, 1998.
- [EVMW] G.C. Ejebe, H.P. Van Meeteren, B.F. Wollenberg, "Fast contingency screening and evaluation for voltage security analysis", *IEEE Trans. Power Systems*, vol. 3, no. 4, Nov. 1988, pp. 1582-1590.
- [EIMORT] G.C. Ejebe, G.D. Irisarri, S. Mokhtari, O. Obadina, P. Ristanovic, J. Tong, "Methods for contingency screening and ranking for voltage stability analysis of power systems", *IEEE Trans. Power Systems*, vol. 11, no. 1, Feb. 1996, pp. 350-356.
- [ECSW] A.O. Ekwue, D.T.Y. Cheng, Y.H. Song, H.B. Wan, "Integrated methods for voltage stability analysis of the NGC system", Colloquium on Voltage Collapse, Digest No. 1997/101 Institution of Electrical Engineers, London, UK.
- [PSerc] P. Sauer, M.A. Pai, S. Fernandes, I. Dobson, F. Alvarado, S. Greene, B. Thomas, H-D Chiang, "Real time control of oscillations of electric power systems", ESEERCO Project EP 95-11, Sep. 1996.
- [FOC90] N. Flatabø, R. Ognedal, T. Carlsen, "Voltage stability condition in a power transmission system calculated by sensitivity methods", *IEEE Trans. Power Systems*, vol. 5, no. 4, Nov. 1990, pp. 1286-1293.
- [FFOCH] N. Flatabø, O.B. Fosso, R. Ognedal, T. Carlsen, K.R. Heggland, "A method for calculation of margins to voltage instability applied on the Norwegian system for maintaining required security level", *IEEE Trans. Power Systems*, vol. 8, no. 2, May 1993, pp. 920-928.

- [FCW97] A.J. Flueck, H-D. Chiang, C-S. Wang, "A novel method of look-ahead contingency ranking for saddle-node bifurcation", Proceedings of the 20th International Conference on Power Industry Computer Applications 1997, Columbus, Ohio, May 11-16, 1997 pp. 266-271.
- [FFHH] O.B. Fosso, N. Flatabø, B. Hakavik, A.T. Holen, "Comparison of methods for calculation of margins to voltage instability", Proceedings Athens Power Tech 1993, Athens, Greece, Sep. 5-8, 1993, pp. 216-221.
- [Gal84] F.D. Galiana, "Bound estimates of the severity of line outages in power system contingency analysis and ranking", *IEEE Trans. Power Apparatus and Systems*, vol PAS-103, no. 9, Sep. 1984, pp. 2612-2624.
- [GZ] C.B. Garcia, W.I. Zangwill, *Pathways to Solutions, Fixed Points, and Equilibria*, Prentice-Hall, Englewood Cliffs NJ, 1983.
- [GVHW] L. L. Garver, P. R. Van Horne and K. A. Wirgau, "Load Supplying Capability of Generation-Transmission Networks," *IEEE Trans. Power Apparatus and Systems*, Vol. PAS-98, No. 3, May/June 1979, pp. 957-962.
- [GV] G. Golub, C. VanLoan, *Matrix Computations*, Johns Hopkins University Press, Baltimore, 1983.
- [GSHT] P.R. Gribik, D. Shirmohammadi, S. Hao, C.L. Thomas, "Optimal power flow sensitivity analysis", *IEEE Trans. Power Systems*, vol. 6, no. 2, May 1991, pp. 969-976.
- [GDA97] S. Greene, I. Dobson, F.L. Alvarado, "Sensitivity of the loading margin to voltage collapse with respect to arbitrary parameters", *IEEE Trans. Power Systems*, vol. 12, no. 1, Feb. 1997, pp. 262-272.
- [GDA98] S. Greene, I. Dobson, F.L. Alvarado, "Contingency analysis for voltage collapse via sensitivities from a single nose curve", paper PE-707-PWRS-2-06-1997, IEEE PES Summer Meeting, Berlin, Germany, July 1997.
- [GDAS] S. Greene, I. Dobson, F.L. Alvarado, P.W. Sauer, Initial concepts for applying sensitivity to transfer capability, NSF Workshop on Available Transfer Capability, Urbana IL USA, June 1997.
- [GreMS] S. Greene, *Constraint at a saddle node bifurcation*, MS thesis, Univ. of Wisconsin-Madison, 1993.

- [GH] J. Guckenheimer, P. Holmes, *Nonlinear Oscillations, Dynamical Systems, and Bifurcations of Vector Fields*, Springer-Verlag, NY, 1983.
- [GP] V. Guillemin, A. Pollack, *Differential Topology*, Prentice-Hall, Englewood Cliffs NJ, 1974.
- [HSS] N. T. Hawkins, G. Shackshaft, M.J. Short, "On-line algorithms for the avoidance of voltage collapse: reactive power management and voltage collapse margin assessment", Proceedings of the IEE Third International Conference on Power System Monitoring and Control, Institution of Electrical Engineers, London, 1991, pp. 134-139.
- [HawPhD] N. T. Hawkins "On-line reactive power management in electric power systems", PhD thesis, University of London, Department of Electrical and Electronic Engineering, Imperial College of Science, Technology, and Medicine, London, 1996
- [Heydt] Heydt, *Computer Analysis Methods for Power Systems*, Macmillan Publishing Company, NY, 1986.
- [HD95] I. Hiskens, R. J. Davy "A technique for exploring the power flow solution space boundary", Proceedings Stockholm Power Tech, Stockholm, June 18-22, 1995 , pp. 478-483.
- [HH91] I. Hiskens, D. Hill, "Dynamic aspects of voltage collapse", in [DCL].
- [HJ] R.A. Horn, C.R. Johnson, *Matrix Analysis*, Cambridge University Press, Cambridge, 1985.
- [Iba] K. Iba et al., "Calculation of critical loading condition with nose curve using homotopy continuation method", *IEEE Trans. Power Systems*, vol. 6, May 1991, pp. 584-593.
- [IEEE1] *Inter-Area Oscillations in Power Systems*, IEEE Special Publication 95-TP-101, 1995.
- [IEEE1] *Voltage stability of power systems: concepts, analytical tools, and industry experience*, IEEE Special Publication 90TH0358-2-PWR, 1990.
- [IEEE3] *Recommended techniques for voltage stability analysis*, Working Group on Voltage Stability, System Dynamic Performance Subcommittee IEEE Special Publication, 1994.

- [Jal92] N. Jaleeli, et. al., "Understanding automatic generation control", *IEEE Transactions on Power Systems*, vol. 7, no. 3, Aug. 1992, pp. 1106-1122.
- [JJC92] R. Jean-Jumeau, H.D. Chiang, "Parameterizations of the load-flow equations for eliminating ill-conditioning load flow solutions", *IEEE Trans. Power Systems*, vol. 8, no. 3, Aug. 1995, pp. 1004-1012.
- [Kundur] P. Kundur, *Power System Stability and Control*, McGraw-Hill, NY, 1993.
- [Kur93] A. Kurita et al., "Multiple time-scale power system dynamic simulation", *IEEE Trans. Power Systems*, vol. 8, no. 1, Feb. 1993, pp. 216-223.
- [Kusic] G.L. Kusic, *Computer-Aided Power Systems Analysis*, Prentice-Hall, Englewood Cliffs, NJ, 1986.
- [Kwa86] H. G. Kwatny, et al., "Static bifurcation in electric power networks: loss of steady state stability and voltage collapse", *IEEE Trans. on Circuit and Systems*, vol. CAS-33, no. 10 Oct. 1986, pp. 981-991.
- [LTA72] G. L. Landgren, H. L. Terhune, R. K. Angel, "Transmission Interchange Capability - Analysis by Computer," *IEEE Trans. Power Apparatus and Systems*, Vol. PAS-91, No. 6, Nov/Dec 1972, pp. 2405-2414.
- [LA73] G. L. Landgren, S. W. Anderson, "Simultaneous Power Interchange Capability Analysis," *IEEE Trans. Power Apparatus and Systems*, Vol. PAS-92, No. 6, Nov/Dec 1973, pp. 1973-1986.
- [LAH95] P.A. Löf, G. Andersson, D. Hill, "Voltage dependent reactive power limits for voltage stability studies", *IEEE Trans. Power Systems*, vol. 10, no. 1, Feb. 1995, pp. 220-228.
- [LöfPhD] Per-Anders Löf, *Steady-State Stability Analysis*, PhD Thesis, Royal Institute of Technology, Stockholm, TRITA-EES-9501, ISSN 1100-1607, 1995.
- [LLT94] J. Lu, C-W Liu, J. S. Thorp, "New methods for computing a saddle-node bifurcation point for voltage stability analysis", *IEEE Trans. Power Systems*, vol. 10, no. 2, May 1995, pp. 978-985.
- [MMH95] Y.V. Makarov, V. A. Maslennikov, D.J. Hill, "Calculation of oscillatory stability margins in the space of power system controlled parameters", *Proceedings Stockholm Power Tech*, Stockholm, June 18-22, 1995, pp. 416-421.

- [MMH96] Y.V. Makarov, V. A. Maslennikov, D.J. Hill, “Revealing loads having the biggest influence on power system small disturbance stability”, *IEEE Trans. Power Systems*, vol. 11, no. 4, Nov. 1996, pp. 2018-2023.
- [MATLAB] *MATLAB* : The Math Works, Inc. , Natick MA.
- [Mar86] N. Martins, “Efficient eigenvalue and frequency response methods applied to power system small-signal stability studies”, *IEEE Transactions on Power Systems*, vol. PWRS-1, no. 1, 1986, pp. 217-226.
- [MS73] C.B. Moler, G.W. Stewart, “An algorithm for generalized matrix eigenvalue problems, *SIAM Journal of Numerical Analysis*, 10, 1973, pp. 241–256.
- [MTK96] H. Mori, H. Tanaka, J. Kanno, “A preconditioned fast decoupled power flow method for contingency screening”, *IEEE Trans. Power Systems*, vol. 11, no. 1, Feb. 1996, pp. 357-363.
- [NTSCO] K.Nara, K. Tanaka, R.R. Shoults, M.S. Chen, P. Van Olinda, “On-line contingency selection algorithm for voltage security analysis”, *IEEE Trans. Power Apparatus and Systems*, vol PAS-104, no. 4, April 1985, pp. 847-856.
- [NERC95] Transmission Transfer Capability Task Force, “Transmission transfer capability”, North American Reliability Council, Princeton, New Jersey, May 1995.
- [NERC96] Transmission Transfer Capability Task Force, “Available transmission capability definitions and determination”, North American Reliability Council, Princeton, New Jersey, June 1996.
- [NorPhD] M. Noroozian, *Exploring benefits of controllable series compensators in power systems*, PhD Thesis, Royal Institute of Technology, Stockholm, TRITA-EES-9402, ISSN 1100-1607, 1994.
- [OloPhD] M. Olofsson, *Optimal operation of the Swedish railway electrical system*, PhD Thesis, Royal Institute of Technology, Stockholm, TRITA-EES-9601, ISSN 1100-1607, 1996.
- [OD91] T.J. Overbye, C.L. DeMarco, “Voltage security enhancement using energy based sensitivities”, *IEEE Trans. Power Systems*, vol. 6, no. 3, Aug. 1991, pp. 1196–1202.

- [PPAV] F. L. Pagola, I. J. Perez-Arriaga and G. C. Verghese, "On sensitivities, residues and participants: Applications to oscillatory stability analysis and control," *IEEE Transactions on Power Systems*, vol. PWRS-4, no. 1, 1989, pp. 278-285.
- [PAVS] I. J. Perez-Arriaga, G. C. Verghese and F. C. Scheweppe, "Selective modal analysis with applicatons to electric power systems, Part I and II," *IEEE Transactions on Power Apparatus and Systems*, vol. PAS 101, no. 9, 1982, pp. 3117-3134.
- [PPTT] J. Peschon, D. S. Percy, W. F. Tinney, O.J. Tveit, "Sensitivity in power systems", *IEEE Trans. Power Apparatus and Systems*, vol PAS-87, no. 8, Aug. 1968, pp. 1687-1696.
- [RHSC] C. Rajagopalan, S. Hao, D. Shirmohammadi, M.K. Celik, "Voltage collapse operating margin analysis using sensitivity techniques", Proceedings Athens Power Tech 1993, Athens, Greece, Sep. 5-8, 1993, pp.332-336.
- [RAMCJ] R. Rajaraman, F. Alvarado, A. Maniaci, R. Camfield, S. Jalali, "Determination of location and amount of series compensation to increase power transfer capability", *IEEE Trans. Power Systems*, vol.13, no.2, May 1998, pp. 294-300.
- [Reid] J. K. Reid editor, *Large Sparse Sets of Linear Equations*, Proceedings of the Oxford conference of the Institute of Mathematics and Its Applications held in April, 1970 Academic Press, London, 1971.
- [RAUPG] N.D. Reppen, R.R. Austria, J.A. Uhrin, M.C. Patel, A. Galatic, "Performance of methods for ranking and evaluation of voltage collapse contingencies applied to a large-scale network", Proceedings Athens Power Tech 1993, Athens, Greece, Sep. 5-8, 1993, pp.337-343.
- [SRP91] P. W. Sauer, C. Rajagopalan and M. A. Pai, "An explanation and generalization of the AESOPS and PEALS algorithms," *IEEE Transactions on Power Systems*, vol. 6, no. 1, Feb. 1991, pp. 293-299.
- [Sau97] P.W. Sauer, "Technical challenges of computing available transfer capability (ATC) in electric power systems", 30th Hawaii International Conference on System Science, Maui, Hawaii, Jan. 1997.
- [SauPai] P. W. Sauer, M. A. Pai, *Power System Dynamics and Stability*, Prentice-Hall, Englewood Cliffs NJ, 1996.

- [SenPhD] Ontoseno Penangsang, *Fast linear screening approach for contingency selection of line outages based on voltage quality*, PhD Thesis, University of Wisconsin–Madison, May 1983.
- [Seydel] R. Seydel, *From equilibrium to chaos; practical bifurcation and stability analysis*, Elsevier, NY, 1988.
- [Sme93] T. Smed, “Feasible eigenvalue sensitivity for large power systems,” *IEEE Transactions on Power Systems*, vol. 8, no. 2, May 1993, pp. 555-563.
- [Spivak] M. Spivak, *Calculus on Manifolds*, Addison-Wesley, NY, 1965.
- [StC53] H. P. St. Clair, “Practical Concepts in Capability and Performance of Transmission Lines,” *AIEE Transactions*, Vol. 72, Part III, Dec. 1953, pp. 1152-1157.
- [Sto74] B. Stott, “Review of load flow calculation methods”, *Proceedings of the IEEE*, Vol. 62, No. 1, July 1974, pp. 916-929.
- [Sto79] B. Stott, “Power System Dynamic Response Calculations”, *Proceedings of the IEEE*, Vol. 67, No. 2, Feb. 1979, pp. 219-241.
- [SM79] B. Stott, J. L. Marinho, “Linear Programming for Power System Network Security Applications,” *IEEE Trans. on Power Apparatus and Systems*, Vol. PAS-98, No. 3, May/June 1979, pp. 837-848.
- [SAA85] B. Stott, O. Alsac, F.L. Alvarado, Analytical and computational improvements in performance-index ranking algorithms for networks, *International Journal of Electrical Energy and Power Systems*, vol. 7, no. 3, July 1985, pp.154-160.
- [TMI83] Y. Tamura, H. Mori, S. Iwamoto, “Relationship between voltage instability and multiple load flow solutions in electric power systems” *IEEE Trans. on Power Apparatus and Systems*, Vol. PAS-102, no. 5, May 1983, pp. 1115-1125.
- [TT88] A. Tiranuchit, R.J. Thomas, “A posturing strategy against voltage instabilities in electric power systems”, *IEEE Trans. Power Systems*, vol. 3, no. 1, Feb. 1988, pp. 87–93.
- [VCK] T. Van Cutsem, K. Vournas, *Voltage Stability of Power Systems*, Kluwer Academic, Boston, 1998.

- [VC91] T. Van Cutsem, "A method to compute reactive power margins with respect to voltage collapse", *IEEE Trans. Power Systems*, vol. 6, no. 1, Feb. 1991, pp. 145–156.
- [VC94] T. Van Cutsem, "Extensions and applications of a mid-term voltage stability analysis method", in [Davos].
- [VC293] T. Van Cutsem, "Analysis of emergency voltage situations", Proceedings 11th Power System Computation Conference, Avignon, France, Aug. 30 -Sep. 3, 1993.
- [VC95] T. Van Cutsem, "An approach to corrective control of voltage instability using simulation and sensitivity", *IEEE Trans. Power Systems*, vol. 10, no. 2, May 1995, pp. 616–622.
- [VC96] T. Van Cutsem, R. Mailhot, "Validation of a fast stability analysis method on the Hydro-Québec system", *IEEE Trans. Power Systems*, vol. 12, no. 1, Feb. 1997, pp. 282–292.
- [VSZ91] V. Venkatasubramanian, H. Schättler, J. Zaborszky, "On the dynamics of differential-algebraic systems such as the balanced large electric power system", in *Systems and Control Theory for Power Systems*, Springer-Verlag, NY, 1991.
- [SMA] G.C. Verghese, I.J. Pérez-Arriaga, F.C. Schweppe, K. W-K. Tsai, "Selective Modal Analysis", EPRI Report EL-2830, Research Project 1764-8, Jan. 1983.
- [wahoo] Data available via ftp at wahoo.ee.washington.edu
- [WS90] L. Wang and A. Semlyen, "Application of sparse eigenvalue techniques to the small signal stability analysis of large power systems," *IEEE Transactions on Power Systems*, vol. 5, no. 2, May 1990, pp. 635-642.
- [Weh95] L. Wehenkel, "Contingency severity assessment for voltage security using non-parametric regression techniques", *IEEE Trans. Power Systems*, vol. 11, no. 1, Feb. 1996, pp. 101-111.
- [WW] A. J. Wood, B. F. Wollenberg, *Power Generation Operation & Control*, Wiley, NY 1984.

- [WRPK] D. Y. Wong, G. J. Rogers, B. Poretta and P. Kundur, "Eigenvalue analysis of very large power systems", *IEEE Trans. Power Systems*, PWRS-5, no. 2, May 1990, pp. 635-642.
- [WF93] T. Wu, R. Fischl, "An algorithm for detecting the contingencies which limit the inter-area megawatt transfer", Proceedings 1993 North American Power Symposium, Washington D.C., Oct. 11-12, 1993, pp.222-227.
- [YHC93] N. Yorino, S. Harada, H. Chen "A Method to approximate a closest loadability limit using multiple load flow solutions", *IEEE Trans. Power Systems*, vol. 12, no. 1, Feb. 1997, pp. 424-429.
- [ZGOY] Z.C. Zeng, F.D. Galiana, B.T. Ooi, N. Yorino, "A simplified approach to estimate maximum loading conditions in the load flow problem", *IEEE Trans. Power Systems*, vol. 8, no. 2, May 1993, pp. 646-653.